January 2021

Integrative Approach For Improved Oil Recovery In Unconventional Reservoirs

Abdulaziz Ellafi

INTEGRATIVE APPROACH FOR IMPROVED OIL RECOVERY IN UNCONVENTIONAL RESERVOIRS

By

Abdulaziz Mustafa Em. Ellafi

Bachelor of Science in Petroleum Engineering, University of Tripoli, 2011

Master of Science in Petroleum Engineering, Missouri University of Science and Technology, 2018

A Dissertation

Submitted to the Graduate Faculty

of the

University of North Dakota

in partial fulfillment of the requirements

for the degree of

Doctor of Philosophy

Grand Forks, North Dakota

December

2021

Name: Abdulaziz Mustafa Em. Ellafi
Degree: Doctor of Philosophy

This document, submitted in partial fulfillment of the requirements for the Degree of Doctor of Philosophy in Petroleum Engineering from the University of North Dakota, has been read by the Faculty Advisory Committee under whom the work has been done and is hereby approved.

Dr. Hadi Jabbari…..……

Name of Chairperson

Dr. Minou Rabiei…..……

Name of Committee Member

Dr. Kegang Ling…..……

Name of Committee Member

Dr. Hui Pu…..……..……

Name of Committee Member

Dr. Kouhyar Tavakolian…..……

Name of Committee Member

This document is being submitted by the appointed advisory committee as having met all the requirements of the School of Graduate Studies at the University of North Dakota and is hereby approved.

_____

Chris Nelson

Dean of the School of Graduate Studies

_____

Date

PERMISSION

Title	**Integrative Approach for Improved Oil Recovery in Unconventional Reservoirs**
Department	Petroleum Engineering
Degree	Doctor of Philosophy

In presenting this dissertation in partial fulfillment of the requirements for a graduate degree from the University of North Dakota, I agree that the library of this University shall make it freely available for inspection. I further agree that permission for extensive copying for scholarly purposes may be granted by the professor who supervised my dissertation work or, in his absence, by the Chairperson of the department or the dean of the School of Graduate Studies. It is understood that any copying or publication or other use of this dissertation or part thereof for financial gain shall not be allowed without my written permission. It is also understood that due recognition shall be given to me and to the University of North Dakota in any scholarly use which may be made of any material in my dissertation.

Abdulaziz Mustafa Em. Ellafi
Dec 16, 2021

ACKNOWLEDGMENTS

First, I would like to thank Allah for giving me the strength, knowledge, ability, and opportunity to accomplish this research. I would like to express my sincere gratitude to my advisor, Dr. Hadi Jabbari who, has been a great teacher, a friend, an inspiration, a role model, and a pillar of support in my guide.

I am thankful to the members of my advisory committee: Dr. Minou Rabiei, Dr. Hui Pu, and Dr. Kegang Ling, for their technical guidance and continuous assistance. Great thanks and appreciation to Dr. Kouhyar Tavakolian for accepting the request to be on the committee; thank you for the support and feedback.

I am grateful to Petroleum Engineering Department and the North Dakota Industry Commission (NDIC) for the financial support during my academic study through the contract NDIC G-045-89.

I also wish to acknowledge Reservoir Engineering Management of the Continental Resources (CLR) for providing with all the field data needed and engineering insights to complete this research.

I would also like to thank the Environmental and Energy Research Center (EERC) for the opportunity to work with them as a Research Assistant/Reservoir Engineer for almost two years; EERC supports really helped a lot in this research.

Vast gratitude also goes out to my fantastic research group (UND PE Research Hawks) for their help, especially co-authors in my publications: Dr. Mohammed Ba Geri and Mouna-Keltoum Benabid.

My greatest appreciation goes to Heba Miloud for her assistance and unlimited support. Also, special thanks to Dr. Lu Jin (EERC); I can never thank you enough for the support, valuable explanation, and guidance throughout this process.

My acknowledgement would be incomplete without thanking the biggest source of my strength, my family. This would not have been possible without their unwavering and unselfish love and support given to me at all times.

DEDICATION

To the loving memories of my parents, Fatima Zidane, and Mustafa Ellafi. Also, to my brothers and sister, Abdulrahim, Mohammed, and Tasnim Ellafi. The world's best family.

ABSTRACT

The hydrocarbon production improvement in unconventional reservoir development has been driven by the application of modern horizontal drilling and multi-stage hydraulic fracturing (MSHF) techniques, which makes it possible to access low porosity (<10%) and low permeability (<0.1 mD) formations. Large stimulated reservoir volumes (SRVs) have been created through breakthroughs in hydraulic fracturing technology; however, fracture treatment is not necessarily effective. Operators have started utilizing tighter spaced clusters, longer stage lengths, and greater proppant volumes to design hydraulic fracture stimulation. However, the ultimate oil recovery reported by several studies is less than 8% due to a rapid decline in unconventional well performance and by approximately 75% within the first two years of well production as a result of several reasons.

This research presents an integrated approach of unconventional reservoir applications to increase well/reservoir contact area (i.e., large stimulated reservoir volumes "SRVs") and efficiently produce more trapped oil in the pore matrix from liquid-rich shale reservoirs. In order to achieve research goals, this dissertation is divided into three phases.

In the first phase, we present a combination of the Diagnostic Fracture Injection Test (DFIT) and post-treatment pressure falloff analysis, which can help to design intelligent production and improve well performance. Our field study from the STACK Play, Anadarko Basin, Oklahoma, explains the objective optimization workflow of diagnostic tools. The falloff pressure analysis provides vital information, assisting operators in fully understanding models for fracture network characterization.

In the second phase, this research aims to study the capability of high-viscosity friction reducers (HVFRs) by examining the produced water from the Bakken Formation through an

integral approach. Surfactant application as an additive to the HVFRs is investigated in high TDS (total dissolved solids) conditions. The results show that using a surfactant mixed with the fracturing fluids can improve proppant transport, fracture conductivity profile, and thus higher effective fracture half-length compared to current practice. It is found that such a fracturing fluid mixed with surfactant can increase Estimated Ultimate Recovery (EUR) by as high as 15% compared with linear gel and HVFRs with produced water (HVFR-PR) due to larger propped SRVs.

In the final phase, the experimental work is presented to evaluate the feasibility of the Enhanced Oil Recovery (EOR) method using the CO2 huff-n-puff (HNP) protocol in the Middle Bakken Formation, the Mountrail County, Williston Basin, ND. The objective is to evaluate the incremental oil recovery from CO2-EOR under several operational and well/reservoir conditions scenarios. The parameters considered in the sensitivity study include temperatures, pressure, soak time, and a number of injection cycles to obtain optimum conditions under which the incremental oil recovery from the MB Formation is increased. The wettability alteration (i.e., contact angle) is also studied using rock-chip samples before and after the HNP experiment at the Bakken reservoir conditions (present, for example, P & T in psi/F). As overall outcomes from this research, the CO2-HNP process has a good potential in the lab and could be succeeded economically in field applications that might reduce the need for refracturing stimulation or infill drilling.

CONTENTS

LIST OF FIGURES

LIST OF TABLES

Nomenclature

$\Delta p_{wb\&per}$: Pressure drops in the wellbore and perforation, m/L.t^2

Δp_{tort}: Pressure drops due to near-wellbore tortuosity, m/L.t^2

$\Delta p_{total\ fric}$: Total Pressure drops in the system, m/L.t^2

$P_{c,nf}$: Created fracture closure pressure, m/L.t^2

$P_{c,mf}$: Natural fracture closure pressure, m/L.t^2

ISIP: Instantaneous shut-in pressure, m/L.t^2

p_1^*: dp_w/dG, Nolte match pressure, m/L.t^2

A_{mf}: Total created fracture surface area, L^2

A_{nf}: Total natural fracture surface area, L^2

x_f: Fracture half-length, L,

R_f: Fracture half-radius, L,

C_L: Leak-off coefficient, L/(t)$^{1/2}$

c_f: Fracture compliance, L^2.t^2/m

τ: Superposition time, dimensionless

p_{ws}: pressure at the end of pumping, m/L.t^2

dp_w/dG: First pressure derivative, m/L.t

PIFs: Proppant-impact-factors, dimensionless

K: Reservoir permeability, L^2

η: Fluid efficiency, dimensionless

α: The area exponent, dimensionless

β_s: Pressure constant ratio, dimensionless

G_c: Closure time, t

E': Young's modulus, m/L.t2

V_p: Total injection volume, L3

$g(\Delta t_D)$: G-function

g_0 $g(\alpha, \Delta t_D = 0)$

t_p Operation time, t

t Falloff time, t

r_p Productive fracture ratio, dimensionless

h_f Total fracture height, L

h Propped fracture height, L

Δt_D: Dimensionless time, dimensionless

p_w: Pressure recorded at the surface during the falloff period, m/L.t^2

Gdp_w/dG:Second pressure derivative, m/L.t^2

TVD: Total vertical depth, L

P_i: Initial reservoir pressure, m/L.t2

CHAPTER 1

Hydraulic Fracturing Application

1.1 Introduction

Over the last decade, advancements in horizontal drilling and multi-stage hydraulic fracturing technologies have resulted in a revolution in oil and gas production via oil-bearing shale reservoirs. The objective of a fracture treatment is to create fissures, or "permeable pathways," in tight formations by injecting a larger fluid volume and high proppant concentration to release trapped oil and gas (Ba Geri et al., 2019a; Ellafi et al., 2019b; Li and Zhang, 2019; McMahon et al., 2015).

Based on the drilling spacing unit (DSU) and governmental regulations, up to 20 wells can be drilled and stimulated from a single well pad to produced economically from unconventional shale plays (Ahmed and Meehan, 2016). Subsequently, domestic oil production from liquid-rich shale (LRS) reservoirs in North America has dramatically increased in the Bakken, Eagle Ford, Niobrara, and Permian Basin from 16.5% in 2008 to reach around 60% of the total oil production in 2019 (The Energy Information Administration (EIA), 2019). Whereas the projection of the natural gas production from unconventional shale gas reservoirs, including the Marcellus and Barnett shale plays expects a significant increased from 5 trillion cubic feet per year in 2010 to 13 trillion cubic feet per year in 2035. The hydraulic fracturing technologies would make the United States top

worldwide gas exporter by 2022, with 49% of total natural gas production from conventional and unconventional reservoirs (EIA, 2019).

The most commonly used fracturing fluids in the U.S shale plays are water-based fracturing fluids, such as Newtonian fluids, non-Newtonian viscous fluids (X-link gels & slickwater), or hybrid fluids (X-link gels/slickwater). The typical composition of these hydraulic fracturing fluids consists of mainly 94% freshwater, 5% proppant, and 1% chemical additives (e.g., biocides, acid, corrosion inhibitor, breaker, surfactants, friction reducers) (Ellafi et al., 2020a; Ba Geri et al., 2019b; Palla et al., 2014).

However, some cases were declared by ExxonMobil, 2017 and FracFocus, 2012, the extreme value of freshwater used as makeup fluid is up to 99.8% of the total fracturing fluids. Therefore, the fracture treatment consumes a large volume of freshwater: around 20,000 to 5 million gals of water in a period of two to five days, depending on the length of the horizontal lateral and geological characteristics (Ellafi et al., 2020a; Almubarak et al., 2019; Van Domelen and Haggstrom, 2011).

For instance, the shale gas horizontal wells in the Barnett shale, Eagle Ford, Haynesville, and Marcellus plays require 2.8, 4.2, 5.7, and 4.5 million gals of injection fracturing fluids (freshwater), respectively as median quantity to stimulate the wells in order to achieve gas production at the economic level (Mohammad-Pajooh et al., 2018).

Figure 1. 1 presents the trend of average freshwater consumption per well in the U.S shale reservoirs. Notably, water usage gradually increased from 2011 to 2016, but suddenly increased from 2017 due to the recovery in oil prices that resulted in new strategies for field development, such as refracturing applications to sustain hydrocarbon production levels from tight formations.

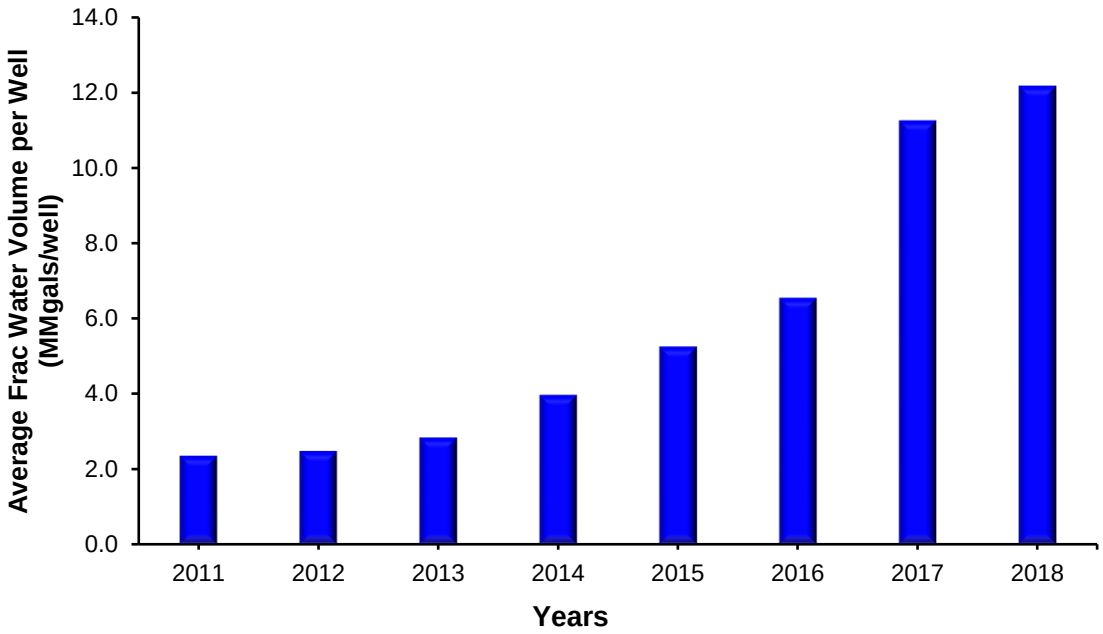

Figure 1. 1 . By year, average consumption of fracturing water per well in the U.S shale plays (Gabriel Collins, 2019; Backstrom, 2019; Oraki Kohshour et al., 2016).

Several comprehensive studies have assessed hydraulic fracturing water usage in all major shale oil and gas plays across the U.S (Campin, 2019; Shrestha et al., 2017; Torres et al., 2016; Kondash and Vengosh, 2015; Scanlon et al, 2014; Freyman, 2014). During unconventional reservoir exploration, hydraulic fracturing treatment requires significant water inputs approximately 89%, with 10% water intensive input for the drilling operation (Ren et al., 2019; USDOE, 2014). In addition, previous studies have addressed hydraulic fracturing applications in shale gas, such as the Marcellus and Barnett shale plays, with significantly more water consumption than the shale oil plays, including the Eagle Ford, Bakken, and Permian Basin, as shown in Figure 1. 2.

Figure 1. 3 illustrates the work by Ba Geri et al. 2020, where they analyzed and summarized data for over 800 wells at each shale play in the U.S from a database of FracFoucs website. Although the Eagle Ford wells are designed with shorter laterals and a lower number of frac stages per well than the Bakken wells, the Eagle Ford wells consume larger quantities of

freshwater: two times more than used in the Bakken wells, as illustrated in Figure 1. 3 (Torres et al., 2016). The reason behind such a difference is that the operation factors (e.g., length of laterals, hydraulic fracturing fluid types, number of frac stages, etc.) as well as formation characterizations are different from one unconventional play to another, which may contribute to lower or higher freshwater demands (Scanlon et al., 2014).

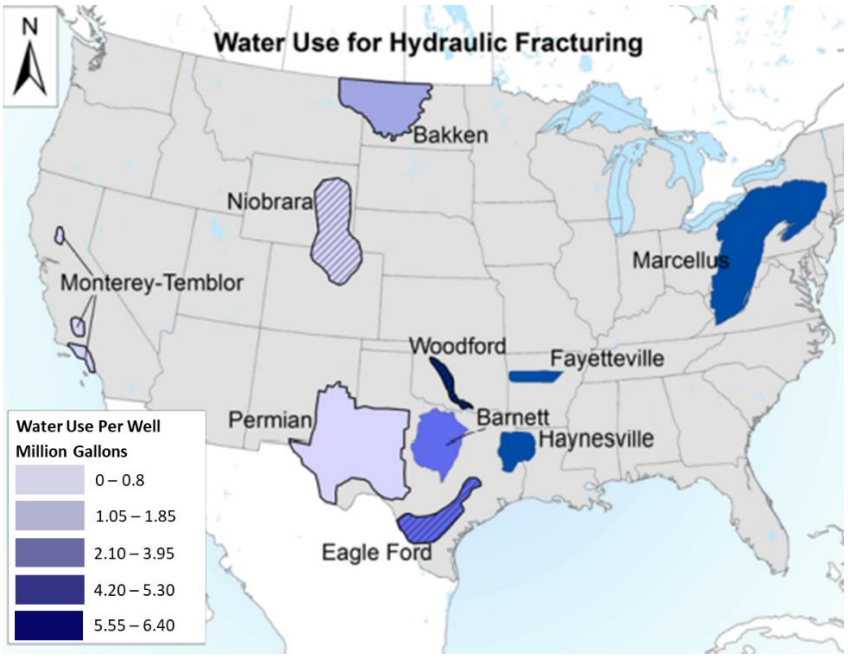

Figure 1. 2. The average water uses in hydraulic fracturing in the main basins in the USA in 2019 (Ba Geri et al. 2020).

In terms of environmental issues, some concerns with the fracking operation are addressed recently, and the treatment process is being re-evaluated the long-term impacts by the producer countries. The primary concerns issues are classified into five categories: 1) water withdrawal, 2) groundwater contamination, 3) water transport, 4) wastewater disposal, and 5) air quality. Shale oil and gas wells in Texas are responsible for wasting 2% of water demand for fracking jobs, an amount of drinkable water sufficient for three million Texans (Environment Texas Research and Policy Center, 2013).

Furthermore, in 2018, total water withdrawal from the Missouri River for hydraulic fracturing purposes was around 1.269 $\times 10^{10}$ gals, which is 10.1% of North Dakota's consumptive water use (NDSWC, 2019). In addition, outlook data for the next ten years suggest that more than 100,000 wells will be drilled and completed, with an expected 70 to 140 billion gals of water per year.

As a result, freshwater availability has decreased with increasing associated costs, which leads to impacts on human health, agriculture, livestock, and wildlife (Kohshour et al., 2016; Torres et al., 2016; Boschee, 2014). On the other hand, in ten years, 212 billion gals of combined flowback and produced water will be generated, and the critics claimed that the used materials would contaminate groundwater resources and toxic air emissions (Chen et al., 2019; Esmaeilirad et al., 2016; Kondash and Vengosh, 2015; Rahm, 2011).

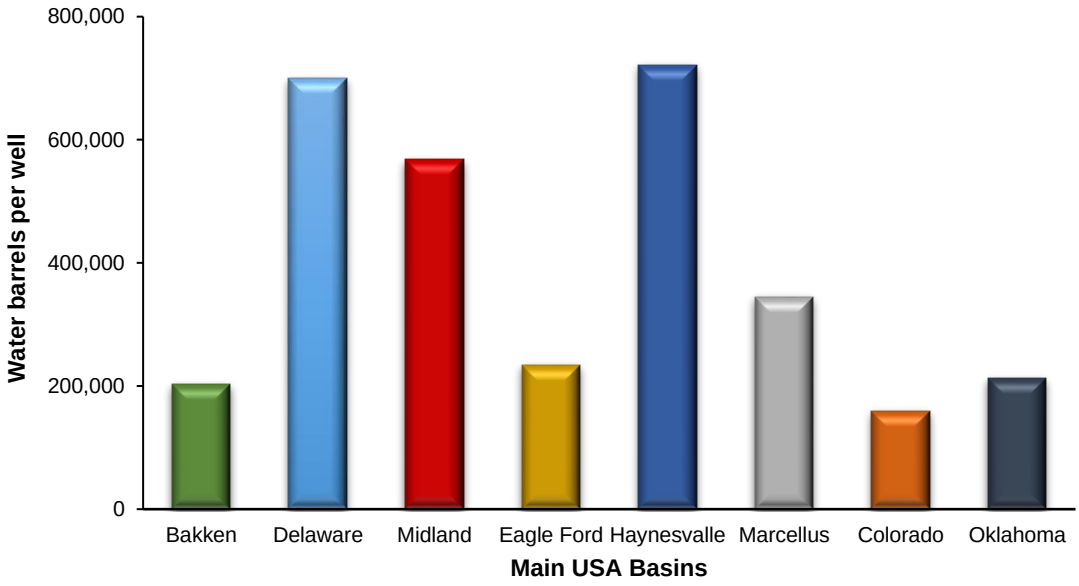

Figure 1. 3. Average freshwater use per well in the U.S shale plays (Kondash and Vengosh, 2015).

1.2 Challenges in Developing Unconventional Reservoirs

In North America, operators face a dramatical increase of produced water by 20 to 30 billion barrels each year due to developments in unconventional resources using hydraulic fracturing

applications consuming large amounts of freshwater mixed with some chemicals as fracturing fluids (Al Battashi et al., 2019; Ba Geri et al., 2019e; Ellafi et al., 2019a; Otton and Mercier, 2015; Li et al., 2014).

In addition, water production increases as the well ages, which may include naturally occurring water that was formed and stored with the hydrocarbon within the pores of the reservoir rocks during the hydrocarbon formation or may be some infiltrating waters from aquifers around the hydrocarbon-bearing rocks (Du et al., 2005). Worldwide oil and gas reservoirs produce approximately 250 million barrels of water daily, where 40% of produced water is discharged into the environment (Iqunnu and Chen, 2012).

Despite the hydrocarbon is significance energy, and the daily petroleum consumption would reach up to 106.6 million barrels of oil by 2030, the volume ratio of water to oil is only 1:3 that associated with a large volume of waste (Iqunnu and Chen, 2012). Figure 1. 4 illustrates that the Bakken formation maintains a water cut of 40% for the entire life of the Bakken wells, which means that most of the produced water is the formation water that produces as a result of water level near the reservoir and due to low percentage of flowback water generate. Also, the Permian Basin behaves similar to the Bakken formation, but with higher water cut that excess of 70% of total liquid production.

On the other hand, the Eagle Ford started with a higher water cut, which mainly represents the flowback water at 30%, then the water depleted to produce at a constant value of around 10%. The change in water cut over time indicates that the geological description of the formation plays an important role in the percentage of produced water production.

In broadly speaking, produced water is defined as an unclean and lower quality water that often contains bacteria and high salinity/hardness. The produced water, including flowback

and formation water consists of a wide range of anions, cations, and heavy metals known as Total Dissolved Solids (TDS) (Li et al., 2010; Ahmadun et al., 2009).

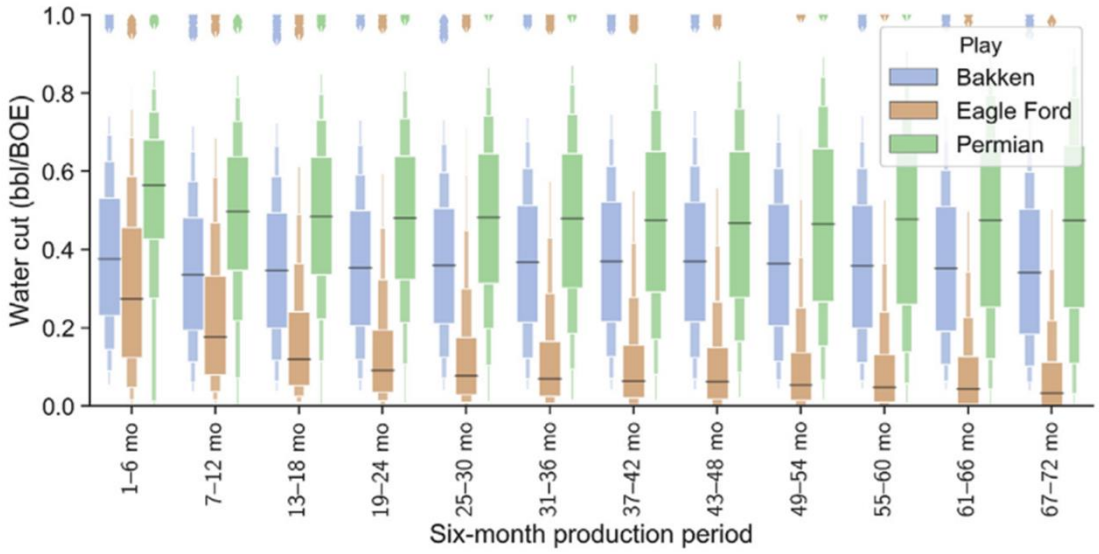

Figure 1. 4. The change in water cut over time in the U.S shale plays (Male, 2019).

Figure. 1. 5 illustrates produced water salinity, with a wide range from a few thousand up to 463,000 ppm Total Dissolved Solids (TDS) in the Williston Basin. The term flowback water refers to volume liquid from a previous treatment job that flows back through the well cleanup, which may contain some portion of the original fracturing fluids. Furthermore, flowback water from previous treatment jobs contains many impurities, such as salt concentrations, heavy metals, oils, grease, dissolved gasses, and volatile and semi-volatile soluble organics (Lord et al., 2013; Du et al., 2005). Therefore, the flowback water is considered the largest proportion of liquid waste in the industry, polluting both surface and underground environments.

Chemicals and other physical attributes of produced water differ significantly depending on the producing reservoir geographical location and condition, general field geographic location, basin era of deposition, and the type of hydrocarbon being produced (Whitfield,

2017; Du et al., 2005). For example, water injection during water flooding activity could also alter the produced water chemicals, depending on the injected volumes (Du et al., 2005). As mentioned above, the real concern in produced water is the salinity level, as this determines the level of treatment that must be applied. In the Bakken produced water, salt contributes to more than 90% of the total dissolved solid content while oil and grease, inorganic and organic compounds introduced as chemical additives to improve drilling and production operations, and naturally occurring radioactive material contribute less than 10% (Haghshenas and Nasr-El-Di, 2014).

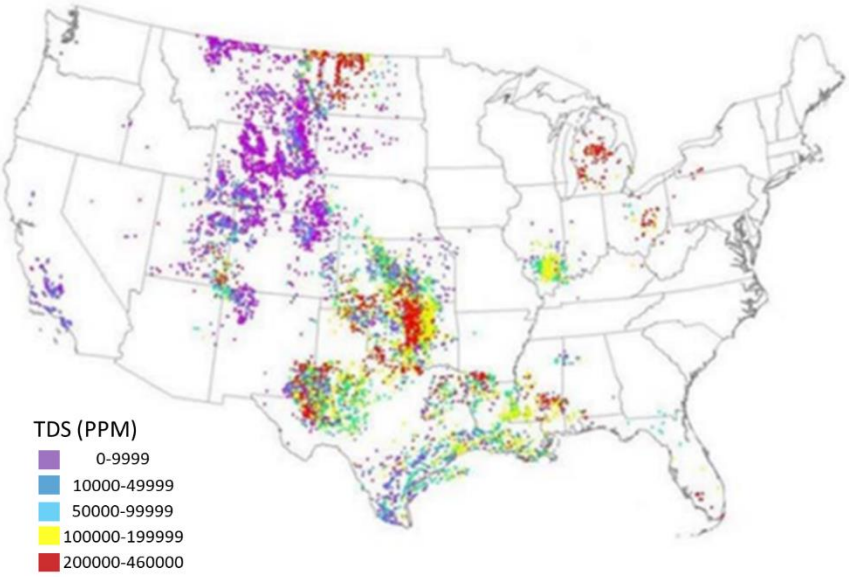

Figure 1. 5. Produced waters salinity range in the United States (Otton and Mercier, 2015).

Produced water may vary depending on the kind of hydrocarbon the reservoir was drilled to produce oil or gas. Produced water from gas production has different characteristics than produced water from oil production. Table 1. 1 lists the typical chemical composition of the diluted sample with mixtures of the metal species ranging from 1 to 100 ppm and the

comparison between the Permian Basin tap water and different flowback water compositions before and after the water treatment process.

In 2013, Fontenelle et al. introduced the electrocoagulation (EC) treatment method that uses electrochemical technology to separate organic and inorganic materials from the flowback water. Although this technology does not remove dissolved ions of the water composition, the variety treated produced water samples were successfully used with fracturing fluids, such as crosslinked and friction reducers fluids.

Table 1. 1. Chemical composition of the produced water analysis from Permian Basin (Ba Geri et al., 2019e; LeBas et al., 2013; Fontenelle et al., 2013).

	Fresh Water	**Produced Water 1**	**Produced Water 2**	**Produced Water 3**	**Produced Water 3 after treated water**
Specific Gravity	1.00	1.20	1.10	1.20	1.10
pH	8.07	4.83	6.21	5.3	7.5
Chloride (ppm)	50-630	163,637	118,000	166,014	166,152
Sulfate (ppm)	11	40	N/D	12	17
Aluminum (ppm)	0	1.42	N/D	1	1
Boron (ppm)	0	20.30	N/D	23.3	28
Barium (ppm)	0	5.69	N/D	8	8
Calcium (ppm)	304	29,222	9,480	29,755	29,875
Iron (ppm)	0	34.60	5.1	13	4
Potassium (ppm)	0	1,660	N/D	1,692	1,705
Magnesium (ppm)	30	4,347	N/D	4,629	4,452
Sodium (ppm)	4	70,342	N/D	74,562	76,427
Strontium (ppm)	0	2,204	N/D	1,777	1,791
TDS (ppm)	237-988	267,588	125,300	275,053	277,095
Hardness (ppm)	328	>20	12,740	36	18

In a reservoir designed to produce gas, in addition to formation water, there would be the presence of condensed water (Du et al., 2005). This water is vapor in both the mixture and the reservoir, but then condenses into a liquid state at the surface during separation. Produced water generated from producing coalbed methane (CBM) also varies from produced water from both oil and gas production activities.

In coalbed methane drilling, oil and grease are less of a concern constituent in the produced water when compared with others. Inclusions of coalbed methane water that need to be considered before reuse are salinity, iron, manganese, and boron (ALL, 2003). The reuse of produced water is not a new concept, but it is challenging under high-salinity reservoirs conditions. Recently, the trend of reusing produced water as fracturing fluids has increased in the field since it offers significant benefits, both environmental and economic.

1.3 Fracture Treatment Fluids in Past and Present.

Since 1947, hydraulic fracturing has been successfully implemented. Hydrocarbon-based treatment fluids were the preferred to use, and water-based treatment was an undesirable option due to the interaction between water and formation mineralogy that causes formation damage. Exposure to drilling fluids can alter the mechanics of chemical formation causing impairments such as: swelling, migration, emulsions, and clay induced and wettability alterations (Jennings Jr, 1996).

In the 1950s, water-based treatment fluids were first introduced to the industry for hydraulic fracturing applications with added polysaccharide material (gelling agents) such as starch, cellulose, and guar gum to water to create linear non-Newtonian fluids. Another objective of using these polymers included their modified variations like carboxymethyl cellulose and carboxymethyl hydroxypropyl guar to enhance the viscosity profile as well as provide some

pipe friction reduction during the operation (Montgomery and Smith, 2010; Maley and O'Neil, 2010).

In the mid-1960s, the industry switched to crosslinked fluids, adding borate ions to hydrated linear gels to enhance fluids' capabilities (transport and suspense proppant). At that time, studies observed that crosslinked fluids can increase viscosity profile, elasticity modulus, share modulus, and fluid stability in high reservoir temperature (Maley and O'Neil, 2010).

In the early 1970s, a revolution in hydraulic fracturing applications occurred, and several types of additives were used to develop hydrocarbon reservoirs. The two main additives utilized were metal ions of zirconium and titanium, which were used as an alternative to borate-based crosslink fracturing fluids since these additives showed better performance in high reservoir temperature (Quintero et al., 2018).

In the last decade, a significant development in oil-bearing shale reservoirs using fracturing fluids by injecting a larger fluid volume and high proppant concentration to create complex fracture geometry and enhance stimulated reservoir volume ensued (SRV) (Ellafi et al., 2020a; Ba Gei et al., 2019a). Nonetheless, the linear gel cost was increased by more than three times, and operators faced challenges in terms of stimulation costs. Several alternative fracturing fluids were attempted instead of linear gel, but the production results showed limited success.

In 2012, the evaluation conducted by the Stim-Lab showed that traditional friction reducer (FR) based fluid can regain conductivity in contrast to linear guar gel. Several companies then replaced the linear gel system with the slickwater fracturing fluids, which are low viscosity fluids and have a low concentration of friction reducers. The chemical definition, known as a "polyacrylamide" or "polyacrylamide" combined with another monomer, which

made of long chain synthetic polymer mixed with ionic functionality. Friction reducer polymers can be anionic, nonionic, or cationic species, as listed in Table 1. 1.

To improve hydration properties and compatibility with different water sources, acrylic acid and AMPS are incorporated (Rodvelt et al., 2015; Sun et al., 2010). The low concentration FR falls in the range between 0.5 to 2 gallons per thousand gallons (gpt), and the average molecular weight of the fluids is 20-25 million Dalton, known by the size of polymers (Ba Geri et al., 2019; Paktinat et al., 2011). The most effective polymer friction reducers are mixed in oil-based fluid and surfactant to maintain the fluid in the state required for use (DeMong et al., 2010).

Therefore, the lowered FR dosages provide a lower footprint and a more cost-effective system. The fluids can be pumped for a high pump rate with a low reduction in operation pressures to promote a more efficient laminar flow and overcome the tubular drag while the pumping pressure is high around 10,878-11,603 psi (Quintero et al., 2019).

This would improve production for extremely low permeability formations with high potential and low cost of the treatment. In addition, some additives can be added to Slickwater, such as clay controls, flowback enhancers, and scale inhibitors to extend capability and performance (Boyer et al., 2014). However, there are several concerns associated with Slickwater use in long lateral horizontal wells. It can be concluded to have poor proppant transport capability, provide low proppant distribution, premature sand screenout, excessive water volume requirements, and environmental issues (Ba Geri et al., 2019a, b, & c; Hu et al., 2018; Van Domelen et al., 2017; Motiee, 2016).

Due to recent restrictions from government regulations to limit the use of freshwater, as well as concerns over the disposal and environmental impact of flowback water, reusing produced

water, (including formation and flowback water) alternative water sourcing is getting important attention in the oil and gas industry since it has many benefits, such as saving high-quality water for domestic and agricultural needs, minimizing environmental footprints, and reducing operating costs (Fontenelle et al., 2013).

Table 1. 2. Types and chemical structures of friction reduces (FRs) (Xiong et al., 2018).

Type of FRs	Chemical Name	Chemical Structure
Non-ionic PAM	Polyacrylamide	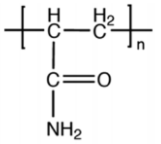
Anionic PAM	Polyacrylamide-co-acrylic acid, hydrolyzed polyacrylamide	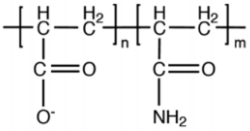
	Poly-acrylamido-2-methylpropane sulfonate	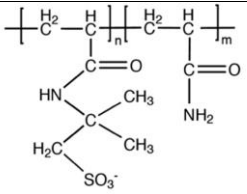
Cationic PAM	Poly (acrylamide-co-N,N,N-trimethyl-2-((1-oxo-2-propenyl)oxy))	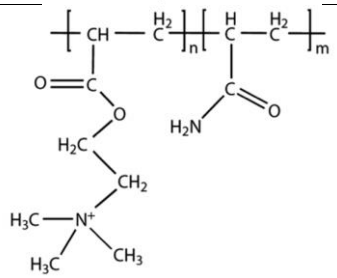

However, recycling water-based fluid treatment is challenging, as the water can contain a high amount of total dissolved solids (TDS), chemicals, suspended solids from previous treatments, and dissolved organic materials (Lord et al., 2013). The results in the literature summarized that the salinity and pH range in the tests did not appear to have a significant effect on the performance of friction reducers. The main concern is the stability of the fracturing fluids when salt content and iron increase in aqueous-based fluids, where most of the treatment fluids fail to carry proppant into the fractures.

Fontenelle et al., 2013 introduced smart water treatment using an electrochemical process for flow back and produced waters, which does not remove dissolved ions. This technology separates colloidal organic and inorganic materials. The results reported the technology minimized the amount of produced water, where the treated water was able to use treatment fracture fluids. In addition, the technology treatment cost is low compared to other water management approaches.

Thus, comprehensive studies in the lab have been conducted to understand the fluid characterization (viscosity and viscoelasticity properties) of the fracturing fluids under harsh brine solution before running simulation and field trials using produced water with fracturing treatment fluids (Almubarak et al., 2019; Ba Geri et al., 2019; Demong et al., 2010; Ellafi et al., 2019b; Seymour et al., 2018; Walters et al., 2009).

To develop and optimize the application of salt-tolerant polyacrylamide-based friction reducers, which is referred to as high viscosity friction reducers (HVFRs), the first generation of HVFRs were not able to tolerate high salinity brines and showed lower performance in terms of viscosity profile and friction pressure reduction compared to industry standard FRs (Quintero et al., 2019). Dynamic measurements of HVFRs in the laboratory are crucial to study, understand and assess the fluid characterizations before running simulation and field trials using produced water with fracturing treatment fluids (Tomomewo et al., 2020a&b; Ellafi et al., 2020b; Ba Geri et al., 2019c, d, & e; Seymour et al., 2018).

Ba Geri et al. (2019a) introduced a critical review study that summarized the recent applications of HVFRs as fracturing fluids. HVFRs are classified into three types: Anionic, Nonionic, and Cationic. The most common type of HVFRs are anionic fluids due to their lower cost and better drag reduction. Although anionic HVFRs tend to have minimum

formation damage, they cannot tolerate a high TDS level of saltwater and are more sensitive to iron constituent. On the other hand, cationic HVFRs have been successfully used in up to 100% of produced water with the lower cost operation, but cationic HVFRs may not be compatible with formations that contain a high amount of quartz and/or clay (Ba Geri et al., 2020; Tomomewo, 2020a).

As a result, formation damage can occur due to the negatively charged formations and interaction with fluids that cause altered rock wettability and release a clay stabilizing agent over time (Xu et al., 2018). Therefore, the authors' goal was describing HVFRs' capability in detail. The study concluded that the proposed fluids give high proppant transport, retain 100% conductivity, offer lower operation cost, reduce the use of chemicals by 50%, have low pipe friction and high pump rate, minimize water consumption, decrease environmental concerns, and are compatible with produced water.

Moreover, Ba Geri et al., (2019b, c, d, & e) addressed the evaluation performance of HVFRs in the high-TDS environment using Wolfcamp shale-produced water. The research aimed to investigate viscoelastic characterization by providing a full lab-based comparison of viscosity and elastic modulus between HVFRs and other fracturing fluids, such as linear guar gel, xanthan, and emulsion. The experimental work results confirmed that HVFRs represent a stable fracturing fluid compared to other types, which have effectual properties in high temperature and high-water salinity for proppant transport and diminishing turbulent flow results, increasing in a pump rate up to 100 bbl./minute.

The study provided the flow behavior index (n') and flow consistency index (k') which determined the rheological properties of HVFRs under high water salinity conditions. These

values were used in our research simulation works to mimic the behavior of HVFRs using 3D hydraulic fracturing simulation.

To solve the problems and challenges of anionic HVFRs in harsh conditions, two key solutions have been employed. First, Seymour et al., 2018 investigated several surfactants to be used as additives to extend the salt tolerance of HVFRs' performance. These researchers performed a series of experiments using a friction flow loop to detect the performance of HVFRs. In addition, sodium and potassium brine effects were examined using the Permian basin-produced water.

This study concluded that the surfactant system extends the HVFRs workability at high TDS conditions. Adding the surfactant to fracturing fluids can assist in changing the intermolecular interaction between polymer fragments. As a result, the fracturing fluids can be utilized to inhibit formation damage and prevent flocculation. A surfactant system with fracturing fluids was reported to be an effective solution to prevent performance degradation in high TDS conditions (Xu et al., 2017; Palla et al., 2014). Few research studies have introduced the surfactant additives in the fracturing fluids with produced water, but the surfactant is well known in the industry, used in different applications, and showing ability in Interfacial Tension reduction and Wettability (WTB) Alteration.

The authors have examined the usability of surfactant as a good candidate to enhance the performance of the fracturing fluids in high TDS conditions as well as improving oil recovery from unconventional shale plays. Recently, the study of Gu et al., 2020 concluded a surfactant–polymer mixture has the advantages of strong shear resistance, drag reduction polymer to mechanical and thermal degradation, and the micelle structure's critical concentration is reduced. Adding surfactants to Slickwater can reduce surface tension, the

contact angle between the fracturing fluids and reservoir fluids and/formation rocks, control the leak-off of the treatment fluids in low-pressure reservoirs, and reduce the well clean up in the flowback period.

DeMong et al., 2010 studied the performance of HVFRs in the Horn River Basin, where the water from surface sources in the winter season can be very cold and lead to serious problems, such as increasing the inversion time that causes reduction in the effectiveness of HVFRs. The research compared the cost and benefit of the surfactant solution compared to heating and/or increasing friction reducer dosages. The conclusion addressed the concern that high concentration surfactants are not preferred options in terms of cost compared to using water treatment and increasing HVFRs loading. However, the surfactant is well known in the industry and is used in different applications to show ability in interfacial tension reduction and wettability (WTB) alteration. The authors have examined the usability of surfactant as a viable candidate to enhance the unfolding time of some of HVFRs in high TDS conditions and cold water as well as improving oil recovery from unconventional shale plays (Paktinat et al., 2011).

In 2009, Walters et al. presented a new clean biopolymer-based fracturing fluid that showed a high capability to be used with produced water. The lab results confirmed that the new fracturing fluids had significant conductivity, stable viscosity under a different range of temperatures, low-pressure loss, and perfect proppant placement in deep fractures. Also, the fluid was used in the field to frac 14 stages over four wells. The field trial assessment reported that, in terms of production, the outcomes show high reservoir production performance because of more effective fracture half-length and proppant transport obtained during the operation.

1.4 HVFR is Environmentally Friendly

The following points are concluded by Ba Geri et al., 2020a, where the authors approved that PAM is widely used in environmental systems including (Xiong et al., 2018; Ba Geri et al., 2019b; Ba Geri et al., 2020a&b):

1. As a flocculant in water treatment and sludge dewatering
2. As a soil conditioning agent in agricultural implementations.
3. As a viscosity enhancer in enhanced oil recovery (EOR) and more recently as a friction reducer in high volume hydraulic fracturing (HVHF)
4. High regains conductivities and less formation damage above 95% compared to linear and crosslinked gels systems.

These insights of using HVFRs concluded that high dosages of HVFRs is an environmentally friendly footprint leads to optimize the compatibility between HVFRs with low water quality "Bakken Produced Water".

1.5 Unconventional Well Performance

The creation of large stimulated reservoir volumes (SRVs) has been achieved through breakthroughs in hydraulic fracturing technology; however, fracture treatment is not necessarily effective (Ellafi and Jabbari, 2021). In the field, operators have started utilizing tighter spaced clusters, lower number of stages, longer stage lengths, and greater proppant volumes to design hydraulic fracture stimulation (Zhang et al., 2021; Jayaram et al., 2019). The aim is to enhance fracture treatment performance in terms of cost-efficiency by reducing the stage number to save bridge plugs in geological engineering along horizontal well. The ultimate oil recovery reported by several studies is less than 8% due to a rapid decline in

unconventional well performance, and by approximately 75% within the first two years of well production.

The decline in the oil production rate is due to several reasons:

1. A low to no hydrocarbon recharge from the ultra-tight matrix blocks since the natural and induced fractures close, and there is a high flow resistance at the matrix-fracture interface; therefore, the increase in net stress leads to a zero-pressure gradient, which obstructs the fluid flow from the rock matrix into the fracture (Ellafi and Jabbari, 2020).
2. Proppant embedment plays a significant role in conductivity and decreasing fracture width since an inappropriate choice may cause proppant deformation, or proppant crush, under closure pressures (Li et al., 2015).
3. High-pressure drawdown may also cause formation rock compression, which leads to a reduction in matrix permeability with changes in reservoir pressure or stress (Nguyen et al., 2020).
4. Diagnostic fracture tools through several case studies show a low efficiency of perforation, where one-third of perforation clusters contribute to the major production along the horizontal wellbore due to the stress shadow effect. This phenomenon is the heterogeneity existing in both rock-mechanical properties and in-situ stresses that cause uneven distribution of fracturing fluids volume during the treatment and an unequal fracture propagation from one cluster to another in each fracture stage (Zhang, F et al., 2021).
5. Fracture hit phenomenon that refers to the type of well interference or interaction during the fracture treatment process. Due to the pressure depletion and stress change around the parent well, fracturing fluids transport from new child wells to the parent well through natural and induced fracture networks that creates an overlap between wells. As a result,

significant production degradation occurs in both parent and child wells while water cut increases suddenly in the parent well (Zhang, S et al., 2021).

1.6 Research Objectives

The primary objective of this research is to improve oil recovery from shale plays using an integrated unconventional reservoir engineering method by increasing well/reservoir contact area (i.e., large stimulated reservoir volumes "SRVs") and efficiently producing more trapped oil in the pore matrix from liquid-rich shale reservoirs. In order to achieve research goals, this dissertation is divided into three phases, and the objective of each phase is described as follows:

- In the first phase, the pressure falloff data tool is used to evaluate fracture designs on a stage-by-stage basis to optimize the overall performance of a well, unlike common performance evaluation methods such as Rate Transient Analysis (RTA) and micro-seismic fracture imaging/mapping (MS). Our target is to overcome some limitations and weaknesses in most of the proposed techniques in the literature by developing a tool that can provide comprehensive information, such as the mechanics of the created open, closed, and propped hydraulic fractures.
- In the second phase, this research aims to conduct simulation studies on HVFRs with surfactant as an additive that could help operator companies reduce costs and develop unconventional wells successfully for a return on their investment.
- In the final phase, the experimental work is presented to evaluate the feasibility of the Enhanced Oil Recovery (EOR) method using the CO2 huff-n-puff (HNP) protocol under several operational and well/reservoir conditions scenarios that may be successful

economically in field applications to reduce the need for refracturing stimulation or infill drilling.

1.7 Research Scope

This research applied the integrated approach on the field data from unconventional reservoirs in evaluating and understanding the contribution of individual fracture stages in order to maximize well performance during both primary production and late stage EOR processes. This dissertation consists of seven chapters as follows:

1. Chapter 1 defines hydraulic fracturing application and a brief explanation of challenges in the development of unconventional resources. It also provides the statement problem in unconventional well performance, fracturing fluids technology, research objective, and dissertation scope.
2. Chapter 2 outlines a combination of the Diagnostic Fracture Injection Test (DFIT) and falloff pressure analysis through an unconventional well case study, which can help to design intelligent production and improve well performance. The chapter presents the paper entitled "*Unconventional Well Test Analysis for Assessing Individual Fracture Stages through Post-Treatment Pressure Falloffs: Case Study*" published in Journal of Energies https://doi.org/10.3390/en14206747.
3. Chapter 3 presents the optimization strategy of fracture treatment design using produced water with HVFRs. The study starts with evaluating an unconventional formation and then building the geomechanical model to assess the three different fracturing fluid scenarios for hydraulic fracture modeling. Chapter 3 is taken from the paper entitled "*Formation Evaluation and Hydraulic Fracture Modeling of Unconventional*

Reservoirs: Sab'atayn Basin Case Study" published in the 53rd US Rock Mechanics/Geomechanics Symposium held in New York, NY, USA, 23–26 June 2019.

4. Chapter 4 is aimed at studying the capability of HVFRs by examining the produced water from the Bakken formation through an integral approach. The application of surfactant as an additive to the HVFRs was investigated in high TDS (total dissolved solids) conditions. This chapter presents the paper entitled "How Does HVFRs in High TDS Environment Enhance Reservoir Stimulation Volume?" published in the International Petroleum Technology Conference held in Dhahran, Saudi Arabia, 13 – 15 January 2020. https://doi.org/10.2523/IPTC-20138-Abstract
5. Chapter 5 shows the experimental work to evaluate the feasibility of CO2-EOR using the huff-n-puff (HNP) protocol. We assess the oil recovery from CO2-EOR under several scenarios of operational and well/reservoir conditions. The parameters considered in the sensitivity study include temperatures, pressure, soak time, number of injections, and wettability alteration. This chapter presents the paper entitled "*Understanding the Mechanisms of Huff-n-Puff, CO2-EOR in Liquid-Rich Shale Plays: Bakken Case Study*" published in the SPE Canada Unconventional Resources Conference held in Calgary, Alberta, Canada, 29 September – 2 October 2020. https://doi.org/10.2118/200001-MS
6. Chapter 7 aims to build a reservoir simulation model of the CO2 huff-n-puff process case study in the Mountrail County, Williston Basin, ND, to investigate the geomechanical coupling effects with molecular diffusion/adsorption mechanisms in both perspectives of production performance and storage. The stress state during injection, soak, and production may lead to changes in petrophysical properties, fluid/rock molecular interactions, and fluid transport, which are investigated by coupling the geomechanics and fluid flow through a two-way method. This integrated workflow can assist us to

understand the relation between geomechanics and CO2-EOR mechanisms in unconventional liquid-rich shale reservoirs. This chapter is taken from the paper entitled "*Coupling Geomechanics with Diffusion/Adsorption Mechanisms to enhance Bakken CO2-EOR Modeling*" published in the 53rd US Rock Mechanics/Geomechanics Symposium held in New York, NY, USA, 23–26 June 2019.

7. Chapter 9 summarizes the dissertation findings includes recommendations and future research that can be carried out.

CHAPTER 2

Unconventional Well Test Analysis

This chapter discusses the paper entitled "***Unconventional Well Test Analysis for Assessing Individual Fracture Stages through Post-Treatment Pressure Falloffs: Case Study***" published in Journal of Energies https://doi.org/10.3390/en14206747.

Abdulaziz Ellafi was responsible to prepare the methodology, analyze the data and validation while Hadi Jabbari provided the data was involved in the methodology development/analyses, and he is the PhD advisor and was the director of the project.

Abstract

Researchers and operators have recently become interested in the individual stage optimization of unconventional reservoir hydraulic fracture. These professionals aim to maximize well performance during an unconventional well's early stage and potential Enhanced Oil Recovery (EOR) lifespan. Although there have been advances in hydraulic fracturing technology that allow for the creation of large stimulated reservoir volumes (SRVs), it may not be optimal to use the same treatment design for all stages of a well or many wells in an area. We present a comprehensive review of the main approaches used to discuss applicability, pros and cons, and a detailed comparison between different methodologies. Our research outlines a combination of the Diagnostic Fracture Injection Test (DFIT) and falloff pressure analysis, which can help to design intelligent production and

improve well performance. Our field study presents an unconventional well to explain the objective optimization workflow. The analysis indicates that most of the fracturing fluid was leaked off through natural fracture surface area and resulted in the estimation of larger values compared to the hydraulic fracture calculated area. These phenomena might represent a secondary fracture set with a high fracture closure stress activated in neighbor stages that was not well developed in other sections. The falloff pressure analysis provides significant and vital information, assisting operators in fully understanding models for fracture network characterization.

2.1 Introduction

The advent of unconventional reservoir development is a turning point in the global oil and gas industry, since these resources contain massive hydrocarbon reserves larger than those found in conventional formations. Domestic oil production from liquid rich shale (LRS) reservoirs in North America has seen significant development, according to the US Energy Information and Administration (EIA), with production dramatically increasing in the 'top producing' American oil shale plays: the Bakken, Eagle Ford, and Permian Basin. This hydrocarbon production improvement has been driven by the application of modern horizontal drilling and multi-stage hydraulic fracturing (MSHF) techniques, which makes it possible to access low porosity (<10%) and low permeability (<0.1 mD) formations (He et al., 2016; Abbasi et al., 2014). The creation of large stimulated reservoir volumes (SRVs) has been achieved through breakthroughs in hydraulic fracturing technology; however, fracture treatment is not necessarily effective (Ellafi and Jabbari, 2020). Operators have started utilizing tighter spaced clusters, longer stage lengths, and greater proppant volumes to design hydraulic fracture stimulation (Jayaram et al., 2019; Parvizi et al., 2018). The

ultimate oil recovery reported by several studies is less than 8% due to a rapid decline in unconventional well performance, and by approximately 75% within the first two years of well production (Figure 2. 1).

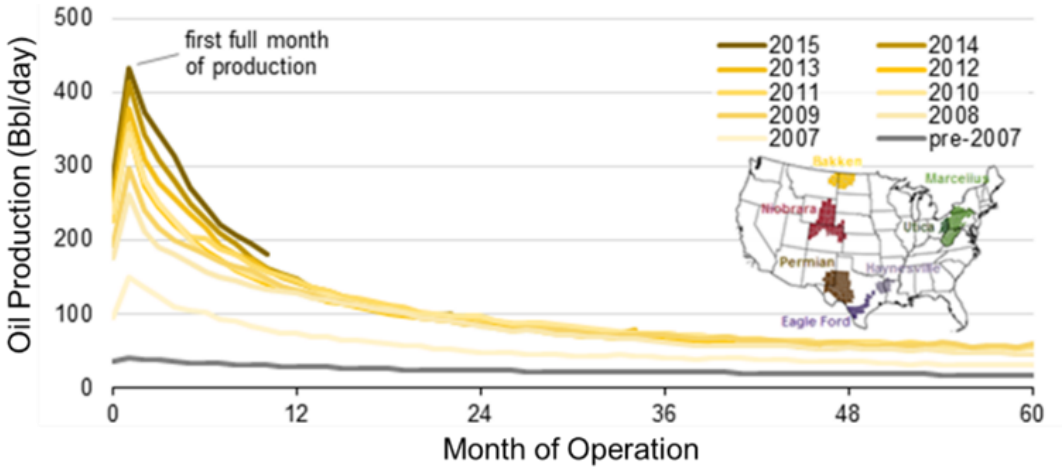

Figure 2. 1. Average oil production per well in the Bakken Formation, Williston Basin, North Dakota (EIA, 2019).

The decline is due to a low to no hydrocarbon recharge from the ultra-tight matrix blocks since the natural and induced fractures close, and there is a high flow resistance at the matrix–fracture interface; therefore, the increase in net stress leads to a zero-pressure gradient, which obstructs the fluid flow from the rock matrix into the fracture (Qin et al., 2021; Ellafi and Jabbari, 2020; Li et al., 2015). Proppant embedment plays a significant role in conductivity and decreasing fracture width since an inappropriate choice may cause proppant deformation, or proppant crush, under closure pressures. High-pressure drawdown may also cause formation rock compression, which leads to a reduction in matrix permeability with changes in reservoir pressure or stress (Ellafi and Jabbari, 2020; Nguyen et al., 2020; Jayaram et al., 2019). The productivity of unconventional wells heavily relies on the effective fracture

contact area or the propped fracture area per cluster, which is critical in evaluating hydraulic fracture treatment performance (Liu et al., 2020).

Performing a successful treatment design depends primarily on evaluating the stimulated formation before and during fracture treatment. Recommendations for the proper selection of slurry type and amount are provided to produce the optimal fracture geometry using a high efficiency assessment (Barree et al., 2014). Current literature suggests that the use of diagnostic tools is critical when assessing unconventional plays since they can reveal opportunities for future exploration, evaluation, delineation, and development (Alfarge et al., 2018); however, currently available traditional methods are not feasible for decision makers, even with the appropriate data. The majority of the previously published research is associated with high uncertainty and lacks a thorough discussion of fracture network characterizations. Only long-term production data were utilized in the past, the application of which caused ambiguity in understanding the hydraulic fracture performance (Economides et al., 2007; Cipolla and Wright, 2002). This ambiguity was caused by the difficulty in utilizing conventional exploration and production techniques to establish commercial production rates (Haskett and Brown, 2005; Ellafi and Jabbari, 2020).

Most of the previous post-treatment analysis studies of unconventional reservoirs do not provide quantitative discussions with detailed support case studies, and very few field studies have discussed the application of pressure falloff data (Liu et al., 2020). We present guidelines to better understand unconventional well test analysis through critical literature reviews and case studies of fracturing treatment analysis to address the lack of quantitative evaluation.

We have concluded that post-stimulation condition performance evaluation using indirect methods, such as pressure falloff data, is the most promising technology. This approach may provide a clear perspective about the created fracture's dimensions and properties; therefore, the effective fracture contact surface area for both natural and induced fractures can be determined from stage to stage during fracture treatment jobs. The application of pressure falloff data is a valuable tool that provides comprehensive information, such as the mechanics of the created open, closed, and propped hydraulic fractures, due to the tool's capability of reflecting the rock and fluid's physical behavior. This technology may overcome some limitations and weaknesses in most of the proposed techniques in the literature, such as production data analysis and micro-seismic methods.

2.2 Research Objectives

The main objective of diagnostic tool usage is to maximize well performance during both primary production and late stage EOR processes by understanding the contribution of individual fracture stages (Nguyen et al., 2020; Abbasi et al., 2014; Cipolla and Wright, 2002). Important pressure falloff data gathered after fracture treatments were generally ignored in the past, even though that detailed information could reveal attributes necessary for successful fracturing evaluation. There were also no precise measurement technologies for recording production rate and pressure during each stage to evaluate each cluster or stage's contribution. The pressure falloff data tool has garnered significant interest in the oil and gas industry since it is a powerful method for defining prime fracture parameters to gain insight into the effectiveness of the treatment jobs' fracture (Liu et al., 2020).

Evaluating fracture designs can be implemented on a stage-by-stage basis to optimize the overall performance of a well, unlike common performance evaluation methods such as Rate

Transient Analysis (RTA) and micro-seismic fracture imaging/mapping (MS). We will investigate the following key parameters to evaluate these designs:

1. The importance of closure stress, including closure behavior and geomechanics parameters, in fracture geometry and the impact of its variation from stage to stage.
2. The variability of geology and mineralogy and their impacts on fracture propagation and geometry.
3. The contribution of natural fractures in created well reservoir contact areas and their impact on fracture geometry.
4. The role of treatment designs on proppant distribution and characteristics, such as conductivity, crush, and embedment, which are related to closure stress and effective stress.
5. Investigate if an optimal fracture contact area would exist for a specified treatment design.
6. Identify optimal treatment design parameters for individual fracture stages, such as proppant volume and mesh size, fracturing fluid amount and type, and pump schedule.
7. Prepare protocols for evaluating the success of individual fracture stages from the viewpoint of production performance, such as post-treatment analysis.
8. Determine the contribution of individual fracture stages in the well's overall performance and determine the right spot for treatment execution.

9. Evaluate the lessons learned from fracturing in the previous stages. Develop a workflow for the real-time treatment design optimization for next-stage application to address good or bad frac-hits, unsuccessful designs, and fracturing in undesired formations.
10. Determine if the expected treatment design optimization by stage would justify the additional cost and treatment design adjustments through case studies.

We have compared common fracture diagnostic tools, discussed DFIT and pressure falloff data, and analyzed fracturing treatment case studies fracturing for unconventional wells. We have also presented the potential of combining DFIT and pressure falloff data in various pressure-time plots to identify fracture and reservoir behavior characteristics. Guidelines to better understand unconventional well test analysis that can lead to real-time optimization and adjustment of fracture job treatments have been provided as we proceed from one stage to another in an MSHF operation.

2.3 Principle of Fracture Diagnostic Tools

Monitoring the growth of fracture networks in the subsurface is the common process during stimulation treatments in unconventional wells. The created fractures are usually simulated by simple bi-wing and single planar fracture model definitions, such as Perkins-Kern-Nordgren (PKN) and Khristianovic-Geertsmade Klerk (KGD) fracture geometry models. These models assume that the hydraulic fractures will primarily stay within the pay zone and extend significantly (Daniels et al., 2007); however, in reality, the fracture networks can grow in an asymmetrical shape due to variable confinement across the geologic interfaces and orientation changes. Fracture growth around natural fractures can add more complexities to the fracture system due to the interaction between the induced and fissure networks (Evans

et al., 1992). An effective fracture network's formation mechanism in shale resources is still largely unknown. As a result of this knowledge gap and the network's complexity, it is difficult to predict, obtain, and verify fracture geometry, such as fracture length, height, and containment. These challenges can lead to suboptimal outcomes when incorrect assumptions are used through fracture diagnostic applications (Barree et al., 2014).

There are several fracture diagnostic applications. These applications allow petroleum engineers to assess the success of the fracture stages and create optimal development strategies for effective reservoir drainage. These tools can also optimize the entire field development regarding well spacing and location, optimal design, and optimum interval/height coverage. Numerous fracture diagnostics are discussed by researchers that provide subsets of knowledge about treatment design optimization (Fu and Liu, 2019; Guo et al., 2014; Cipolla and Wright, 2002): (a) direct far-field fracture diagnostic techniques, such as micro-seismic fracture mapping and tiltmeter, (b) direct near-wellbore fracture diagnostic techniques, such as production and temperature logging tools and radioactive tracers, and (c) indirect fracture-diagnostic techniques, such as transient pressure and rate transient analysis "PTA/RTA" and fracture modeling "net pressure analysis". We have focused on indirect fracture-diagnostic techniques in this review paper. Table 2. 1 provides a brief discussion and comparison reference for widely used diagnostic tools with their strengths and limitations explained.

The analysis of source rock and fluid behaviors is detected by the fracture diagnostic tools, highlighting the fracture and reservoir properties; therefore, the combination of diagnostic tools provides more confidence and allows fracture engineers to make decisions in real-time. DFIT, post-treatment pressure falloff, micro-seismic, flowback, and other data can be

collected and interpreted in real-time to assess the created contact surface areas and evaluate fracture design properties, such as fracture half-length, number of clusters, proppant loading, and fracture complexity and direction. The pump schedule can be adjusted from stage to stage by assessing the proppant placement and injection volumes to ensure the maximum pay zone proppant coverage. An optimal well stimulation strategy should be established to avoid some far-field issues, such as well interventions and frac-hits (Barree et al., 2014).

Applying the DFIT methodology and using post-treatment pressure falloff data as a fracture diagnostic tool may assist us in monitoring the pressure interference and offset well intervention based on the survey comparison mentioned in Table 2. 1. This technology will provide valuable information needed to improve individual fracture stage treatment design and enhance the production of the propped fracture surface area in real-time.

Table 2. 1. Comparison of different diagnostic methods for fracture treatment performance analysis.

a) Production Data Analysis as a Diagnostic Method:			
Pros	**Cons**	**Results**	**Authors**
• The data are readily available at low costs, and their analysis is straightforward. • This application is critical for using historical production data for various purposes: a) Characterize reservoir and well stimulation properties, b) Predict production performance for development plans and reserve estimations. • Production data analysis is useful for checking the consistency of the data and identifying the flow regimes over time. • There are a couple of ways to apply production data techniques:	• High-frequency measurements are required to obtain a reasonable analysis. • The results suffering from some degree of uncertainty; therefore, more information is required, such as geology, phase behavior, and completion practices. This information needed is more complex compared to other approaches. • Traditional production data analysis assumes that all clusters are similar, which appears to be an oversimplification of the problem. • All production data analysis methods are non-uniqueness associated with well and	• Fracture permeability. • Conductivity. • Storage coefficient. • Fracture half-length. • SRVs. • Hydrocarbon in place. • Reservoir permeability. • Thickness product. • Skin. • Performance forecast.	Ehlig-Economides et al., 2006 Ilk et al., 2011 Abbasi et al., 2014 Kurtoglu et al., 2015 Ezulike et al., 2016 Xu et al., 2016

a) Type curve analysis, b) Straight line (flow regime) analysis, c) Analytical and numerical simulation, d) Empirical methods to quantify the hydraulic fracture performance at different unconventional well life stages. • Production analysis is a tool to study linear flow regimes when assessing the productivity and effectiveness of completion designs. The impact of fracture hit, and offset stages can also be evaluated.	reservoir properties; therefore, the different methods must be validated and cross-checked. • The production data approaches for conventional rate transient methods need further modifications to analyze the MSHW data. • Production data analysis does not offer any procedures for quick and measured adjustments of completion designs and production operations.		

b) Microseismic Fracture Imaging/Mapping			
Pros	**Cons**	**Results**	**Authors**
• Microseismic imaging provides the best resolution and lowest uncertainties when characterizing fracture geometries in most cases. • Microseismic mapping can be coupled with real-time simulations to accurately predict fracture growth in the target zone. This combination can be utilized to assess the effectiveness of flushing an unexpected screenouts, imaging proppant placement, synthetic Microseismic event prediction, and fracture geometry control. • Microseismic imagery is also helpful during postmortem well performance analysis to: a) Calibrate numerical simulations, b) Optimize stimulation design, c) Investigate frac-hit phenomena, d) Test new fracturing procedures,	• This technology is not widely used due to its high cost. • This application is associated with a few uncertainties due to source mechanisms: a) Receiver-coupling resonances, such as improper sensor couplings with rock properties, including velocity-model limitations, formation anisotropy, noise, and mislocation. b) The interference of fluid leakoff and stress effects in some formations, such as shale plays. • Fracture geometries obtained from Microseismic monitoring may not be accurate enough in certain situations; therefore, the geometries must be validated and cross-checked with other diagnostic tools. • The extent of fractures parallel to the lateral might be difficult to interpret from	• Fracture direction. • Fracture dimension: a) Fracture half-length, b) Fracture height. • Fracture complexity. • SRVs.	Maxwell et al., 2002 Fisher et al., 2004 Daniels et al., 2007 Maxwell and Cipolla, 2011 Warpinski et al., 2013 Xu et al., 2016 Jayaram et al., 2019

e) Assess well drainage patterns, f) Optimize economics, such as NPV and ROR.	microseismicity alone, such as in the case of microseismicity vs. dimensions. • Microseismic imaging cannot provide accurate information on individual fractures and cracks, or whether they are open, closed, or propped/unpropped. • It is not clear why Microseismic may not detect the tensile failure at the advancing tip of a hydraulic fracture.		

c) Transient Pressure Analysis "DFIT and Post-Treatment Falloff Pressure"			
Pros	**Cons**	**Results**	**Authors**
• It is a simple approach that only requires shut-in pressure versus time. • The data are recorded right after fracture treatments with no additional cost. • It is a unique method to assess the state of created fractures, whether they are open, closed, or propped. • It does not require long periods of shut-in data, as required in conventional buildup tests. • A half-hour period for pressure recordings after the main fracturing treatment would be enough to reliably obtain falloff pressure analysis and diagnostic plots to determine: a) Total contact of natural fracture surface area, b) Total contact of induced fractures surface area. • This technique can be used at any time during the life of the well and can also be integrated with intelligent production studies.	• The application of fracture falloff pressure analysis is still in its infancy, and its theory is based on the assumptions of DFIT: a) The whole surface of created fractures/cracks would contribute to the fluid flow. Further research is necessary to improve the current effective well/fractures contact area workflow estimation fracture. We recommend the inclusion of proppant-impact-factors (PIFs) in the estimation of the effective contact areas to improve the DFIT assumptions. • It may not be used independently as an accurate diagnostic tool to assess fracture network growth. It is recommended that this tool be integrated with other methods, such as: a) Microseismic, where the fracture height is required for area estimation, given by MS,	• Fracture permeability. • Conductivity. • Storage coefficient. • Fracture dimension: a) Fracture half-length, b) Fracture width. • Fracture surface areas: a) Natural fracture surface area, b) Main Hydraulic fracture surface area. • Assessment of treatment design parameters: a) Fluid efficiency, b) Leakoff coefficients, c) Net pressure, d) Closure pressure, e) Friction losses,	Ehlig-Economides et al., 2006 Economides et al., 2007 Liu and Ehlig-Economides, 2019 Wang, and Sharma., 2019 Liu et al., 2020 Wang et al., 2021

• This technique may facilitate the real-time evaluation of the created contact areas between the well and reservoir at each fracture stage, representing the success of a fracturing treatment job. • The method provides the flow regimes and fracture/reservoir behaviors before and after closure. • Evaluating individual fracture stages through this technique can assist in stage-by-stage treatment job optimization and further design improvements.	b) Production logging data, c) Fiber-optic information, d) Rate transient analysis. • This technique has not yet been used for real-time fracturing treatment optimizations. • A low-pressure gauge resolution can cause inaccurate diagnostic plots and unreliable results. We recommend a measurement of the shut-in pressure period at a time interval of one second using high-resolution pressure gauges, which can assist in solving data quality issues and minimize the effects of water hammers.	f) ISIP, g) Type of leak-off behavior, Fracture complexity. • Reservoir properties: a) Permeability, b) Reservoir pressure.

2.4 Diagnostic Fracture Injection Test (DFIT)

A DFIT has been widely used in the oil and gas industry over the last 20 years. This approach is based on the pressure transient data procured immediately after fracture treatments to obtain a reliable assessment of fracture and reservoir properties. A DFIT is a standard well testing technique for ultra-low-permeability formations, where a traditional pressure transient test, such as a buildup test, is impractical. A DFIT analysis does not require a long shut-in time to reach the radial flow regime.

The pressure falloff data are analyzed in DFIT to estimate the in-situ stress, fluid efficiency, leak-off coefficient, reservoir properties, and net pressure, which are the critical factors used to design and implement a successful main fracture treatment. A DFIT provides the representative properties of an undamaged formation since the test creates a large area of investigation that can extend beyond the damaged near-wellbore zone. The results from a DFIT can be used in several ways: (a) characterizing in-situ stresses and fracture compliance

(Wang and Sharma, 2019), (b) modeling hydraulic fracture propagation (Gonzalez et al., 2015), (c) designing fracture treatment jobs (Wright et al., 1996), (d) modeling reservoir simulation (Jabbari and Zeng, 2012), and (e) post-fracture treatment analysis (Kurtoglu et al., 2015). This application can also be utilized in geologic carbon sequestration, nuclear waste repositories, and geothermal energy exploitation (Ilk et al., 2011; Witherspoon, 2004; Evans et al., 1992).

A DFIT implementation and interpretation should be studied in detail before any field execution or analysis. We have presented lessons learned and recommendations that may help operators design the optimum fracture jobs.

2.4.1 DFIT Design and Tactics

A typical DFIT operation pumps a small volume of the treatment fluid, such as water, without proppant at a constant rate for a short period of approximately 3–5 minutes. The injection pressure increases above the reservoir fracturing pressure, or breakdown pressure, creating a short artificial fracture in the target layer. The leak-off behavior is small during the injection period, and no filter cake forms on the fracture wall. The pressure falloff data is a recorded function during shut-in time immediately after the treatment. The injected fluid begins to leak-off into the formation until the fracture wall comes into contact, or closure. The pressure falloff period recorded in the case studies we analyzed was extended for days or even weeks to observe the radial flow regime, depending on the reservoir characteristics.

Figure 2.2 displays a typical pressure profile of a DFIT in the absence of natural fractures and weak planes. Two distinct periods of before and after closure (BC and AC) were analyzed to characterize the properties of the created fractures and reservoirs. These two periods were

separated by the fracture closure event, which is the primary outcome and supplies us with the fracture closure pressure, or minimum in-situ stress. The fracture and reservoir properties were obtained by analyzing the typical flow regimes observed during the BC, before closure for fracture-dominated, and AC, after closure for reservoir-dominated, respectively (Figure 2. 3).

The conditions of modeling in unconventional reservoirs are more complex than in conventional formations. Significant conflict exists on how to model the fracture closure behavior since most of the models assume that the fracture surface is perfectly smooth; however, fractures exist everywhere in the subsurface in the form of small-scale cracks and fissures, and large-scale joints and faults. The mechanical resistance and fluid transport properties found in unconventional formations are complicated and controlled by several factors, such as in-situ stress, compliance, or stiffness (Equation 2. 1), rock mineralogy, fracture-surface roughness, treatment fluid pressure inside the fractures, and leak-off rate (Wang and Sharma, 2019; Hawkes et al., 2018; Barree et al., 2014). A proper DFIT model must account for the effects of pressure-dependent leak-off and dynamic fracture compliance to precisely capture the fracture pressure response and obtain a realistic estimation of the fracture closure pressure and fluid leak-off behavior (Wang and Sharma, 2019; Liu and Ehlig-Economides, 2018). These parameters are crucial factors necessary for calculating the fracture surface contact areas to obtain proper hydraulic fracture modeling and accurate post-treatment assessment.

Investigating compelling field evidence using a downhole measurement that indicates what exactly occurs in the subsurface is paramount. Figure 2. 4 illustrates the tiltmeter measurements of well #2B from the Gas Research Institute/Department of Energy M-site,

which is defined as an indication of fracture displacement or fracture width (Warpinski et al., 1997).

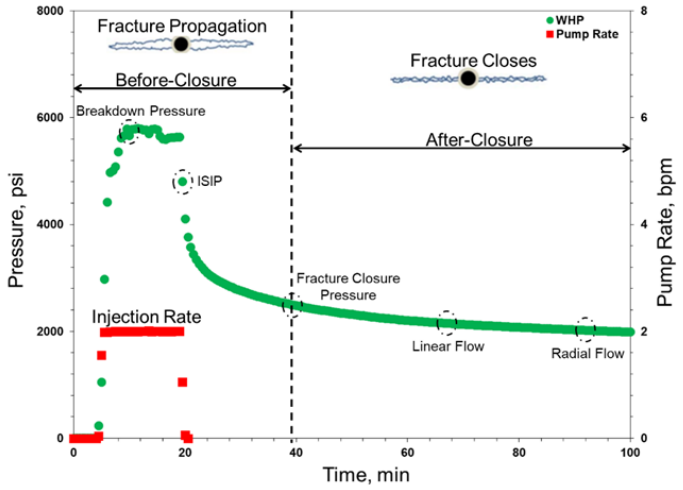

Figure 2. 2. Typical pressure behavior includes a sequence of main events observed in a DFIT. ISIP is instantaneous shut-in pressure.

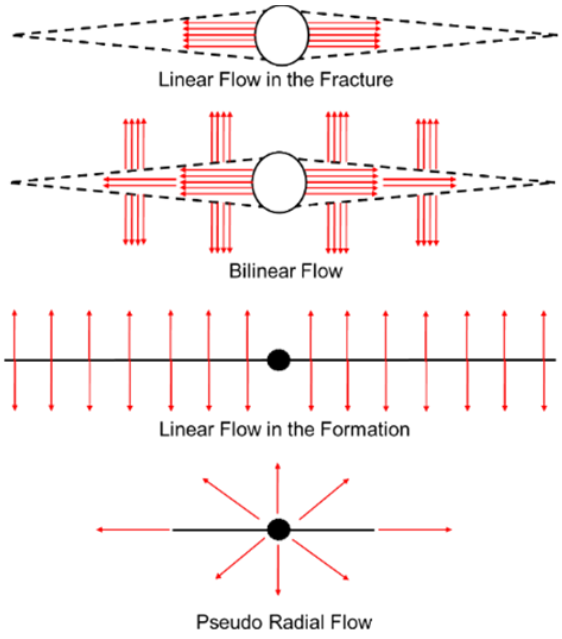

Figure 2. 3. Typical flow regimes before and after closure behaviors.

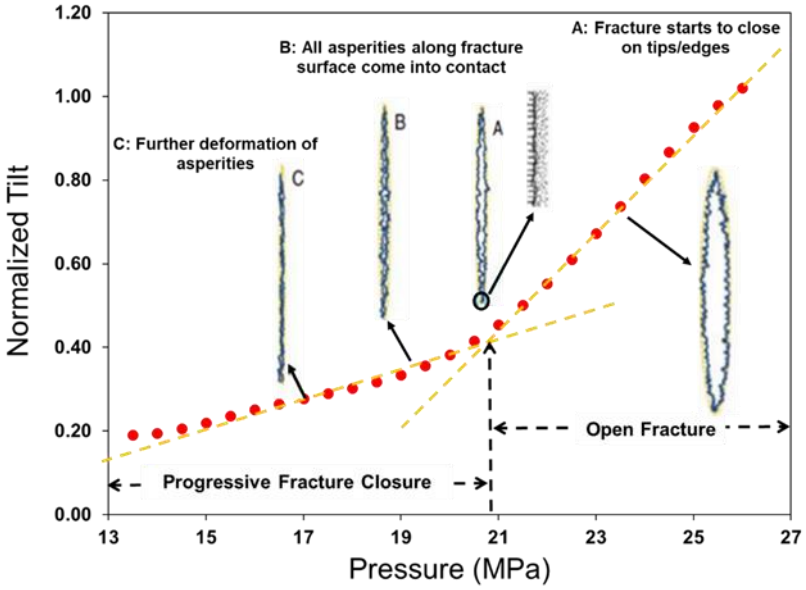

Figure 2. 4. Observation of fracture closure behavior.

Wang and Sharma (2019) used recorded data to explain the relationship between normalized tilt and formation pressure (Figure 2. 4). The data for this downhole field measurement were recorded and gathered immediately after the end of the several week-long test. The Y-axis presents the normalized tilt calculated by dividing each tiltmeter measurement by the maximum fracture displacement. The data were plotted vs. the wellbore pressure to generate the diagnostic plot (Figure 2. 4), demonstrating a direct measurement of the rock deformation during the fracture closure behavior. The results indicate that the pressure falloff data response on a normalized tilt vs. formation pressure plot (Figure 2. 4) is proportional to the fracture compliance, or inversely proportional to fracture stiffness, and the fracture closure behavior is a function of average displacement and fracture volume.

The fracture volume is proportional to the average fracture width as the pressure continues to decrease, and two distinct periods are indicated on the diagnostic plot: (1) The trend of the pressure falloff data is a linear decline until the point of measured pressure inside the fracture,

or closure pressure, is greater than 21 MPa (3046 psi). At this point, the fractures are still open, the stiffness factor is constant, and the surface area remains constant until the fracture wall comes into contact, or closure. The fracture geometry can then be estimated directly using Table 2. 2. (2) The pressure falloff data begin to deviate from a straight line at the inflection point on the plot, where the closure pressure is marked with a dashed green line; therefore, the fracture stiffness increases gradually, as a result of the fracture closure on the asperities of the fracture edges or tips.

Table 2. 2. Fracture geometry models.

Fracture Model	**PKN**	**KGD**	**Radial**	**Equation #**
Area exponent (α)	4/5	2/3	8/9	-
Fracture compliance (c_f)	$\frac{\pi\beta_s h_f}{2E'}$	$\frac{\pi\beta_s x_f}{E'}$	$\frac{16\beta_s R_f}{3\pi E'}$	(2. 1)
g_0	1.41	1.48	1.38	-
β_s	4/5	0.9	3 π^2/32	-

This information coincides with downhole measurements but is not a parameter in the available DFIT models; therefore, this application assists us with measuring the appropriate closure pressures and provides more information on the mechanics of the created hydraulic fractures, such as if they are open or closed. This information may assist us in developing DFIT assumptions by adding proppant-impact-factors (PIFs), which can be used in the post-treatment pressure falloff data analysis to estimate an effective contact fracture surface area, such as the propped fracture area per cluster.

2.4.2 Fundamentals of DFIT

The leak-off behavior term was introduced in Nolte's work (1979, 1986), where he pioneered DFIT as a reliable test method before executing main fracture jobs. A poroelastic closure

model was used to describe the pressure falloff behavior when fracturing fluid leak-off entered the fractures and formations. Equations (2. 2) – (2. 10) are used for analyzing a DFIT to capture normal leak-off behavior. This analysis is based on the following assumptions, which are assumed in several models: (1) power-law fracture growth, (2) negligible spurt loss, (3) constant fracture surface area immediately after the end of the test if there is constant leak-off area and constant fracture compliance or stiffness, and (4) Carter's leak-off model, which defines one-dimensional fluid leak-off across a constant pressure boundary. The leak-off behavior is not pressure-dependent, and the solution to the diffusivity equation predicts that the leak-off rate will scale with the inverse of the square root of time.

These assumptions may be realistic due to the characterization of the fracturing fluids and unconventional formations; therefore, Nolte's technique may not work for unconventional formations and may yield overestimated results in parameters such as fluid efficiency, leak-off coefficient, and storage coefficient. This technique is a reliable application under some circumstances and is derived based on the G-function approach (Equation (2. 2)). The pressure and G-function time are analyzed on log-log graphs to obtain the fracture closure point and other parameters, such as fluid efficiency and leak-off coefficient.

$$p_{ws} - p_w(\Delta t_D) = \frac{\pi r_p C_L \sqrt{t_p}}{2c_f} G(\Delta t_D) \tag{2. 2}$$

$$p_1^* = \frac{\pi r_p C_L \sqrt{t_p}\left(A_{mf} + A_{nf}\right)}{2c_{mf} A_{mf}} \tag{2. 3}$$

$$c_{mf} A_{mf}\left(ISIP - p_{c,mf}\right) = V_p - 2r_p C_L \sqrt{t_p}\left(A_{mf} + A_{nf}\right) g_o \tag{2. 4}$$

where, p_{ws} is the pressure at the end of pumping, p_w is the pressure recorded at the surface during the falloff period, and Δt_D is the dimensionless time defined by:

$$\Delta t_D = \frac{t - t_p}{t_p} \quad (2.5)$$

τ is the superposition time defined by:

$$\tau = \frac{\Delta t + t_p}{\Delta t} \quad (2.6)$$

With pumping time t_p, falloff period t, productive fracture ratio $r_p = h/h_f$, fracture height h_f, propped height h, leak-off coefficient C_L, and fracture compliance c_f, p_1^*: dp_w/dG at the closure point.

The pressure derivative equation is defined by:

$$\tau \frac{d\Delta p_w}{d\tau} = (\Delta t_D + \Delta t_D^2) \frac{d\Delta p_w}{d\Delta t_D} \tau \frac{d\Delta p_w}{d\tau} = (\Delta t_D + \Delta t_D^2) \frac{d\Delta p_w}{d\Delta t_D} \quad (2.7)$$

$$G(\Delta t_D) = \frac{4}{\pi}[g(\Delta t_D) - g_0] \quad (2.8)$$

where the g-function of time is approximated by:

$$g(\Delta t_D) = (1 + \Delta t_D)\, sin^{-1}(1 + \Delta t_D)^{-1/2}\ \alpha = 1/2, \text{ low fluid efficiency.} \quad (2.9)$$

$$g(\Delta t_D) = (4/3)\left((1 + \Delta t_D)^{3/2} - \Delta t_D{}^{3/2}\right)\alpha = 1, \text{ high fluid efficiency.} \quad (2.10)$$

$g(\Delta t_D)$ is the loss-volume function, approximated analytically by Nolte (1979, 1986) with the bounding values of the area exponent, α, and g_0 is $g(\alpha, \Delta t_D = 0)$, see Table 2.

Castillo (1987) later introduced a new G-function plot to address the assumption of pressure-dependent behavior by linearizing the relationship between the pressure falloff and time during the closure behavior. The relation is the time, such as the G-function time and the square root of time, on the X-axis vs. falloff pressure and the pressure derivative on the Y-axis. This approach reduces the uncertainty of estimating fracture fluid efficiency and the leak-off coefficient, while overestimated outcomes have resulted from Nolte's method. The

diagnostic plot estimates accurate pressure parameters, such as instantaneous shut-in pressure "ISIP," closure pressure "Pc," and Nolte match pressure "p_1^*".

Barree and Mukherjee (1996) presented several types of abnormal leak-off behaviors: (a) natural fracture opening or pressure-dependent leak-off, (b) fracture tip extension or recession, (c) height recession, (d) pressure-dependent fracture compliance, and (e) transient flow in the fracture. The authors developed Nolte's work (1979, 1986) for various closure behavior types and removed the ambiguity associated with understanding the complex fracture networks. The diagnostic plots allow us to predict an accurate estimation of the in-situ stress, fluid efficiency, leak-off coefficient, and pressure parameters. The G-function plot in the proposed models is the relationship between the following terms: falloff pressure, pw, first pressure derivative, dpw/dG, and second pressure derivative, Gdpw/dG, on the Y-axis vs. the G-function time on the X-axis. The closure event is the point where the curve deviates from the straight line. Equations (2. 11) through (2. 13) are used to determine the primary outcomes, as listed in Table 2. 3. This method enables us to identify the proper leak-off behavior for accurately estimating the hydraulic fracture geometries.

Table 2. 3. Primary outcomes from a DFIT based on stipulated fracture geometry.

Results	**Fracture models**			**Equation**
	PKN	**KGD**	**Radial**	
Fluid efficiency, η	$\eta = \frac{G_c}{G_c + 4g_0/\pi}$	$\eta = \frac{G_c}{G_c + 4g_0/\pi}$	$\eta = \frac{G_c}{G_c + 4g_0/\pi}$	(2. 11)
Fracture dimensions, x_f or R_f	$x_f = \frac{(1-\eta)V_p E'}{2\beta_s g_0 p*}\left[\frac{1}{2h_f{}^2}\right]$	$x_f{}^2 = \frac{(1-\eta)V_p E'}{2\beta_s g_0 p*}\left[\frac{1}{4h_f}\right]$	$R_f{}^3 = \frac{(1-\eta)V_p E'}{2\beta_s g_0 p*}\left[\frac{3\pi}{32}\right]$	(2. 12)
Leak-off coefficient, C_L	$C_L = \frac{\beta_s p*}{r_p\sqrt{t_p}E'}[h_f]$	$C_L = \frac{\beta_s p*}{r_p\sqrt{t_p}E'}[2x_f]$	$C_L = \frac{\beta_s p*}{r_p\sqrt{t_p}E'}\left[\frac{32R_f}{3\pi^2}\right]$	(2. 13)

Where, Gc, closure time, E', Young's modulus, Vp, total pumping volume, and βs, the ratio of the average net pressure inside fractures to the maximum net pressure at the wellbore during the shut-in time (Table 2. 2).

A DFIT uses the basis of conventional mini-fracture treatments that focus on acquiring treatment design parameters, such as fluid efficiency and leak-off behavior; however, this application is subtly different for unconventional formation analysis. This approach is used to acquire significantly more information on the created fractures and formation properties, such as pore pressure, closure pressure, and fracture gradients (Wang and Sharma, 2019; Liu and Ehlig-Economides, 2018; Barree et al., 2014), process zone stresses (Li et al., 2015), transmissibility values (Soliman et al., 2010), leak-off mechanisms (Li et al., 2015), natural fracture properties (Li et al., 2015), fracture stiffness and un-propped fracture conductivity as a function of closure stress (Wang and Sharma, 2019), and stimulation complexity and net pressure (Potocki et al., 2012).

We can evaluate the properties of the main hydraulic fractures and natural fractures in a fracture treatment job by adopting the DFIT analysis method with no proppant. This method may not be ideal due to its tendency to ignore the impact of the proppant; however, it can be used with caution to evaluate post-treatment production and unconventional well performance.

2.4.3 DFIT Models: Before-Closure Analysis

Several analytical or semi-analytical models have been proposed for before-closure analysis (BC) (Liu and Ehlig-Economides, 2015; Craig and Blasingame, 2006; Mayerhofer and Economides, 1993; Nolte., 1986; Hagoort, 1981; Nolte., 1979), where all BC models were based on two

fundamental concepts underlying the proposed methodology: (1) a material balance equation before fracture closure, and (2) the diffusive flow in the formation after closure. These models were founded based on two main conditions: (1) the total injection volume is equal to the sum of the fracture volume and cumulative leak-off volume, and (2) the fracture volume is estimated from the linear elasticity theory and a 2D fracture geometry during the pressure falloff period.

Cramer and Nguyen (2013) reported that it would be rare to observe a normal leak-off behavior in the field, and closure behavior is commonly related to the abnormal leak-off concepts (Figure 2. 5); therefore, the BC analysis must correctly address abnormal leak-off behaviors and near-wellbore friction losses. Liu and Ehlig-Economides (2019) presented a model that was not limited to normal leak-off behavior compared to previous BC models (Wang and Sharma, 2019; Craig and Blasingame, 2006; Mayerhofer and Economides, 1993; Hagoort, 1981). These BC models relied on the assumptions of ideal leak-off behavior: (1) constant injection rate, (2) constant fracture surface area after shut-in, (3) creation of one main hydraulic fracture cluster without the effects of natural fractures, (4) constant fracture compliance during the operation, (5) assumption of similar fracture closure stresses for all stages, and (6) assumption that all injected fluid at the surface flows into the created fracture, meaning that the impact of the wellbore storage (WBS) is insignificant. Most current studies do not provide a quantitative discussion and do not address factors such as formation geology and mineralogy, resistance-dependent fluid distribution, and geomechanics parameters.

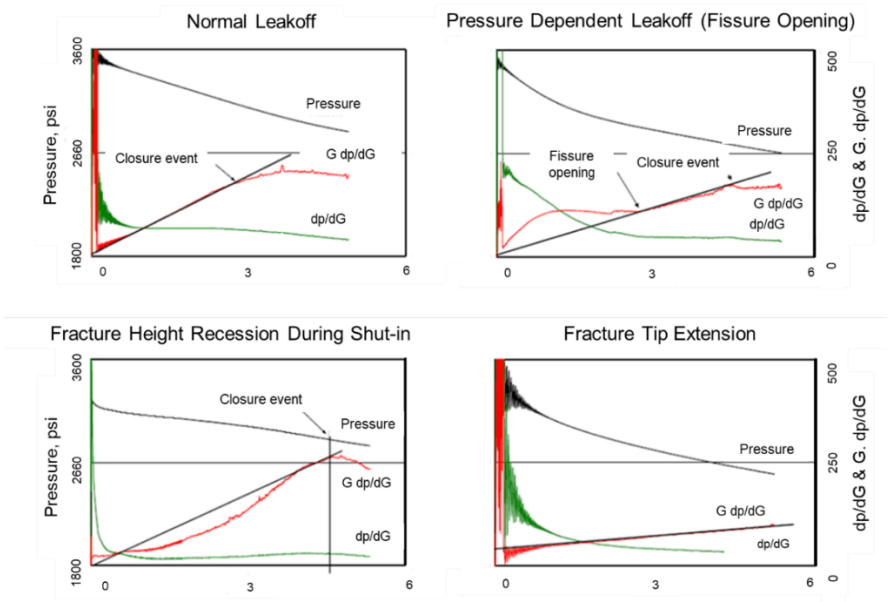

Figure 2. 5. G-function characteristics for different leak-off mechanisms (Craig and Blasingame, 2006).

Table 2. 4. Main results and methodologies of DFIT analysis.

Period	Results	Methods
Before closure	Total injection volume	• Record time and rate.
Before closure	Fracture volume	• Pressure falloff analysis by assuming linear elasticity and 2D fracture geometry (PKN and KGD models).
Before closure	Leak-off volume	• Cater leak-off model. • Diffusive linear flow from the fracture into the matrix.
After closure	Reservoir parameter	• Conventional PTA.

Table 2. 4 summarizes DFIT analysis methods and the details of the fracture/reservoir property estimations from each period in a DFIT BC and AC. Table 2. 5 lists the different leak-off models commonly used to analyze a DFIT, while Table 2. 6 presents the outcomes from each model for several case studies. We have added our conclusions by summarizing the pros and cons of recently published models on abnormal leak-off behaviors (Table 2. 7).

Table 2. 5. Definition of two main leak-off behaviors.

Type of Leak-off Behavior	Definition
Normal leak-off behavior	• Two scenarios can be considered for normal leak-off behavior: a) All injected fluids leak-off through the fracture network. The fracturing fluid is accumulated and stored in the induced fractures, b) All injected fluids leak-off across the contact surface area of the hydraulic fracture and are then recovered during flowback. • The survey in this paper indicates that the assumptions mentioned above may not be appropriate for DFIT analysis in most field cases.
Abnormal leak-off behavior	• In abnormal leak-off models, part of the injected fluids may leak-off into active secondary fractures. • This behavior can be detected on the diagnostic plots from the following signature: a) Higher stress on the diagnostic plot, compared to that of the main HF, may indicate the closure behavior of the secondary fracture network. The main hydraulic fracture propagates to the minimum principal stress.

We suggest developing the concept of DFIT to address this lack of a quantitative evaluation, allowing us to evaluate the post-treatment pressure falloff analysis in real-time fracture treatment job optimization. The accurate estimations of closure pressure, ISIP, and perforation and tortuosity friction losses can be obtained to prevent some far-field issues, such as well interventions, frac-hits, high apparent net pressure, and stress shadow. An effective evaluation of a stimulated formation before and during fracture treatment can identify optimal treatment design parameters for individual fracture stages.

Table 2. 6. DFIT's outcomes from several field studies.

Type of Leak-Off Behavior	Duration	Results
Normal leak-off behavior	BC	• Leak-off coefficient. • Fluid efficiency. • Fracture dimensions, such as fracture width and fracture half-length.
	AC	• Permeability and skin. • Reservoir pressure.
Abnormal leak-off behavior	BC	• Friction losses in the wellbore. • Perforation and near-wellbore tortuosity. • Net pressure during and after shut-in. • ISIP. • Type of leak-off behavior and leak-off coefficient. • Extension of secondary fractures. • Tip extension distance after shut-in. • Fracture surface area for natural fractures. • Fracture geometry, such as fracture width and fracture half-length.
	AC	• Permeability and skin. • Reservoir pressure.

Table 2. 7. Recently published DFIT models under the conditions of abnormal leak-off behaviors.

Model	Pros	Cons
Craig and Blasingame, 2006	• This type-curve method enables the analysis of the whole pressure falloff data, BC, and AC, unlike previous methods (Nolte, 1979; Hagoort, 1981; Nolte, 1986) developed for only a specified portion of pressure falloff data, BC or AC.	• The model does not account for fluid loss into natural fractures, such as diagnostic plots modeled based on normal leakoff behavior assumptions. The outcomes, such as the leakoff coefficient, fluid efficiency, and fracture surface area, are associated with high uncertainty.
McClure et al., 2014	• This study investigated the effect of changing fracture compliance on pressure transience for unconventional formations, previously neglected during the closure behavior by previous research; therefore, the model provides	• The standard models, such as PKN and KGD, simulate the created fractures; however, the actual fracture geometry is more complex due to the interaction between induced and fissure networks. Newtonian injection fluids and a fracture

	accurate estimates of closure pressure analysis.	with uniform leakoff along the fracture face were assumed to form fracture geometry equations.
Liu and Ehlig-Economides, 2015, 2018, and 2019	• This model involves the impact of secondary fractures on fluids leakoff, where multiple closure events are observed on the G-function and Bourdet pressure derivative plots. • This approach reduces the need for a rate step-down test since this model allows us to perform a DFIT analysis to determine friction losses from near-wellbore tortuosity. • This model can be used for the main fracture treatment design since it accounts for fluid leakoff into the natural and induced fractures.	• The fluid efficiency estimated from the normal leakoff behavior is smaller than that of Nolte's model. The model indicates inconsistency with other approaches. • This work assumes that leakoff behaviors, such as closure behavior in secondary and created fractures, are governed by one constant leakoff coefficient for all apparent closure events. • The surface fracture area calculations are associated with uncertainty due to ignoring the impact of the proppant. We recommend the inclusion of PIFs to estimate the effective contact areas to improve the DFIT assumptions.
Wang and Sharma, 2017, 2018, and 2019	• This model accounts for fracture stiffness/compliance changes as the fracture closes; leakoff rate is a function of fracture pressure. • This new concept promotes an understanding of pressure falloff and coupled behaviors during a DFIT with detailed support case studies.	• This model assumes the closed fracture still retains fracture conductivity. • Fluid leakoff remains constant through the fracture surface area before and after closure behavior.

2.4.4 Recommendations When Conducting and Interpreting DFIT

Table 2. 8 provides suggestions and recommendations that interpreters and operators should follow before any field execution or analysis to correctly perform a DFIT and achieve the research goals.

Table 2. 8. Important points that extended in planning, executing, and achieving the successful DFIT.

Authors	**Suggestions and Recommendations**	
	Field Execution	**Data Analysis**
Marongiu-Porcu et al., 2014	• The authors suggest injecting fracturing fluids at a low pumping rate for a short period to create a short fracture.	• Reduce the time to reach fracture closure and AC pseudo linear and pseudo-radial flow.
Barree et al., 2015	• The pumping rate for a DFIT should be set at a rate close to the planned rate, at least 75%, of the fracture treatment job.	• A successful DFIT design provides reliable closure identification and

	• The same fracturing fluids should be used for both DFIT and fracture treatment operations. • The range of the injection period should be between 3 to 5 minutes for a DFIT. The test should end by performing a rapid step-down test.	representative fracture and reservoir properties. • A major assumption may not always be true.
Hawkes et al., 2018	• The final execution relies on several factors, such as the design of the wellhead manifold, pressure gauge types and sampling time, stated objectives, time schedules, wellbore conditioning, pump rate, and pump volume. • There are three surface located pressure gauges that should adhere to the specifications of 0.02% full-scale accuracy and 0.01 psi resolution. • The test should be performed at the toe stage to fill the well with fracturing fluid. This process will activate pressure and bleeds back by circulating the treatment fluid until trapped gas bubbles are removed. • Testing should be performed on the well casing, packers, tubing, and wellhead at high pressure. • A diesel fluid should be injected on top of the wellbore water to avoid surface line and wellhead freezing.	• Fracture engineers should not use an over tuning or smoothing method to analyze pressure falloff data since this approach yields no identifiable flow regimes. • Distinguishing between actual flow regime behavior and false look-alikes is critical. • Reservoir engineers should link the fundamentals of fracture mechanisms with a physical response. • The analysis of DFIT depends on the pressure accuracy; therefore, pressure sources can mitigate erroneous or uninterpretable DFIT pressure responses.

2.4.5 Lessons Learned from DFIT Operations

Table 2. 9 provides lessons learned using a comparison study from DFIT field cases that have been reported in peer-reviewed journal articles. The objective is to explain the impact of operation conditions on DFIT interoperation and analysis of the outcomes.

Table 2. 9. Field case studies of DFIT operations and lessons learned.

Authors	Field/Country	Description	Results
Rohmer et al., 2015	Vaca Muerta Shale/Argentina	• Two similar DFITs were performed in the same formation: a) The first DFIT was performed with a	• Diagnostic plots of both DFITs presented abnormal leakoff behaviors, but the difference in the closure signature was unexpected.

			small volume (20.8 bbl) and a low rate (≤5.5 bpm). b) The second DFIT was designed with a large volume (155 bbl) and a high rate (≤14 bpm).	a) The diagnostic plots confirmed the transverse storage/height recession behavior for the first DFIT and the pressure-dependent leakoff (PDL) behavior for the second DFIT, b) The final closure events were chosen using a holistic methodology, and the outcomes exhibited consistent values from both DFITs.
Rizwan., 2017	NIMR/Oman		• Two successive informative field DFITs were reported, where they were performed in the same zone in a tight gas formation. a) A small volume (24.8 Bbl) at a low rate (0.94–1.38 bpm) was injected in the first DFIT, b) The second DFIT was designed to pump a larger volume (158 Bbl) at a higher pumping rate in the range of 12.6 to 18.7 bpm.	• The results demonstrated a different fracture closure behavior. a) The diagnostic plot of the first DFIT presented wellbore storage (WBS) followed by limited tip extension that defines a simple BC trend close to the behavior of normal leakoff, b) The second DFIT illustrated a complicated BC behavior of variable fracture compliance under different categories that could be pressure-dependent leakoff (PDL), apparent height recession, or transverse storage, c) The BC analysis was not consistent with the closure pressures quantified in both DFITs.
Nicholson et al., 2017	Eastern Alberta Shallow/Canada		• The authors conducted the interpretation of two successive DFITs in a shallow gas-shale formation with a thrust fault setting. a) The first injection had a relatively large volume, at 33.2 Bbl, and a high rate at 6.3 bpm compared to the second injection, with an ultra-small volume of 0.82 bbl.	• The results demonstrated a different fracture closure behavior. a) The diagnostic plots of the first DFIT presented the behavior of transverse storage/height recession closure behavior, while the second DFIT illustrated a normal leakoff behavior, b) The final closure chosen from those two DFITs was consistent but with different closure behavior types. The created fractures did not reopen due to a very small injection volume in the second DFIT.

2.4.6 How DFIT Analysis Is Applicable for Pressure Falloff Data of Main Fracture Treatments

Both DFIT and fracture treatment operations in unconventional horizontal wells have some similarities, especially in the created fractures and behavior of the pressure falloff data immediately after the treatment; however, several dissimilarities in the primary assumptions and operation conditions exist between the two techniques that must be addressed, examined, and basic formulae must be modified to obtain a representative analysis for pressure falloff behavior on a stage-by-stage basis in real-time. Very few studies (Liu et al., 2020) have analyzed pressure falloff data applications on a stage-by-stage basis in a horizontal wellbore. We have addressed the main differences between the two tests:

1. A DFIT is performed by pumping a small volume (24.8 Bbl) at a low rate (0.94–1.38 bpm), while the injection volume of the main fracture treatment in each stage is higher; therefore, the formation pore pressure may not be accounted for. We account for the formation pore pressure during the DFIT analysis.

2. A DFIT only operates with water that does not include proppant, but the role of proppant exists in the main fracture treatment jobs. We recommend the inclusion of PIFs to improve the DFIT assumptions. We can apply the DFIT methodology to the main fracture treatment pressure falloff data to estimate an effective contact fracture surface area.

3. A DFIT operation creates only one fracture, while hydraulic fracture treatments generate multiple perforation clusters in each stage. The fracture geometry is different from stage to stage on a well due to several factors, such as stress shadow effects, formation heterogeneity, formation lithology, and resistance-dependent fluid distribution.

4. The falloff period immediately after DFIT is relatively long, up to a week compared to a short period of half an hour in the hydraulic fracture treatment, which is enough to perform the analysis.

2.5 Effective Fracture Surface Area Calculations

This section presents the workflow to analyze post-treatment pressure falloff data in order to estimate effective fracture surface areas for both natural fractures and hydraulic fractures on a stage-by-stage basis. Figure 2. 6 illustrates our methodology, and Table 2. 10 lists the main Equations (2. 14) through (2. 19) that are used to determine the primary outcomes.

Table 2. 10. Hydraulic fracture geometry calculations.

Fracture Half Length	Fracture Models	Equation
$x_f = \frac{V_p E'}{\pi \beta_s \left[ISIP - p_{c,mf} + 4p_1^* g_o/\pi\right]} \left(\frac{1}{h_f^2}\right)$	PKN	(2. 14)
$x_f = \sqrt{\frac{V_p E'}{\pi \beta_s \left[ISIP - p_{c,mf} + 4p_1^* g_o/\pi\right]} \left(\frac{1}{2h_f}\right)}$	KGD	(2. 15)
$R_f = \sqrt[3]{\frac{V_p E'}{\pi \beta_s \left[ISIP - p_{c,mf} + 4p_1^* g_o/\pi\right]} \left(\frac{3\pi}{16}\right)}$	Radial	(2. 16)
Effective Fracture Surface Area	**Fracture Models**	**Equation**
$A_{mf} = 4x_f h_f$	PKN/KGD	(2. 17)
$A_{mf} = \pi R_f^2$	Radial	(2. 18)
$A_{nf} = A_{mf}\left[\frac{2c_{mf}P_1^*}{\pi r_p C_L \sqrt{t_p}} - 1\right]$	PKN/KGD/Radial	(2. 19)

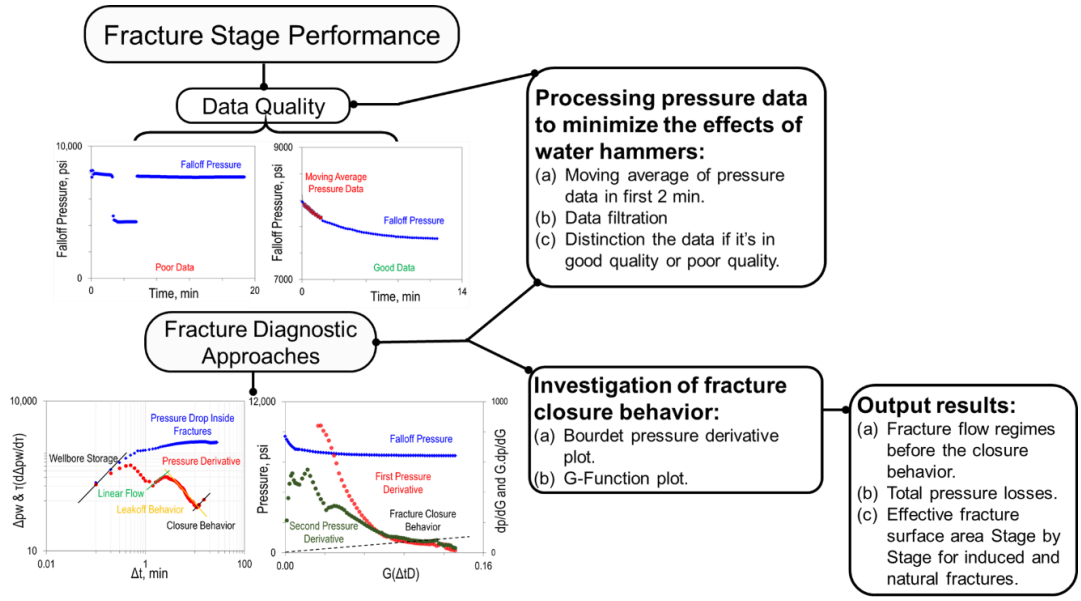

Figure 2. 6. Workflow of research methodology to determine fracture stage performance.

The same concept was used to analyze the pressure falloff data by Liu et al. (2020), who determined the total fracture surface area for both natural fractures and hydraulic fractures on a stage-by-stage basis. In this paper, we modified the workflow, which enables us to calculate fracture half-length and identify the main fracture flow regimes after the treatment of the Meramec Formation, STACK Play of the Anadarko Basin, Oklahoma.

2.6 Unconventional Well Case Study

2.6.1 Case Study Description

The DFIT was performed at the toe stage of an unconventional horizontal well (Well #2) in the Meramec Formation, STACK Play of the Anadarko Basin, Oklahoma. The STACK Play is a multi-layered tight oil reservoir "Meramec and Woodford Formations" with porosity lying in the range of 3% to 10%, and permeability in the range of 0.0001 to 0.01 mD. The plug and perf stimulation technique was used to complete the well. The wellbore was prepared before testing by filling it with fracturing fluids, typically water, to pressurize the top of the wellbore up to the point of completion so the formation did not break down if there

were no pre-existing fractures. The fracturing fluid was pumped into the formation through the first casing interval with an inner diameter (ID) of 4.67 inches, a total vertical depth (TVD) of 9648 ft, and a measured depth (MD) of 19,635 ft. The pressure rises linearly with the injection volume during the injection period, while the injection rate remains constant (Figure 2. 7). Figure 2. 7 presents the injection and pressure profiles for our DFIT case study, where the surface injection rate was maintained at 12 bpm for approximately 40 minutes. The first shut-in period was measured for the same injection period, then the injection test was performed again with a higher injection rate of approximately 13 bpm. The test was then completed, and the pressure falloff data were recorded during the next 4–5 days.

The main fracture treatment job was performed in the same well (Well #2) based on the evaluation report from the DFIT analysis. Figure 2. 8 presents the main hydraulic fracturing operation, where the job consists of several pump schedule stages, as shown in the figure by green and blue colors, and the slurry rates and proppant concentrations were changed during the operation. The total job period is around 160 min at an average 100 bpm slurry rate. At the end of the job, the falloff pressure was recorded for a period of time of approximately 15 min on average for all fracture stages. The fracture treatment strategy was applied with a constant pump schedule to create 36 frac stages, where each stage consisted of four to five clusters with 50 ft spacing.

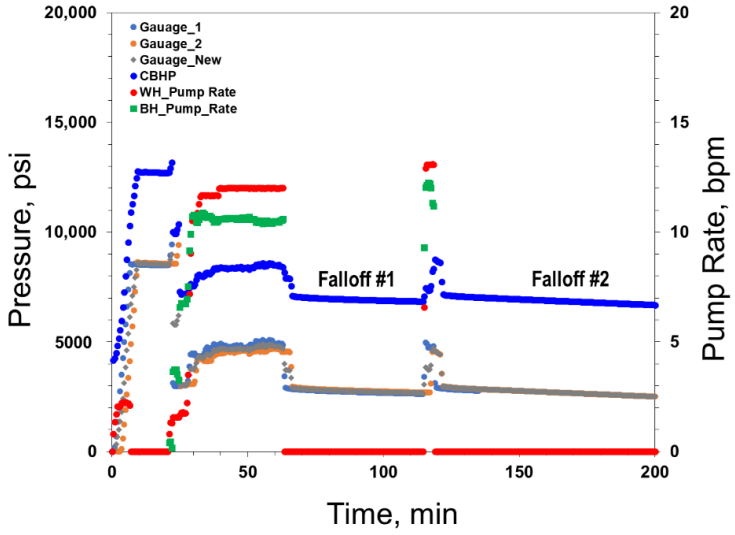

Figure 2. 7. DFIT operations for the Well #L2, presenting injection and pressure profiles.

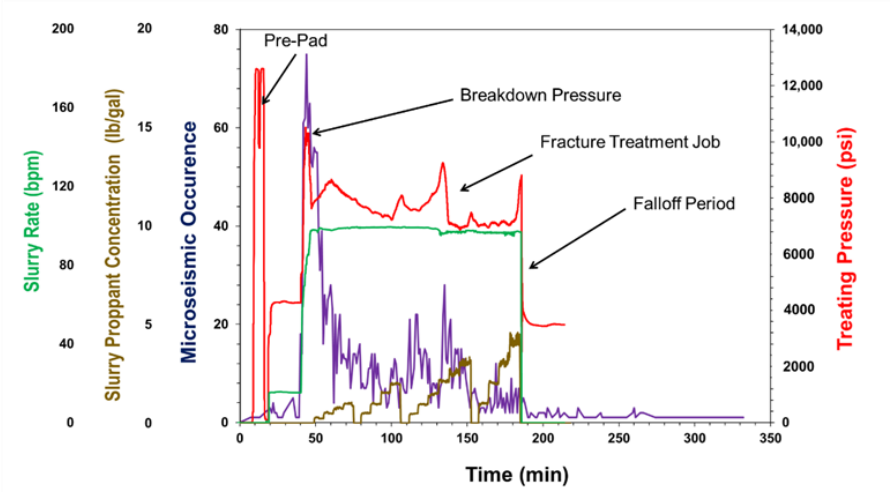

Figure 2. 8. Main hydraulic fracturing operations for the Well #L2, presenting injection, pressure, proppant concentration profiles, and micro-seismic events.

This section presents a case study of the unconventional horizontal well, where Table 2. 11 shows the main fracture treatment operation parameters as well as preprocessing data quality for each fracture stage. The combination of DFIT and pressure falloff data immediately after the treatment was used to identify fracture and reservoir behavior characteristics to assess the evaluation of the fracture stages.

Table 2. 11. Main hydraulic fracturing and well parameters and preprocessing post-treatment pressure data quality.

Stage	Cluster Count	Pumping Time	Falloff Period	P_{ws}	ISIP	TVD	Data Quality
(#)	(#)	(min)	(min)	(Psi)	(Psi)	(ft)	(-)
1	1	128	14	8112	7214	9676	Poor
2	5	171	15	7959	7629	9678	Poor
3	5	169	18	8465	7769	9682	Poor
10	5	168	17	8726	8117	9722	Poor
11	5	172	16	8179	7924	9732	Good
12	5	162	18	10,002	8047	9734	Good
13	5	166	30	9144	8055	9742	Good
14	5	166	17	9033	8146	9745	Poor
15	5	168	16	9147	8118	9755	Good
16	5	176	16	9399	8121	9766	Good
17	5	166	9	8954	8010	9766	Good
27	5	159	16	9405	8859	9818	Good
28	5	166	15	9685	8868	9821	Good
29	5	160	17	9146	8740	9830	Good
30	5	158	17	9530	8676	9834	Good
31	5	159	17	9697	8554	9829	Good
32	5	159	19	8943	8575	9836	Good
35	5	156	13	9322	8002	9903	Good
36	5	153	18	9907	8559	9923	Good
Max		176	20	10,186	9399	9923	
Min		128	9	7985	7214	9676	
Avg		162	17	9092	8210	9779	

2.6.2 Results of Case Study Including DFIT and Main Fracture Treatment Analysis

Figures 2. 9 and 2. 10 illustrate the analysis of the DFIT test using two diagnostic plots: (1) a Bourdet pressure derivative plot (Bourdet et al., 1989) (Figure 2. 9), and (2) the plot of the G-function diagnostic analysis (Figure 2. 10). Both plots indicate consistent results and the same leak-off signature, which is the height recession leak-off. The mechanisms of this closure fracture behavior are defined as most of the fracturing fluid's leak-offs into neighboring layers, a common behavior for unconventional formations. The plots also indicate that natural fractures have contributed to the multiple fracture closure events observed before the closure analysis.

Different trends, such as circle 1, appear to be wellbore storage coupled with friction dissipation. The following flat trend, circle 2, appears to be tip extension with limited growth distance, as shown in Figure 2. 11. Linear flow with ½ signature, circle 3, is indicated on the plot before the closure behavior, marked by the green dashed line. Two closure events overlay on a 3/2 slope, circle 4, that depicts the closure behavior of the natural and induced fractures. The reservoir dominated flow observed after the closure analysis with two flow regimes started by linear flow, a ½ slope, circle 5, was followed by radial flow, and a zero slope, circle 6, where formation permeability can be estimated.

The main results from DFIT analysis are listed in Table 2. 12, where the formation is classified with low permeability in the range of 0.004 md and closure pressure in 6100 psi. The same concept was used to analyze the pressure falloff data by Liu et al. (2020), who determined the total fracture surface area for both natural fractures and hydraulic fractures on a stage-by-stage basis. However, we modified the workflow to improve the data quality, minimizing the effects of water hammers for the first 2 min in falloff pressure data and

including the analysis of the G-function plot in order to validate fracture flow regimes, as well as considering variable parameters for each stage. This methodology has not been applied before in the literature, and it is more precise with low uncertainty compared to previous research, where constant values were used for all stages to estimate total fracture surface areas. Our case study shows three different behaviors after the main fracture treatment as follows:

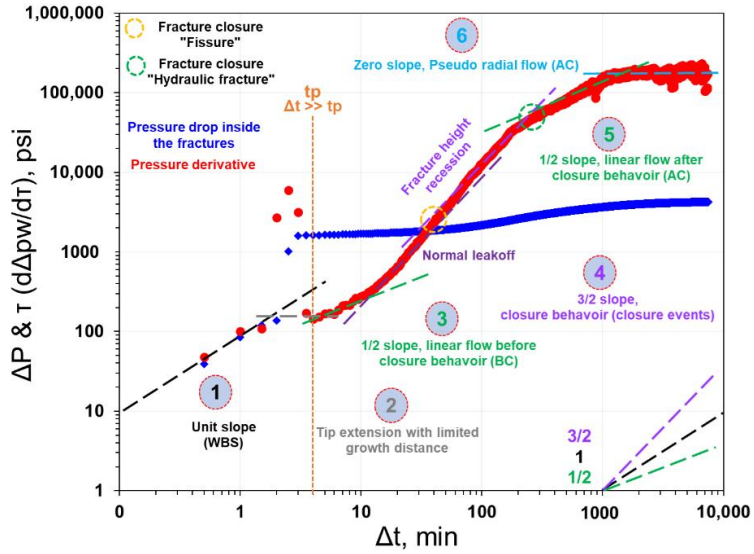

Figure 2. 9. DFIT analysis, Bourdet pressure derivative plot for the Well #2.

1. Case #1, ¼ slope, tip extension of the main fracture: Figure 2. 12 presents the behavior of tip extension of the main hydraulic fracture, where the results showed that the fracture surface area for the main fracture is higher than the total fracture surface area for the natural fracture. The reason is that low total pressure losses and more fracturing fluids leak-off through main fractures instead of nearby neighbor layers.

2. Case #2, –1/2 and –1 slope, fracture height recession: Figure 2. 13 shows the behavior of fracture height recession, where the results confirmed the DFIT signature for the

Meramec formation. The reason is that more fracturing fluids are leaking off through nearby neighbor layers instead of creating a longer fracture half-length.

3. Case #3, 0 slope, open fissures. Figure 2. 14 illustrates the behavior of open fissures, where the treatment created a high natural fracture surface area compared to the main hydraulic fracturing area as a result of communications with neighbor stages. The reason is that the treatment generated higher total pressure losses compared to two previous cases with shorter fracture half-length since all fracturing fluids leaked off through natural fracture. Additionally, this behavior indicates frac-hit phenomena due to interaction and communication between child and parent wells.

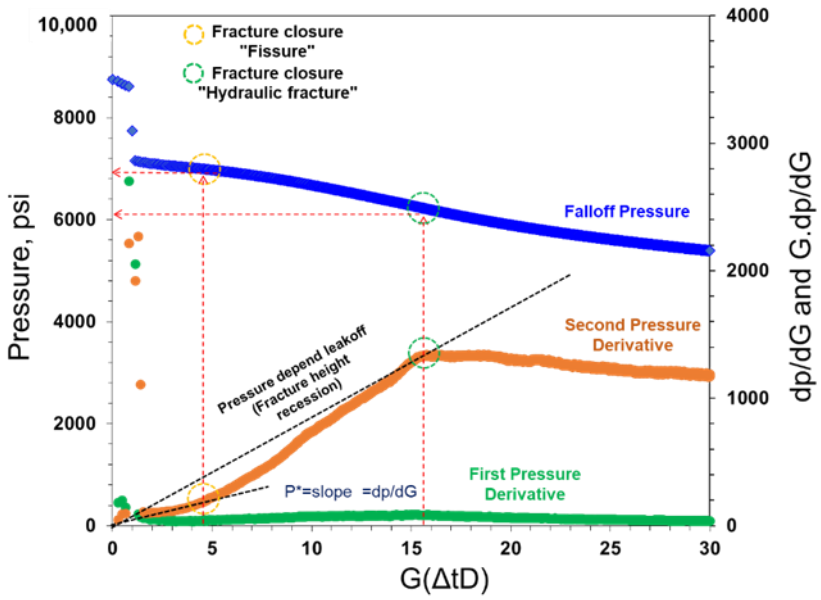

Figure 2. 10. DFIT analysis, G-function plot for the Well #L2.

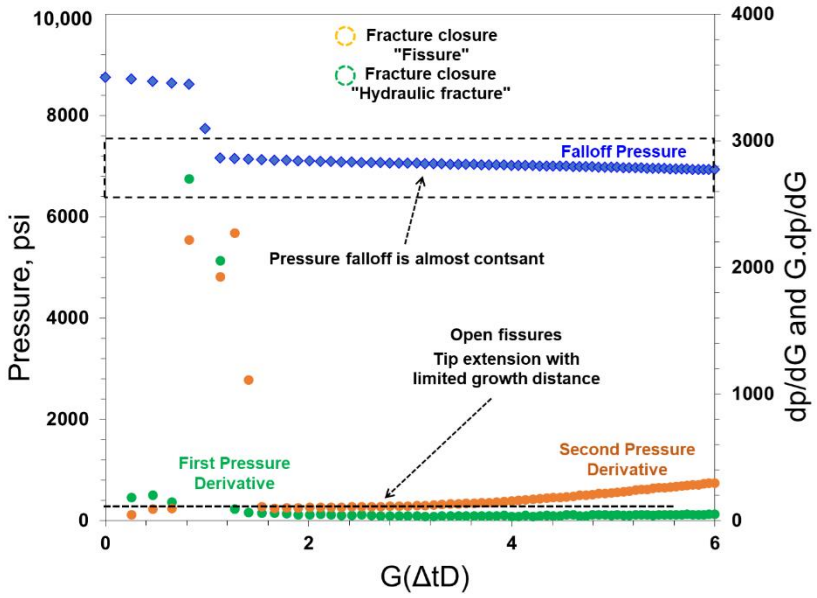

Figure 2. 11. DFIT analysis, observation of open fissures' behavior through G-function plot for the Well #L2.

Table 2. 12. Summary of the main DFIT outcomes of the Meramec Formation, Well #L2.

Flow Regime Behaviors	Slopes	Pressure, psi	Time, min	Permeability, md
WBS	1			
Tip extension	0			
Linear flow	½			
Fracture closure (Fissures)	1.5	6944	31.5	
Fracture closure (HF)	1.5	6125	210	
Linear flow	½			
Radial flow	0			
Pi =		4521		
k =				0.0038
P*1 =		48		
P*2 =		79		
ISIP =		7535		

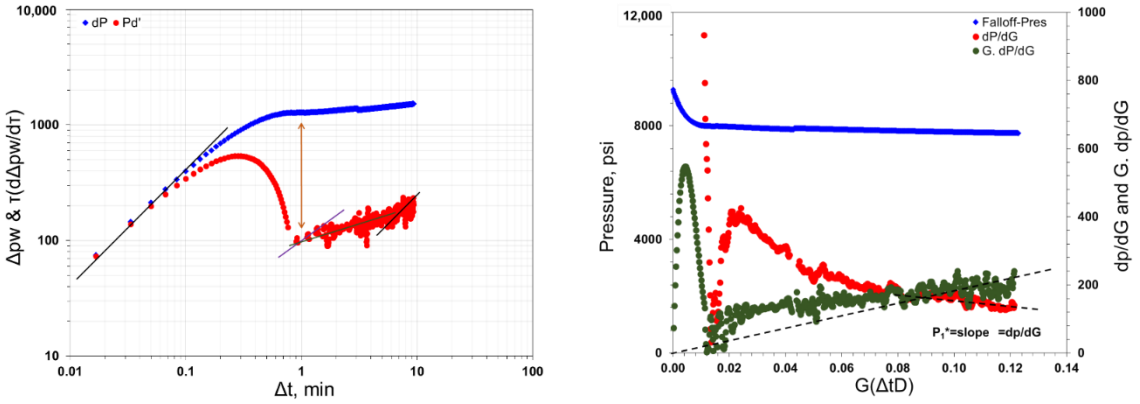

(a) (b)

Figure 2. 12. (a) Case #1, Bourdet pressure derivative plot for the main hydraulic fracture treatment of Well #L2. (b) Case #1, G-function plot for the main hydraulic fracture treatment of Well #L2.

For more detailed results, Table 2. 13 provides the analysis outcomes, including friction pressure losses and total fracture surface area.

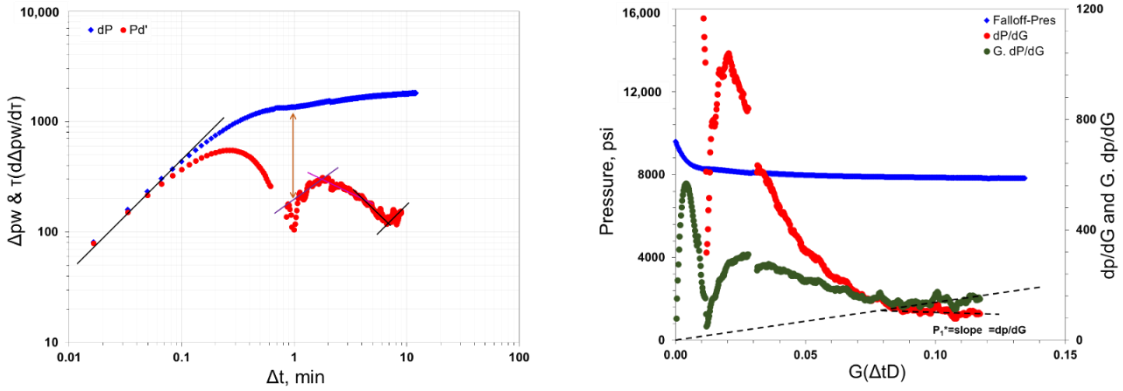

(a) **(b)**

Figure 2. 13. (a) Case #2, Bourdet pressure derivative plot for the main hydraulic fracture treatment of Well #L2. (b) Case #2, G-function plot for the main hydraulic fracture treatment of Well #L2.

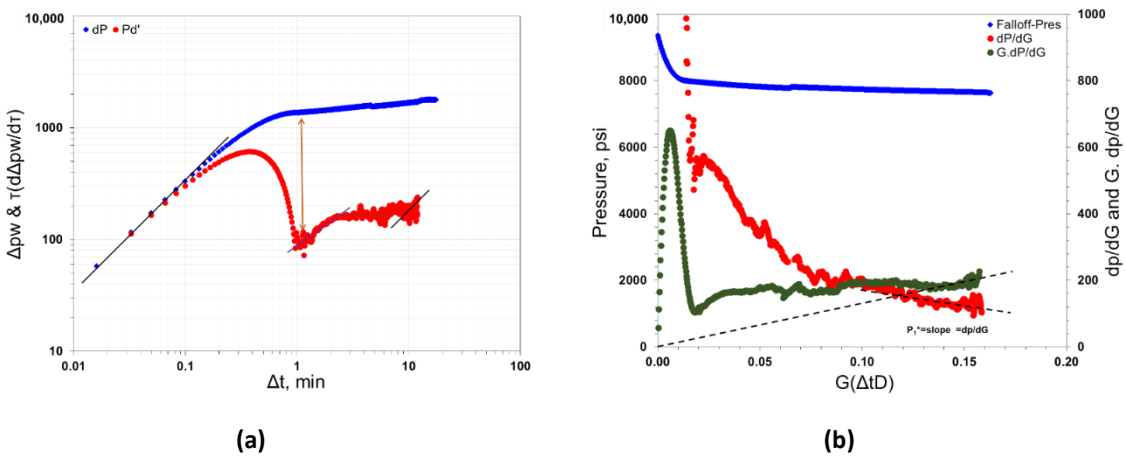

Figure 2. 14. (a) Case #3, Bourdet pressure derivative plot for the main hydraulic fracture treatment of Well #L2. (b) Case #3, G-function plot for the main hydraulic fracture treatment of Well #L2.

Table 2. 13. Outcomes from the pressure falloff analysis of the main hydraulic fracture treatment for the Well #L2.

Stage	$\Delta p_{wb\&per}$	Δp_{tort}	$\Delta p_{total\ fric}$	$P_{c,nf}$	$P_{c,mf}$	ISIP	p_1^*	A_{mf}	A_{nf}
(#)	(Psi)	(Psi)	(Psi)	(Psi)	(Psi)	(Psi)	(Psi)	(ft^2)	(ft^2)
11	944	340	1283	7778	7530	7891	1789	225,162	392,586
13	948	318	1266	8002	7780	8091	1704	231,059	380,939
15	598	244	842	7964	7676	8051	1247	230,521	325,202
32	451	261	712	8226	8044	8575	568	274,479	33,713
35	704	287	991	8207	7786	8321	1574	74,499	161,706
36	1022	419	1441	8620	8012	8818	1400	115,360	214,029

2.7 Past, Present, and Future Research Directions

Very few studies (Liu et al., 2020) have investigated the pressure falloff behavior combined with DFIT analysis to evaluate the effectiveness of fracture treatment conditions stage-by-stage; however, the assessment of fracture design quality stage-by-stage must still be studied,

especially after treatment. The principle of DFIT needs to be adjusted by counting PIFs to estimate the effective fracture contact area, or the propped fracture area per unit length of lateral, which is one key factor for evaluating post-treatment performance. An integral approach using several diagnostics tools is necessary to develop the technology for determining the contribution of individual fracturing treatments when multiple factors are considered. This approach can be accomplished using a series of neural network models to predict fracture geometry, fracture directions, number of clusters needed, proppant loading, fracture complexity, and treatment costs during fracture treatment. A data-driven model must be created to apply an integral approach in real-time, a challenge that must be addressed with thorough discussion, especially given the lack of literature on this subject. These combination methods involve machine learning tools that can assist us in understanding fracture treatment effectiveness, assess new completion technologies, and evaluate which formations are the most productive. This technology is feasible for real-time analysis to apply an optimum pump schedule for the current and next treatment stages on a well.

2.8 Summary

In this study, we employed an integral approach to identify fracture and reservoir behavior characteristics to assess the performance of hydraulic fractures stage-by-stage. The research findings highlight the following:

- Diagnostic tools have become attractive to the oil and gas industry since they are powerful methods for identifying fracture and reservoir characteristics. The analysis of these approaches is based on data type, which guides the assessment of complex fracture networks generated by hydraulic fracture treatment operations.

- The use of falloff pressure data is a simple approach since it does not require more information than shut-in pressure vs. time. The data are recorded immediately after shut-in at no additional cost; however, micro-seismic monitoring is expensive, and the production data analysis has high uncertainty.

- The models proposed by Liu and Ehlig-Economides (2018) allowed us to perform DFIT analysis to determine flow friction losses in the wellbore, perforation, and near-wellbore tortuosity separately without the need for rate step-down tests. These models are the primary means by which we can calculate the total fracture surface area for the secondary fractures and hydraulic fractures and gain insight into the effectiveness of the hydraulic fracturing process.

- Barree et al. (2014) and Liu and Ehlig-Economides (2018) reported that their data supported a holistic methodology that allows them to pick the hydraulic fracture closure, which contradicts the variable fracture compliance approach from McClure et al. (2014).

- Rizwan (2017) created an alternative methodology to apply a DFIT, where a change in the test operation strategy may cause a change in fracture closure behavior. This study provided insight into expected fracture closure behavior during the main fracture treatment.

- We concluded that evaluating the performance of post-stimulation conditions on a stage-by-stage basis using indirect methods, such as pressure falloff data analysis, is the most promising technique for providing a wide range of information covering the mechanics of the hydraulic fracture, such as open, closed, and propped. This method may overcome

limitations and weaknesses found in many of the proposed techniques reported in peer-reviewed journal articles, such as production data analysis and micro-seismic methods.

- This technology is a critical factor in the economic development of unconventional reservoirs since the well completion cost is a significant portion of the capital cost compared to other expenses, and heavily influences production rate or ultimate recovery.

- We suggest combining static and dynamic diagnostic methods to better estimate fracture geometry through pressure data, diagnostic fracture injection tests (DFIT), micro-seismic fracture mapping, distributed temperature sensing (DTS), production logs, and production data. The full suite of information can provide valuable evidence concerning the details of the treatment and well performance from complicated shale plays.

- Three different cases were observed through diagnostic plots, where mainly the analysis indicates that most of the fracturing fluid was leaked off through the natural fracture surface area and resulted in the estimation of larger values compared to the hydraulic fracture calculated area. These phenomena might represent a secondary fracture set with a high fracture closure stress activated in neighbor stages that was not well-developed in other sections.

- This conclusion fits with our discussion that provided detailed information with support case studies to apply the technology of post-treatment pressure analysis in real-time.

References

Abbasi, M.A.; Ezulike, D.O.; Dehghanpour, H.; Hawkes, R.V. A comparative study of flowback rate and pressure transient behavior in multi-fractured horizontal wells completed in tight gas and oil reservoirs. J. Nat. Gas Sci. Eng. 2014, 17, 82–93, https://doi.org/10.1016/j.jngse.2013.12.007.

He, J.; Lin, C.; Li, X.; Wan, X. Experimental investigation of crack extension patterns in hydraulic fracturing with shale, sandstone, and granite cores. Energies 2016, 9, 1018, https://doi.org/10.3390/en9121018.

Ellafi, A.; Jabbari, H. Understanding the mechanisms of huff-n-puff, CO2-EOR in liquid-rich shale plays: Bakken case study. In Proceedings of the SPE Canada Unconventional Resources Conference, Calgary, AL, Canada, 18–19 March 2020, https://doi.org/10.2118/200001-ms.

Jayaram, V.; Hull, R.; Wagner, J.; Zhang, S. Hydraulic fracturing stimulation monitoring with distributed fiber optic sensing and microseismic in the Permian Wolfcamp shale play. In Proceedings of the SPE/AAPG/SEG Unconventional Resources Technology Conference 2019, Denver, CO, USA, 22–24 July 2019; https://doi.org/10.15530/urtec-2019-291.

Parvizi, H.; Gomari, S.R.; Nabhani, F.; Monfared, A.D. Modeling the risk of commercial failure for hydraulic fracturing projects due to reservoir heterogeneity. Energies 2018, 11, 218, https://doi.org/10.3390/en11010218.

Li, K.; Gao, Y.; Lyu, Y.; Wang, M. New mathematical models for calculating proppant embedment and fracture conductivity. SPE J. 2015, 20, 496–507, https://doi.org/10.2118/155954-pa.

Qin, Q.; Xue, Q.; Ma, Z.; Zheng, Y.; Zhai, H. Hydraulic fracturing simulations with real-time evolution of physical parameters. Energies 2021, 14, 1678, https://doi.org/10.3390/en14061678.

Nguyen, T.; Pande, S.; Bui, D.; Al-Safran, E.; Nguyen, H. Pressure dependent permeability: Unconventional approach on well performance. J. Pet. Sci. Eng. 2020, 193, 107358, https://doi.org/10.1016/j.petrol.2020.107358.

Liu, G.; Zhou, T.; Li, F.; Li, Y.; Ehlig-Economides, C.A. Fracture surface area estimation from hydraulic-fracture treatment pressure falloff data. SPE Drill. Complet. 2020, 35, 438–451, https://doi.org/10.2118/199895-pa.

EIA. Annual Energy Outlook 2019 with Projections to 2050; US Department of Energy: Washington, DC, USA, 2019. Available online: https://www.eia.gov/ out-looks/aeo (20 November 2019).

Barree, R.D.; Miskimins, J.L.; Gilbert, J.V. diagnostic fracture injection tests: common mistakes, misfires, and misdiagnoses. SPE Prod. Oper. 2014, 30, 84–98, https://doi.org/10.2118/169539-pa.

Alfarge, D.; Wei, M.; Bai, B. Evaluating the performance of hydraulic-fractures in unconventional reservoirs using production data: Comprehensive review. J. Nat. Gas Sci. Eng. 2018, 61, 133–141, https://doi.org/10.1016/j.jngse.2018.11.002.

Cipolla, C.L.; Wright, C. Diagnostic techniques to understand hydraulic fracturing: What? Why? and How? SPE Prod. Facil. 2002, 17, 23–35, https://doi.org/10.2118/75359-pa.

Economides, M.J.; Ehlig-Economides, C.A.; Tosic, S. Application of pressure-transient and production-data analysis for hydraulic-fracture-treatment evaluation. In Proceedings of the

SPE Hydraulic Fracturing Technology Conference 2007, College Station, TX, USA, 29–31 January 2007.

Haskett, W.J.; Brown, P.J. Evaluation of unconventional resource plays. In Proceedings of the SPE Annual Technical Conference and Exhibition 2005, Dallas, TX, USA, 9–12 October 2005.

Daniels, J.L.; Waters, G.A.; Le Calvez, J.H.; Bentley, D.; Lassek, J.T. Contacting more of the Barnett shale through an integration of real-time microseismic monitoring, petrophysics, and hydraulic fracture design. In Proceedings of the SPE Annual Technical Conference and Exhibition 2007, Anaheim, CA, USA, 11–14 November 2007.

Evans, K.F.; Kohl, T.; Rybach, L.; Hopkirk, R.J. The effects of fracture normal compliance on the long-term circulation behavior of a hot dry rock reservoir: A parameter study using the new fully coupled code “fracture”. Geotherm. Resour. Counc. Trans. 1992, 16, 449–456.

Fu, C.; Liu, N. Waterless fluids in hydraulic fracturing—A review. J. Nat. Gas Sci. Eng. 2019, 67, 214–224, https://doi.org/10.1016/j.jngse.2019.05.001.

Guo, T.; Zhang, S.; Qu, Z.; Zhou, T.; Xiao, Y.; Gao, J. Experimental study of hydraulic fracturing for shale by stimulated reservoir volume. Fuel 2014, 128, 373–380, https://doi.org/10.1016/j.fuel.2014.03.029.

Wang, H.; Sharma, M.M. A novel approach for estimating formation permeability and revisiting after-closure analysis of diagnostic fracture-injection tests. SPE J. 2019, 24, 1809–1829, https://doi.org/10.2118/194344-pa.

Gonzalez, M.; Taleghani, A.D.; Olson, J.E. A cohesive model for modeling hydraulic fractures in naturally fractured formations. In Proceedings of the SPE Hydraulic Fracturing Technology Conference 2015, The Woodlands, TX, USA, 3–5 February 2015.

Wright, C.A.; Weijers, L.; Germani, G.A.; MacIvor, K.H.; Wilson, M.K.; Whitman, B.A. Fracture treatment design and evaluation in the Pakenham field: A real-data approach. In Proceedings of the SPE Annual Technical Conference and Exhibition 1996, Denver, CO, USA, 6–9 October 1996; https://doi.org/10.2118/36471-MS.

Jabbari, H.; Zeng, Z. Hydraulic fracturing design for horizontal wells in the Bakken formation. In Proceedings of the 46th US Rock Mechanics/Geomechanics Symposium 2012, Chicago, IL, USA, 24–27 June 2012.

Kurtoglu, B.; Salman, A.; Kazemi, H. Production forecasting using flow back data. In Proceedings of the SPE Middle East Unconventional Resources Conference and Exhibition 2015, Muscat, Oman, 26–28 January 2015; https://doi.org/10.2118/spe-172922-ms.

Ilk, D.; Okouma, V.; Blasingame, T.A. Characterization of well performance in unconventional reservoirs using production data diagnostics. In Proceedings of the SPE Annual Technical Conference and Exhibition 2011, Denver, CO, USA, 30 October–2 November 2011; https://doi.org/10.2118/147604-ms.

Witherspoon, P.A. Development of underground research laboratories for radioactive waste isolation. In Proceedings of the Second International Symposium on Dynamics of Fluids in Fractured Rock, Berkeley, CA, USA, 10–12 February 2004; pp. 3–7.

Hawkes, R.V.; Bachman, R.; Nicholson, K.; Cramer, D.D.; Chipperfield, S.T. Good tests cost money, bad tests cost more—A critical review of DFIT and analysis gone wrong. In

Proceedings of the SPE International Hydraulic Fracturing Technology Conference and Exhibition, Muscat, Oman, 16–18 October 2018; https://doi.org/10.2118/191458-18ihft-ms.

Liu, G.; Ehlig-Economides, C. Comprehensive before-closure model, and analysis for fracture calibration injection falloff test. J. Pet. Sci. Eng. 2018, 172, 911–933, https://doi.org/10.1016/j.petrol.2018.08.082.

Warpinski, N.; Branagan, P.; Engler, B.; Wilmer, R.; Wolhart, S. Evaluation of a downhole tiltmeter array for monitoring hydraulic fractures. Int. J. Rock Mech. Min. Sci. 1997, 34, 329.e1–329.e13, https://doi.org/10.1016/s1365-1609(97)00074-9.

Ezulike, O.; Dehghanpour, H.; Virues, C.; Hawkes, R.V.; Jones, R.S. Flowback fracture closure: A key factor for estimating effective pore volume. SPE Reserv. Eval. Eng. 2016, 19, 567–582, https://doi.org/10.2118/175143-pa.

Xu, Y.; Ezulike, O.D.; Zolfaghari, A.; Dehghanpour, H.; Virues, C. Complementary surveillance microseismic and flowback data analysis: An approach to evaluate complex fracture networks. In Proceedings of the SPE Annual Technical Conference and Exhibition 2016, Dubai, UAE, 26–28 September 2016; https://doi.org/10.2118/181693-MS.

Fisher, M.; Heinze, J.; Harris, C.; Davidson, B.; Wright, C.; Dunn, K. Optimizing horizontal completion techniques in the Barnett shale using microseismic fracture mapping. In Proceedings of the SPE Annual Technical Conference and Exhibition 2004, Houston, TX, USA, 26–29 September 2004.

Maxwell, S.; Urbancic, T.; Demerling, C.; Prince, M. Real-time 4D passive seismic imaging of hydraulic fracturing. In Proceedings of the SPE/ISRM Rock Mechanics Conference 2002, Irving, TX, USA, 20–23 October 2002; https://doi.org/10.2118/78191-ms.

Warpinski, N.R.; Mayerhofer, M.J.; Agarwal, K.; Du, J. Hydraulic-fracture geomechanics and microseismic-source mechanisms. SPE J. 2013, 18, 766–780, https://doi.org/10.2118/158935-pa.

Nolte, K. A general analysis of fracturing pressure decline with application to three models. SPE Form. Eval. 1986, 1, 571–583, https://doi.org/10.2118/12941-pa.

Nolte, K.G. Determination of fracture parameters from fracturing pressure decline. In Proceedings of the SPE Annual Technical Conference and Exhibition 1979, Las Vegas, NV, USA, 23–26 September 1979; https://doi.org/10.2118/8341-ms.

Castillo, J. Modified fracture pressure decline analysis including pressure-dependent leakoff. In Proceedings of the SPE/DOE Joint Symposium on Low Permeability Reservoirs 1987, Denver, CO, USA, 18–19 May1987; https://doi.org/10.2118/16417-ms.

Barree, R.; Mukherjee, H. Determination of pressure dependent leak off and its effect on fracture geometry. In Proceedings of the SPE Annual Technical Conference and Exhibition 1996, Denver, CO, USA, 6–9 October 1996; https://doi.org/10.2118/36424-ms.

Soliman, M.Y.; Miranda, C.G.; Wang, H.M. Application of after-closure analysis to a dual-porosity formation, to CBM, and to a fractured horizontal well. SPE Prod. Oper. 2010, 25, 472–483, https://doi.org/10.2118/124135-pa.

Potocki, D.J. Understanding induced fracture complexity in different geological settings using DFIT net fracture pressure. In Proceedings of the SPE Canadian Unconventional Resources Conference 2012, Calgary, AL, Canada, 30 October–1 November 2012; https://doi.org/10.2118/162814-ms.

Craig, D.P.; Blasingame, T.A. Application of a new fracture-injection/falloff model accounting for propagating, dilated, and closing hydraulic fractures. In Proceedings of the SPE Gas Technology Symposium 2006, Calgary, AB, Canada, 15–17 May 2006.

Hagoort, J. Waterflood-Induced Hydraulic Fracturing. Ph.D. Thesis. Delft University, Delf, The Netherlands, 1981.

Mayerhofer, M.; Economides, M. Permeability estimation from fracture calibration treatments. In Proceedings of the SPE Western Regional Meeting 1993, Anchorage, Alaska, 26–28 May 1993; https://doi.org/10.2118/26039-ms.

Cramer, D.D.; Nguyen, D.H. Diagnostic fracture injection testing tactics in unconventional reservoirs. In Proceedings of the SPE Hydraulic Fracturing Technology Conference 2013, The Woodlands, TX, USA, 4–6 February 2013.

Marongiu-Porcu, M.; Retnanto, A.; Economides, M.J.; Ehlig-Economides, C. Comprehensive fracture calibration test design. In Proceedings of the PE Middle East Unconventional Resources Conference and Exhibition 2015, Muscat, Oman, 4–6 February 2015; https://doi.org/10.2118/168634-ms.

Bourdet, D.; Ayoub, J.A.; Pirard, Y.M. Use of pressure derivative in well test interpretation. SPE Form. Eval. 1989, 4, 293–302, https://doi.org/10.2118/12777-pa.

Rohmer, B.; Raverta, M.; de la Combe, J.-L.B.; Jaffrezic, V. Minifrac analysis using well test technique as applied to the Vaca Muerta shale play. In Proceedings of the EUROPEC 2015, Madrid, Spain, 1–4 June 2015, https://doi.org/10.2118/174380-ms.

Rizwan, Y. Pressure Transient Analysis for Minifracs/DFIT and waterflood induced fractures. Master's Thesis, The Delft University of Technology, Delf, The Netherlands, 2017.

Nicholson, A.K.; Bachman, R.C.; Hawkes, R.V. How diagnostic fracture injection tests (DFITs) show horizontal plane tensile and shear fractures in various stress settings. In Proceedings of the SPE/AAPG/SEG Unconventional Resources Technology Conference 2017, Austin, TX, USA, 24–26 July 2017; https://doi.org/10.15530/urtec-2017-2670018.

McClure, M.W.; Blyton, C.A.J.; Jung, H.; Sharma, M.M. The effect of changing fracture compliance on pressure transient behavior during diagnostic fracture injection tests. In Proceedings of the SPE Annual Technical Conference and Exhibition 2014, Amsterdam, The Netherlands, 27–29 October 2014; https://doi.org/10.2118/170956-ms.

CHAPTER 3

Formation Evaluation and Hydraulic Fracture Modeling

This chapter discusses the paper entitled "***Formation Evaluation and Hydraulic Fracture Modeling of Unconventional Reservoirs: Sab'atayn Basin Case Study***" published in the 53rd US Rock Mechanics/Geomechanics Symposium held in New York, NY, USA, 23–26 June 2019.

Abdulaziz Ellafi was responsible to prepare the methodology, analyze the data, validation and writing the paper. Co-authors are Mohammed Ba Geri, Bailey Bubach, and Hadi Jabbari were involved in the review and editing of the draft. Hadi Jabbari is the PhD advisor and was the director of the project.

Abstract

Basement fractured reservoirs have proven to yield significant contributions of hydrocarbon production in several countries. Sab'atayn Basin in Yemen has potential production and is classified as an unconventional reservoir. Due to poor reservoir quality from low porosity and ultra-low permeability, understanding the petrophysical properties and geomechanical characterization can lead to optimize the design for hydraulic fracturing treatments. The workflow in this research started by evaluating the formation of interest, then building the

geomechanical model to assess the three different fracturing fluid scenarios for hydraulic fracture modeling. The results showed hydrocarbon potential in the fractured oil-bearing zone with a dominated fracture porosity of almost 2.2% and a high amount of shale content. As a new study area, the geomechanical property results are compatible within the typical range of several basement fractured reservoirs worldwide. As a fracturing fluid, produced water is the appropriate fluid treatment in terms of creating a high fracture half-length with low damage and environmental footprint. However, the high viscosity friction reducer fluid has more potential to transport the proppant deeper into the fracture. The research findings provide a deep understanding of geomechanical models, which could be used as guidance for fracture engineers to design and optimize fracturing treatments.

3.1 Introduction

Natural Fractured Reservoirs (NFRs) are defined as formation rocks that are characterized by a series of discontinuous fractures/faults/fissures/or bedding planes, and their lithology can be carbonates, sandstones, or crystalline rocks. Several researchers reported that these reservoirs have been successfully proven to be a significant contribution to hydrocarbon production, since a large proportion of produced hydrocarbon worldwide are NFRs (Nelson, 1985; Aguilera, 1996; Badakhshan et al., 1998; Nelson, 2001; Rodriguez et al., 2004; Nicolas et al., 2011). However, the detection and evaluation processes for these sweet spots are challenging for geologists, geophysicists, and petroleum engineers due to heterogeneity in the pore structure of the rock (El Sharawy, 2015). In the last decade, discovery and development in these reservoirs has increased rapidly due to advances in horizontal drilling and hydraulic fracturing technologies. Landes et al., 1960 and Aguilera 1996 defined fractured basement formations as metamorphic or igneous rocks (regardless of age) which

are unconformably overlain by a sedimentary sequence. As a result, faults were led to create fracture networks and pore space through diagenetic processes. Furthermore, hydrocarbon was formed and stored in the natural fractures due to tectonic activity. In addition to sandstone or carbonate formations, the basement reservoirs are usually found in the lower zone of the oil-bearing formations with a significant amount of hydrocarbons that accumulated in the natural fracture between the rock matrix. These resources are considered to have a sedimentary origin, which are fractured quartzite or granites (North, 1990; Koning 2013). In 1979, Nelson characterized the NFRs into four different categories; most of the basement formation fall into the category that the reservoirs have relatively low permeability and no or low matrix porosity. Therefore, these reservoirs are classified as unconventional resources that are the primary target to produce additional oil and gas (Nicolas et al., 2011; Pascal and Priscilla, 2017). There has been little exploration conducted on this complex reservoir type, fractured basement granite rocks are attractive to the oil and gas industry because of their popularity in more than 30 different countries, such as Algeria, China, Vietnam, Canada, India, Yemen, UK, Libya, and Egypt (Sircar 2004; Gutmanis, 2009). Since 1975, Vietnam has large discoveries, where the Bach Ho oil field has estimated two billion barrels of oil reserves in the Cuu Long Basin's offshore field (Keggin and Alaaraji, 2017). In contrast, Yemen had a large onshore exploration in last 20 years, where ten blocks of basement fractured granite reservoirs were detected in the Masilah and the Sab'atayn Basins. Because of the poor reservoir quality (low porosity and ultra-low permeability), only five of the ten blocks are producing, and East Shabwa has the highest daily oil production around 11,765 m3 /day (74 M Rbbl/day) (Nicolas et al., 2011; Bawazer et al., 2018). This case study emphases understanding the petrophysical properties and geomechanical characterization of

fractured granite basement reservoirs as an unconventional resource in the Middle East region to gain insight into the optimum design for hydraulic fracturing treatments.

3.2 Overall About the Area of Study

The basement formation are hydrocarbon-rich fractured granite rocks that served as unconventional oil and gas resources, in the Sab'atayn Basin. This formation was deposited during the Precambrian Era, around 600 million years ago. The reservoir top is around 2,621.25 m (8,600 ft) and varies in thickness from 61 m to 85 m (200 ft to 280 ft). This formation is the lowest zone that is isolated and overlain by a thin shale bed. The reservoir fluid is classified as black oil, where reservoir pressure, bubble point pressure, reservoir temperature, oil specific gravity (API gravity), and formation volume factor are 2.7×10^7 Pa (4,000 psi), 2.3×10^7 Pa (3,354 psi), 93 °C (200 °F), 0.83 (39.5 °API), and 1.68 m^3/m^3 (1.68 Rbbl/STB), respectively.

Furthermore, the evaluation of its characterization, according to the literature, showed that the average range of unfeatured porosity matrix is less than 5% and, the reservoir rock permeability in the range of 7 μD. As a result, the formation rocks have poor connectivity to the matrix porosity. Therefore, the combination of horizontal drilling and hydraulic fracturing techniques plays a key role to access the unlocked formation by creating a path from the reservoir to the wellbore. Then, it is necessary to evaluate the petrophysical and geomechanical properties of unconventional resources to design a successful hydraulic fracturing operation.

3.3 Methodology

Figure 3. 1 illustrates the workflow in this research starting with the formation evaluation step, where various open-hole log data was gathered and checked for QC/QA analysis. Figure 3. 2 shows that all data evaluated includes total GR, Spectral GR, Caliber and Bit size, Neutron porosity, Photoelectric, Bulk density logs, Sonic and Shear wave, and Resistivity logs. Next, these data were interpreted to investigate reservoir characterization of fractured basement rocks using fracture system identification by resistivity log analysis. Furthermore, cross plots were used to define the formation lithology for the unconventional reservoir. In addition, our results were compared with the analysis outcomes from the previous work in the same area.

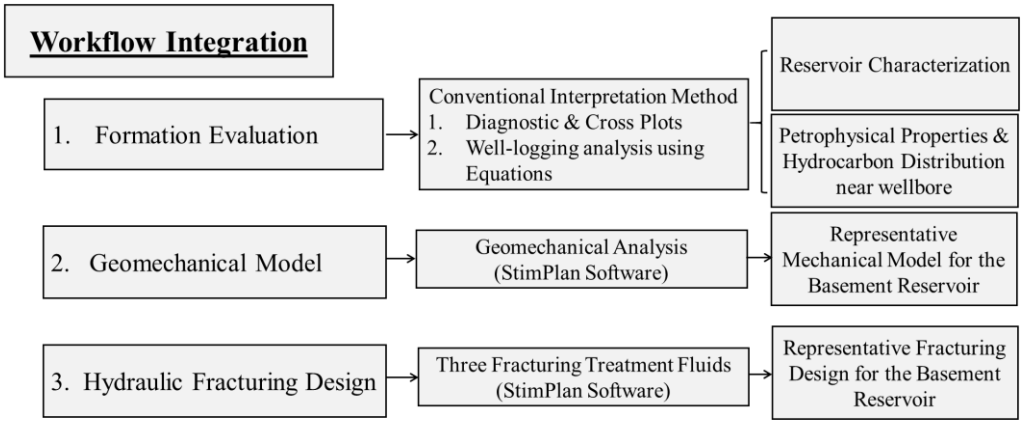

Figure 3. 1. The workflow description for the research scope.

After that, conventional log interpretation was utilized to determine the volume of shale, effective and total porosity, and water and hydrocarbon distributions near the wellbore region. Moreover, analysis of the Bulk density and sonic wave logs were performed using StimPlan commercial software (NSI Technologies) to build a geomechanical property model that represent the basement fractured granite formation. Finally, the optimum hydraulic

fracturing model was designed using three scenarios of the fracture fluid to perform the applicable model for the unconventional formation.

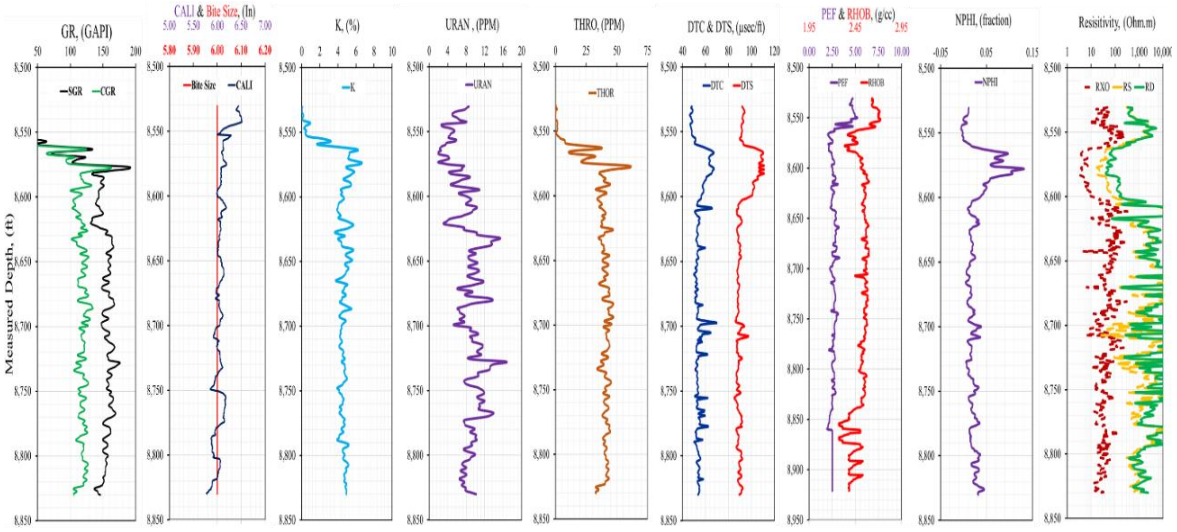

Figure 3. 2. Open-hole logs for the fractured basement formation.

3.4 Results and Observations

3.4.1 Formation Evaluation of the Basement Reservoir

Open-hole logs were analyzed using conventional well logging interpretation methods to evaluate and build a reservoir evaluation model for the formation of interest. The overall well-logging analysis in this paper shows the natural fractures behavior in the reservoir, as shown in Figure 3. 2. The characterization of fractures is noticed by the reflection of caliber log results that are around the standard bit size, which means an increase in borehole diameter. Also, the separation between the sonic and shear wave curves is associated with high reflection in total GR log content, as well as spectral GR log (Potassium, Uranium, and Thorium) is an indicator of the presence of the natural fracture system in the formation. In addition, the spike in the reading values, especially in the compression travel time, indicates the presence of fissures and cracks in the target formation. On the other hand, the resistivity

ratio identification plot was utilized to confirm the presence of the fractured formation. This is the relationship between the deep resistivity log and the ratio of deep to shallow resistivity logs, as demonstrated in Figure 3. 3.

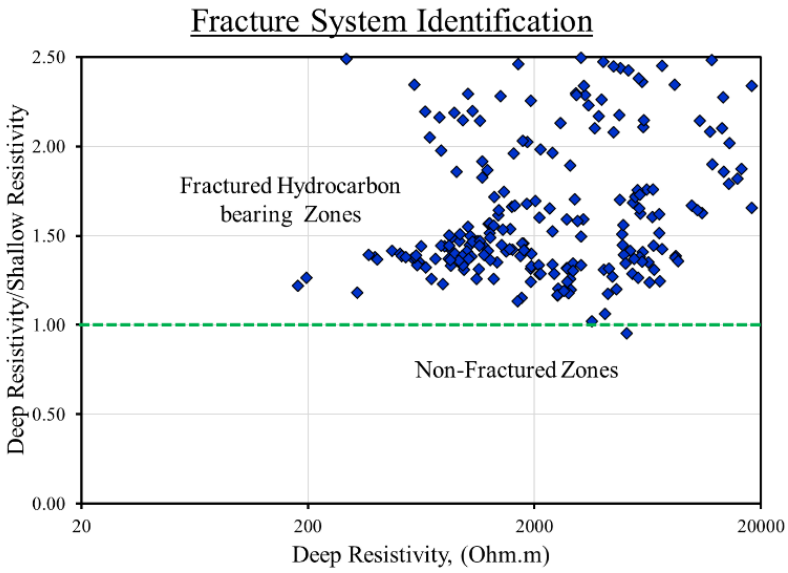

Figure 3. 3. Natural fractures diagnostic plot.

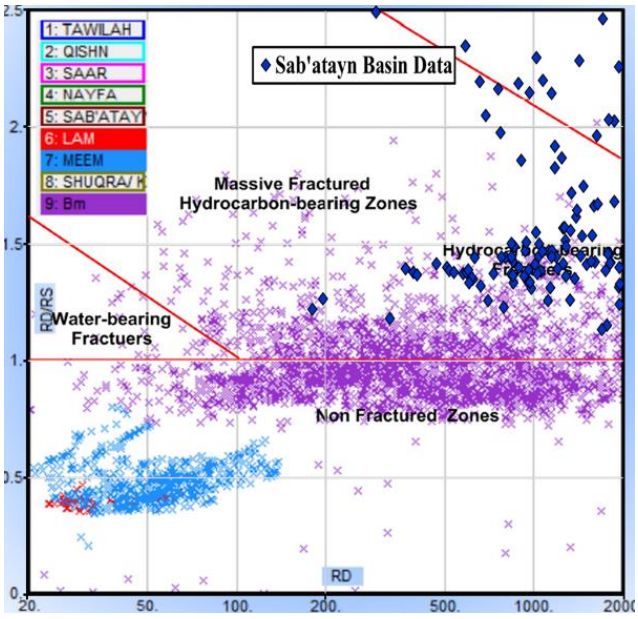

Figure 3. 4. Fractures identification plots for Sab'atayn basement reservoir overlay on Bawazer's study in Yemen (Modified from Bawazer et al., 2018).

The results showed that most of the data points have fallen above the unit line (Rd/Rs=1) on the fractured hydrocarbon-bearing zones. Therefore, this confirms the analysis with the previous technique. Moreover, the Bawazer et al., 2018 study was used to compare with our results since both studies are in the same region. Our interpretation which is represented by blue diamonds were overlain on the cross plots, as shown in Figure 3. 4. The results for the comparison confirm that the reservoir is a fractured hydrocarbon bearing zone, based on the location of the data points in the Figure.

3.4.2 Lithology of the Basement Reservoir

Lithology in the basement reservoirs is characterized by heterogeneity in the lithological composition. The formation mineralogy consists of many components, such as granite, quartzite or gneiss, amphibolite, and epidote quartz breccia, etc. According to the literature review, the construction of the granite is from a high amount of quartz around 30% plus alkali feldspars and mica (Schlumberger, 1989). In this research, the lithology identification logs (Photoelectric log) reads around 2.5 during the formation of interest, where this value represents the granite rock, while the potassium log reflection shows feldspar content. Furthermore, the cross plot was used to define the rock lithology by plotting the uranium content on the x-axis versus thorium content on the y-axis (Serra, 1984).

The results indicate the formation lithology, as illustrated in Figure 3. 5, where the data points that are represented by the red circle are located outside of the region for granite classification. The reasoning for this could be due to the clay content, which affects the location of the data points on the graph and places the data out of range.

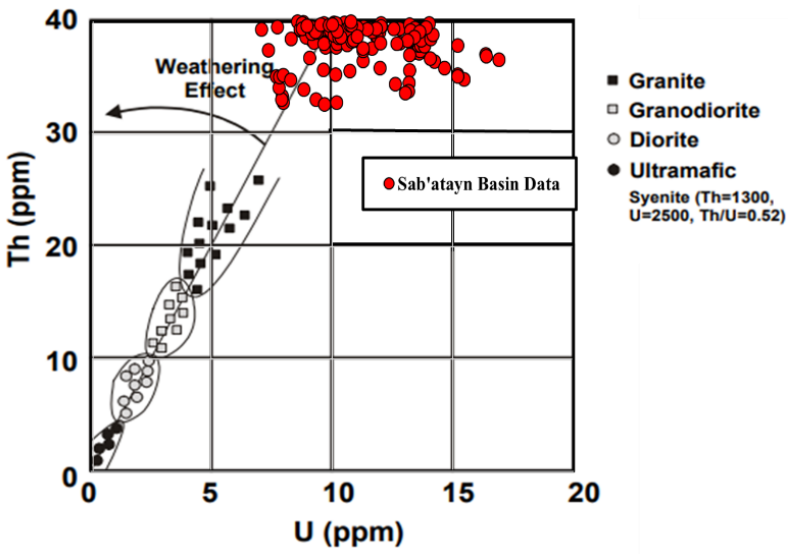

Figure 3. 5. Lithology indication using thorium versus uranium contents (Modified from Serra, 1984).

3.4.3 Petrophysical Properties of the Basement Reservoir

One of the main petrophysical properties that are responsible for the reservoir classification is the porosity. Unconventional reservoirs are characterized by low reservoir porosity compared to conventional resources. According to several studies, the basement fractured granite reservoirs depend on the fracture porosity to storage hydrocarbon, where these resources formed with low to no matrix porosity. The sonic travel time wave and bulk density logs were utilized to estimate the basement porosity using Equations 3. 1 and 3. 2 (Schlumberger, 1989).

$$\phi_{sonic} = \frac{\Delta t_{log} - \Delta t_{ma}}{\Delta t_{fluid} - \Delta t_{ma}} \quad (3.\ 1)$$

$$\phi_{RHOB} = \frac{\rho_{ma} - \rho_{RHOB}}{\rho_{ma} - \rho_{fluid}} \quad (3.\ 2)$$

Where: ϕ_{sonic}: Sonic derived porosity, (fraction), Δt_{log}: Interval transient time of the formation, (µsec/ft), Δt_{ma}: Interval transient time of the matrix, (168.14 µsec/m (51.25 µsec/ft)), Δt_{fluid}: Interval transient time of the fluid, (620 µsec/m (189 µsec/ft)), ϕ_{RHOB}: Rock bulk density derived porosity, ρ_{RHOB}: Bulk density of the formation, ρ_{ma}: Bulk density of the matrix, (2.68 g/cc), and ρ_{fluid}: Bulk density of the fluid, (1.19 g/cc)

The results are shown in Figure 3. 6, where Sonic and neutron logs have close to exact porosity values compared to density logs that show larger porosity in the basement fractured granite zone. This is an indicator for the fractured behavior, where the density log reads the porosity from the natural fractures, while the sonic and neutron logs measured the matrix reservoir porosity. This explanation is based on the principle for both sonic and neutron logs, where compression wave travels only through the solid formations, while neutron log also captures the hydrogen ion found in the matrix formation. After that, total porosity and effective porosity were determined using Equations 3. 3 and 3. 4.

$$\phi_{total} = \sqrt{\frac{\phi_{Neutron}^2 + \phi_{RHOB}^2}{2}} \quad (3.\ 3)$$

$$\phi_{effective} = \phi_{total} \times \left[1 - V_{shale}\right] \quad (3.\ 4)$$

Where: ϕ_{total}: Total porosity, (fraction), $\phi_{effective}$: Effective porosity. (fraction), and V_{shale}: Volume of shale content, (fraction)

Figure 3. 7 illustrates the total and effective porosity versus depth, where the red line is the effective porosity that represents only the connected pores, while the blue line is the total porosity that defines the sum of porosity in connected and unconnected pores. As we noticed, the separation between both curves is small, which is the indicator if fracture porosities dominate the basement reservoir.

In order to define the reservoir lithology and hydrocarbon fluid distribution through depth, shale volume and Archie's Equations 3. 5, 3. 6, and 3. 7 were utilized to perform the volume and fluid plots by determining initial water saturation, moveable hydrocarbon saturation, and unmovable hydrocarbon saturation versus the formation depth (Schlumberger, 1989).

$$V_{shale} = \frac{GR_{log} - GR_{min}}{GR_{max} - GR_{min}} \quad (3.\ 5)$$

$$Sw = \left[\frac{F \times R_w}{R_t}\right]^{\frac{1}{n}} \quad (3.\ 6)$$

$$S_{xo} = \left[\frac{F \times R_{mf}}{R_{xo}}\right]^{\frac{1}{n}} \quad (3.\ 7)$$

Where: Sw = Water saturation, (fraction), S_{xo} = Flush zone saturation, (fraction), F = Formation resistivity factor, $F = \frac{a}{\phi_{effective}^{m}}$, $\phi_{effective}$ = Effective porosity, (fraction), m = Cementation factor, which ranges from 1.7 to 3, but normally 2, a = Tortuosity, normally 1, n = Saturation exponent, which ranges from 1.8 to 4, but normally 2, R_w = Formation water resistivity, (ohm.m), R_t = True formation resistivity, (ohm.m), R_{mf} = Mud filtrate resistivity, (ohm.m), and R_{xo} = Flush zone resistivity, (ohm.m).

Finally, Figure 3. 8 and 3. 9 illustrate the volume and fluid plots for the basement fractured reservoir, where these plots help the reservoir engineer to evaluate and detect the pay zone thickness as well as the petrophysical properties for the target formation. We can notice that the formation interval is in the depth of 2,621 m to 2,691 m (8,600 ft to 8,830 ft) with availability of hydrocarbon content. The volume plot demonstrates the volume of shale, volume of granite, and porosity, which are shown by gray, yellow, and green, respectively.

In contrast, the fluid plot represents the initial water saturation, movable oil, and unmovable oil by blue, red, and green, respectively.

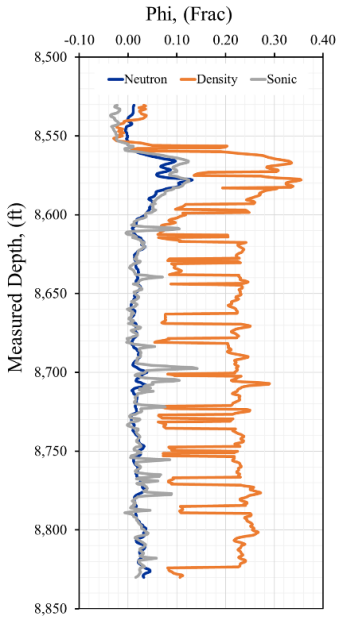

Figure 3. 6. Porosity estimation versus depth from sonic, neutron, rock density logs.

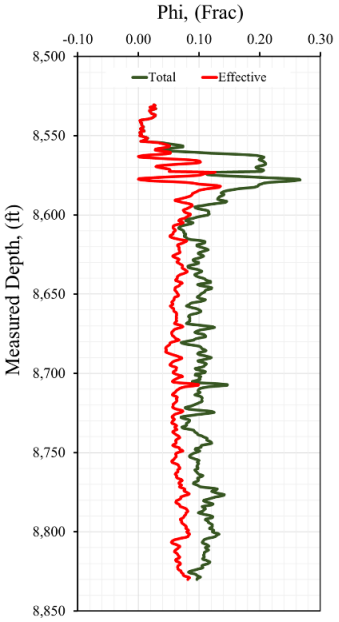

Figure 3. 7. Total and effective porosity versus formation depth.

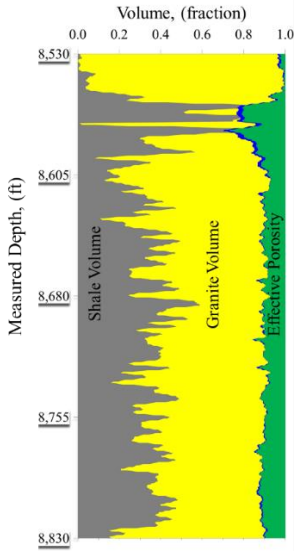

Figure 3. 8. Volume distribution plot versus the formation depth.

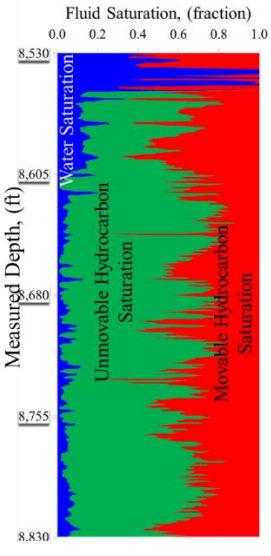

Figure 3. 9. Fluid distribution plot versus the formation depth.

3.4.4 Fracturing Design of Basement Reservoirs

Stimulation processes by applying the combination of horizontal multilateral wells and hydraulic fracturing in unconventional reservoirs, has been implemented in the recent decades. In order to produce profitably from a large naturally fractured basement formation, a successful hydraulic fracturing treatment is required. Lacking knowledge of geomechanical characterization of Sab'atayn naturally fractured basement reservoir could potentially cause complete or partial failure of hydraulic fracturing design. Therefore, this paper investigated the geomechanical properties of Sab'atayn basement formation to fill the gap that is required for appropriate fracturing design. The objective of this study is to provide a full understanding of geomechanical properties of natural fractured basement reservoir rocks that could help optimize the hydraulic fracturing design. Based on well logging date and reservoir properties, numerical hydraulic fracturing simulator (StimPlan) was used to predict the unknown geomechanical property of the basement reservoirs in the Sab'atayn Basin. This study found that the static Young's modulus of the basement formation is around 48.263 GPa (7 MMpsi), and the dynamic Young's modulus is approximately 57.226 GPa (8.3 MMpsi) which is larger than the static modulus by 9%. In addition, the range of Poisson's ratio is around 0.21. Also, the fluid loss coefficient was calculated as approximately 8.46×10-5 m/sqrt(min) (0.0001 ft/sqrt(min)).

Understanding petrophysical and geomechanical properties of natural fractured basement reservoirs is a significant key to design an efficient hydraulic fracturing treatment. Modulus of elasticity or Young's modulus (E) is classified into dynamic and static modulus.

The dynamic Young's modulus can be calculated from elastic waves (Δt_s & Δt_p) and density logs (ρ_{RHOB}), while the static Young's modulus is measured experimentally by measuring

rock deformation or using correlation based on the rock type Equations 3. 8 and 3. 10 (McCan and McCan 1977; Onalo et al., 2018).

$$E_{dynamic} = 1.34 \times 10^{10} \frac{\rho_{RHOB}}{\Delta t_s^2} \left[\frac{3\Delta t_s^2 - 4\Delta t_p^2}{\Delta t_s^2 - \Delta t_p^2} \right] \quad (3.\ 8)$$

$$E_{static} = 0.69 E_{dynamic} + 6.4 \quad (3.\ 9)$$

The Poisson's ratio (v) of the basement reservoir can be estimated from the Equation 2. 10.

$$v = \frac{\frac{1}{2}\left(\frac{\Delta t_s}{\Delta t_p}\right)^2 - 1}{\left(\frac{\Delta t_s}{\Delta t_p}\right)^2 - 1} \quad (3.\ 10)$$

The desirable execution fracturing treatment relies on accuracy of estimation for these three principle stresses, such as vertical stress (S_v), maximum horizontal stress (S_H), and minimum horizontal stress (S_h). This is due to the tendency for fractures to propagate perpendicular on minimum horizontal stress (Roussel et al., 2013). The importance of estimating the geomechanical properties aids in avoiding job screen-out or early failure of proppant transport.

The results show that Sab'atayn basement formation has normal fault due to Sv = 6.89×10^7 Pa (10,000 psi) > Sh = 4.2×10^7 Pa (6,100 psi). Figure 3. 10 and 3. 11 show the geomechanical properties that were estimated using simulator model (StimPlan) based on well logging data analysis at the basement formation.

Table 3. 1 illustrates the geomechanical characterization results of the natural fractured basement formation. The case study results fit within the typical range of granite rocks from previous studies. The results are in good agreement with Bawazer et al. (2018), where they estimated the basement porosity less than 5% and the porosity of our results is 2.2%. Due to the availability of inadequate information on the geomechanical properties of the Sab'atayn basement formation, this work calculated them and found that the Young's modulus is 57.2 GPa and, Poisson's ratio is 0.21. These results are consistent with the findings of Valley and Evans 2003, and Kumar 1976.

Table 3. 1. Geomechanical properties of natural fractured basement (granites) rocks.

Parameters	**Our case study results**	**Pervious work results**	**Typical range**	**Source**
Porosity (%)	2.2	< 5	0.1 – 5	Bawazer et al. 2018
Permeability (mD)	$3.6\ 10^{-3}$	$5*10^{-5}$	10^{-3} - 10^{-8}	Geraud, 2010
Young's Modulus (GPa)	57.2	55	40 - 70	Valley & Evans, 2003
Poisson's Ratio	0.21	0.25	0.2 – 0.3	Kumar, 1976

Analyzing simulation results including the stress profile, fluid efficiency, net pressure, and fracture geometry is an essential step to design a pump schedule. Designing a hydraulic fracturing operation an adequately for naturally fractured basement reservoirs requires induced long fracture half-length (Xf) because the basement rocks have ultra-low permeability and very low porosity. Therefore, the pumping schedule treatment and fluid selection with a proper concentration of proppant are the main keys for effective proppant distribution and placement within the fractures. Several types of fracking fluids have been applied, including the use of slickwater, linear gel, and crosslinked based in the US and

Canada basins (Jabbari and Zeng, 2012). The success of a fluid selection process in a confined formation depends primarily on fracture half-length, proppant distribution and placement in fracks (Hofmann et al. 2012). Thus, understanding fluid composition, ability to create a complex fracturing system, and the ability to carry and transport proppant deep into the fracture, is crucial for success in the fracking treatment.

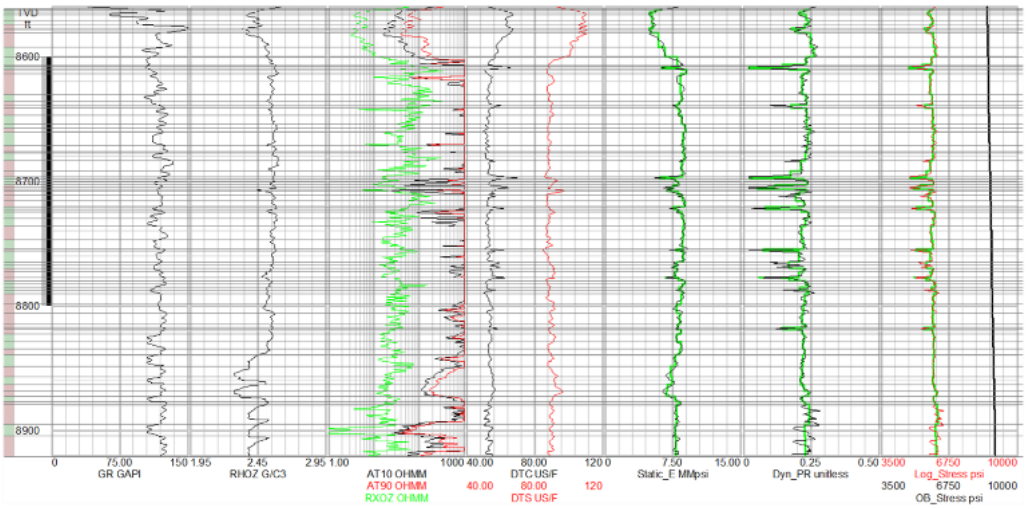

Figure 3. 10. Formation evaluation and geomechanical properties of the fractured granite basement reservoir.

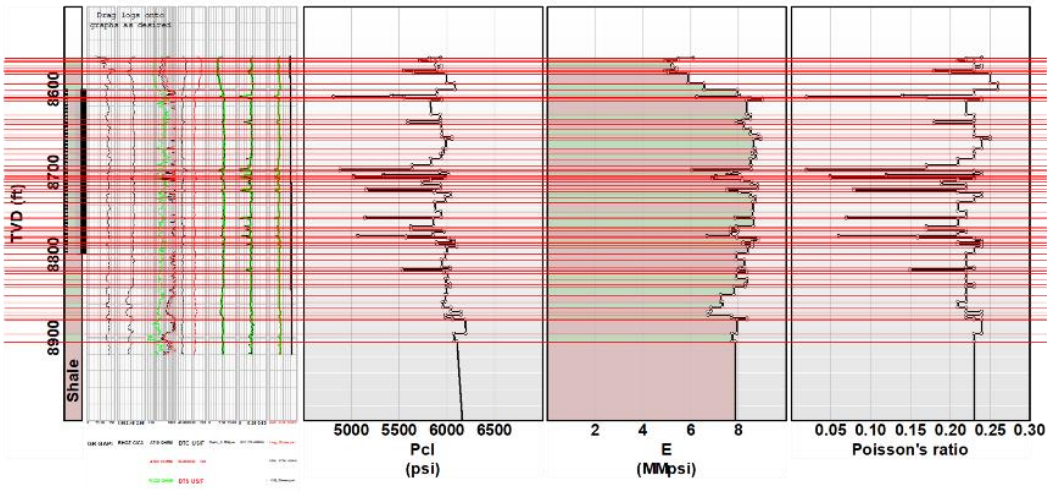

Figure 3. 11. Representative geomechanical model of the fractured granite basement reservoir.

Mesh size, Ottawa 20/40, the target fracture half-length (Xf) is 152 m (500 ft); Several parameters effect fracture treatment, such as fluid type, proppant size, proppant type, and proppant concentration, Three different hydraulic fracturing scenarios were designed to evaluate fracturing fluid type including produced water, linear gel, and high viscosity friction reducers (HVFRs). All three scenarios were conducted using the same conditions, such as proppant type Ottawa size 20/40mesh, slurry volume (7.57 m3 (2 M-Gal)), fracture half-length (Xf = 152m (500 ft)). Proppant properties are listed in Table 3. 2.

The first scenario using produced water during hydraulic fracturing process was selected based on the fact that to minimize usage of fresh water in hydraulic fracturing, reduces environmental impacts. Al-Muntasheri, 2014 reported high salinity produced water that was used in hydraulic fracturing applications with the total dissolved solids (TDS) 267,588 mg/L, total hardness solids (TSS) 10,623, and specific gravity is 1.2 g/cc. This study used the same composition that was reported by AlMuntasheri, 2014 in his study to mimic the real composition of high TDS produced water in fracturing treatments. Furthermore, the linear gel fracture fluid was used as a second scenario. The concentration of linear gel was 20 ppt, which is within the common concentrations range used for guar-based fluids (Ba Geri et al. 2019). The last scenario followed the recent trend of using HVFRs as alternative fracturing fluids instead of using guar-based fluids. Ba Geri et al. 2019 represented comprehensive investigation of HVFRs concentrations that are commonly used in field case studies which are around 2.6 gpt. This simulation work used 2 gpt loading of HVFR.

Table 3. 2. Proppant data – Ottawa Sand 20/40 (Jabbari and Zeng, 2012).

Specific Gravity				2.65	
Damage Factor (1.0 = No Damage)				0.70	
Proppant Stress	0	2000	4000	8000	16,000
Kf @ 2#/sq ft md-ft	4800	3850	2750	990	50

Promising results were observed from using HVFRs comparing to the other two fracture fluid systems e.g., produced water and linear gel because HVFRs has many advantages including create complex fracture system network, the ability of carrying and transport proppant deep into the fractures, less formation damage, and reducing the operational cost, and minimizing environmental footprint effect due to using fewer chemicals.

Figure 3. 12 shows fracture half-length (Xf) as a function of hydraulic fracturing type. Produced water has the highest Xf which is around 137 m (450 ft), while the Xf of using linear gel is 110 m (360 ft) because viscosity profile of produced water is less than linear gel and the relationship between fluid viscosity and Xf is proportional inversely (Brannon and Bill, 2011).

Figure 3. 13 presents the fracture propped area (FPA) as a function of different fracturing fluids. The FPA can be calculated using Equation 3. 11 (Hofmann et al., 2012).

$$FPA = 2L_F\ h_F \tag{3. 11}$$

Where: L_F is the fracture propped length (ft), and h_F is the fracture height (ft).

Even though, using produced water is able to create the largest X_f (137 m (450 ft)) and the X_f of HVFR is 119 m (391 ft); HVFR has the capability of transporting proppant farther into the fracture. Figure 3. 13 clearly shows that HVFR has the largest fracture propped area which leads to increased well productivity as a result of increasing fracture conductivity.

While linear gel also has a high fracture propped area, but due to formation damage the cost to use linear gel could be significantly more than using HVFRs (Motiee et al. 2016). Brannon and Bill, 2011 studied the effect of fracturing fluid viscosity on facture half-length and fracture complexity by using slickwater and linear gel represented low viscous and high viscous fracturing fluids, respectively.

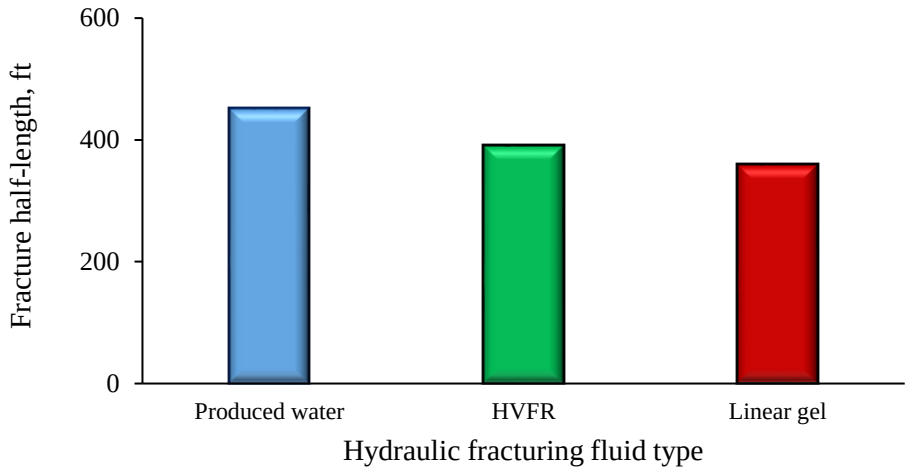

Figure 3. 12. Fracture half-length for all three different scenarios.

The investigation of their study concluded that using slickwater (low viscous) created a complex fracture system with long fracture length, but with a poor ability to carry proppant, while linear gel (high viscous) had desirable proppant transport and placement, but less fracture complexity and fracture half-length. Also, using linear gel generated higher fracture propped area than fracture propped area of using produced water, 30,480 m^2 and 15,240 m^2, correspondingly. This paper has the same trend of fracture propped area from using produced water and linear gel. Furthermore, this work highlights studying new fracture fluid system HVFR, and the results are promising since fracture propped area in this case study in natural fractured basement reservoirs provided a much better proppant transport and placement than using conventional fracture fluid systems e.g., slickwater and linear gel.

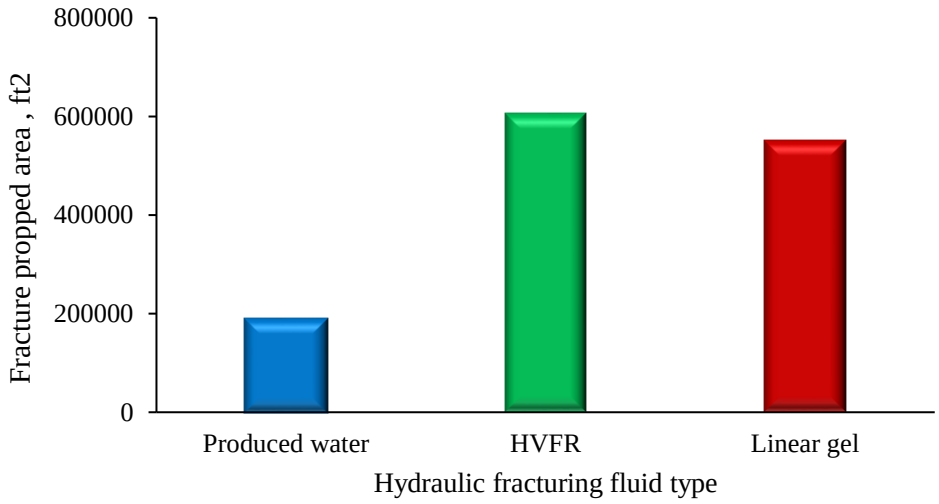

Figure 3. 13. Propped fracture length for all three different scenarios.

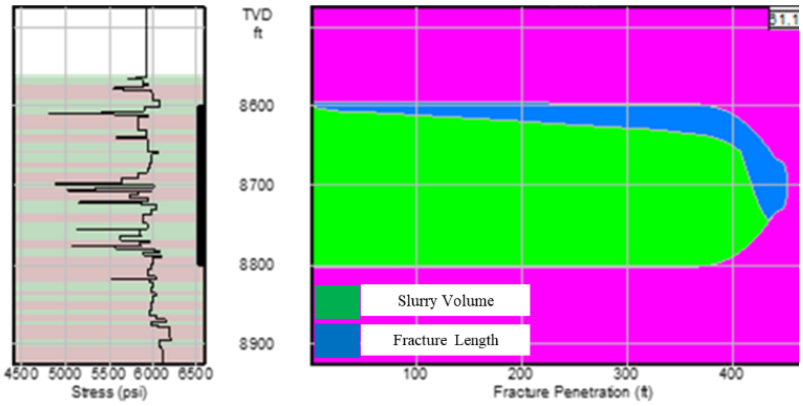

Figure 3. 14. Optimum hydraulic fracturing design of the fracture granite basement reservoir using produced water.

Figure 3. 14, 3. 15, and 3. 16 show the cross section view of the fracture penetration and proppant distribution through the basement formation using produced water, linear gel, and HVFR, respectively as a fracture fluid treatment.

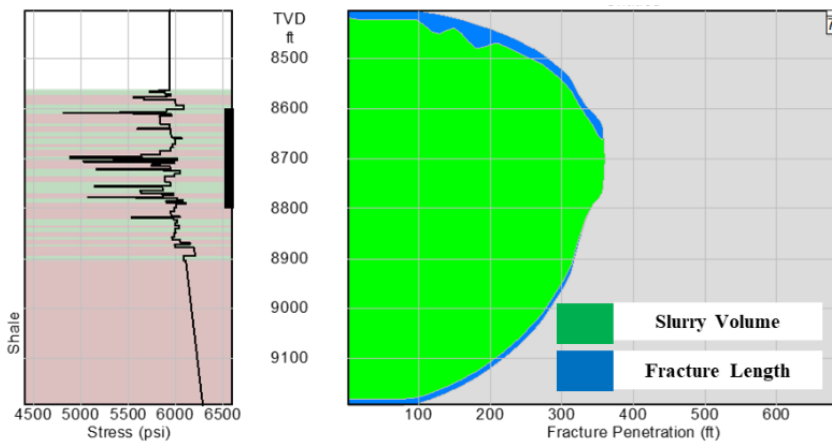

Figure 3. 15. Optimum hydraulic fracturing design of the fracture granite basement reservoir using linear gel.

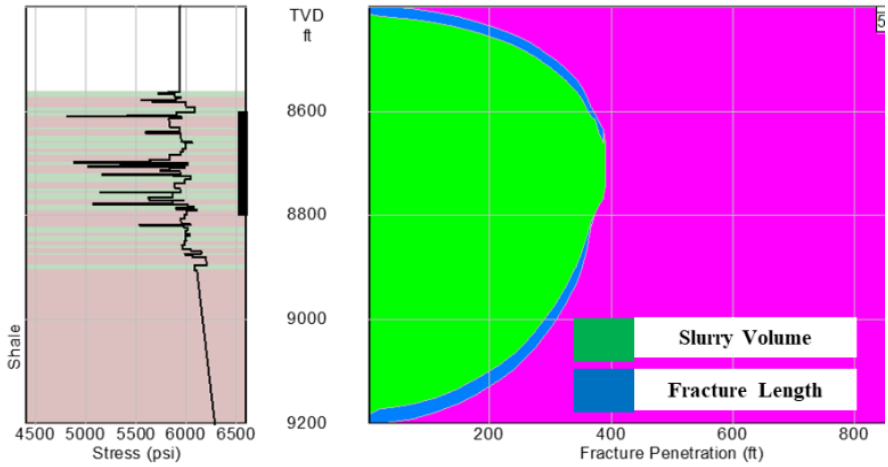

Figure 3. 16. Optimum hydraulic fracturing design of the fracture granite basement reservoir using HVFR.

3.5 Conclusion

The aim of this paper was to conduct a comprehensive study on the fractured granite basement reservoir to design the optimum hydraulic fracturing model. Based on various well-logging data, the formation characterization and hydrocarbon potential in the fractured basement granite reservoir were defined using well-logging interpretation techniques. The conventional analysis showed that the reservoir is an unconventional reservoir with high

hydrocarbon fracture zones, where the dominated porosity is fractured porosity (2.2 %) with a significant amount of hydrocarbon.

Also, it can be concluded the reservoir lithology is a granite formation with a high amount of shale content. Therefore, this type of reservoir is the primary target to add additional oil and gas reserves. Although there is lacking knowledge and no previous studies on the geomechanical properties in this area, our results are compatible within the typical range of several basement fractured reservoirs worldwide.

Furthermore, the geomechanical model is the main key to apply hydraulic fracturing design and access the unlocked formation. Based on the three fracture treatment fluid scenarios, produced water is the appropriate fluid type for a formation like granitic rocks, where the results showed a high fracture half-length with low damage and environmental contamination.

On the other hand, the high viscosity friction reducer has adequate fracture half-length and desirable fracture propped area than other fracture fluid systems (produced water and Linear gel).

References

Aguilera R. (1996). Servipetrol Technical Notes on the Subject of 'Naturally Fractured Reservoirs'. Technical Note No.3 - Undiscovered Naturally Fractured Reservoirs. August.

Al-Muntasheri, G. A. 2014. A critical review of hydraulic fracturing fluids for moderate to ultralow permeability formations over the last decade. Society of Petroleum Engineers. doi:10.2118/169552-PA

Areshev, E. G., T. L. Dong, N. T. San, and O. A. Snip, 1992. Reservoirs in fractured basement on the continental shelf of southern Vietnam. Journal of Petroleum Geology, 15, 451- 464.

Valley, B., and K.F. Evans, 2003. Strength and elastic properties of the soultz granite." 2nd year report, http://www.mirarco.org/files/publications/1292 527243valley_06_strength_585283.

Ba Geri, M., A. Imqam, and R. Flori. 2019a. A critical review of using high viscosity friction reducers as fracturing fluids for hydraulic fracturing applications. In Proceedings of the SPE Oklahoma City Oil & Gas Symposium, Oklahoma, 7 – 11 April 2019. https:// doi:10.2118/195191-MS

Ba Geri, M., A. Imqam, A. Bogdan, A.L. Shen. 2019b. Investigate the rheological behavior of high viscosity friction reducer fracture fluid and its impact on proppant static settling velocity. In Proceedings of the SPE Oklahoma City Oil & Gas Symposium, Oklahoma, 7 – 11 April 2019. https:// doi:10.2118/195227-MS

Ba Geri, M., A. Imqam, and M. Suhail. 2019c. Investigate Proppant Transport with Varying Perforation Density and its Impact on Proppant Dune Development Inside Hydraulic Fractures. In Proceedings of the SPE Middle East Oil and Gas Show and Conference, Manama, Bahrain, 18 – 21 March 2019. https:// doi:10.2118/195018-MS

Badakhshan, A., H. Golshan, H.R. Musavi-Nezhad, and F.A. Sobbi. 1998. The Impact of Gas Injection On the Oil Recovery of a Giant Naturally Fractured Carbonate Reservoir. The Journal of Canadian Petroleum Technology, No. 98-12-01. http://dx.doi.org/10.2118/98-12-01.

Bawazer W, A. Lashin, M.M. Kinawy. 2018. Characterization of a fractured basement reservoir using high-resolution 3D seismic and logging datasets: A case study of the Sab'atayn Basin, Yemen. PLOS ONE 13(10): e0206079. https://doi.org/10.1371/journal.pone.0206079

Brannon, H.D, W.D. Wood, and R.S. Wheeler. 2005. The quest for improved proppant placement: investigation of the effects of proppant slurry component properties on transport. In Proceedings of the SPE Annual Technical Conference and Exhibition, Dallas, 9 – 12 October 2005. SPE 95675-MS

El Sharawy M. 2015. Fractured basement reservoir identification using geophysical well log data, Gulf of Suez, Egypt. Pelagia Research. Adv Appl Sci Res. 2015; 6(8):17–35.

Gutmanis, J. 2009. Basement Reservoirs - A review of their geological and production characteristics. In Proceedings of the International Petroleum Technology Conference, Doha, Qatar, 7 – 9 December 2009. doi:10.2523/IPTC-13156-MS

Gutmanis, J. and T. Batchelor. 2010. Hydrocarbon production from fractured basement formations. In GeoScience Limited, version 11.

Hofmann H, T. Babadagli, and G. Zimmermann. 2012. Hydraulic fracturing scenarios for low temperature EGS heat generation from the Precambrian basement in northern Alberta. GRC Transactions, Vol.36:459–468

Kumar, J. 1976. The Effect of Poisson's Ratio on Rock Properties. In Proceedings of the 51stAnnual Fall Technical conference and Exhibition of the Society of Petroleum Engineers of AIME, Dallas, TX, 3 – 6 October 1976. https://doi.org/10.2118/6094-MS

Jabbari, H., and Z. Zeng. 2012. Hydraulic fracturing design for horizontal wells in the Bakken Formation. In Proceedings of the 46th US Rock Mechanics / Geomechanics Symposium, Chicago, IL, 24 – 27 June 2012.

Keggin, J. and W. Alaaraji. 2017. Detecting basement reservoir fractures on Vietnam's first ocean bottom seismic survey in the Cuu Long Basin. GeoExpro Vol. 14, No. 2-2017

Koning, T., 2013. Fractured and weathered basement reservoirs: Best practices for exploration and production- Examples from USA, Venezuela, and Brazil. In Proceedings of the AAPG Annual Convention, Pittsburgh, Pennsylvania, 21 May 2013.

Landes, K.K., J.J. Amoruso, L.J. Charlesworth, F. Heaney, and P.J. Lesperance. 1960. Petroleum resources in basement rocks. AAPG Bull. 44 (10): 1682–1691.

Legrand, N., J. De Kok, P. Neff, and T. Clemens.2011. Recovery mechanisms and oil recovery from a tight, fractured basement reservoir, Yemen. Society of Petroleum Engineers. doi:10.2118/133086-PA

McCann, D., and C. McCann. 1977. Application of borehole acoustic logging techniques in engineering geology. In Proceedings of4th European Formation Evaluation Symposium, SPWLA London Chapter, October 1976.

Motiee, M., M. Johnson, B, Ward, C. Gradl, M. McKimmy, and J. Meeheib. 2016. High concentration polyacrylamide-based friction reducer used as a direct substitute for guar-based borate crosslinked fluid in fracturing operations. In Proceedings of the SPE Hydraulic Fracturing Technology Conference, Woodland, TX, 9-11 February 2016. https://doi:10.2118/179154-MS

Nelson, R.A. 1979. Natural Fracture Systems: Description and Classification. AAPG Bull., Vol.63, No.12, pp.2214-2221.

Nelson, R.A. 2001. Geologic Analysis of Naturally Fractured Reservoirs. Gulf Publishing Co. Book Division, 2nd Edition, 332.pp.

North, F. K., 1990. Petroleum Geology. Second Ed.: Winchester, Mass, Unwin Hyman Ltd, 631 pp

Onalo, D, O. Oloruntobi, S. Adedigba, F. Khan, L. James, & S. Butt. 2018. Static Young's modulus model prediction for formation evaluation. Journal of Petroleum Science and Engineering, 171, 394-402.

Pascal, D., and S. Pricilla. 2017. Fractured Basement in Mature Basin Exploration: New Play Analog in Central Sumatra Basin. In Proceedings of the AAPG 2017 Asia Pacific Region Technical Symposium, Bandung, Indonesia, 13-14 September 2017.

Rodriguez, F., J.L. Sanchez, and A. Galindo-Nava. 2004. Mechanisms and main parameters affecting nitrogen distribution in the Gas Cap of the Supergiant Akal Reservoir in the Cantarell Complex. In Proceedings of the SPE Annual Technical Conference and Exhibition, Houston, TX, 26–29 September 2004. http://dx.doi.org/10.2118/90288-MS.

Roussel, N. P., H. Florez, and A.A. Rodriguez. 2013. Hydraulic fracture propagation from infill horizontal wells. In Proceedings of the SPE Annual Technical Conference and Exhibition, New Orleans, Louisiana, 30 September–2 October 2013. doi:10.2118/166503-MS

Schlumberger. 1989. Log interpretation principles and applications. Sugar Land, Texas

Serra, O. 1984. Fundamentals of Well–Log Interpretation. 1 – the acquisition of logging data. Elsevier Science Publishers B.V.

CHAPTER 4

HVFRs in High TDS Environment

This chapter discusses the paper entitled "***How Does HVFRs in High TDS Environment Enhance Reservoir Stimulation Volume?***" published in the International Petroleum Technology Conference held in Dhahran, Saudi Arabia, 13 – 15 January 2020. https://doi.org/10.2523/IPTC-20138-Abstract

Abdulaziz Ellafi was responsible to prepare the methodology, analyze the data, validation and writing the paper. Co-authors are Hadi Jabbari, Xincheng Wan, Vamegh Rasouli, Mohammed Ba Geri, were involved in the review and editing of the draft, and Waleed Al-Bazzaz presented the presentation in the conference. Hadi Jabbari is the PhD advisor and was the director of the project.

Abstract

Improvement in hydrocarbon production from unconventional reservoirs, such as the Bakken Formation, is driven by drilling horizontal wells and multi-stage hydraulic fracturing. The main objective of a frac treatment is to create complex fracture geometry to increase well/reservoir contact area (i.e., large SRV; stimulated reservoir volume) by injecting larger fluid volume and high proppant concentration. The success of the treatment relies substantially on selecting appropriate fracturing fluids that transport the proppant particles

deep enough into the fractures. This research is aimed at studying the capability of high-viscosity friction reducers (HVFRs) by examining the produced water from the Bakken Fm through an integral approach. The application of surfactant as an additive to the HVFRs was investigated in high TDS (total dissolved solids) conditions. To assess the current industry practice for hydraulic fracturing in the Williston Basin, these tasks were performed: a) rate trainset analysis (RTA) to evaluate the current completion in Bakken wells by estimating fracture half-length and SRV properties, b) 2D/3D fracture simulation to study the impact of treatment fluids on fracture-network/SRV properties, and c) reservoir simulation to predict the estimated ultimate oil recovery (EUR) for identifying optimum hydraulic fracturing design. The results show that using a surfactant mixed with the frac fluids can lead to improved proppant transport, fracture conductivity profile, and thus higher effective fracture half-length compared to current practice. It was found that such a frac fluid mixed with surfactant can result in improved EUR by as high as 15% compared with linear gel and HVFRs with produced water (HVFR-PR) due to larger SRVs. Reusing produced water, including formation and flow back water can be a wise decision to minimize environmental footprint and reduce operating costs. The findings from this research can be applied to other unconventional shale plays, such as Eagle Ford and Permian Basin for comparison and optimization purposes.

4.1 Introduction

In the last decade, it a revolution in oil and gas production has been observed due to significant development in oil-bearing shale reservoirs using advancement technologies in horizontal drilling and multi-stage hydraulic fracturing. The objective of the treatment is to create complex fracture geometry by injecting a larger fluid volume and high proppant

concentration to enhance stimulated reservoir volume (SRV). The success of the treatment strongly relies on selecting appropriate fracturing fluids that transport and fill the proppant particles deeper into the fractures, while unsuccessful implementation design causes lower incremental oil recovery from SRV (Ba Geri et al., 2019d; McMahon et al., 2015; Li & Zhang, 2019). Therefore, research works have been done on improving the fracturing parameters, such as conductivity of fracture networks and fracture half-length using new fracturing fluids to produce efficiently more trapped oil in the pore matrix, minimize the formation damage due to fracturing fluids, and reduce environmental footprint (Kurtoglu, 2013; Ellafi et al., 2019b; Ba Geri et al., 2019d). Although Newtonian fluids (slickwater) and non-Newtonian viscous fluids are lower-cost fracturing fluids that are commonly used in the North America shale plays, these traditional fracturing fluids create poor fracture conductivity and short effective fracture half-length, causing smaller SRV proportionally to the total reservoir volume. In addition, the treatment consumes a large volume of freshwater, which is around 20,000 to 5 million gals of water, depending on the length of the horizontal lateral. Furthermore, reusing produced water, including formation and flow back water is getting great attention in the oil and gas industry since this alternative water source has many benefits, such as saves high-quality water for domestic and agricultural needs, minimize environmental footprint, and reduce operating costs (Fontenelle et al., 2013). Recycling water-based fluid treatment is challenging, which can contain a high amount of total dissolved solids (TDS), chemicals and suspended solids from previous treatments, and dissolved organic materials (Lord et al., 2013). The main concern is the stability of the fracturing fluids when salt content increases in aqueous-based fluids, where most of the treatment fluids are failed to carry proppant into the fractures. Thus, comprehensive studies in the lab have been conducted to understand the fluid characterization (viscosity and

viscoelasticity properties) of the fracturing fluids under harsh brine solution before run simulation and field trial using produced water as makeup fluid with fracturing treatment fluids (Walters et al., 2009; Demong et al., 2010; Seymour et al., 2018; Ellafi et al., 2019; Ba Geri et al., 2019; Almubarak et al., 2019).

In 2009, Walters et al. presented a new clean biopolymer-based fracturing fluid that showed a high capability to use with produced water. The lab results confirmed that the new fracturing fluids have significant conductivity, stable viscosity under different range of temperatures, low-pressure loss, and perfect proppant placement in deep fractures. Also, the fluid was used in the field to frac 14-stages over four wells. The field trial assessment reported that the outcomes in terms of production show high reservoir production performance as a result of more effective fracture half-length and proppant transport obtained during the operation. Ba Geri et al., (2019 a) introduced a critical review study that summarized the recent applications of high viscosity friction reducer (HVFRs) "typically long-chain polyacrylamides (PAM)" as fracturing fluids. The authors' goal was describing HVFRs capability in details, and the study concluded that the proposed fluids give high proppant transport, retain 100% conductivity, low operation cost, reduce of using chemicals by 50%, low pipe friction, high pump rate, minimize water consumption, decrease environmental concerns, and compatible with produced water. Moreover, Ba Geri et al., (2019 b, c, d, & e) addressed the evaluation performance of HVFRs in the high-TDS environment using Wolfcamp shale produced water. The research aimed to investigate the viscoelastic characterization by providing a full lab-based comparison of viscosity and elastic modulus between HVFRs and other fracturing fluids, such as linear guar gel, xanthan, and emulsion. The experimental work results confirmed that HVFRs is a stable fracturing fluid

compared to other types, which has good properties in high temperature and high-water salinity to proppant transport and diminishing turbulent flow results increase in pump rate up to 100 bbl/ min. The study provided the flow behavior index (n') and flow consistency index (k') that determined the rheological properties of HVFRs under high water salinity conditions. These values were used in our research simulation works to mimic the behavior of HVFRs using 3D hydraulic fracturing simulation.

In 2018, Seymour et al. investigated several surfactants to be used as additives to extend the salt tolerance on HVFRs performance. This research performed a series of experiments using a friction flow loop to detect the performance of HVFRs. Also, sodium and potassium brine effects were conducted using the Permian Basin produced water. This study concluded that the surfactant system extends the HVFRs workable at high TDS conditions. Adding the surfactant to fracturing fluids can assist in changing the intermolecular interaction between polymer fragment. As a result, the fracturing fluids can be utilized to inhibit formation damage and prevent flocculation. A surfactant system with fracturing fluids was reported to be an effective solution to prevent performance degradation in high TDS conditions (Palla et al., 2014; Xu et al., 2017). Limited research studies have introduced the surfactant additives in the fracturing fluids with produced water, but the surfactant is well known in the industry which was used in different applications and show ability in Interfacial Tension reduction and Wettability (WTB) Alteration. The authors have examined the usability of surfactant as a good candidate to enhance the performance of the fracturing fluids in high TDS conditions as well as improving oil recovery from unconventional shale plays.

This study is an extended work to our previous publications (Ba Geri et al., 2019 and Ellafi et al., 2019) to study the capability of HVFRs with produced water in unconventional rich

liquid reservoirs (ULR) using an integral approach (3D/2D Pseudo hydraulic fracturing simulator and numerical reservoir simulation). In this paper, optimizing hydraulic fracturing treatment is applied using Rate Transient Analysis (RTA) to enhance Bakken oil production by improving fractures networks around SRV using HVFRs with a surfactant in high TDS environment.

4.2 Case Study: Middle Bakken Formation

Figure 4. 1 presents the schematic of well-A, which is a parent oil well that was drilled horizontally with 9,800 ft lateral in one of the unit spaces of the Siverston field in the McKenzie County, Williston Basin, ND. The Middle Bakken Formation is the target zone at the measuring depth of 10,866 ft and 55 ft net pay thickness. The well hydraulically fractured using a sliding sleeve completion to frac 24 stages along the horizontal lateral. The spacing between the stages is 300 ft, and Table 4. 1 lists the main treatment design parameters used as a base case to create the representative treatment for the Middle Bakken using 3D-Pseudo simulation.

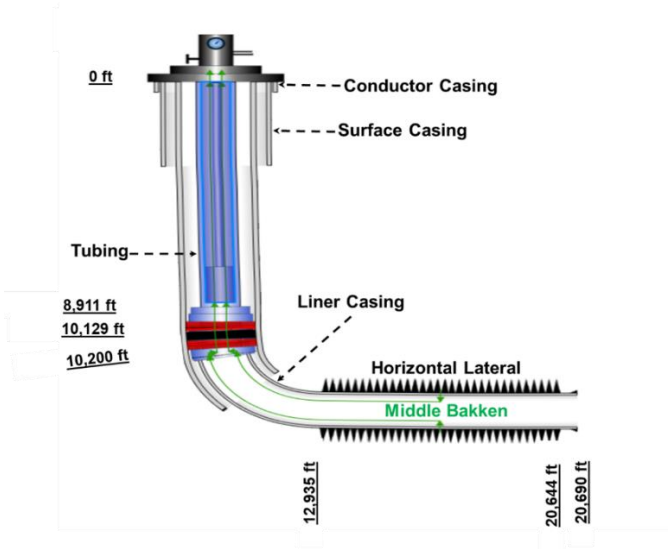

Figure 4. 1. Well schematic for Well-A.

Figure 4. 2 shows the production in well-A, which started in May 2011 to December 2015. In early 2016, the well was closed due to a sharp decline in production rate as a result of unsuccessful hydraulic fracturing design. Then, the fractures network around the SRV were depleted faster, while slow to no feed hydrocarbon production from the rock matrix.

Table 4. 1. Treatment parameters for the well-A "Base Case".

Fracturing Fluid Type (-)	Proppant Type (mesh)	Slurry Volume (U.S. gal)	Pump Rate (bmp)	Initial Proppant Concentration (lbm/gal)	Final Proppant Concentration (lbm/gal)
Slickwater	40/70 Sand	86,984	50	0.25	2

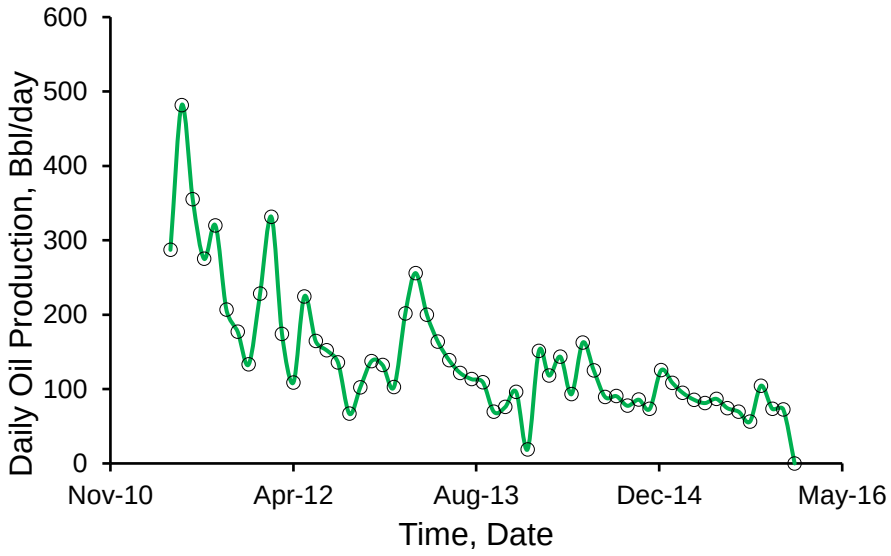

Figure 4. 2. Oil production history of the well-A.

4.3 Geomechanical Modeling of the Bakken Petroleum System (BPS)

One of the most important factors in designing hydraulic fracturing stimulation is geomechanical modeling, especially in unconventional shaly plays, such as the Bakken Petroleum System, which presents different magnitude and orientation of principal stress between Bakken Members.

Table 4. 2. Geomechanical properties of the Bakken Petroleum System.

Formation Name (-)	TVD @ Bottom (ft)	MD @ Bottom (ft)	Stress Gradient (Psi/ft)	Stress (Psi)	Young's Modulus (MMPsi)	Poisson's Ratio (-)
Lodgepole	10,867.1	11,024.7	0.610	6,609	7.40E+6	0.27
Upper Bakken	10,886.0	11,115.7	0.600	6,502	1.50E+6	0.28
Middle Bakken	10,941.0	-	0.590	6,535	6.00E+6	0.23
Lower Bakken	10,991.0	-	0.637	6,996	1.50E+6	0.25
Three Forks	11,091.0	-	0.641	7,110	6.00E+6	0.24

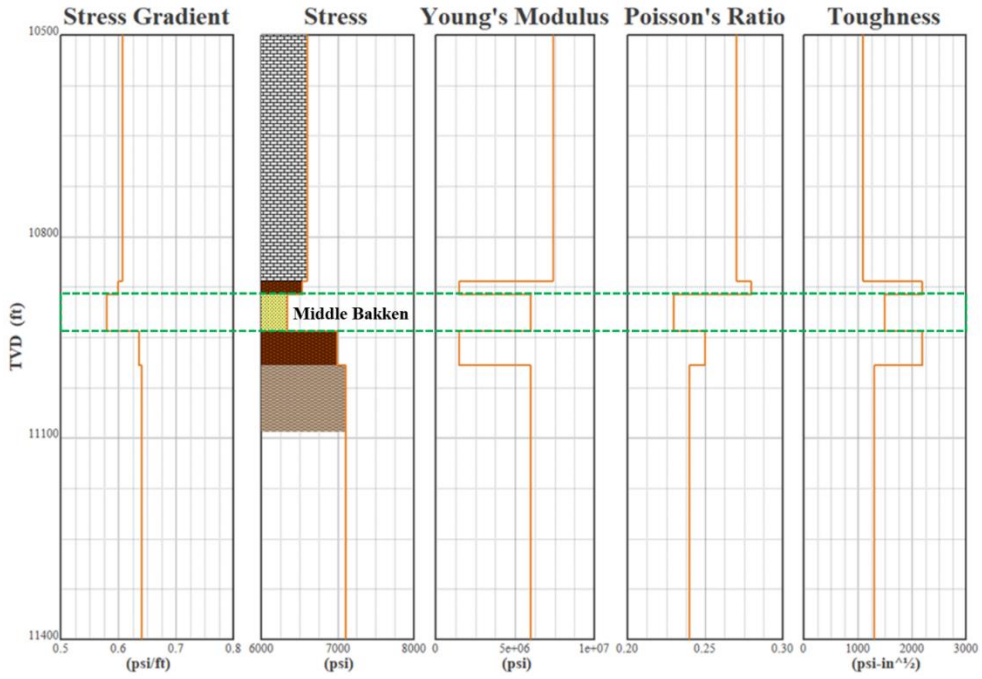

Figure 4. 3. Geomechanical model of the Bakken Petroleum System.

The microseisms studies suggested that the stress state could be a normal or strike-slip fault environment. The stress state is crucial to define, which can influence the hydraulic fracturing initiation and propagation (Yang et al., 2013).

The mechanical properties such as Young's modulus, Poisson's ratio, in-situ stress distribution, and rock strength of the target formation have an essential role to understand pre-existing fractures, create an effective design, and avoid complete or partial failure in hydraulic fracturing application in the shale oil reservoirs. Table 4. 2 shows the collected geomechanical parameters based on the Bakken Formation literature review in order to build proper geomechanical modeling using 3D-Psudo frac simulation. Figure 4. 3 illustrates the geomechanical model that represent Bakken layers, where our focus in on the Middle Bakken Formation.

4.4 Methodology

Figure 4. 4 illustrates the workflow used in this paper, which started by gathering the main reservoir and hydraulic fracturing data from the literature review and Oil and Gas Division-North Dakota Industrial Commission (NDIC) website. The next step, well logs data were used to build the geomechanical model that represents the Bakken Petroleum System in order to obtain a successful implementation design. After that, a representative Bakken case study hydraulic fracturing was designed using 2D/PKN model. The main data in Table 4. 1 were utilized as input to generate the optimum pump schedule based on 6 stages from a total of 24 stages along the lateral section of the well. Then, the base case model (slickwater), as shown in Figures 4. 5 and 4. 6 was created using a 3D Pseudo hydraulic fracturing simulator. Figure 4. 7 demonstrates the symmetric model that was built for simulation purposes using a commercial compositional simulator (CMG/GEM). Tables 4. 3 and 4. 4 lists the main reservoir parameters and model description, where the model simulated the hydraulic fractures explicitly using Local grid refinement (LGR), and the Peng-Robinson equation of

state (PR-EOS) was utilized to mimic the Bakken oil behavior under a wide range of pressures and temperatures, as listed in Table 4. 5.

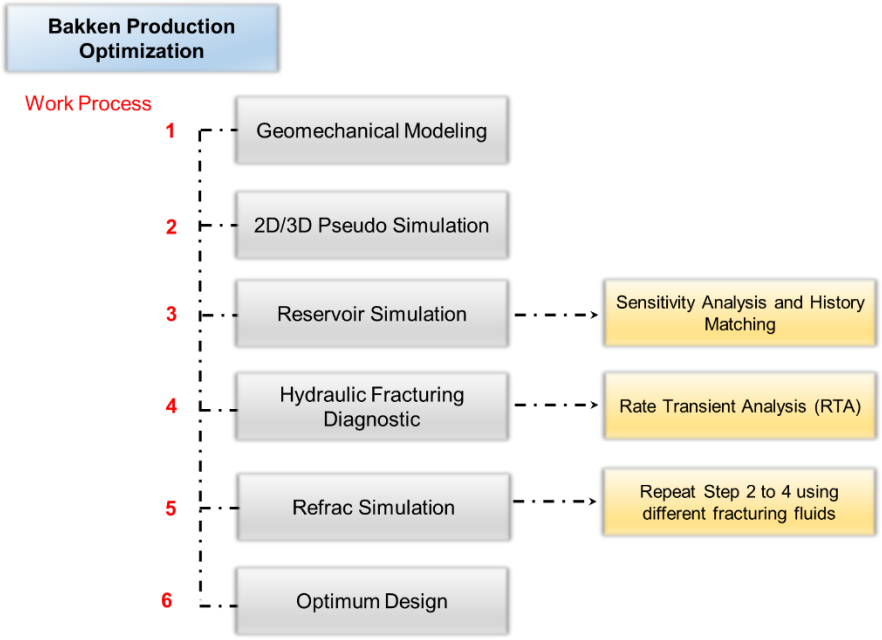

Figure 4. 4. Workflow process for the Bakken production optimization.

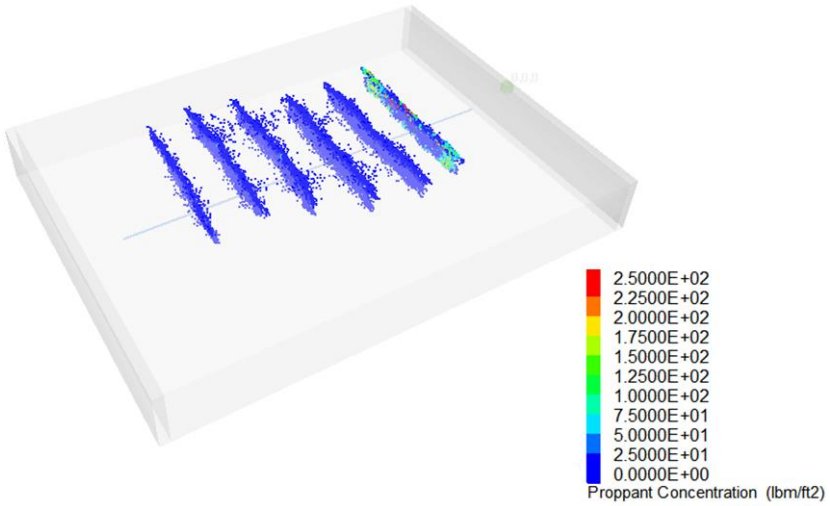

Figure 4. 5. Hydraulic fracturing treatment of the base case model through 6 stages.

The hydraulic fracturing file outputs were imported directly to the numerical reservoir simulator. Then, the calibration processes were performed for reservoir and fractures properties including relative permeabilities for both matrix and fractures. The main effective parameters on history matching of oil and water production trend were detected by sensitivity analysis. Reducing the global error method was applied through a history matching technique by using the CMOST reservoir simulation process, as shown in Figures 4. 8 and 4. 9.

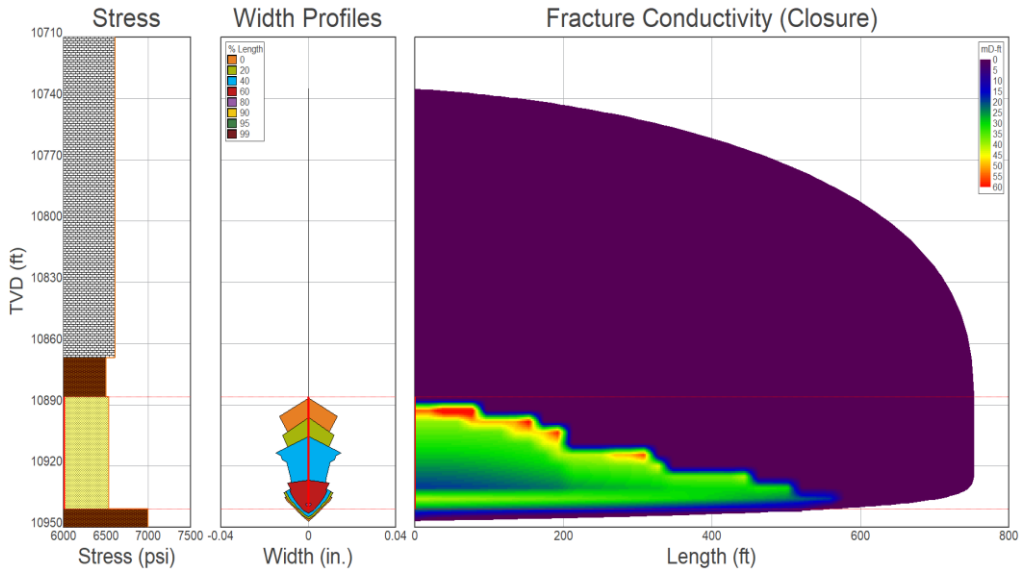

Figure 4. 6. Fracture conductivity profile effect of the base case model through single stage.

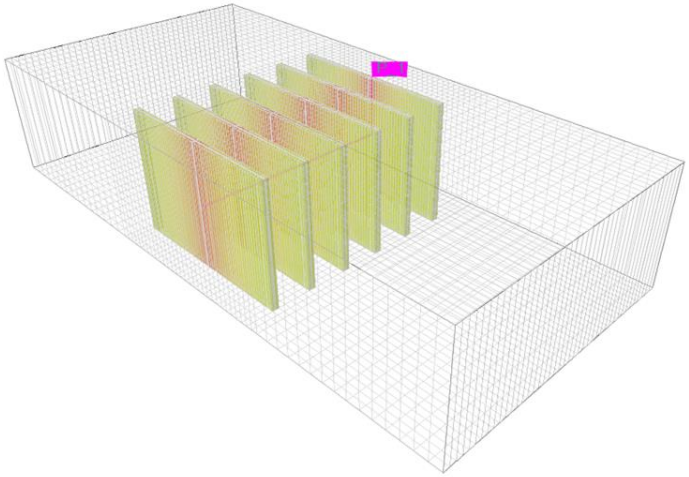

Figure 4. 7. The symmetric model with 6 stages of hydraulic fracturing.

Table 4. 3. The typical range of formation properties in Bakken Members.

Parameters	Bakken Members	Median Value
Thickness, (ft)	Upper Bakken	19
	Middle Bakken	55
	Lower Bakken	50
Porosity, (%)	Upper Bakken	4
	Middle Bakken	6
	Lower Bakken	4
Permeability, (µd)	Upper Bakken	0.010
	Middle Bakken	5
	Lower Bakken	0.010
Initial Water Saturation, (Fraction)	Middle Bakken	0.40
Total compressibility, (Psi^{-1})	Middle Bakken	1.00E-6

Table 4. 4. The model description and reservoir conditions.

Parameters	Value
Number of Grid, (#)	60×42×1
Model Dimensions, (ft)	5280×2520×55
Horizontal Well Length, (ft)	2,520
Number of Stages, (#)	6
Total Number of Fractures, (#)	42
Reservoir Pressure, (Psi)	6,555
Reservoir Temperature, (deg F)	213
Production Period, (Years)	5
Forecast Period, (Years)	5
Depletion Pressure (Psia)	1500

The main objective of the model was to generate as accurate bottom-hole pressure (BHP) as possible to reflects the production trend so to be used in the rate transient analysis tool (RTA) to diagnostic the production behavior using analytical and numerical models. Furthermore, the refracturing application was studies using alternative fracturing fluids (HVFRs) to extend

and enhance stimulation reservoir volume (SRV) in order to optimize the estimated ultimate oil recovery (EUR) for the Bakken oil well. Finally, the optimum design was chosen based on sensitivity analysis to obtain higher EUR in 5 years.

Table 4. 5. Bakken crude oil composition and PR-EOS parameters.

Component (-)	Mole Fraction fraction	Critical Pressure (atm)	Critical Pressure (k)	Molecular Weight g/gmole	Omega A (-)	Omega B (-)
CO2	0.0024	72.80	304.20	44.01	0.457	0.078
N2	0.0198	33.50	126.20	28.01	0.457	0.078
C1	0.2814	45.40	190.60	16.04	0.554	0.094
C2	0.1304	48.20	305.40	30.07	0.374	0.062
C3-NC4	0.1680	36.23	387.49	40.16	0.457	0.078
IC5-C8	0.1675	33.89	560.09	98.26	0.457	0.078
C9toC12	0.0943	20.13	687.81	127.51	0.457	0.078
C13toC18	0.0716	14.46	809.33	251.44	0.457	0.078
C19toC29	0.0547	14.42	893.97	326.02	0.457	0.078
C30toC44	0.0099	12.60	944.00	589.70	0.457	0.078

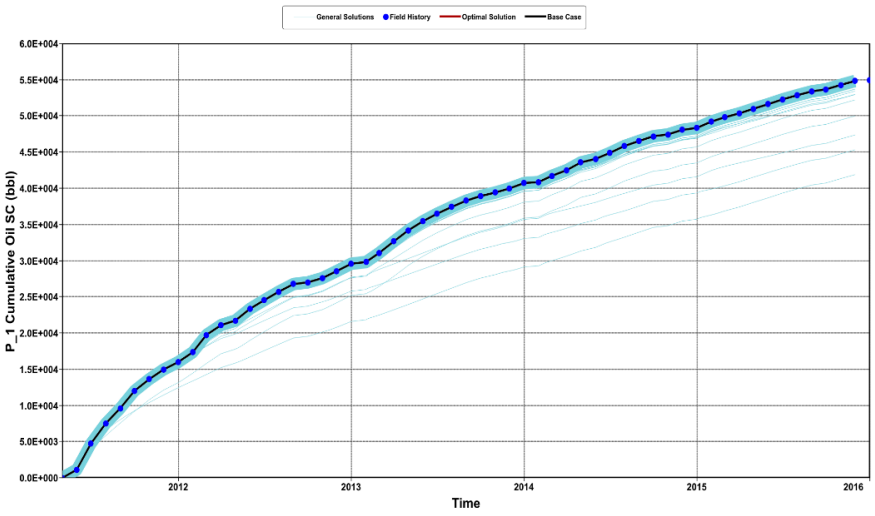

Figure 4. 8. History match of cumulative oil production.

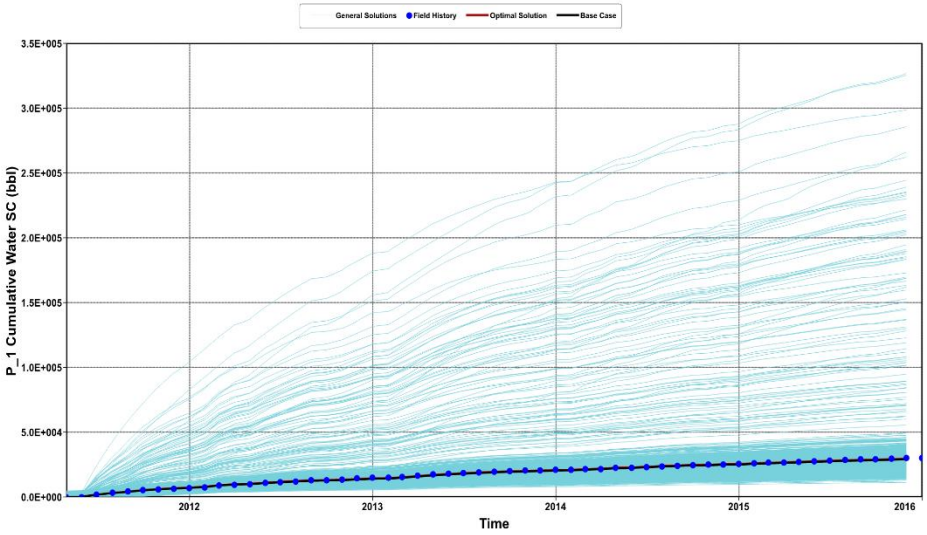

Figure 4. 9. History match of cumulative water production.

4.5 Pre-Refracturing Simulation Well Flow Behaviors

Figure 4. 10 presents the superposition plot, which consists of normalized pressure versus material balance square root of time. The diagnostic plot was used to investigate the production behavior of the pre-refracturing stimulation job. RTA analysis could be a powerful tool to understand and evaluate the completion status before and after applying hydraulic fracturing applications. In this paper, the superposition plot shows an initial linear flow at the early time when data point overlays on the straight line. It can be observed that the linear flow period is a short time interval that corresponds to the small SRV and short an effective fracturing half-length (Xf). The analytical solution results gave the first estimate of Xf and KSRV values, which are 255 ft and 0.0261 md, respectively.

On the other hand, Figure 4. 11 illustrates the boundary dominated flow, where there is a departure in the production trend from the straight line due to flow transition from initial linear flow to secondary pseudo linear flow that occurred outside of SRV. This is a common

behavior in the Bakken wells, where the rock matrix supports the fractures by pressure to feed more hydrocarbon through boundary dominated flow, as shown in Figure 4. 11.

The numerical validation results approved that the effective fracturing half-length is short in the range of 300 ft compared to total fracturing half-length 753 ft. The findings are in a good agreement with fracturing simulation results, where the propped fracturing half-length is approximately 330 ft. This concluded that the base case model (slickwater) was not able to transport the proppant into deeper fractures due to poor proppant packing. As a result, the production rate was declined sharply due to low fracture network conductivity that created small SRV. Table 4. 6 shows a comparison between RTA analysis and 3D Pseudo fracturing simulations. Based on these RTA results, the base case design was an unsuccessful implementation design and refracturing operation might be a wise decision to reproduce more effectivity from the Bakken well.

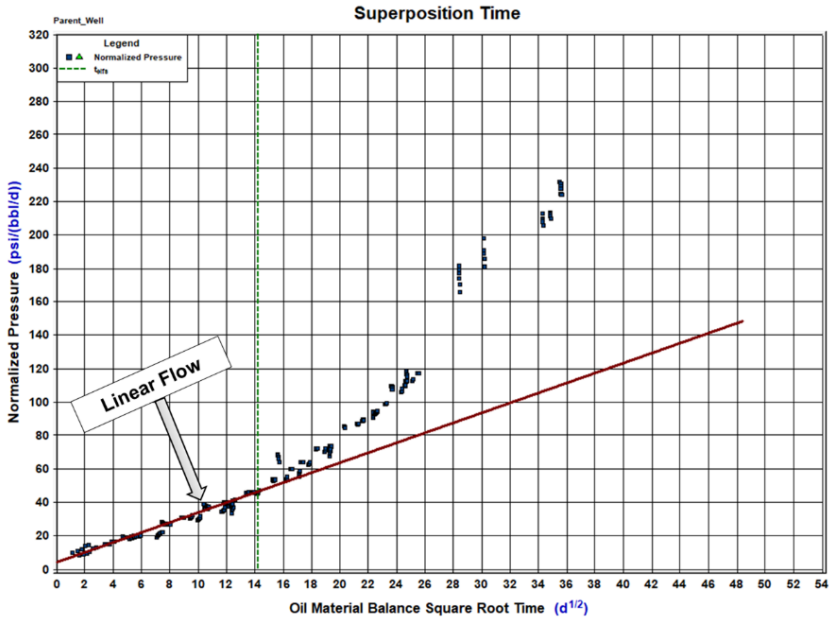

Figure 4. 10. Superposition time of the Base case model.

Table 4. 6. Results comparison between 3D Pseudo simulation and RTA numerical analysis.

Parameters	3D Pseudo Frac Simulation	RTA Analysis
X_f (ft)	330	300
F_{CD} (-)	12.5	9.7
K_{SRV} (md)	-	0.0193
X_i (ft)	-	150
A_{SRV} (acres)	-	25

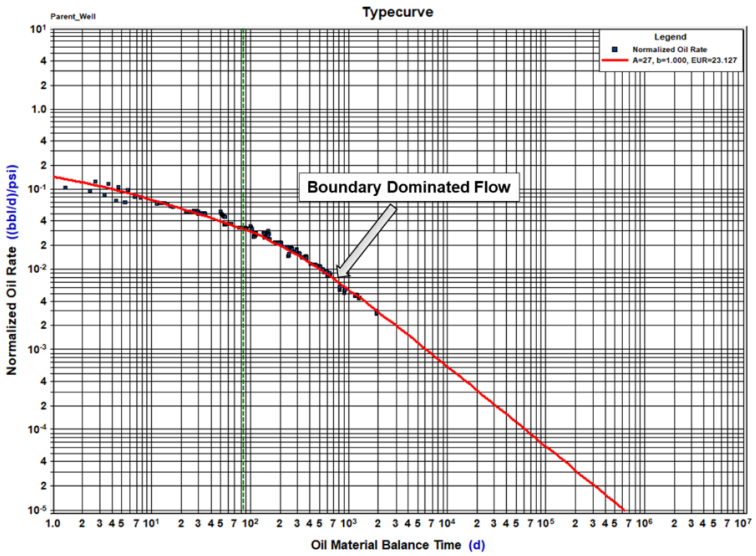

Figure 4. 11. Type curve of the Base case model.

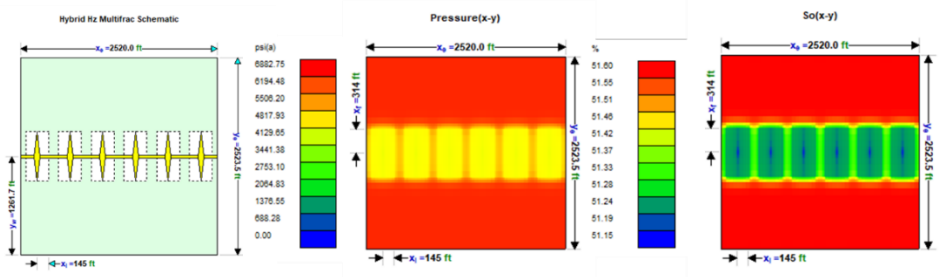

Figure 4. 12. Numerical schematic model, pressure distribution, and oil saturation distribution around SRV.

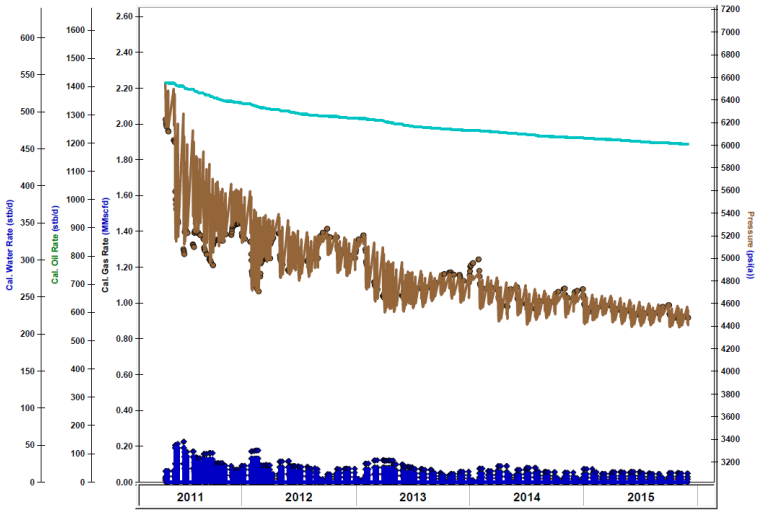

Figure 4. 13. Pressure history matching using oil volatile numerical model.

4.6 Refrac Simulation

Table 4. 7 shows the refracturing case studies, where the study was divided into three scenarios based on the fracturing fluid types as follows: Linear Gel, HVFR-PR (mixed with produced water), HVFR-PRS (mixed with produced water plus surfactant as additives). The sensitivity analysis was performed to investigate the production forecasting in 5 years in order to obtain the optimum design.

Table 4. 7. Summary of restimulation case scenarios.

Treatment Cases (#)	Type of Fluids (Name)	Pump Rate (bpm)	Final Proppant Concentration (Ibm/gal)	Proppant Size (mesh)
Case Study #1	Linear Gel	50	2	40/70
Case Study #2	HVFR-PR	50	2	40/70
Case Study #3	HVFR-PRS	50	2	40/70

4.7 Results and Analysis

Case Study #1: In this scenario, Linear Gel fracturing fluid was selected as an alternative fluid to compare with the base case model. Figures 4. 14 and 4. 15 present better designs

with higher conductivity and propped length area compared to the slickwater case. However, this model showed shorter fracture half-length with high fracture height that extended to Lower and Upper Bakken Formations.

Case Study #2 In the second scenario, produced water with HVFRs treatment fluid was investigated and compared with the base case model. Figures 4. 16 and 4. 17 illustrate high fracture half-length, which is around 500 ft compared to 400 ft using Linear Gel fluids that generated shorter X_f. However, the fracture conductivity profile in both fluids shows similar and closer results, which is not common in the HVFRs applications. This may be due to the fact that, the high-water salinity impacted the usual performance of HVFR and provided lower proppant transport due to degradation phenomena.

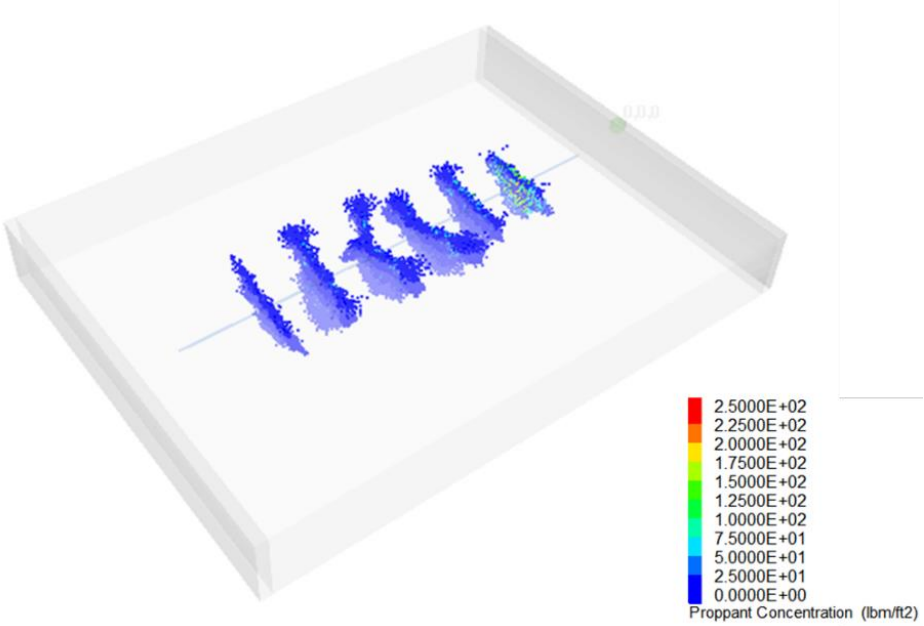

Figure 4. 14. Six stages of refracturing process using Linear Gel.

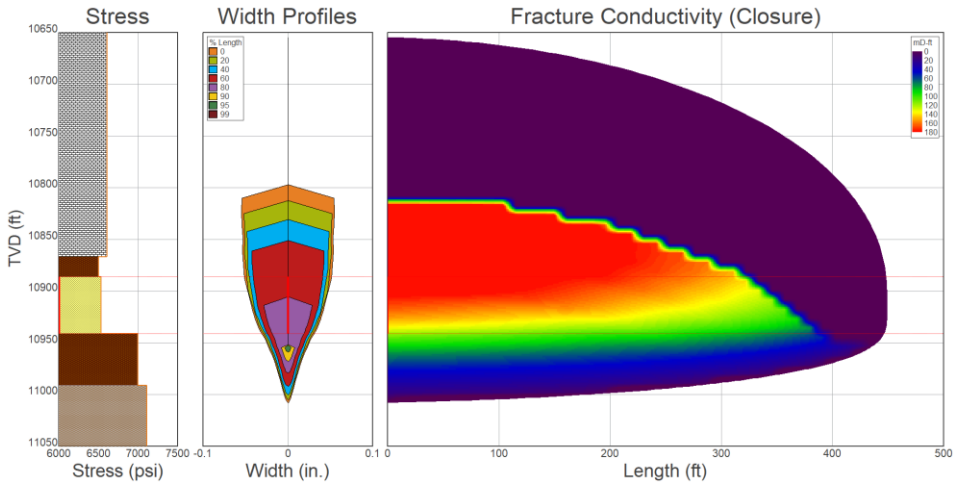

Figure 4. 15. Fracture conductivity profile effect of refracturing process using Linear Gel.

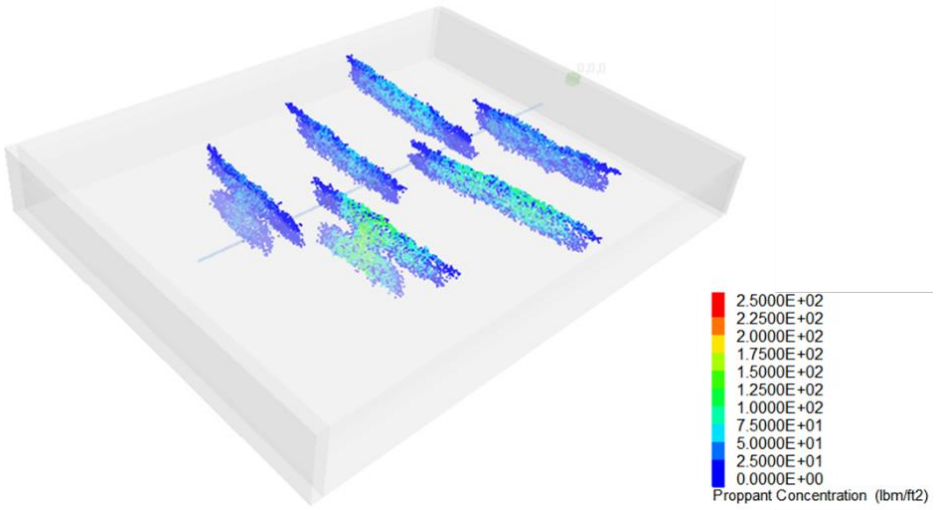

Figure 4. 16. Six stages of refracturing process using HVFR-PR.

Case Study #3 For the final case, HVFR with surfactant (HVFR-PRS) was tested as an optimized fluid and compared with the previous scenarios. The presented results in Figures 4. 18 and 4. 19 show better proppant transport, fracture conductivity profile, and high effective fracture half-length compared to other models. For example, the fracture half-length is around 500 ft compared to 550 ft using HVFR-PR. However, the fracturing conductivity is in the range of 36 md-ft, which is higher than the HVFR-PR case that created only 20 md-

ft. Also, proppant concentration in the surfactant scenario shows higher than HVFR-PR study by almost 40%.

Also, both cases 2 and 3 generated high fracture height that extended to Three Forks Formation. In the real field, this kind of design will cause more contribution to oil production from Three Forks Formation. But this might negatively impact the production performance by causing a frac-hit problem to the well that drilled in Three Forks Layer.

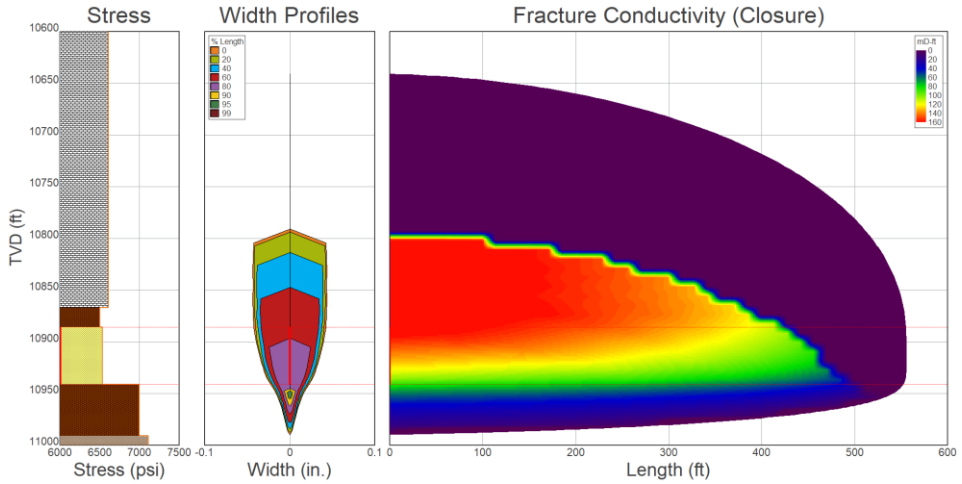

Figure 4. 17. Fracture conductivity profile effect of refracturing process using HVFR-PR.

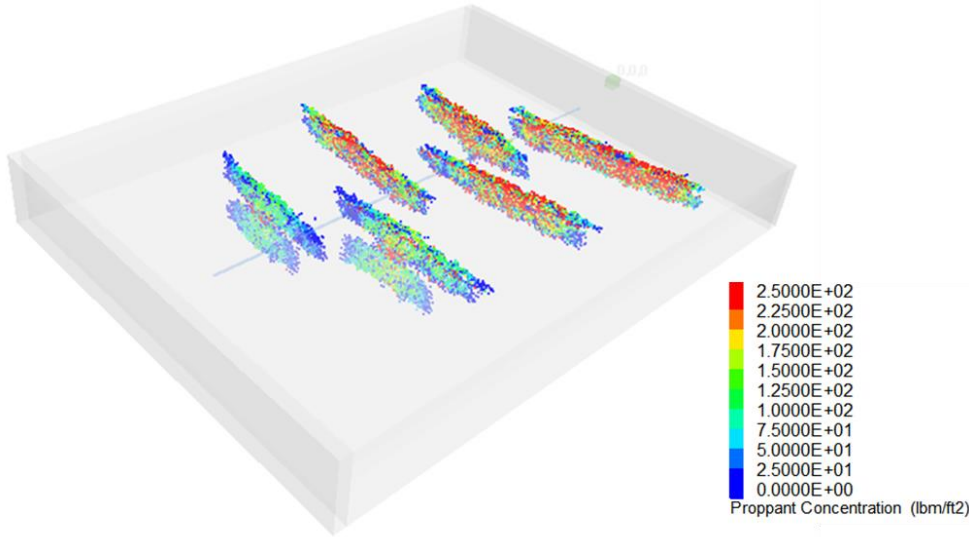

Figure 4. 18. Six stages of refracturing process using HVFR-PRS.

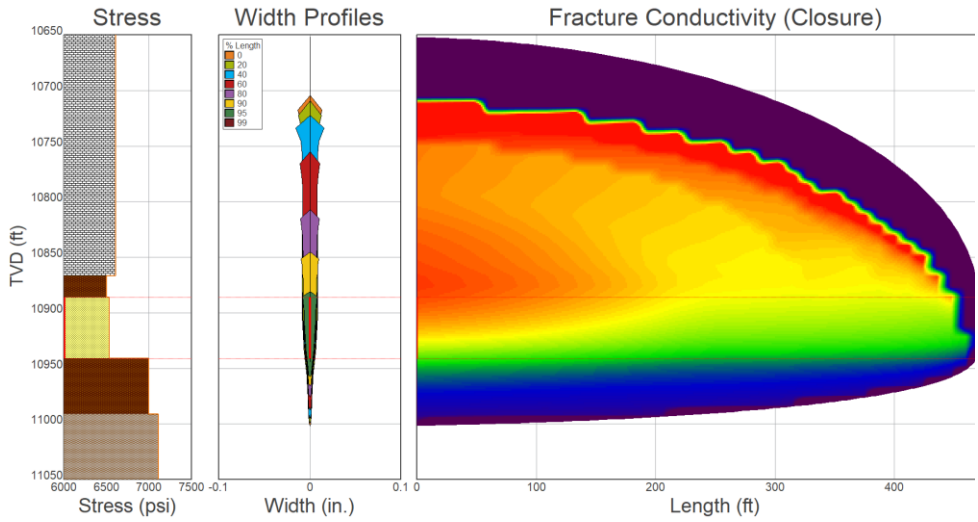

Figure 4. 19. Fracture conductivity profile effect of refracturing process using HVFR-PRS.

The surfactant as additives modified the rheological properties of HVFRs with produced water by preventing degradation, reduce viscosity and expand fluid viscoelasticity, and extend the flow behavior index (n') and flow consistency index (k') performance of the fracturing fluids to be able to carry proppant deeper up to secondary and tertiary fractures under high reservoir temperature, high TDS environment, and high to low shear rates, as shown in Figure 4. 18.

Interestingly, our simulation results are consistent with the experimental findings of Seymour et al., 2018, where they concluded that adding surfactant to treatment fluids can assist in changing the intermolecular interaction between polymer fragments. This suggests that the viscoelasticity model is the most important parameter for the fracturing fluids than viscosity to generate the optimum frac design.

This study does not consider the wettability alteration term in reservoir simulation. However, based on surfactant capability, the oil production performance in unconventional reservoirs

would be higher due to its function to change wettability from oil-wet toward water-wet conditions.

4.8 Effect of Fracturing Fluid Types on Bakken Oil Well Production

Restimulation application was developed for the Bakken well to enhance SRV as well as oil recovery at the depletion pressures. In this section, the numerical model was utilized to generate three case studies, as illustrated in Figures 4. 20 to 4. 25.

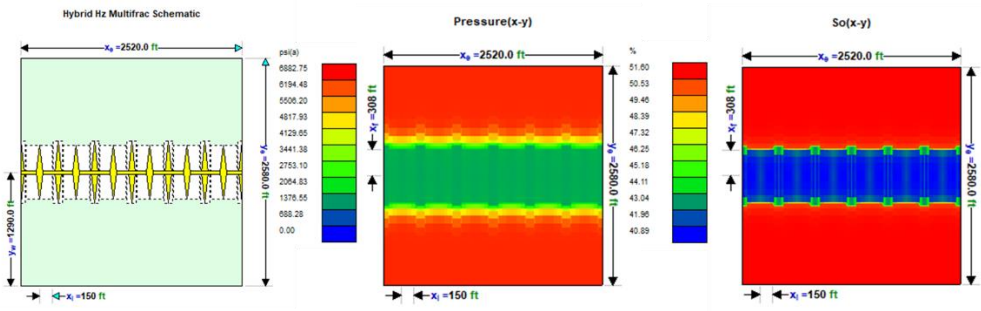

Figure 4. 20. Production forecast (Linear Gel), pressure distribution, and oil saturation distribution around SRV.

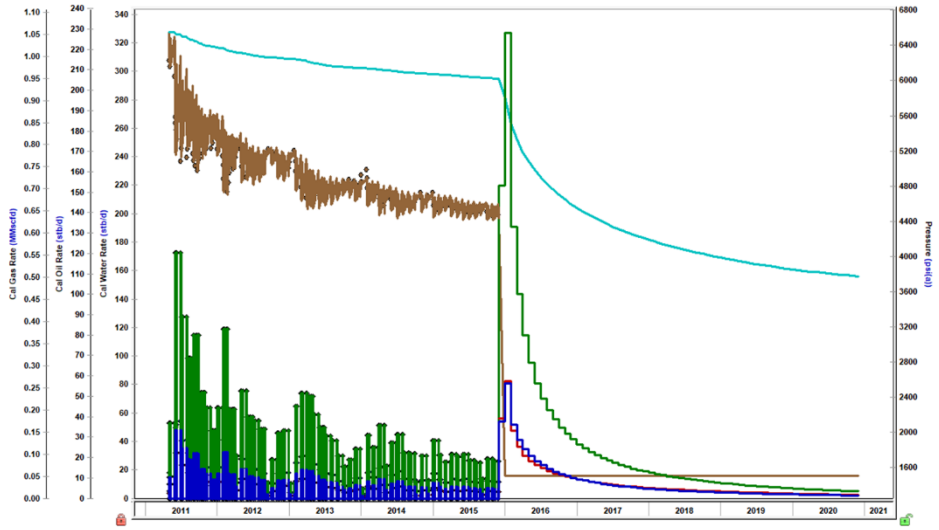

Figure 4. 21. Production forecast (Linear Gel) using oil volatile numerical model.

The findings are compatible with the 3D Pseudo hydraulic fracturing simulation. The ultimate oil recovery results are depicted in Figure 4. 26, where the oil recovery increased by 33% when the HVFR-PRS was used. This is a significant increase in EUR compared with Linear Gel and HVFR-PR due to extend and improve SRV region.

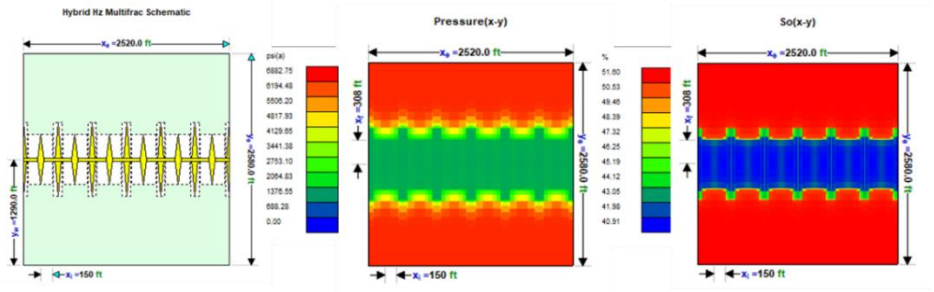

Figure 4. 22. Production forecast (HVFR-PR), pressure distribution, and oil saturation distribution around SRV.

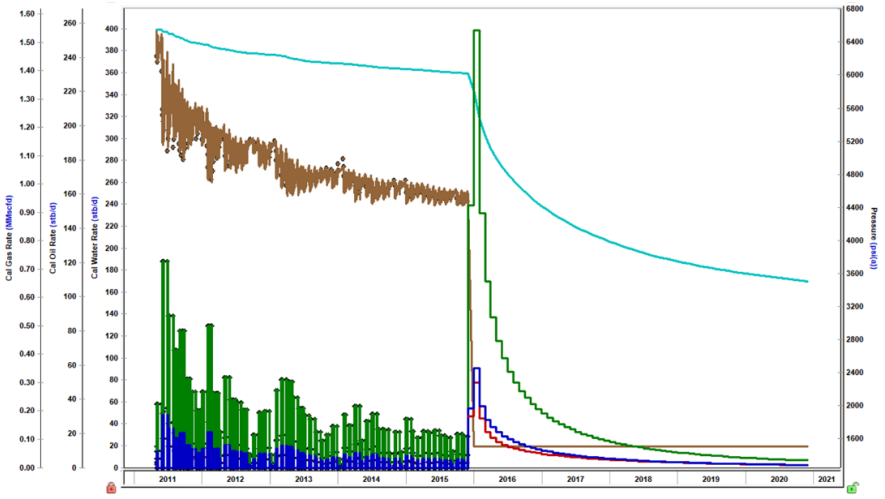

Figure 4. 23. Production forecast (HVFR-PR) using oil volatile numerical model.

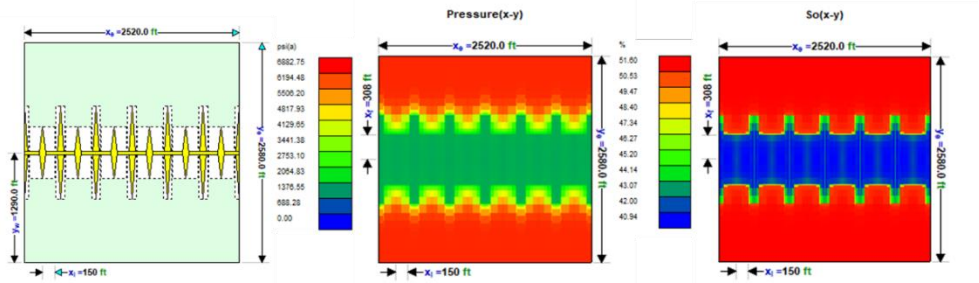

Figure 4. 24. Production forecast (HVFR-PRS), pressure distribution, and oil saturation distribution around SRV.

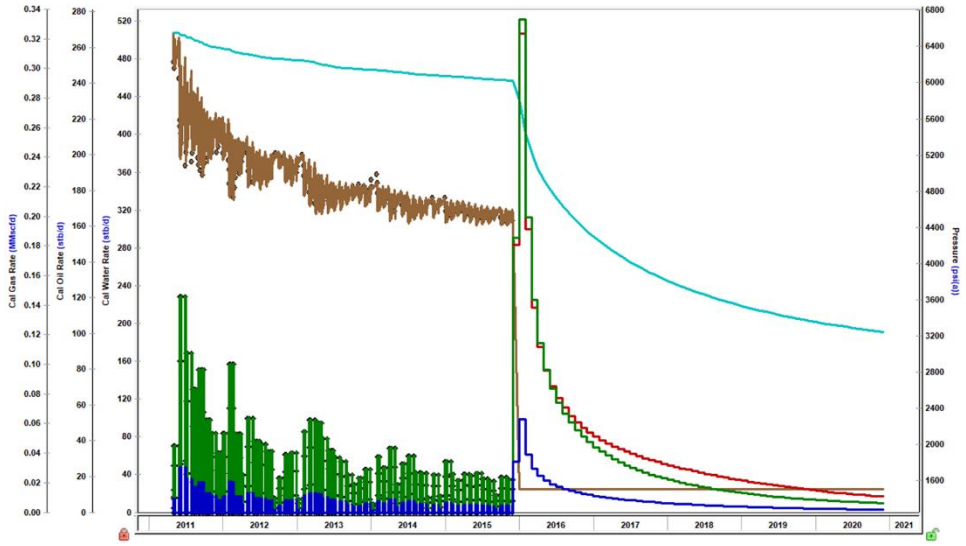

Figure 4. 25. Production forecast (HVFR-PRS) using oil volatile numerical model.

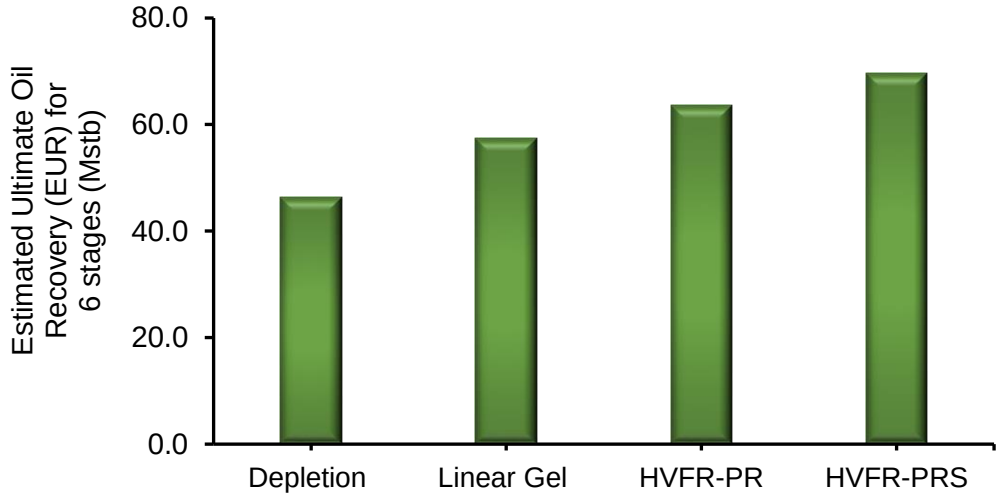

Figure 4. 26. Forecasting production using different operation Scenarios "Depletion Vs. Refracturing Application".

4.9 Conclusions

In this study, an integral approach was employed for frac treatment optimization in unconventional shale plays, such as the Bakken Formation. The research findings point out the following:

- The results from RTA (specialized square-root of time plot) of the Bakken wells understudy presented a boundary-dominated flow followed by a departure from the straight line indicating a secondary pseudo linear flow that occurred outside of SRV.
- Based on RTA, the slickwater model would provide smaller SRV region, where the effective fracture half-length is short, about 300 ft compared to a total fracture half-length of 753 ft. Therefore, using alternative fracturing fluids is essential to improve production in Bakken wells. The application of RTA to assess well/reservoir performance can be very helpful; especially, when microseismics data are not available.
- Hydraulic fracturing simulation (2D/3D) proved that utilizing surfactant and HVFR as fracking fluid can enhance proppant transport (i.e., longer effective frac half-length) and fracture conductivity, which means larger SRVs and improved stimulated wells performance.
- The surfactant as additives modified the rheological properties of HVFRs with produced water by preventing degradation, reducing viscosity, expanding fluid viscoelasticity, and extending the flow behavior index (n') and flow consistency index (k') performance of the fracturing fluids to be able to carry proppant deeper up to secondary and tertiary fractures.
- The surfactant model gives a significant increase by 15% in EUR compared with Linear Gel and HVFRs with produced water (HVFR-PR) due to extend and improve in the SRV region.

- Reusing produced water, including formation and flow back water has many benefits, such as saves high-quality water for domestic and agricultural needs, minimize environmental footprint, and reduce operating costs.

References

Almubarak, T., AlKhaldi, M., Ng, J. H., & Nasr-El-Din, H. A. (2019, August 1). Design and Application of High-Temperature Raw-Seawater-Based Fracturing Fluids. Society of Petroleum Engineers. doi:10.2118/195597-PA

Assady, A., Jabbari, H., Ellafi, A. M., & Goudarzi, B. (2019, August 28). On the Characterization of Bakken Formation: Oscillating-Pulse, Pulse-Decay Permeability Measurement & Geomechanics. American Rock Mechanics Association.

Ba Geri, M., Ellafi, A., Flori, R., Noles, J., & Kim, S. (2019d, October). Viscoelastic Characterization Effect of High-Viscosity Friction Reducers and Proppant Transport Performance in High-TDS Environment. Society of Petroleum Engineers. https://doi:10.2019/196014-MS

Ba Geri, M., Ellafi, A., Flori, R., Noles, J., & Kim, S. (2019e, November). A Comprehensive Review of Formation Damage Caused by High-Viscosity Friction Reducers: Wolfcamp Case Study. Society of Petroleum Engineers. https://doi:10.2019/197081-MS

Ba Geri, M., Imqam, A., & Flori, R. (2019a, April 8). A Critical Review of Using High Viscosity Friction Reducers as Fracturing Fluids for Hydraulic Fracturing Applications. Society of Petroleum Engineers. doi:10.2118/195191-MS

Demong, K. L., Sherman, D., & Affleck, B. (2010, January 1). The Tradeoff Between Surfactant Costs and Water Heating to Enhance Friction Reducer Performance. Society of Petroleum Engineers. doi:10.2118/138027-MS

Ellafi, A., & Jabbari, H. (2019a, August 28). Coupling Geomechanics with Diffusion/Adsorption Mechanisms to Enhance Bakken CO2-EOR Modeling. American Rock Mechanics Association.

Ellafi, A., Ba Geri, M., Bubach, B., & Jabbari, H. (2019b, August 28). Formation Evaluation and Hydraulic Fracture Modeling of Unconventional Reservoirs: Sab'atayn Basin Case Study. American Rock Mechanics Association.

Ellafi, A., Jabbari, H., Ba Geri, M., & Alkamil, E. (2019c, November). Can HVFRs Increase the Oil recovery in Hydraulic Fracturing Applications?. Society of Petroleum Engineers. https://doi:10.2019/197744-MS

Geri, M. B., Ellafi, A., Ofori, B., Flori, R., & Sherif, H. (2019c, July 31). Successful Implementation of High Viscosity Friction Reducers from Laboratory to Field Scale: Middle Bakken Case Study. Unconventional Resources Technology Conference. doi:10.105530/urtec-2019-447

Geri, M. B., Flori, R., & Sherif, H. (2019b, July 25). Comprehensive Study of Elasticity and Shear-Viscosity Effects on Proppant Transport Using HFVRs on High-TDS Produced Water. Unconventional Resources Technology Conference. doi:10.105530/urtec-2019-99

Jabbari, H., & Benson, S. A. (2013, January 1). Hydraulic Fracturing Design Optimization—Bakken Case Study. American Rock Mechanics Association.

Jabbari, H., & Zeng, Z. (2012, January 1). Hydraulic Fracturing Design for Horizontal Wells in the Bakken Formation. American Rock Mechanics Association.

Kurtoglu, B. 2013. Integrated Reservoir Characterization and Modeling in Support of Enhanced Oil Recovery for Bakken. Ph.D. dissertation, Colorado School of Mines.

Li, S., & Zhang, D. (2019, April 1). How Effective Is Carbon Dioxide as an Alternative Fracturing Fluid? Society of Petroleum Engineers. https://doi:10.2118/194198-PA

Lord, P., Weston, M., Fontenelle, L. K., & Haggstrom, J. (2013, June 26). Recycling Water: Case Studies in Designing Fracturing Fluids Using Flowback, Produced, and Nontraditional Water Sources. Society of Petroleum Engineers. doi:10.2118/165641-MS

McMahon, B., MacKay, B., & Mirakyan, A. (2015, April 13). First 100% Reuse of Bakken Produced Water in Hybrid Treatments Using Inexpensive Polysaccharide Gelling Agents. Society of Petroleum Engineers. doi:10.2118/173783-MS

Oil and Gas Division-North Dakota Industrial Commission (NDIC). 2019. https://www.dmr.nd.gov/oilgas/

Palla, C., Weaver, J. D., Benoit, D., Lu, Z., & Vera, N. (2014, November 10). Impact of Surfactants on Fracture Fluid Recovery. Society of Petroleum Engineers. doi:10.2118/171732-MS

Seymour, B., Friesen, D., & Sanders, A. (2018, August 9). Enhancing Friction Reducer Performance in High Salt Conditions. Unconventional Resources Technology Conference. doi:10.15530/URTEC-2018-2902709

Walters, H. G., Stegent, N. A., & Harris, P. C. (2009, January 1). New Frac Fluid Provides Excellent Proppant Transport and High Conductivity. Society of Petroleum Engineers. https://doi:10.2118/119380-MS

Wan, X., Rasouli, V., Damjanac, B., Torres, M., & Qiu, D. (2019, August 28). Numerical Simulation of Integrated Hydraulic Fracturing, Production and Refracturing Treatments in the Bakken Formation. American Rock Mechanics Association.

Xu, L., Lord, P., He, K., Riley, H., Koons, J., Wauters, T., & Weiman, S. (2017, April 3). Case Study: A Two-Part Salt-Tolerant Friction Reducer System Enables the Reuse of Produced Water in Hydraulic Fracturing. Society of Petroleum Engineers. doi:10.2118/184508-MS

Yang, Y., Zoback, M., Simon, M., & Dohmen, T. (2013, August 12). An Integrated Geomechanical and Microseismic Study of Multi-Well Hydraulic Fracture Stimulation in the Bakken Formation. Unconventional Resources Technology Conference. doi:10.1190/urtec2013-056

CHAPTER 5

Mechanisms of Huff-n-Puff, CO2-EOR: An Experimental Work

This chapter discusses the paper entitled "***Understanding the Mechanisms of Huff-n-Puff, CO2-EOR in Liquid-Rich Shale Plays: Bakken Case Study***" published in the SPE Canada Unconventional Resources Conference held in Calgary, Alberta, Canada, 29 September – 2 October 2020. https://doi.org/10.2118/200001-MS

Abdulaziz Ellafi was responsible to prepare the methodology, analyze the data, validation and writing the paper. Hadi Jabbari is the PhD advisor and was the director of the project.

Abstract

A revolution of unconventional reservoirs is a turning point in the global oil and gas industry since these resources have massive reserves with large potential in contributing to hydrocarbon production. Previous EOR laboratory experiments and simulation studies in the literature illustrated promising results in terms of recovery factor for different EOR applications, such as CO2, surfactant, and natural gas. However, pilot tests performance reported contrast behavior due to misleading predicting for the EOR physics processes. This paper presents the experimental work to evaluate the feasibility of CO2-EOR using the huff-n-puff (HNP) protocol in the Middle Bakken (MB) Formation, the Mountrail County,

Williston Basin, ND. We evaluate the oil recovery from CO2-EOR under several scenarios of operational and well/reservoir conditions. The parameters considered in the sensitivity study include temperatures, pressure, soak time, and number of injection cycles to obtain optimum conditions under which the incremental oil recovery from the MB Formation is increased. The wettability alteration (i.e., contact angle) was also studied using rock-chip samples before and after the HNP experiment at the Bakken reservoir conditions (present for example P & T in psi/F). The outcomes indicated on the effect of the reservoir temperature and pressure on the performance of the CO2, where the recoverable oil increases as the temperature and pressure increase until reach the optimum. As a previous research outcome, the number of cycling and soaking time are crucial design parameters for the HNP experiment and on the field as well to let the CO2 time to diffuse into the deep formation and swell more oil. In addition, the wettability alteration was changed by CO2-EOR as injection pressures increase and the wetting phase move from the oil-wet toward the water-wet system. As overall outcomes from this research, the CO2 HNP process has a good potential in the lab and could be succeeded economically in field applications that might reduce the need for refracturing stimulation or infill drilling.

5.1 Introduction

A revolution of unconventional reservoirs is a turning point in the global oil and gas industry since these resources have massive reserves with large potential in contributing to hydrocarbon production. In recent years, the domestic oil production from liquid-rich shale (LRS) reservoirs in North America have shown immense development, and the production has dramatically increased in the “top producers” American oil fields: Bakken, Eagle Ford, and Permian Basin. The total U.S oil production from conventional and unconventional

reservoirs 16.5% was produced in 2008 compared to nearly 60% in 2019 (The Energy Information Administration (EIA), 2019). Currently, these shale plays have the most drilling and completion activities in the U.S., with the number of wells in each play at over 12,000 producing either oil or gas (EIA, 2020; Drilling Info, 2019; FracFoucs, 2019). EIA outlook data in 2050 shows that the U.S. shale plays' daily production rate will be extended to 70% of the total U.S. daily oil production. This improvement in hydrocarbon production is driven by applying modern horizontal drilling and multi-stage hydraulic fracturing that make it a reality to access low porosity (<10%) and low permeability (<0.1 mD) formations (Ellafi et al., 2020a; Ba Geri et al., 2019a). In the Bakken Formation, a complex-fracture geometry system is often generated as a result of significantly distributed in natural fractures. Although breakthroughs in unconventional technologies have been achieved to create larger stimulated reservoir volume (SRV), the oil recovery is believed to be less than 8% due to sharply decline in oil production rates after the fractures depletion with small to no recharge from the ultra-tight matrix blocks (Jin et al., 2017; Sheng, 2015). The estimated oil reserves in the Bakken Sweet Spots is around 500 billion barrels of oil, and only 30 to 40 billion barrels of oil can be produced with current technology (Energy & Environmental Research Center (EERC), 2019; Continental Resources, 2018). Therefore, the unrecovered hydrocarbon from tremendous storage is isolated in tight pores without using unconventional applications, such as improving oil recovery (IOR) and enhanced oil recovery (EOR) methods. The common questions are asking by people in the industry and required to answer: what are the methods, how the process works, and can these applications enhance incremental oil recovery in a commercial way.

The current options that are used and gaining more attention in the industry to revive the performance in unconventional wells are infill drilling and refracturing treatment applications. The refrac treatment is performed by injecting fracking fluids, such as high viscosity friction reducers (HVFRs) through the fractures of the previous job and/or new entry points to create new fracture clusters with smaller fracture spacing in order to enhance production performance (Ellafi et al., 2020a; Ba Geri et al., 2019b). Based on the drilling spacing unit (DSU) and imposed government regulations, up to 20 wells can be drilled and stimulated from a single well pad to produce economically sound and financially profitable oil from unconventional shale plays (Ahmed and Meehan, 2016). However, these development applications of shale reservoirs have reached a challenging point, where the operators in North America face problems in terms of management and environmental issues. For example, the successful restimulation application is required a careful selection of the design parameters: treatment fluids, proppant type, completion method (diversion or isolation), design of refrac stages, and the selection of proper well candidate (Ellafi et al., 2020b; Ba Geri et al., 2020). As a result, the uncertainty is significant and difficult to infer which the most critical factors due to high cost and unavailable diagnostic tools to improve prediction of post refracture treatment design. On the other hand, the treatment process is being re-evaluated the long-term impacts on environmental perspective, where the critics claimed that the hydraulic fracturing uses materials would contaminate groundwater resources and toxic air emissions (Ellafi et al., 2020b; Chen et al., 2014).

There are a number of papers mentioned that refracturing process is crucial methodologies to expand the oil and gas production from unconventional reservoirs, while others (Jin et al., 2019; Gubian, 2017; Cipolla and Wallace, 2014) claimed that the increase in the well lateral

length, number of fracture stages, and proppant mass loading will not improve the incremental oil recovery more enough proportionally to operating cost. Furthermore, seeking a way to keep sustainability and enhance oil recovery in unconventional reservoirs, such as EOR has become an emerging technology to access more remaining oil and improve the long-term well productivity from cost-effective operations (Ellafi et al., 2020a; Ellafi and Jabbari, 2019a; Lashgari et al., 2018; Kurtoglu, 2013; Shoaib and Hoffman, 2009).

According to EIA, increasing in one percent of the oil recovery in LRS reservoirs could lead to increase the technically recoverable oil by 10 to 25 billion barrels of oil as well as improve the net present value (NPV) of a field (Jin et al., 2019). Therefore, any effort to improve the recovery factor through an EOR process, such as gas-injection is worthwhile. The extraction technique would reduce the remaining oil from the nano-darcy pores media and increase the oil recovery factor up to 10% (Mahzari et al., 2019). Most recent EOR experimental investigations and numerical simulation studies reported that miscible and immiscible gas injection processes, such as associated-produced gases (C1, C2, & C3), carbon dioxide (CO2), and nitrogen (N2) are the most effective EOR agents due to larger injectivity and lower viscosity (Alfarge et al., 2017; Kurtoglu, 2014). These applications might take tight formations to the level up to 20% of incremental oil recovery (Wang et al., 2019; Thakur, 2019). In contrast, Bakken Formation makes traditional EOR processes are extremely challenging to implement due to its lower characterization rock quality. As a result, normal water flooding or continuous gas injection are not applicable for unconventional reservoirs due to poor seep efficiency and low injectivity that can take long payback period. The only way can overcome mitigate the negative effect of fractures in unconventional reservoirs if the huff-n-puff (HNP) approach is used to inject large volume of gas into high conductivity

fracture extend area, then produce oil through the same well at different time interval (Yu et al., 2014; Gamadi, et al., 2013).

Hawthorne et al. 2013 summarized the gas injection EOR process in unconventional reservoirs in five conceptual steps as follows: 1) gas flows into and through the fracture networks, 2) injected gas exposed at the fracture surfaces into rock matrix, 2) the gas penetrates the tight pores carrying some hydrocarbon inside the rock matrix by pressure, but this step assists to reduce the oil viscosity by swelling mechanism and extract more oil out of the nano-porous media, 4) by swelling and viscosity reduction mechanisms, the hydrocarbon migrates to micro-porous media (fractures system), and 5) the migrate process caused by gas injection pressure gradient that becomes smaller, then molecular diffusion mechanism drives oil flow slowly from nano-porous to the fracture networks. Based on Hawthorne's explanation, unconventional reservoirs have shown two distinguishable flow regimes: viscous flow in the high permeability fracture network and diffusion dominated flow in the low permeability rock matrix. Improving incremental oil recovery in tight formations relies on enhancing the ability of diffusion mechanisms from the rock matrix with significant oil recovery to the fracture system (Jin et al. 2017). Understanding the HNP mechanism, which is the focus of this paper, guide to enhance oil recovery and improve the long-term well productivity. Subsequently, this process is a profitable operation that might reduce and/or limit the need for refracturing stimulation and/or infill drilling, especially when the oil prices are going down (Jin et al., 2016; Hawthorne et al., 2013).

However, the pilot tests assessment report in the Bakken Formation showed contrast behavior due to misleading predicting for the EOR physics processes from lab to field. Today, the industry needs to know many of the key questions remaining unanswered regarding the

optimum HNP operation conditions, uncertainty factors of unconventional EOR adsorption/diffusion mechanisms in the field scale, solvent-fluid-rock minerals interaction, nano-confined oil (PVT) effect during depletion and EOR process, damage because of changing in fluid composition and reservoir conditions (asphaltene precipitation), and the full economic analysis study compared to current options (i.e. refrac & infill drilling).

This study presents a comprehensive review and experimental investigation to assess the feasibility of CO2-EOR using the HNP protocol in LRS reservoirs. We first reviewed several publications to gain a deeper understanding of the CO2-EOR mechanisms and address opportunities and challenges in the Williston Basin. In the lab, we evaluate the oil recovery from CO2-EOR using the Middle Bakken (MB) formation, the Mountrail County, Williston Basin, ND core samples under several scenarios of operational and well/reservoir conditions. The design parameters considered in the sensitivity study include temperatures, pressure, soak time, number of injection cycles, and depletion pressure to obtain optimum conditions under which the incremental oil recovery from the MB core samples is increased. Moreover, the wettability alteration (i.e. contact angle) was also studied using rock-chip samples before and after the HNP experiment at the Bakken reservoir conditions (present for example P & T in psi/F).

5.2 Bakken Petroleum System (BPS), Williston Basin

The Williston Basin is a shared area between the United States and Canada. The basin occupies about 225,000 square miles of the subsurface and covers parts of Eastern Montana, Southern Saskatchewan, Manitoba, and Western North Dakota. The most productive formation in the Williston Basin is the Bakken Formation or known as the Bakken Petroleum System (BPS). The initial oil in place is estimated between 100 to 900 billion barrels of oil,

and cumulative oil production in the last 10 years is approximately 1 billion barrels (bbl) of oil from several reservoirs through over 10,000 wells in Parshall, Sanish, Reunion Bay, Bailey, Murphy Creek, Antelope, and Elm Coulee Fields (North Dakota Industrial Commission (NDIC), 2019; Jin et al., 2016). This recoverable oil represents approximately 1-2% of the total unconventional oil reserve with the available technologies today (Sheng, 2015; North Dakota Council, 2012). Figure 5. 1 demonstrates the Bakken production performance in December 2019 of several counties in North Dakota State (ND), where our study focuses on Mountrail County as marked by the gold star.

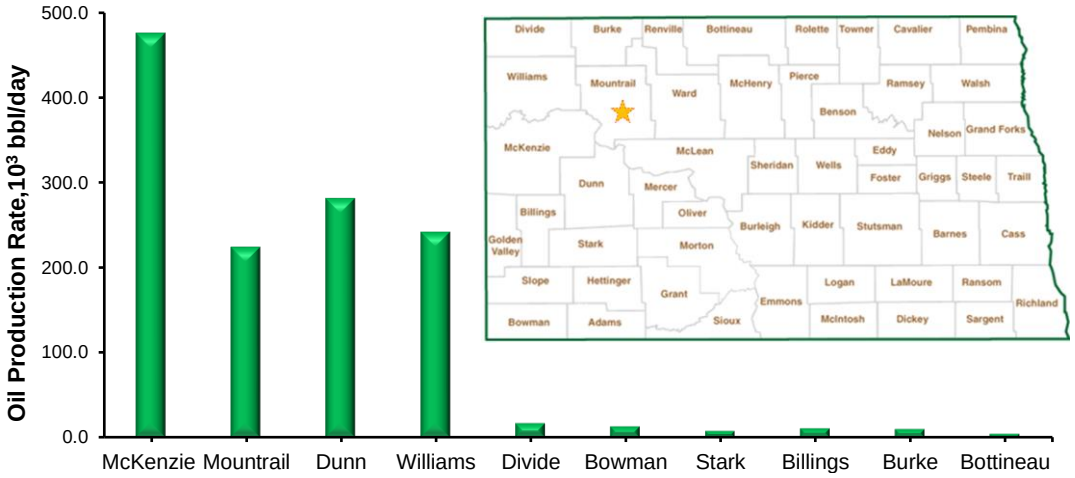

Figure 5. 1. Bakken oil production performance of North Dakota counties in December 2019 (NDIC, 2019).

5.3 Bakken Well Performance

Most unconventional wells spend years producing by primary depletion in the transient flow until hydrofractures around SRV begin to deplete, and the wells switch to boundary-dominated flow (BDF) (Male, 2019). For instance, Figure 5. 2 presents the average Bakken wells oil production rate begin with a high production rate due to high initial reservoir pressure (initial pressure greater than 6,500 psi) and significant conductivity and connectivity

between fractures. Moreover, the rapid decline was observed by around 75% after two years of begin producing because of large flow resistance at the matrix-fracture interface due to closure of natural and/or induced fractures. Thus, the increase in net stress leads to a zero-pressure gradient (formation pressure equal to initial reservoir pressure) of the fluid flow from the rock matrix into the fracture.

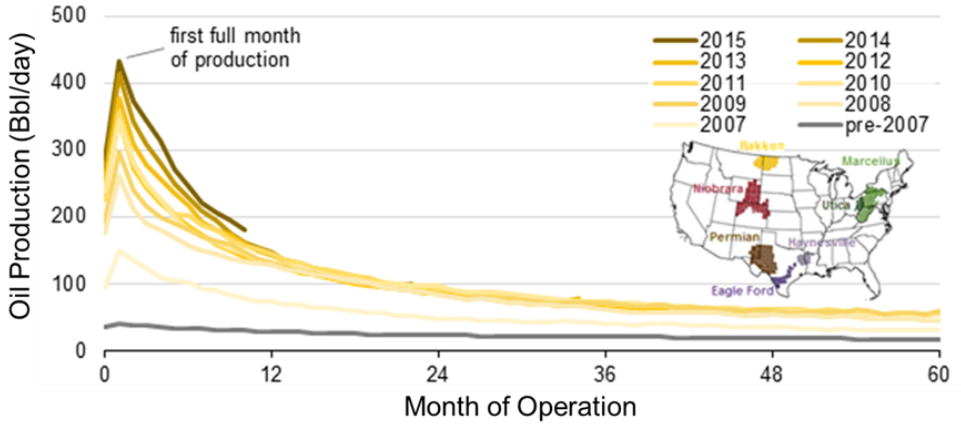

Figure 5. 2. Average oil production per well in the Bakken formation (EIA, 2019).

Figure 5. 3 illustrates Male's research that show water cut maintains constant over entire life of the Bakken wells at 40%. This means most of the produced water is the formation water that produces as a result of water level near the reservoir (the overlying Lodgepole Formation), while low percentage of flowback water caused by treatment fluids. The Permian Basin behaves similar to the Bakken Formation, but with higher water cut that excess of 70% of total liquid production.

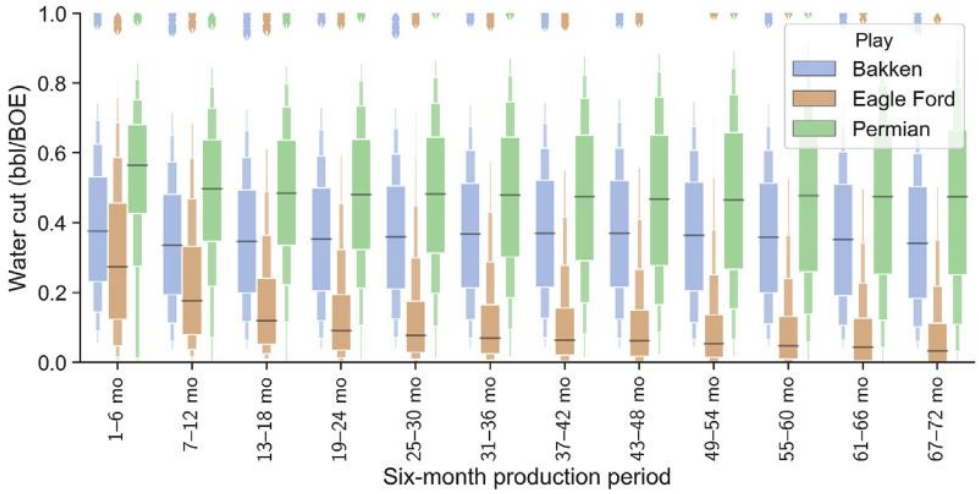

Figure 5. 3. The change in water cut over time in the Bakken Formation compared to other U.S. shale plays (Male, 2019).

On the other hand, the Eagle Ford started with a higher water cut, which is likely caused by the flowback water at 30%, and then the water depleted to produce at a constant value of around 10%. The change in water cut over time indicates that the geological description of the formation plays an important role in the percentage of produced water production. In case of the Middle Bakken tight formation, the capillary effect is greater than the gravity segregation due to a stabilized water cut that indicates the pore space contains both free water and oil (Jin et al. 2017).

As shown in Figure 5. 4 gas/oil ratio (GOR) remains constant over entire life of the Bakken wells at average 1,000 Scf/Stb compared to Eagle Ford and Permian Basin, where GOR started at 2,000 SCF/STB and increased to reach around 4,000 SCF/STB over the first three years of production. GOR behavior in the Bakken Formation indicates that most of the gas is dissolved into oil and confined in the formation, and the primary production mechanism is the oil expansion drive with slowly releasing the gas with oil production.

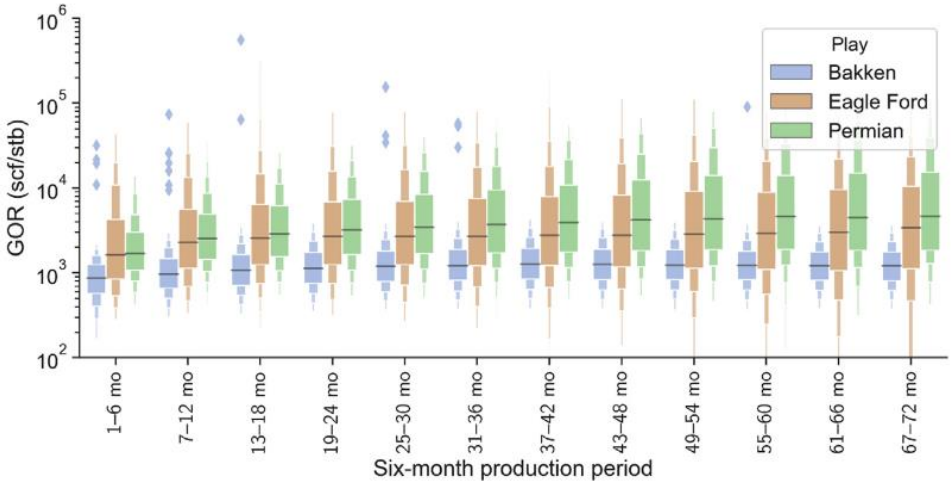

Figure 5. 4. The change in gas/oil ratio over time in the Bakken Formation compared to other U.S. shale plays (Male, 2019).

Tran et al. 2011 published a research study that introduced the types of well production trends in unconventional wells and the outcomes of the interpretation utilize to calculate original oil in place (OOIP) and the area of matrix drainage between fractures (Acm). The research is mainly focused on the Bakken Formation, where 146 wells with twenty years of the production histories in the nine different counties in North Dakota were analyzed, and the work classified the production performance into three categories using production decline analysis and semi-analytical of linear dual-porosity Stehfest. Half of the wells are under Type I, which is defined as the production behavior when the reservoir pressure drops below the bubble point pressure, and the trend can be recognized on the GOR curve versus time plot.

In addition, the type I is divided into three sub-types production performance as follows: a) production behavior has less support from the rock matrix, which is shown a fast decline then after a period of time the behavior changes to a steady and a slow decline in production, b) strong support from the rock matrix, it can be noticed with a short rapid decline at the beginning of production followed by an almost steady production 6 trend, and c) the

production behavior has not any support, and the oil recovery is only through the fracture network. The behavior can be recognized as a sharp decline in the oil production trend and continues for the entire well life, as summarized in Figure 5. 5.

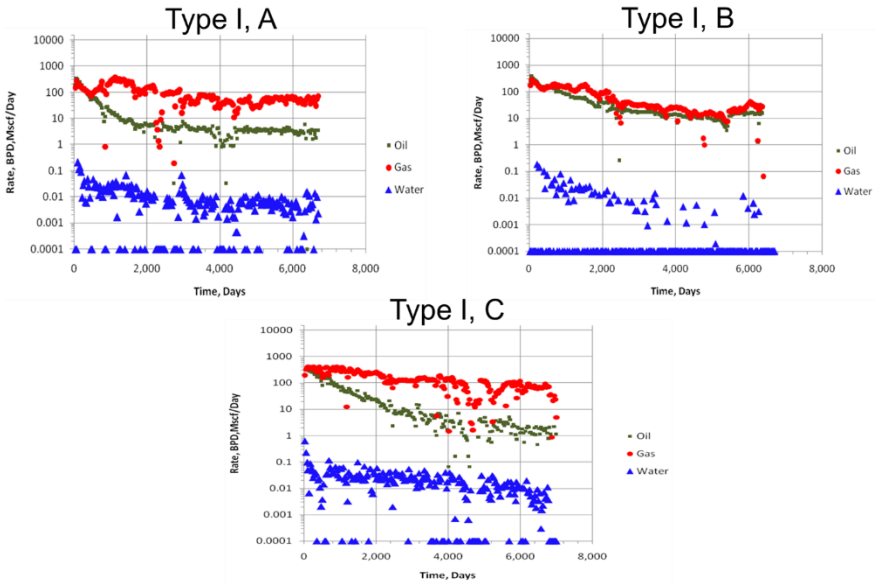

Figure 5. 5. The production trend for the Bakken wells under Type I (Tran et al. 2011).

Furthermore, Figure 5. 6 demonstrates the Type II, which is observed for some wells, as a half-slope on the log-log plot of the oil rate versus time when the reservoir pressure is above the bubble point pressure, and the produced oil flow is linear from the matrix into the fractures (oil production only from the matrix). Also, the GOR is almost constant for the entire production life, as illustrated in Figure 5. 6. Finally, the rest of the wells are under Type III, which is shown unclear behavior of the production trend due to scattering data that leads to uncorrected analysis.

In 2013, Kumar et al. quantified the production contribution in both shale layers in the Bakken using reservoir simulation models by considering the effect of adsorption and diffusion mechanisms to involve the significant mode of fluid storage and recovery

mechanism in nanopores scale. The observation of sensitivity analysis suggested that the Upper and Lower Bakken Shale contribute from 12% to 52% of the total oil production from the three Bakken Layers. The finding addressed that the shale layers are in interference with the Middle Bakken Formation and improvements in fracture treatment application yield to more contribution and support for recovery mechanisms.

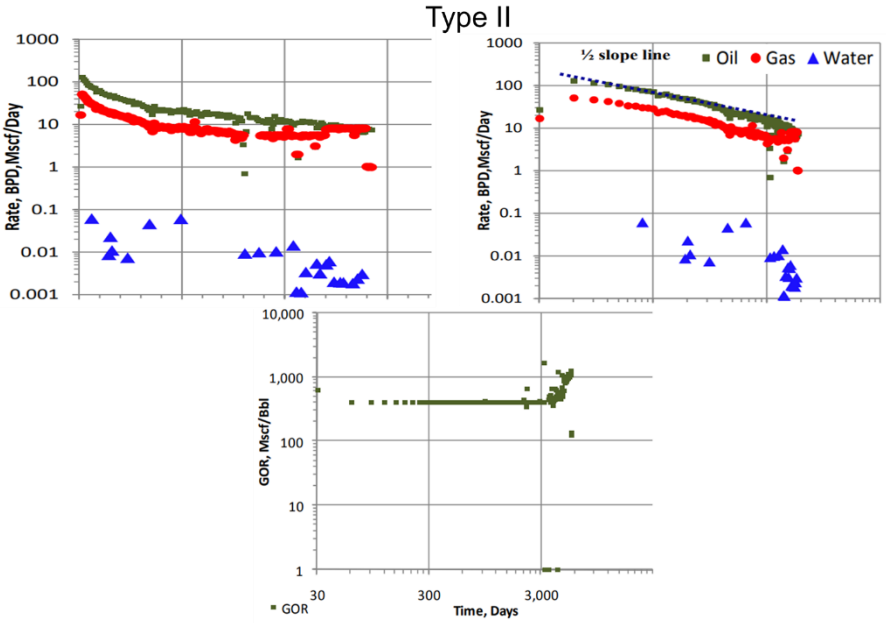

Figure 5. 6. The production trend for the Bakken wells under Type II (Tran et al. 2011).

5.4 Characteristics of the Middle Bakken Formation

Figure 5. 7 illustrates the description of the sequence in the Bakken Formation, which is "two, black fissile shales separated by light grey to grey-brown fine-grained sandstone". The Bakken shale play is subdivided into three distinct stratigraphic members: Upper Bakken (UB), Middle Bakken (MB), and Lower Bakken (LB), listed from top to bottom. The MB member acts as a reservoir rock and the target pay-zone for horizontal wells with a thickness of 85 ft. The formation is characterized by low porosity (<10%) and ultra-low permeability

(<0.01md). The total organic carbon (TOC) content in the middle member is low ranging from 0.1 to 0.3 wt.%, which is an organic poor compared to upper and lower members, as illustrated in Figure 5. 5. Based on these reservoir properties, the MB Layer is classified as an unconventional play (Ellafi et al., 2019b; Ba Geri et al., 2019c; Assady et al., 2019; Kurtoglu, 2013; Klenner et al., 2014). Furthermore, geostatistics modeling has indicated that the reservoir properties in the MB Member is highly heterogeneous throughout the Williston Basin (Jin et al. 2017).

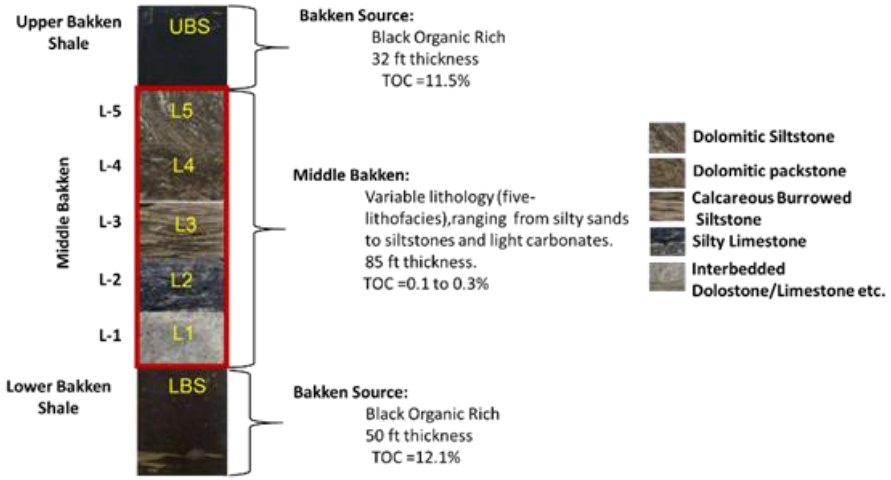

Figure 5. 7. Schematic of Bakken Petroleum System stratigraphy (Sorensen J., 2016; Klenner, et al., 2014).

Also, the fluid transport is governed through the fracture networks (natural and artificial fracture) at both the micro and macro-scale (Klenner et al., 2014). History field data of long-term pressure and rate transient analysis (RTA) of the Bakken wells identify that natural fractures can play a significant role in unconventional wells performance as well as can have both positive and negative impacts on the effectiveness of an EOR scheme (Kurtoglu, 2013). In addition, reservoir properties, especially the wettability of the reservoir is really important and must be investigated, which has the main role in the relative permeability, capillary pressure, electrical properties, and EOR process (Zhu et al. 2011).

To assess and gain a deeper understanding of the CO2-EOR mechanisms in unconventional reservoirs, rock and oil properties of the Bakken Formation as well as CO2-fluid-rock minerals interaction need carefully reviewing to address opportunities and challenges in the Williston Basin.

5.4.1 Bakken Reservoir Permeability

Assady et al., 2019 conducted an experimental study to characterize the MB core samples using both steady state and unsteady-state permeability measurements. They explored the range of reservoir permeability of the core samples from the Mountrail County wells, ND, which are the same wells and depths of our study. Figure 5. 8 presents the comparison between the three methods used, and the conclusion showed that the pulse decay permeability measurement is in close agreement with the permeability range of the tight formation in the literature. Kurtoglu, 2013 pointed out that the permeability magnitude in the laboratory is 10-4 to 10-5 mD while in the field scale measurement is 10-1 to 10-2 mD due to significant contribution of a micro-fracture network. In the field application, the only way to estimate the reservoir permeability is from a diagnostic fracture injection test (DFIT), and the research by Melcher et al., 2020 summarized the analysis of thirty-three DFIT tests and reservoir permeability in the MB Member reported as mean value around 0.022 mD that represents the upper-bound estimation value.

Despite research findings of Assady et al., 2019 observed that the pulse-decay is associated with some of the errors; its outcomes are still more reliable compared to steady state and oscillating approaches. In the case of complex pore throat configurations, the steady state and oscillating methods are associated with high errors since these approaches are used to determine core samples in medium and high permeabilities ranges using Darcy's law. On the

other hand, the foundation of pulse-decay based on the Darcy-Klinkenberg Fibonacci calculation model that reduces the uncertainty for permeability measurement for unconventional reservoirs. The results of the experiment showed a significant effect on the reservoir permeability due to change in confining pressure and pore pressure. As can be seen in Figure 5. 8, the permeability in the three methods is high at low pressure, while the reservoir permeability is gradually decreased as confining pressure and pore pressure are increased. Therefore, the outcomes using pulse-decay, steady state, and oscillating methods are decreased by 75%, 68%, and 56%, respectively when the pressure is increased from 1,045 psi to 2,205 psi.

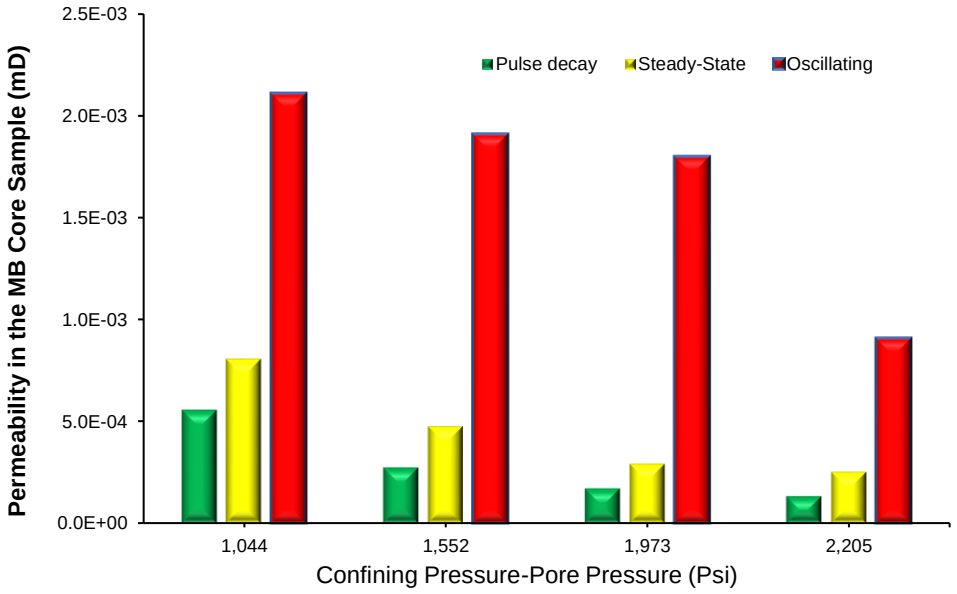

Figure 5. 8. Comparison between three methods of the Middle Bakken permeability measurements (Assady et al., 2019).

A clear statement was proposed in the work of Assady et al., 2019 that the running of the hysteresis technique can be modeled the fluid flow during EOR (injection and soak), as well as production depletion in unconventional reservoirs. The matrix permeability in tight formations is stress-dependent that significantly impact early and long-term production.

Thence, understanding EOR mechanisms in unconventional reservoirs, such as molecular diffusion rate relies on the permeability hysteresis that highlights the impact of micro-fractures and nano-pores in tight formations under different conditions of pore pressure and confining stress.

Teklu et al., 2018 addressed the importance of permeability hysteresis information in reservoir development strategy by studying of fracture and matrix permeability dependency on stress during loading cycle (depletion process) and unloading cycle (injection process). They observed that the major role of the stress dependency and hysteresis of permeability is larger in nano-pores than mirco-proes media. The pore interconnectivity of the effective porosity and permeability of the tight formation depends on the net effective (σ_{eff}) stress that govern the deformation of the rock and can affect material properties (Civan, 2019). This term is defined as the difference between applied confining pressure (external stress, (σ) and the internal pore pressure, (p), as described in Equation 5. 1 (Terzaghi, 1943).

$$\sigma_{eff} = \sigma - \alpha p \tag{5. 1}$$

Where α is a porirelastic (Biot's) coefficient.

For example, Figure 5. 9 shows during loading cycle that represents production depletion (depressurization mechanism), the pressure drop in pore pressure is equivalent to increase in applied effective stresses to the reservoir, which leads to significant decrease in the MB core samples permeability up to 37%, and microcracks could not be open to enhance bulk permeability. On the other hand, during unloading cycle (injection) when the effective stress is decreased, a significant hysteresis with 24% restored permeability was observed for the Bakken cores (Teklu et al., 2018).

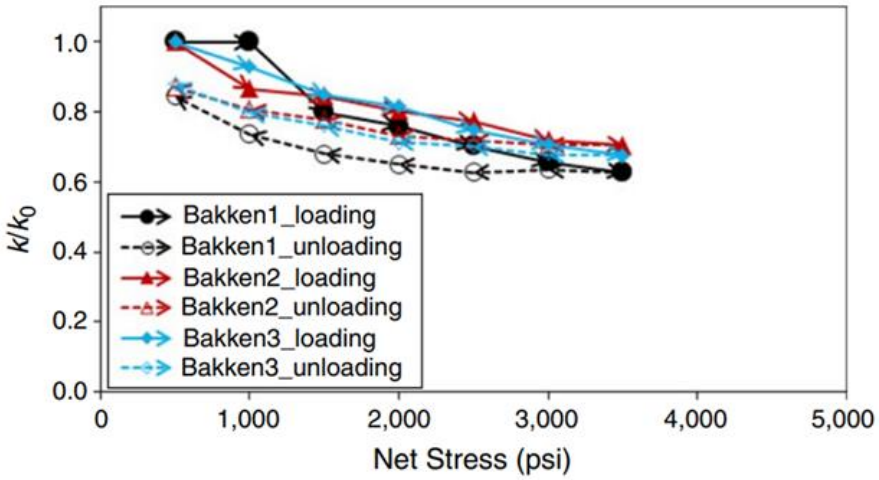

Figure 5. 9. The permeability hysteresis of the Bakken core samples during loading and unloading cycles (Teklu et al., 2018).

Figure 5. 10 shows similar trend behavior in the work of Assady et al., 2019, where the reduction observed is around 31%. It can be concluded that the fluid flow in unconventional formations depends on reservoir properties and micro-pore structure that influenced through stress changes. As a result, the reservoir petrophysical properties may change during the production and/or injection process, and this leads to affect the storage capacity of the formation. Furthermore, unconventional reservoir properties are not important for only understanding primary depletion process, but also may play an important role in success in the implementation of CO2-EOR and/or CO2 sequestration applications, where the stress dependency might cause an altering of permeability magnitude (Wang et al., 2019). Also, in high reservoir temperature reservoir, such the Bakken reservoir (220 to 240 deg F), the increasing in temperature enhances the diffusion mechanism, which might lead to increase the effective permeability of the rock matrix. In fact, the reservoir permeability is much affected by confining pressure than injection pressure, where minimizing the permeability change due to injection pressure can be done by extending the injection pressure period until it reaches the optimum time (Wang et al., 2019).

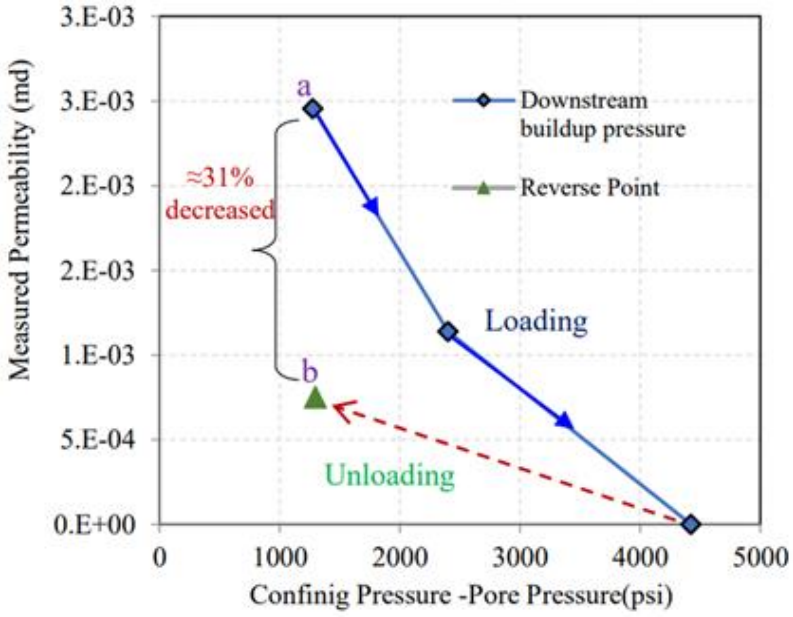

Figure 5. 10. Loading/unloading effects on permeability of Bakken core samples (Assady et al., 2019).

5.4.2 Bakken Reservoir Porosity

In unconventional shale reservoirs, the pore structures are a crucial factor that can affect the site for accumulation and storage capacity of hydrocarbon include chemical properties of the rock. In addition, the pores provide the flow paths (permeability), which might influence the fluid flow mechanisms during the production and EOR process. Unlike conventional reservoirs, there are three types of existing porosity: matrix porosity (inorganic), organic porosity, and fracture porosity with pore sizes ranging from nanoscale to microscale level. It is necessary to answer the question of the nature of fracture networks in the scale of macro and micro within the reservoir properties to consider the potential use of CO2 injection in the Bakken.

The high resolution of SEM images (Scanning Electron Microscopy) is the most used method to quantify porosity in shale reservoirs, where multiscale pore level can provide rock characterization information such as pore shape, pore size, pore location, and pore

connectivity. (Liu et al., 2018; Liu and Ostadhassan, 2017) these authors reported that the matrix and fracture porosity are main dominated hydrocarbon storage capacity in the MB Formation, while Eagle Ford shale both organic and matrix porosity prevails the major storage volume.

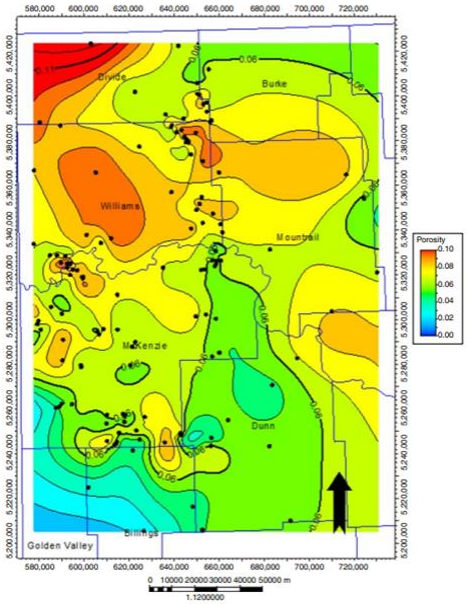

Figure 5. 11. Porosity distribution map in the Middle Bakken, Williston Basin (Luo et al., 2019).

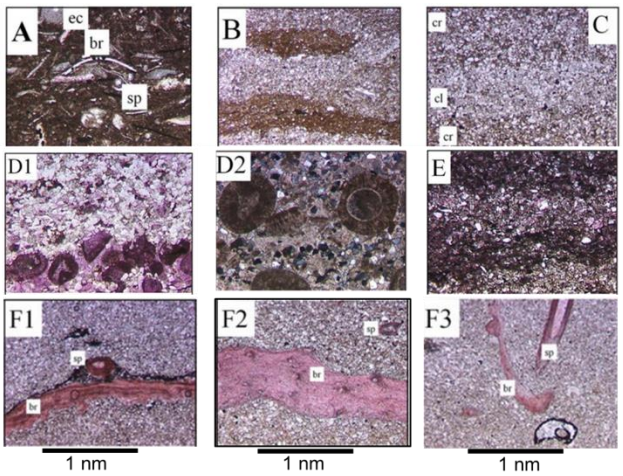

Figure 5. 12. Photomicrographs of the Middle Bakken facies, Williston Basin (Kowalski and Sonnenberg, 2013).

Furthermore, the porosity outcomes for the MB Member are low, most samples that measured by Liu et al., 2018 reported porosity below 10%. This confirmed by Luo et al., 2019, and Figure 5. 11 presents porosity distribution ranges from 2 to 10% over various counties in the Williston Basin, ND. In another study by Kowalski and Sonnenberg, 2013, the porosity showed varying values by changing the facies, where they concluded that facies with high calcite cement and illite/smectite (clay) provide low to no porosity.

In contrast, the high porosity presents if the formation contains a high concentration of quartz, as shown in Figure 5. 12. The secondary porosity and both induced and natural fractures were observed also using photomicrographs, (see Figure 5. 12, Facies E & F). This causes by a large amount of dolomite as a result of the dissolution process and diagenetic alteration during burial and forming a history of the rock. Overall reported results from the literature review conclude that the average porosity in the MB Formation is around 6% with significant connected and open pore space, as shown in Figure 5. 13.

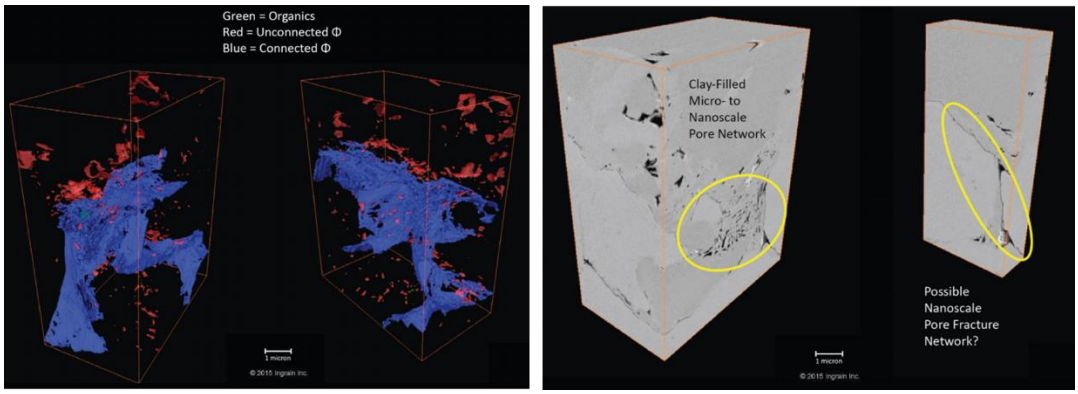

Figure 5. 13. FIB-SEM analysis of the Middle Bakken lithofacies, Williston Basin (Sorensen et al., 2016).

In 2016, Sorensen et al. proposed advanced analytical method to characterize twenty-six samples from the Bakken Formation using an integral approach, which is a combination of advanced computer tomography (CT) imaging and scanning electron microscopy (SEM)

techniques, including whole-core and micro x-ray CT imaging, field emission (FE)–SEM, and focused ion beam (FIB)–SEM. The multiscale workflow was utilized to improve and support the characterization technique of the geomodels analysis for more representative studies of fluid flow pathways within various lithofacies of the MB Formation.

The observation from this study show evidence that the network of pore structures in the MB Formation could serve as the main pathway to diffuse CO2 into the rock matrix through the diffusion-dominated flow and then mobilized more hydrocarbons by viscosity reduction mechanism to keep the viscous flow in the fractures, as shown in Figure 5. 13 significant connected porosity was observed using FIB-SEM analysis.

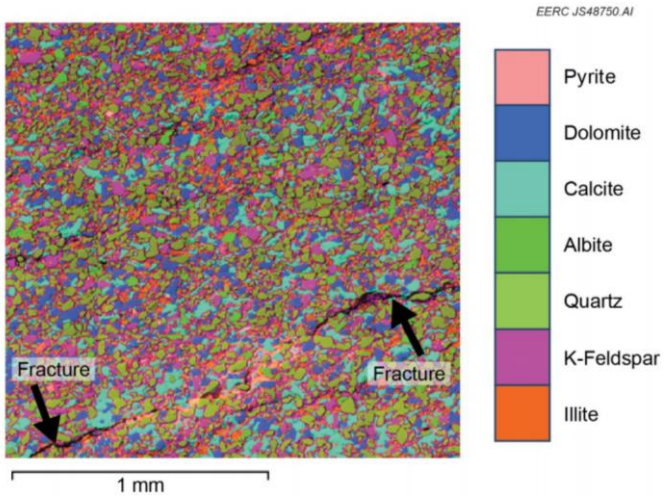

Figure 5. 14. SEM images and mineral map of the Middle Bakken lithofacies "laminated zone", Williston Basin (Sorensen et al., 2015).

Figure 5. 14 demonstrates the laminated zones in the MB Formation, which is geomechanically weaker with higher porosity and permeability, but also tends to micro-fracturing as a result of fracture treatment job, and characterization applications approved that these lithofacies are most favorable zones to CO2 EOR more easily than others (Sorensen et al., 2015).

As shown in Figure 5. 14, might answer the question of the role of fractures of CO2 movement into the rock matrix. A fracture network in the reservoir can serve as a means of more beneficial effects of CO2 to expose more oil-saturated rock when the generated fractures are higher density and limited near the wellbore. Then, the surface area of the formation is a lager contact with CO2, and lower maintained pressure is needed to optimize more effective miscible CO2. Otherwise, CO2 quickly migrates away from the productive area, and higher pressure is required to operate CO2-EOR (Sorensen et al., 2015).

5.4.3 Bakken Rock Mineralogy

The mineral composition of the unconventional reservoir is a key factor for successful IOR/EOR applications, which is crucial to understand the pore structure and estimate the fluid transport and storage in the nano and micro scale. Additionally, the rock composition is fundamental that has a main role to assess the best zone for hydraulic fracturing jobs, thus improving the hydrocarbon oil recovery from tremendous oi resource, such as Bakken Shale Play (Jarvie et al., 2007). The rock mineralogy directly relates to geomechanical properties (i.e, Poisson's ratio, Young's modulus, etc..), which can reduce or increase the brittleness of the tight formation and provides a poor or significant fracture network between the wellbore and micro and nano-pores media. The brittleness index is defined as the ability control to create and maintain the fracture, and the research findings from previous studies concluded that the MB Formation is more densely and prone to develop fractures compared to other shale plays due to low clay content (Bhattacharya and Carr, 2019; Kurtoglu, 2014). For the EOR application, the high brittle formation generates a large surface area that counts as advantages, and the SRV would be exposed to a large volume of the gas injection and unlimited solvent oil contact to increase incremental oil recovery.

Li et al., 2019 and Liu et al., 2017 studied the characterization of the Bakken Layers using X-ray diffraction (XRD) analysis in the laboratory. The research aimed to determine the physical parameters and deposition environment of the Bakken Shale by experimenting with more than twenty-five samples from different locations to identify the mineral composition, clay type, and clay abundance of the Bakken Formation. Their results were gathered and analyzed using the box plot, as shown in Figure 5. 15, where the mineralogy analysis in the MB Formation is described as quartz, pyrite, feldspar, clay, dolomite, calcite, and ankerite with median values, as listed in Table 5. 1. The dominated components in the MB Formation are quartz, feldspar, clay, and dolomite. The main clay types are: smectite, chlorite, kaolinite, and illite/ mica. All previous studies agreed that the primary clay type is illite in moderate amounts of around 13.1% and the lithology of the layer is defined as a mix of sandstone and limestone (Kurtoglu, 2014). The tight oil reservoirs are typically sedimentary rocks, which contain unstable minerals (e.g., calcite, dolomite, K feldspar, and albite).

One of the remaining questions that is required to answer is how CO2 interacts with the rock matrix mineralogy. Al Ismail and Zobach, 2017 highlighted the point that the contact between CO2 and rock mineralogy cannot be ignored, which is a crucial factor to understand the behavior of permeability changes, the transport mechanism of CO2 in nano porous reservoirs, and design the optimum CO2-EOR implementation pilot test.

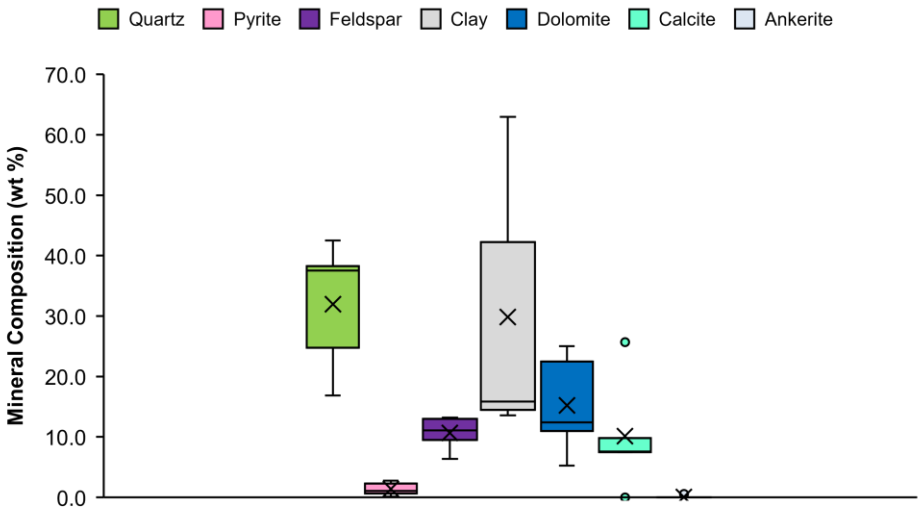

Figure 5. 15. Mineral analysis results of the Middle Bakken Formation samples.

Table 5. 1. Statistical analysis of the Middle Bakken Formation mineral composition.

	Quartz (wt %)	**Pyrite (wt %)**	**Feldspar (wt %)**	**Clay (wt %)**	**Dolomite (wt %)**	**Calcite (wt %)**	**Ankerite (wt %)**
Minimum	15.24	0.10	5.36	9.36	2.25	0.00	0.00
Q1	17.70	1.39	7.17	14.83	11.35	7.53	0.00
Median	31.14	2.62	10.85	19.19	21.07	9.68	0.00
Q3	38.48	3.57	13.15	25.19	32.92	14.82	0.00
Maximum	42.56	4.98	25.36	62.94	38.57	25.70	0.56
Mean	29.22	2.57	11.37	24.66	20.78	10.93	0.06
Range	27.32	4.88	20.00	53.58	36.32	25.70	0.56
St. D	6.83	1.22	5.00	13.40	9.08	6.43	0.14

Q1: First quartile (25%), Q3: Third quartile (75%), and St. D: Standard deviation.

Beside XRD analysis, the bulk chemistry of the MB Formation is very important to detect and quantify, where x-ray fluorescence (XRF) was used in the work by Jin et al. 2016, as shown in Figure 5. 16. The outcomes clearly show that silicon, calcium, and aluminum are

the most chemical elements in the MB Layer with a significant percentage of calcium as a result of the basin composition of carbonate rock contains an abundant amount of calcium.

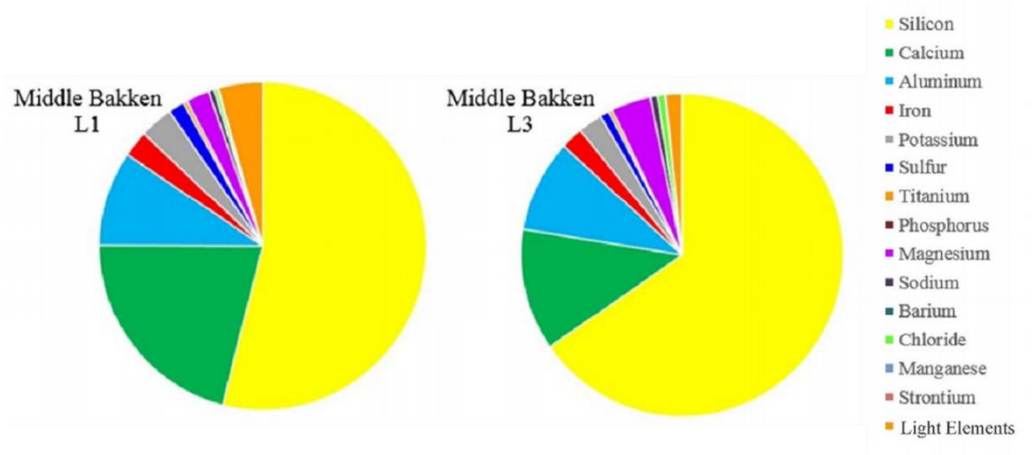

Figure 5. 16. X-ray fluorescence (XRF) analysis for the Middle Bakken core samples (Jin et al. 2016).

The reservoir rock is classified as hydrophilic when the formation is rich with silicon and aluminum and poor with iron. Then, the wettability of the formation may be induced by CO2-EOR, which causes to change the petrophysical properties of the whole reservoir (Zhu et al. 2011). The interaction in the soaking period between CO2 and formation rock can partially dissolve the skeletal grain minerals and cement of the rock. As a result, the rock mineralogical and pore structural properties alter, and the mineral dissolutions can generate macropores or even microfractures that result in altering the properties of the rock mineralogy (Li et al. 2020).

Heller and Zoback, 2014, conducted experimental work to investigate the relationship between gas adsorption capacity and TOC and minerals that represents Barnett, Montney, Marcellus, and Eagle Ford Formations. The results showed that the high TOC value, the maximum absolute adsorption capacities, where Barnett and Montney have TOC in range of 5.3% and maximum adsorption around 40.8 gmole/g. Also, the rich shale members contain

the kerogen that is the primary organic matter component that has micro porosity, spanning micrometer to nanometer in scale. On the other hand, the study by Smith et al. 2019 concluded that the MB Formation is considered as lower adsorptive potential with ten times compared to UB and LB Layers due to its low amount of clay, as shown in Figure 5. 17.

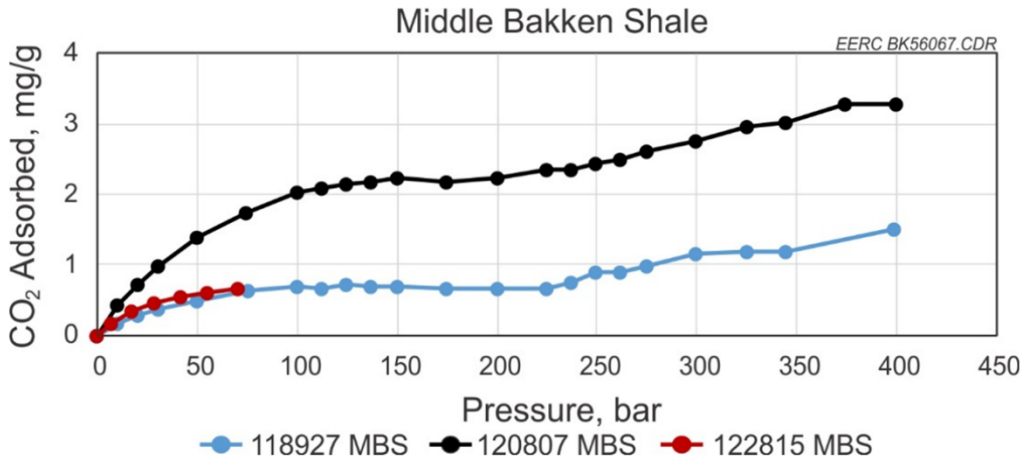

Figure 5. 17. Carbon dioxide adsorption isotherms on samples from the Middle Bakken Formation (Smith et al. 2019).

In the work by Kurtoglu, 2013, they discussed that the main pathway for solvent injection into a tight shale play would be through the micro-fracture networks for transporting the solvent into the tight matrix. Obviously, the abundance and favorable distribution of fracture networks yield better solvent exposure and control the contact time that the solvent has with the oil and thus higher Bakken wells productivity in an EOR process. In addition, the Bakken Formation is characterized by the oil-wet system that using the waterflooding process will not be an effective technique. Therefore, based on the above characteristics of the MB Formation that approve the formation is under a high intensity naturally fractured and/or hydraulically fractured formations, the solvent injection (e.g., CO2) could be an effective EOR technique.

5.5 CO2 Huff-n-Puff Protocol in Unconventional Reservoirs

The results from several studies on gas injection EOR, such as carbon dioxide (CO2), nitrogen (N2), rich natural gases (C1 "70%" and C2 + "30%"), and lean gas (primary methane) proved that the application is a more feasible EOR technique in shale plays due to their low viscosity and easier transport into matrix that dissolves in oil and cases oil swelling and reduced viscosity (Alfarge et al., 2017; Sheng, 2015). Furthermore, most of the recent studies reported that CO2 injection is preferred application due to several reasons (Alfarge et al., 2018; Zhang et al., 2016; Kurtoglu et al., 2014): 1) CO2 requires lower miscibility pressure to reach miscibility than other gases, which makes CO2 miscible injection attainable under wide range of reservoir pressures. 2) The injectivity of CO2 injection is favorable as a result of continuous gas pathways from fracture and penetrating into the rock matrix to swell oil through the diffusion mechanism. Due to their ultra-tight permeability in shale plays, the simulation studies and experiment works have proved that the single-well HNP (cyclic gas injection) process would be an effective EOR approach for LRS reservoirs.

A CO2 flooding process as compared to HNP may take a considerably long time for the injection transient pressure to propagate towards the producing well. Sheng, 2015 showed that in fractured reservoirs (naturally and fracked wells), the HNP approach has a better recovery performance compared to the gas flooding process. They explained that the complex fracture networks around a production well could cause early breakthrough or viscous fingering which means poor sweep efficiencies or an underperformed flooding performance. Therefore, the industry has resolved this issue by drilling a single horizontal well that acts as both production and injection well (Wan and Sheng, 2015). Also, the presence of natural fractures will benefit the recovery by increasing the contact area of the

injected solvent with reservoir rocks. Figure 5. 18 illustrates the method, which starts with a huff stage by injecting the solvent at high pressure; then the first or multiple contact miscibility occurs, where the injection fluid mixes with the formation oil, resulting in a single-phase fluid flow. Next, a soaking period begins when the well is shut-in for a specified period. In this step, the CO2 diffuses into the rock matrix and interacts with the host rock and fluid. Then, as the puff step, the well is put on the production for a certain period and under specified depletion pressure so that the mixture of CO2 and shale oil expand and flow to the surface in one phase. This application has been successfully implemented for the steam injection process, but it has also been used recently to face challenges of tight formations during CO2-EOR injection.

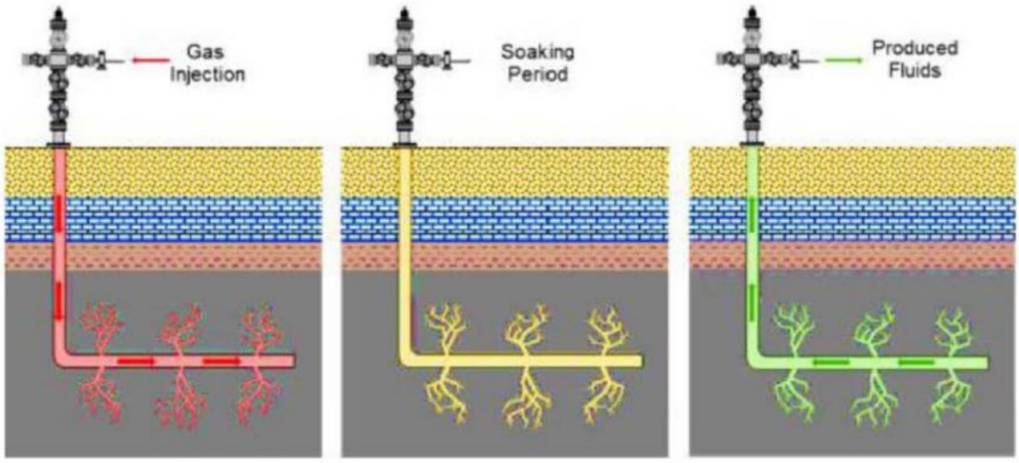

Figure 5. 18. Typical gas HNP process for unconventional EOR application (Pankaj, et al., 2018).

Generally speaking, understanding of the key parameters controlling the CO2 HNP process requires testing the recovery under several scenarios with different well, reservoir (rock, fluid, rock-fluid, etc.), and operational parameters. The oil viscosity reduction ratio with CO2 injection and oil swelling factors as well as recovery at different conditions (e.g., p, T, soak period, # of injection cycles, etc.) are summarized below in this work. The HNP process was

firstly evaluated by Wan et al. 2013, where they used numerical reservoir simulation to quantify the oil recovery from this EOR process in shale oil plays. They concluded that fracture networks are crucial for improving oil recovery in ultra-tight shale formations. Furthermore, Hawthorne et al. 2013 conducted experiments using core samples size 10 mm diameter in 40 mm long, to determine the effects of CO2 exposure time on recovering hydrocarbons from the UB, LB, and MB formation at conditions of 110°C and 5,000 psi. Their results indicated that CO2 injection is a promising method for enhancing oil recovery from both source and reservoir rocks of the Bakken if the operations meet the two conditions of long exposure time and wide contact area.

Moreover, Gamadi et al. 2013 performed an experimental study of the HNP process using N2 as the injection fluid on core plugs of the Barnett, Marcos, and Eagle Ford shales. They studied the impact of operating pressure, shut-in time, and a number of cycles on the N2 injection performance. Their results indicated that the peak recovery factor can be reached if the injection pressure is near miscibility. The work of Hawthorne et al. in 2013, 2014 and 2017 gave the observation about the effect of minimum miscibility pressure (MMP) on the incremental oil recovery, where they approved in fractured tight reservoirs with light hydrocarbons like Bakken, the recovery process does not rely on the flushing mechanism but strongly controlled by solubility/diffusion mechanisms in a soaking period. The reason behind that the injection solvent would favor lighter hydrocarbon components due to its higher solubility, then the diffusion rate is improved. In contrast, Tovar et al. 2018 discovered that in organic-rich shale, increasing pressure beyond the MMP leads to increase oil recovery factors. This major change in operation philosophy compared to inorganic formations due to differences in mechanisms that taking place during CO2 injection. Moreover, the number of

cycles is also critical design parameter, and the observed outcomes from previous works concluded the majority of oil production is in the first and second cycles, and then the recovery stabilization has reached. In addition, the depletion condition appeared to be a crucial factor as well to design the HNP operation in order to enhance oil recovery application.

In 2014, Gamadi et al. repeated the previous experiments using CO2 injection and the same core samples and operation conditions. The results supported the hypothesis that higher pressures than MMP may not be an effective strategy to increase the oil recovery from tight reservoirs. Tovar et al., 2014 discussed the results of two experiments using the HNP CO2 method on Barnett core samples. They modified a Hassler core holder to simulate CO2 HNP process by surrounding the core samples by glass beads (to emulate fractures) and plugging both ends by two Berea sandstone to allow the high-pressure CO2 always in contact with the matrix (cores) and prevent the glass beads to escape the chamber. Therefore, the high permeability media surrounding the core samples was saturated with the solvent at constant pressure (1,600 and 3,000 psi) and temperature (150 °F) during the experiment. They reported that the high permeability media (the glass beads) provided a high surface area to perform CO2 injection, while it is not possible when CO2 is injected directly into the core sample. Such a new design would resolve the problem of low to zero injection into a tight core from a shale play. The significant improvement in the incremental oil recovery was observed, and the estimated recovery was between 10 to 55% of the pore volume of the core samples. The methodology used in the experiment (x-ray computed tomography, [CT]) indicated that the increase in oil volumes was driven by diffusion and reduction in capillary forces.

Lately, in 2017, Jin et al. conducted an experiment on CO2 exposure for some Bakken core samples with small dimensions (1.1 cm diameter and 4 cm in length) at the pressure and temperature of 5,000 psi and 230 °F, respectively. They aimed at a better understanding of the microstructure and diffusion dominated flow in ultra-low permeability formations during a CO2-EOR process. The results concluded that CO2 is able to extract more oil recovery as high as 68% during 24 hrs exposure time from the UB and LB formation. Both layers content generally high content of total organic content (TOC) in a range of 10-15 wt%, and small pore-throat size in a range of 3-7 nm, known as mesopores with important number of micropores. These factors can impact the oil recovery due to their roles in residual oil trapping. The shale formations with a high amount of TOC contain kerogen, which is organic matter, and its surface is oil-wet with complex pore structure and confining oil inside. As a result, CO2 could not diffuse and displace hydrocarbon molecules easily due to large capillary pressure. The presence of organic matter in unconventional reservoirs has significant impact on the EOR mechanisms and reservoir depletion behavior. On the other hand, the core samples from MB and TF formations have larger pore sizes (>50 nm), known as macropores and low TOC level, which assists in a more favorable flow for both CO2 and hydrocarbon molecules. The ultimate oil recovery reported is 99% of the total pore volume during 24 hrs of CO2 exposure under Bakken conditions. In the work by Tovar et al., 2018, CO2 injection was studied to investigate the operation philosophy and understand the recovery mechanisms. They used a similar Hassler core holder to simulate the behavior of fractures around the core (i.e., rock matrix). Their work provides some experimental observations on the effects of pressure, soak time, rock transport, and oil and injection gas compositions on recovery mechanisms.

CO2-EOR technologies have the potential to add millions of barrels of incremental production to the Williston Basin oil recovery. In general, CO2 injection is a fast method with promising potential that might succeed economically compared to refrac and infill drilling applications. CO2 operations include capture, compression, and transportation has started to consider as economic application as a result of the extension and expansion of Federal 45Q tax credits, which provides $50/ton for CO2 stored for 12-year period in saline aquifers, while $35/ton for CO2 captured in depleted formations during CO2-EOR. To provide economy of scale and, potentially, additional subsidy for saline aquifer injection through CO2 sales, CO2-EOR likely needs to be part of the system (Holubnyak et al., 2019). However, there is a wide range of uncertainties associated with operating such a process in shale plays, which need to be addressed prior to meaningful pilot tests in the field.

5.6 Methodology Details

5.6.1 Experimental Setup

Figure 5. 19 shows the schematic of the experimental setup used in this work to simulate the HNP process. The setup consists of high-pressure vessels containing up to three rock samples together in each run. As illustrated in the figure, the core and chip samples were numbered and loaded as a stack. The space between the vessel and core samples represents the fractures with high permeability to allow CO2 to contact with the whole core samples. The stainless-steel vessel is designed for high pressure and high temperature conditions to mimic the operational parameters in the Bakken formation.

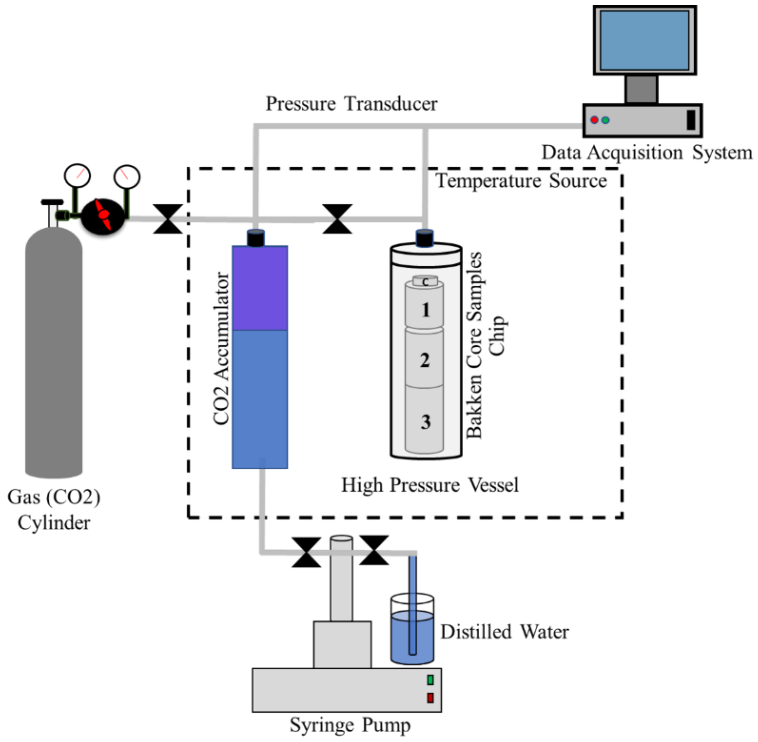

Figure 5. 19. The experimental setup used for testing a typical huff-n-puff process on Bakken core samples.

The vessel is connected to a CO2 accumulator, and both are placed in an oven with a maximum operating temperature of 300 °C. The gas is supplied from a commercial CO2 cylinder with the purity of 99.99% under a maximum pressure of 900 psi. If pressures higher than 900 psi is desired, a syringe pump can be used to increase the pressure depending upon the operational conditions of the experiment. The syringe pump works by injecting distilled water to fill up the accumulator and push the piston up in order to increase the CO2 pressure in the system. All components of the system are connected to a data acquisition system to monitor and control the temperature and pressure by using two transducers in the vessel and CO2 accumulator. This system is a modified design of the original core flood setup in order to simulate the HNP process in a tight shale play (see Figure 5. 19). The materials used in the experiments are as follows:

1. Dead oil Bakken fluid was used to fully saturate the rock and chip samples, where the properties of the fluid are listed in Table 5. 2.

Table 5. 2. Bakken crude oil properties.

Oil Type	Density, gm/cc	Viscosity, cp
Dead oil	0.86	2.46

2. Six core and chip samples from the MB formation from two different wells and depths were studied to evaluate their recoveries and to assess the proceeding wettability alteration by measuring the contact angle before and after each HNP run. Table 5. 3 shows the well number, formation depth, dimensions, surface areas, and bulk volumes of the samples, respectively.

Table 5. 3. Core sample information, dimensions, surface areas, and bulk volumes.

Sample, #	Well, #	Formation Depth, ft	L, in	D, in	SF-A, in^2	BV,CC
1	24779	10,242.6-10,248.4	1	1	1.5708	12.8704
2	24779	10,242.6-10,248.4	1.5	1	2.3562	19.3056
3	24779	10,242.6-10,248.4	2	1	3.1416	25.7408
4	25688	10,645.5-10,680.0	1	1	1.4945	12.7648
5	25688	10,645.5-10,680.0	1.5	1	2.4752	19.4167
6	25688	10,645.5-10,680.0	2	1	3.2468	25.8436
C	25688/24779	10,242.6-10,680.0	Chip size = 0.394 in × 0.394 in			

3. A precise scale was utilized to weigh the core samples before saturation, after saturation, and at each CO2-EOR experiment run in order to determine the incremental oil recovery.

4. A wettability tester was used to determine the contact angle of the chip samples in order to study the wettability alteration from CO2-EOR. In this research, the contact angle was

measured to assess the wettability in different scenarios in order to identify the conditions under which wettability would act in favor of a CO2 HNP process.

5.6.2 Experimental Protocol

Core Saturation Process*:* This study was started with cleaning all core samples using the Dean Stark extraction, where the mixture of toluene and methanol was used as cleaner solvent at low temperatures to remove the fluid and salt contents by vaporizing the solvent mixture. The cores are placed in such a fluid mixture for almost a week until the color of the mixture shows no more change. Next, the cores are placed in the oven at 70 °F overnight to dry and are weighed by using a high accuracy point scale. Then, the same apparatus, as shown in Figure 5. 20 is utilized to saturate the core samples with the Bakken dead oil.

Figure 5. 20. Saturated the MB core samples.

$$PV = \frac{Wt_{sat} - Wt_{dry}}{\rho_{oil}} \tag{5. 2}$$

Where: PV : Pore volume, cc, Wt_{sat} : Weight of the core sample when saturated, gm, Wt_{dry} : Weight of the core sample when dry, gm, and ρ_{oil} : Bakken oil density, gm/cc

Table 5. 4. The saturation process results.

Sample, #	Wt. D, gm	Wt. Sat, gm	PV, CC
1	37.2840	37.5995	0.3668
2	49.2208	49.7635	0.6309
3	62.3863	63.8770	1.7330
4	36.911	37.1112	0.2328
5	50.1234	50.7384	0.7151
6	62.9674	64.4776	1.7560

This process took almost five days to allow the oil to penetrate deep into the rock samples. Finally, the samples are saturated, as shown in Figure 5. 20, then weighed and the pore volume can be estimated from Equation 5. 2. The results of this step are shown in Table 5. 4 where the cores, taken from different depths, present different pore volumes due to the high heterogeneity in the MB formation.

5.6.3 Experiment Procedure of Huff-n-Puff CO2-EOR

The huff-n-puff experiments were conducted on the six MB core samples and rock chips with different characteristics. As shown in the schematic of the experimental setup (Figure 5. 19), the whole surface area of the cores is exposed to the injected CO2. Before the experiment begins, the original wettability of the cores (chips) were measured through the contact angle. Next, the core samples were loaded in the high-pressure vessel. Then, a four-step procedure was followed: a) inject CO2 injection at a certain rate and temperature until it reaches the desirable pressure, b) close the system and let it soak with CO2 for a specified soak period so that the CO2 can diffuse into the cores, dissolve in oil, and finally reduce the oil viscosity, c) depressurize the system gradually to simulate depletion process to assist the CO2 to swell the oil out of rock matrix, d)open the vessel and measure the weight of each core sample and determine the oil recovery using Equation 5. 3.

$$RF\ at\ each\ cycle.i = \frac{Wt_{sat} - Wt_i}{\rho_{oil}} \times 100 \quad (5.\ 3)$$

Where: $RF\ at\ each\ cycle.i$: Recovery factor, fraction and Wt_i : Weight of the core sample after each CO_2 injection cycle, gm.

In addition, the factor of shut-in time was investigated, where the samples were soaked for three, four, ten, twelve, twenty-four hours, and two days. Furthermore, seven injection cycle were applied to study its effect on the recovery factor. Moreover, five steps were used to show the impact of depletion pressure on the incremental oil, where the core sample was depleted during one hour from 3,500 psi to 1,800 psi.

5.6.4 Contact Angle Measurements

Different methods have been introduced the wettability measurements, where the approaches are classified as quantitative and qualitative methods. The most typical quantitative method is used to measure the wettability of a rock-aqueous phase fluid system is the contact angle as present in the Young Equation 5. 4 or using the force acting on the balance, as written in Equation 5. 5. The contact angle is the angle formed between the liquid and solid interfaces. In this study, the wettability alteration from CO2-EOR was investigated through the measurement of contact angle for each rock chip of MB wells. By using, the equipment in our laboratory can handle the chip size with the dimensions, as listed in Table 5. 3. First, the chip sample of the MB formation is placed in a cell before injecting CO2. Next, distilled water (1 µL) drop is injected into the cell on the top of the measured surface followed by oil in the air at room conditions. A high-resolution camera is used to record the oil drop evolving on the rock surface.

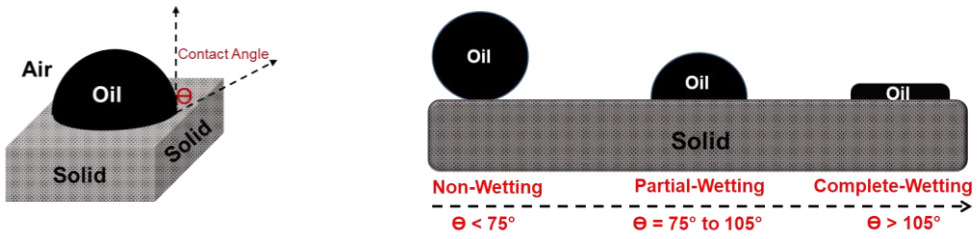

(a) (b)

Figure 5. 21. Contact angle measurements (a) and wettability conditions for different rock samples (b).

$$\gamma_{wg} \times \cos\theta = \gamma_{sg} - \gamma_{sw} \quad (5.4)$$

$$\cos\theta = \frac{(F - F_b)}{P\,\gamma_L} \quad (5.5)$$

Where: γ_{wg}: The interfacial between the aqueous phase and the gas phase, N/m, γ_{sg}: The interfacial between the surface and the gas phase, N/m, γ_{sw}: The interfacial between the surface and the water phase, N/m, θ: The contact angle, degree, F: The measured vertical force, N, F_b: The buoyancy force, N, P: The wetted length, m, and γ_L: The surface tension of the test liquid, N/m.

After that, Image analysis is performed on the drop formed using the provided software. Then, the contact angle measured between the edge of the oil drop and the rock surface. Figure 5. 21 a and b present large contact angle values that indicate less water wet occur on the rock surface when the angle measurement is higher than 90 degrees. On the other hand, lower contact angle values when the contact angle results below 90 degrees and show a more water-wet surface. The main factors that can affect the wettability of the reservoir formations are the complexity of the rock, reservoir temperature, reservoir pressure, gas properties, liquid properties, and the rock surface properties, including rock mineralogy (Craig, 1971).

This experiment was repeated several times at the Bakken temperature and under different CO2 operation pressures.

5.7 Sensitivity Runs to Reduce Uncertainty

5.7.1 Effect of Temperature on Recovery:

Sensitivity runs were performed to study the impact of temperature on oil recovery from a HNP CO2 injection under a constant injection pressure of 875 psi (i.e., gas phase). As depicted in Figure 5. 22, three temperatures were considered: 70°F (lab temperature), 120°F (mid-range), and 220°F (average temperature in the Middle Bakken). The results indicate that there is a relatively high increase in oil recovery (3.56%) from 70°F to 120°F while it reaches a plateau at high temperatures, i.e., from 120°F to 220 °F.

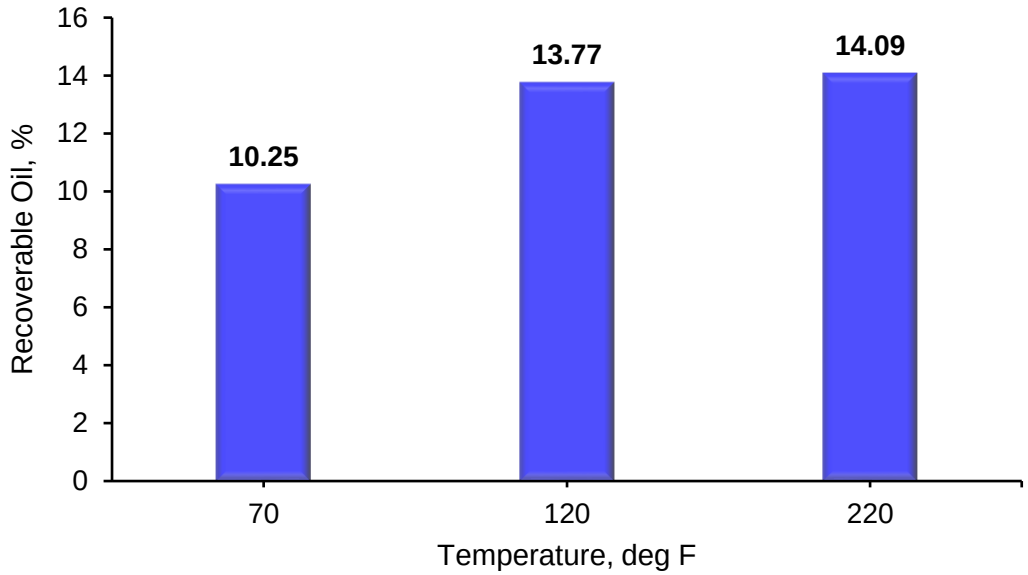

Figure 5. 22. The effect of temperature on oil recovery factor at 875 Psi; duration of CO2 huff-n-puff.

The reason is that the injected CO2 will not be miscible at those lower temperatures while it becomes first-contact miscible at the injected pressure and high temperatures. The improvement in oil recovery was observed from low to medium temperatures till the recovery

factor reaches the plateau and the stable conditions beyond which we may not observe substantial increase in recovery factor.

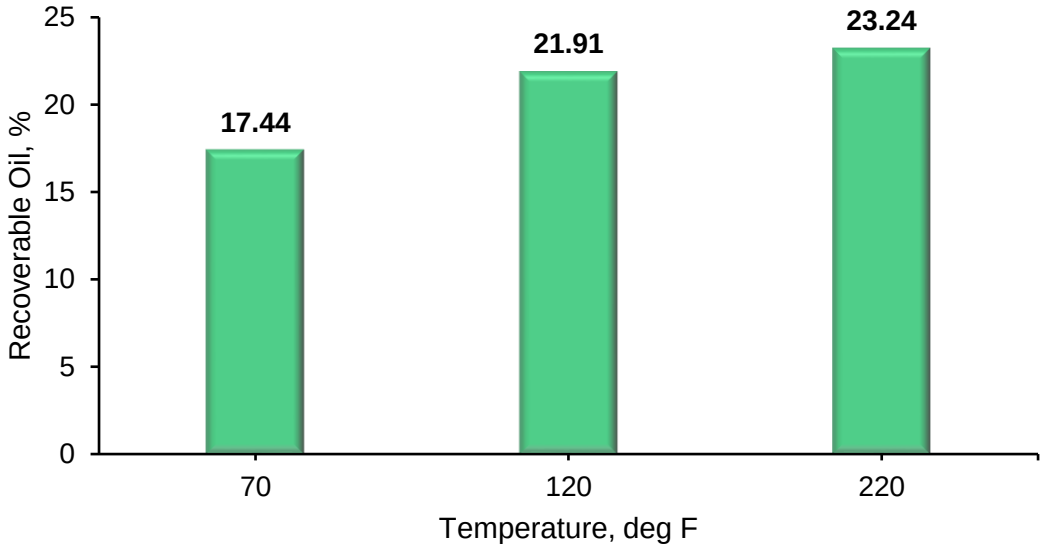

Figure 5. 23. The effect of temperature on oil recovery factor at 1,600 Psi; duration of CO2 huff-n-puff.

Figure 5. 23 presents the effect of temperature under a higher injection pressure of 1,600 psi, but it is still below the miscibility pressure. It shows a similar trend as observed in Figure 5. 22. The incremental oil recovery is increased by 4.46 when temperature increases from 70°F to 120°F. The incremental oil recovery increase is again higher from low to medium temperatures compared to medium to high temperatures. Furthermore, Figure 5. 24 presents similar results for the cases under 3,500 psi injection pressure (above MMP). This graph demonstrates that the impact of temperature at higher pressures is more substantial since the system reaches the miscibility under medium to high temperatures. The higher improvement in the oil recoveries in this case is mainly due to the miscibility of CO2 which diffuses better into the rock sample and lowers the viscosity and swells the oil.

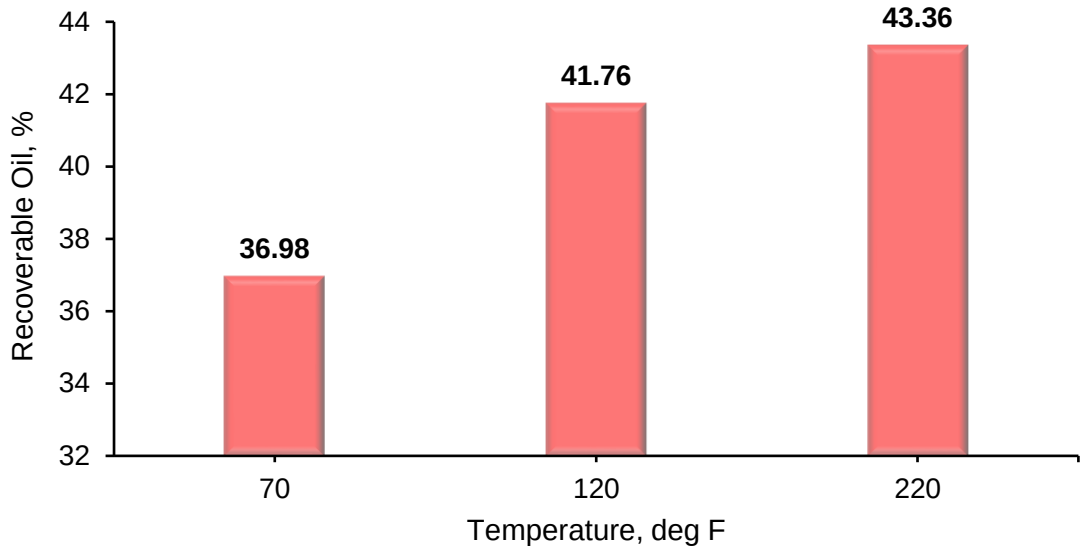

Figure 5. 24. The effect of temperature on oil recovery factor at 3,500 Psi; duration of CO2 huff-n-puff.

5.7.2 Effect of Injection Pressure on Recovery

The core samples from two Bakken wells were acquired and used in this study to evaluate the effect of CO2 injection pressure (phase behavior) on the incremental oil recovery in one HNP cycle and at the Bakken Formation temperature (~220 °F). Figure 5. 25 and Figure 5. 26 show that the injection pressure has a substantial impact on the incremental recovery, especially, when it is elevated to MMP and beyond. Obviously, at those high pressures CO2 is miscible and will diffuse more easily into the rock samples that reduces the viscosity and causes oil swelling.

In the cases with near miscibility injection pressure, the experiments show promising improvements in oil recovery compared to that under 714 psi injection pressure. The ultimate recovery from both samples under similar operating conditions show almost equal results being 50% recovery factor after three cycles.

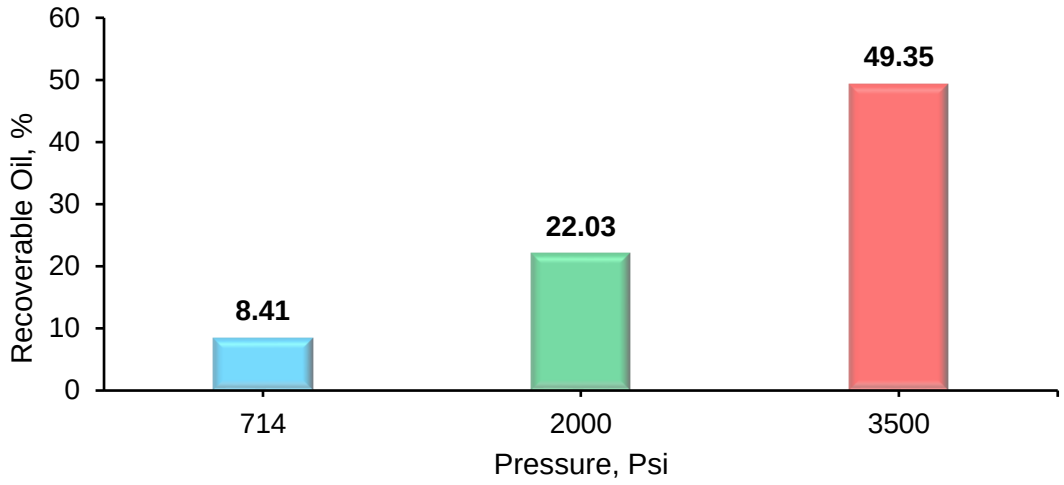

Figure 5. 25. The effect of injection pressure on recovery at 220 °F for sample #1.

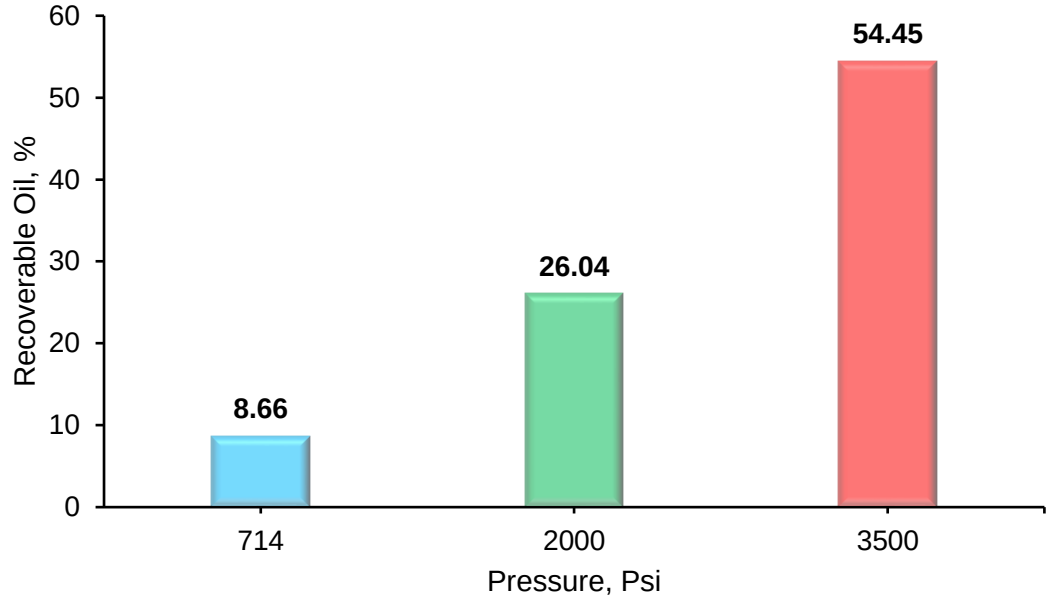

Figure 5. 26. The effect of injection pressure on recovery at 220 °F for sample # 2.

5.7.3 Effect of Number of Huff-n-Puff Cycles

In this study, the recovery factor was investigated from one cycle and seven cycles of huff-n-puff. This helps us to better understand the effect of the number of cycles on both recoverable oil and to identify optimal number of cycles. Samples were used in the huff-n-puff experiments at the Bakken Formation temperature (220 °F) and under the pressure 2,000

psi (near miscibility). The results from both samples show improvements in recovery factor, but the number of cycles needs to be optimized (see Figure 5. 27).

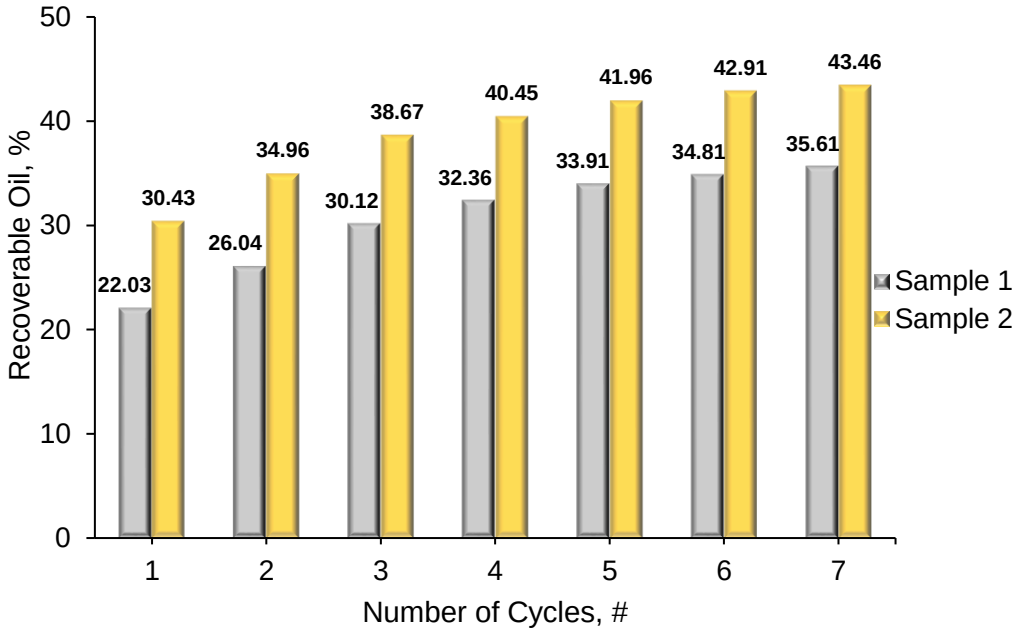

Figure 5. 27. The effect of number of huff-n-puff cycles on oil recovery at 220 °F and 2,000 psi.

5.7.4 Effect of Soaking Time on Recovery

The effect of soaking time was studied for two samples with different bulk volumes (i.e., contact area) and pore volumes. The oil recovery increases as high as 6% only from soaking sample 24 hrs longer. A higher soaking time means more time for the injected CO2 to diffuse into matrix and interact more with the oil and thus higher recovery factor (see Figure 5. 28 and Figure 5. 29). However, this parameter needs to be optimized since there is a tradeoff between higher soaking time and lower rate of recovery which impacts the economy of the EOR project.

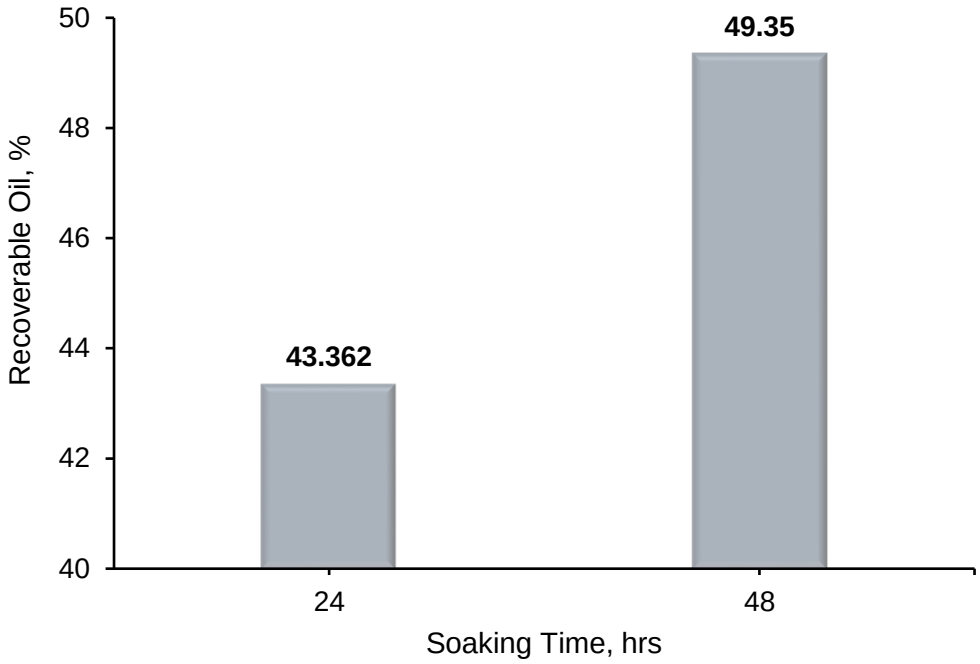

Figure 5. 28. The effect of soaking time on CO2 huff-n-puff recovery at 220 °F and 3500 psi.

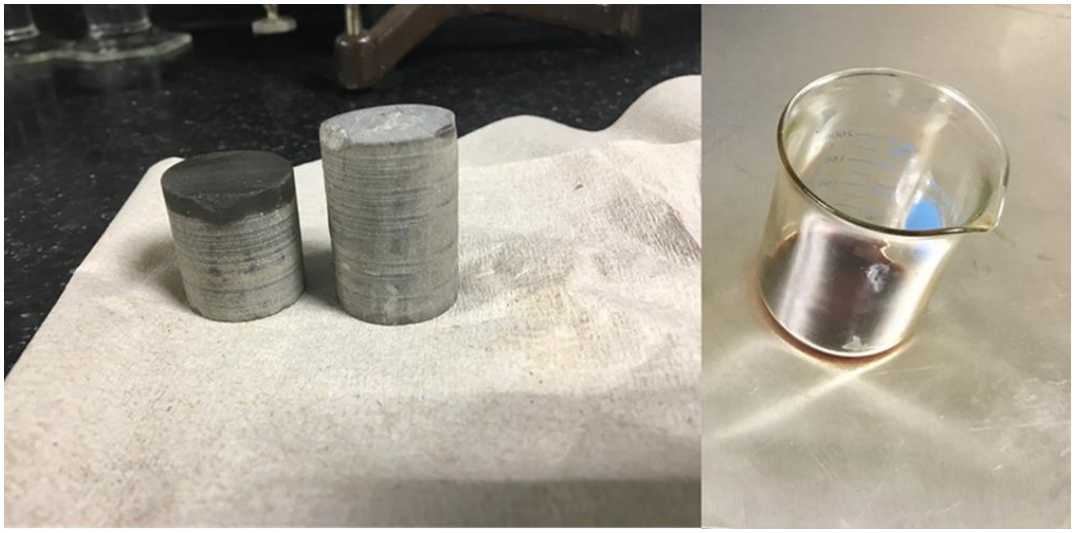

Figure 5. 29. The MB core samples after CO2 injection.

5.7.5 Effect of Wettability on the Recovery from CO2 Huff-n-Puff

Generally speaking, the wettability of the Bakken Formation tends to be more oil-to intermediate-wet. The wettability of some Bakken rock-chip samples were measured using a contact-angle measuring instrument that also confirmed this observation. The wettability

was measured before and after rock exposure to CO2 from which the impact of CO2 on the state of wettability was examined. When the contact angle of an oil droplet is lower than 90°, the rock is considered to be intermediate-to oil-wet (Figure 5. 30). The contact angle of the sample was measured before applying CO2 (i.e., original wettability) and turned out to be ~99° which indicates more oil wet.

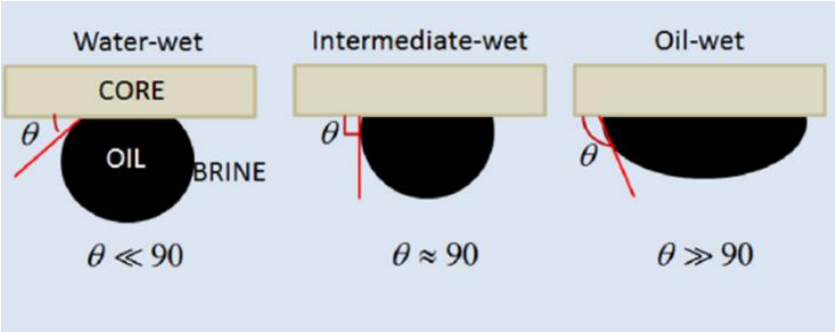

Figure 5. 30. Wettability conditions of different rock samples (Teklu et al., 2015).

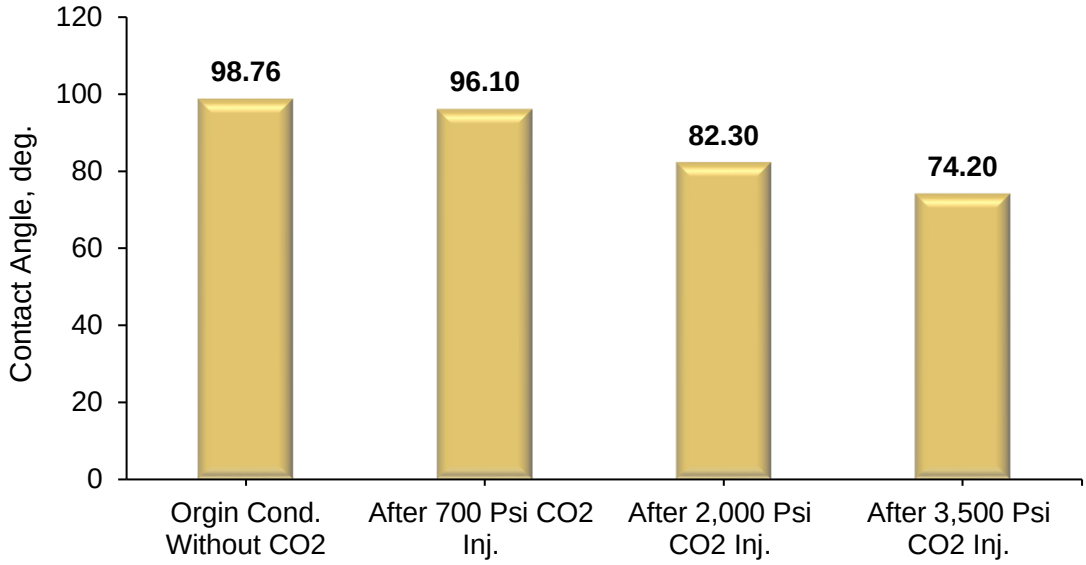

Figure 5. 31. Contact angle measurements for the Middle Bakken Fm. at different conditions before and after applying CO2-EOR.

The contact angles of the sample measured before and after applying CO2 huff-n-puff to study the impact of CO2 on the state of wettability. It is clear from Figure 5. 31 that the

contact angle decreases (i.e., becoming more intermediate- to water-wet) as the CO2 injection pressure increases from 700 psi to 3500 psi (at reservoir temperature) as a result of CO2 interaction with the host rock. In fact, the recovery increases as CO2 diffuses into the matrix, alters the wettability in favor of oil flow (i.e., less oil wet), and reduces oil density and viscosity from CO2 miscibility and oil swelling.

5.8 Conclusion

This work studies the potential of CO2 huff-n-puff in the Bakken Formation, Williston Basin and examines the factors affecting the recovery performance. The production from the huff-n-puff experiments we conducted on Bakken core samples resulted up to 50% ultimate recovery factor under different reservoir conditions. The following results can be drawn from this work:

- The outcomes indicated on the effect of the reservoir temperature on the performance of the CO2, where the recoverable oil increases as the temperature increase until reach the optimum depends on the injection pressure phase. On the other hand, high injection pressure yielded higher amount of produced oil.
- The surface contact area is a crucial factor for the diffusion mechanism, which plays a main important role to contact the CO2 flow to whole core samples, then the oil production increases as the contact surface area increases.
- As a previous research outcome, the number of cycling and soaking time are crucial design parameters for the huff-n-puff experiment and on the field as well to let the CO2 time to diffuse into the deep formation and swell more oil.

- The wettability condition behavior in the Middle Bakken Formation is generally found as the oil wet to intermediate wetting phase, where the contact angle obtained bigger than 90 deg. The wettability alteration was changed by CO2-EOR as injection pressures increase and the wetting phase move from the oil wet toward the water wet system.

- As overall outcomes from this research, the CO2 huff-n-puff process has a good potential in the Lab and could be succeeded economically in field applications.

References

Ahmed, U, and Meehan, N., 2016. “Unconventional Oil and Gas Resources: Exploitation and Development”, Taylor Francis Group, Baker Hughes 2016, https://www.crcpress.com/Unconventional-Oil-and-Gas-ResourcesExploitation-and-Development/Ahmed-Meehan/p/book/9781498759403.

Al Ismail, Maytham, and Mark Zoback. "CO 2-Based Technologies in Unconventional Resources: Impact of Rock Mineralogy on Adsorption." SPE Kingdom of Saudi Arabia Annual Technical Symposium and Exhibition. Society of Petroleum Engineers, 2017.

Alfarge, D., M. Alsaba, M. Wei, and B. Bai. 2018. Miscible Gases Based EOR in Unconventional Liquids Rich Reservoirs: What We Can Learn. In Proceedings of the SPE Improved Oil Recovery Conference, Tulsa, Oklahoma, USA, 14-18 April 2018.

Alfarge, D., M. Wei, and B. Bai. 2017. IOR methods in unconventional reservoirs of North America: Comprehensive review. In Proceedings of the SPE Western Regional Meeting, Bakersfield, California, 23-27 April 2017.

Assady, A., Jabbari, H., Ellafi, A. M., & Goudarzi, B. (2019, August 28). On the Characterization of Bakken Formation: Oscillating-Pulse, Pulse-Decay Permeability Measurement & Geomeachanics. American Rock Mechanics Association.

Ba Geri, M., Ellafi, A., Flori, R., Belhaij, A., & Alkamil, E. H. K. (2019c, November 11). New Opportunities and Challenges to Discover and Develop Unconventional Plays in the Middle East and North Africa: Critical Review. Society of Petroleum Engineers. doi:10.2118/197271-MS

Ba Geri, M., Flori, R., Ellafi, A., Noles, J., Essman, J., Kim, S., & Alkamil, E. H. K. (2019b, November 11). Correlated Friction Reduction and Viscoelastic Characterization of Utilizing

the Permian Produced Water with HVFRs during Hydraulic Fracturing. Society of Petroleum Engineers. doi:10.2118/197748-MS

Ba Geri, Noles, J., Kim, S., & Ellafi, A. (2020). New Developed Mathematical Model for Predicting Viscosity Profile and Proppant Transport Utilizing HVFRs Dosage with Produced Water. Society of Petroleum Engineers. doi:10.2118/ 201433-MS

Bhattacharya, Shuvajit, and Timothy R. Carr. "Integrated data-driven 3D shale lithofacies modeling of the Bakken Formation in the Williston basin, North Dakota, United States." Journal of Petroleum Science and Engineering 177 (2019): 1072-1086.

Chen, C., Balhoff, M.T., and Mohanty, K.K. 2014. Effect of Reservoir Heterogeneity on Primary Recovery and CO2 Huff 'n' Puff Recovery in Shale-Oil Reservoirs. SPE Res Eval & Eng14(03): 404-413. SPE-164553-PA. http:// dx.doi.org/10.2118/164553-PA

Cipolla, Craig and Wallace, Jon. 2014. Stimulated reservoir volume: a misapplied concept? Proc., SPE Hydraulic Fracturing Technology Conference.

Civan, F. (2019, October 1). Effective Correlation of Stress and Thermal Effects on Porosity and Permeability of Naturally Fractured Formations by a Modified Power Law. Society of Petroleum Engineers. doi:10.2118/198893-PA

Continental Resources. 2018, https://clr.com/

DrillingInfo website. 2019, from https://info.drillinginfo.com/

EIA. 2019. Annual Energy Outlook 2019 with projections to 2050, U.S. Department of Energy, https://www.eia.gov/outlooks/aeo (January 2019).

Ellafi, A., & Jabbari, H. (2019a, August 28). Coupling Geomechanics with Diffusion/Adsorption Mechanisms to Enhance Bakken CO2-EOR Modeling. American Rock Mechanics Association.

Ellafi, A., Jabbari, H., Ba Geri, M., & Alkamil, E. (2019b, November 11). Can HVFRs Increase the Oil Recovery in Hydraulic Fractures Applications? Society of Petroleum Engineers. doi:10.2118/197744-MS

Ellafi, A., Jabbari, H., Tomomewo, O., Mann, M., and Ba Geri, M. (2020b) 'Future of Hydraulic Fracturing Application in Terms of Water Management and Environmental Issues: A Critical Review ', Society of Petroleum Engineers (SPE), (SPE-199993-MS)

Ellafi, A., Jabbari, H., Wan, X., Rasouli, V., Ba Geri, M., & Al-Bazzaz, W. (2020a). How Does HVFRs in High TDS Environment Enhance Reservoir Stimulation Volume? International Petroleum Technology Conference (IPTC) 2020 IPTC-20138

Energy & Environmental Research Center (EERC). 2019, https://undeerc.org/

FracFocus website. 2019, from http://fracfocus.org/.

Gamadi TD, Sheng JJ, Soliman MY, Menouar H, Watson MC, Emadibaladehi H. An experimental study of cyclic CO2 injection to improve shale oil recovery. In: SPE IOR Symposium; 2014

Gamadi TD, Sheng JJ, Soliman MY. An experimental study of cyclic gas injection to improve shale oil recovery. In: SPE ATCE; 2013.

Geri, M. B., Ellafi, A., Ofori, B., Flori, R., & Sherif, H. (2019a, July 31). Successful Implementation of High Viscosity Friction Reducers from Laboratory to Field Scale: Middle Bakken Case Study. Unconventional Resources Technology Conference. doi:10.15530/urtec-2019-447

Gubian, Emilie. Changes in shale well design: Reaching the limits? IHS Markit, https://ihsmarkit.com/research-analysis/changes-in-shale-well-design-reaching-the-limits.html.

Hawthorne, S. B., C.D Gorecki, J.A. Sorensen, E.N. Steadman, J.A Harju, and S. Melzer. 2013. Hydrocarbon mobilization mechanisms from Upper, Middle, and Lower Bakken reservoir rocks exposed to CO2. In Proceedings of the SPE Unconventional Resources Conference, Calgary, Alberta, Canada, 5–7 November 2013.

Hawthorne, S. B., Miller, D. J., Grabanski, C. B., Sorensen, J. A., Pekot, L. J., Kurz, B. A., Gorecki, C. D., Steadman, E. N., Harju, J. A., Melzer, S. (2017, February). Measured crude oil MMPs with pure and mixed CO2, methane, and ethane, and their relevance to enhanced oil recovery from middle Bakken and Bakken shales. In SPE Unconventional Resources Conference. Society of Petroleum Engineers.

Heller, Robert, and Mark Zoback. "Adsorption of methane and carbon dioxide on gas shale and pure mineral samples." Journal of unconventional oil and gas resources 8 (2014): 14-24.

Holubnyak, Y., Dubois, M., Hollenbach, J., & Hasiuk, F. (2019, September 23). Challenges and Opportunities for Commercial-Scale Carbon Capture and Storage in Kansas. Society of Petroleum Engineers. doi:10.2118/196186-MS

Jarvie, D. M., Hill, R. J., Ruble, T. E., and Pollastro, R. M., 2007, "Unconventional shale-gas systems: The Mississippian Barnett shale of north-central Texas as one model for thermogenic shale-gas assessment," AAPG Bulletin, v. 91, no. 4, pp. 475–499.

Jin, L., Sorensen, J. A, Hawthorne, S. B., Smith, S. A, Bosshart, N. W., Burton-Kelly, M. E.,… Harju, J. A (2016, February 24). Improving Oil Transportability Using CO2 in the Bakken System - A Laboratory Investigation. Society of Petroleum Engineers. doi :10.2118/178948-MS

Jin, L., Sorensen, J. A., Hawthorne, S. B., Smith, S. A., Pekot, L. J., Bosshart, N. W., … Harju, J. A. (2017, August 1). Improving Oil Recovery by Use of Carbon Dioxide in the

Bakken Unconventional System: A Laboratory Investigation. Society of Petroleum Engineers. doi:10.2118/178948-PA

Jin, X. (Jacob), Pavia, M., Samuel, M., Shah, S., Zhang, R., & Thompson, J. (2019, July 31). Field Pilots of Unconventional Shale EOR in the Permian Basin. Unconventional Resources Technology Conference. doi:10.15530/urtec-2019-506

Klenner, R. C. L., Braunberger, J. R., Sorensen, J. A, Eylands, K. E., Azenkeng, A, & Smith, S. A (2014, August 25). A Formation Evaluation of the Middle Bakken Member Using a Multimineral Petrophysical Analysis Approach. Unconventional Resources Technology Conference. doi:10.15530/URTEC-2014-1922735

Kumar, Amit, Ron Glen Dusterhoft, and Shameem Siddiqui. "Completion and production strategies for liquids-rich wells in ultra-low-permeability reservoirs." SPE Annual Technical Conference and Exhibition. Society of Petroleum Engineers, 2013.

Kurtoglu B. Integrated reservoir characterization and modeling in support of enhanced oil recovery for Bakken [Doctoral Dissertation]. Colorado School of Mines; 2013.

Kurtoglu, B., H. Kazemi, R. Rosen, W. Mickelson, and T. Kosanke. 2014. A Rock and Fluid Study of Middle Bakken Formation: Key to Enhanced Oil Recovery. In Proceedings of the SPE/CSUR Unconventional Resources Conference, Calgary, Alberta, Canada, 30 September – 2 October 2014

Lashgari, H.R., A. Suna, T. Zhanga, G.A. Pope, and L.W. Lake. 2018. Evaluation of carbon dioxide storage and miscible gas EOR in shale oil reservoirs. Journal of Fuel.

Li, C., Kong, L., Ostadhassan, M., & Gentzis, T. (2019). Nanoscale Pore Structure Characterization of Tight Oil Formation: A Case Study of the Bakken Formation. Energy & Fuels, 33(7), 6008-6019.

Li, Chunxiao, et al. "Multi-scale evaluation of mechanical properties of the Bakken shale." Journal of materials science 54.3 (2019): 2133-2151.

Liu, K.; Ostadhassan, M.; Zhou, J.; Gentzis, T.; Rezaee, R. Nanoscale Pore Structure Characterization of the Bakken Shale in the USA. Fuel 2017, 209, 567−578.

Luo, G., Tian, Y., Bychina, M., & Ehlig-Economides, C. (2019, August 1). Production-Strategy Insights Using Machine Learning: Application for Bakken Shale. Society of Petroleum Engineers. doi:10.2118/195681-PA

Mahzari, P., Oelkers, E., Mitchell, T., & Jones, A. (2019, June 3). An Improved Understanding About CO2 EOR and CO2 Storage in Liquid-Rich Shale Reservoirs. Society of Petroleum Engineers. doi:10.2118/195532-MS

Male, F. (2019): "Using a segregated flow model to forecast production of oil, gas, and water in shale oil plays," Journal of Petroleum Science and Engineering, 180, 48–61.

Melcher, H., Mayerhofer, M., Agarwal, K., Lolon, E., Oduba, O., Murphy, J., … Weijers, L. (2020, January 28). Shale Frac Designs Move to Just-Good-Enough Proppant Economics. Society of Petroleum Engineers. doi:10.2118/199751-MS

North Dakota Council. 2012. https://www.ndoil.org/

Oil and Gas Division-North Dakota Industrial Commission (NDIC). 2019. https://www.dmr.nd.gov/oilgas/

Pankaj, P., Mukisa, H., Solovyeva, I., and Xue, H. 2018. Enhanced Oil Recovery in Eagle Ford: Opportunities Using Huff-n-Puff Technique in Unconventional Reservoirs. Presented at SPE Liquids-Rich Basins Conference - North America,

Sheng, J. J. Enhanced oil recovery in shale reservoirs by gas injection. J. Nat. Gas Sci. Eng. 2015, 22, 252−259.

Shoaib, S., and B.T. Hoffman. 2009. CO2 flooding the Elm Coulee Field. In Proceedings of the Rocky Mountain Petroleum Technology Conference, Denver, Colorado, 14-16 April 2009.

Sorensen, J. A., Braunberger, J. R., Liu, G., Smith, S. A., Hawthorne, S. A., Steadman, E. N., & Harju, J. A. (2015, July 20). Characterization and Evaluation of the Bakken Petroleum System for CO2 Enhanced Oil Recovery. Unconventional Resources Technology Conference. doi:10.15530/URTEC-2015-2169871

Sorensen, J., B. Kurz, S. Hawthorne, L. Jin, S. Smith, and A. Azenkeng. 2016. Laboratory characterization and modeling to examine CO2 storage and enhanced oil recovery in an unconventional tight oil formation. Elsevier Ltd, 5460-5478.

Teklu, T. W., Alameri, W., Kazemi, H., & Graves, R. M. (2015, July 20). Contact Angle Measurements on Conventional and Unconventional Reservoir Cores. Unconventional Resources Technology Conference. doi:10.15530/URTEC-2015-2153996

Teklu, T. W., Li, X., Zhou, Z., & Abass, H. (2018, June 1). Experimental Investigation on Permeability and Porosity Hysteresis of Tight Formations. Society of Petroleum Engineers. doi:10.2118/180226-PA

Terzaghi, K. 1943. Theoretical Soil Mechanics. New York: Wiley.

Thakur, Ganesh. "Enhanced Recovery Technologies for Unconventional Oil Reservoirs." Journal of Petroleum Technology 71.09 (2019): 66-69.

Tovar FD, Eide O, Graue A, Schechter DS. Experimental investigation of enhanced recovery in unconventional liquid reservoirs using CO2: a look ahead to the future of unconventional EOR. In: SPE Unconventional Resources Conference; 2014.

Tovar, F. D., Barrufet, M. A., & Schechter, D. S. (2018, April 14). Gas Injection for EOR in Organic Rich Shale. Part I: Operational Philosophy. Society of Petroleum Engineers. doi:10.2118/190323-MS

Tran, Tan, Pahala Dominicus Sinurat, and Bob A. Wattenbarger. "Production characteristics of the Bakken shale oil." SPE Annual Technical Conference and Exhibition. Society of Petroleum Engineers, 2011.

Wan, T., and Sheng, J. 2015. Compositional Modelling of the Diffusion Effect on EOR Process in Fractured Shale-Oil Reservoirs by Gasflooding. J Can Pet Technol 54(02): 107-115. SPE-20214-1891403-PA. http:// dx.doi.org/10.2118/2014-1891403-PA

Wan, T., Sheng, J. J., & Soliman, M. Y. (2013, August 12). Evaluate EOR Potential in Fractured Shale Oil Reservoirs by Cyclic Gas Injection. Unconventional Resources Technology Conference. doi:10.1190/urtec2013-187

Wang, Leizheng, and Wei Yu. "Mechanistic simulation study of gas Puff and Huff process for Bakken tight oil fractured reservoir." Fuel 239 (2019): 1179-1193.

Yu, W., Lashgari, H., & Sepehrnoori, K. (2014, April 17). Simulation Study of CO2 Huff-n-Puff Process in Bakken Tight Oil Reservoirs. Society of Petroleum Engineers. doi:10.2118/169575-MS

Zhang, K., Kong, B., Zhan, J. et al. 2016. Effects of Nanoscale Pore Confinement on CO2 Immiscible and Miscible Processes. Presented at the SPE Low Perm Symposium, Denver, Colorado, USA. 10.2118/180256-MS.

CHAPTER 6

CO2-EOR Diffusion/Adsorption Mechanisms

This chapter discusses the paper entitled "***Coupling Geomechanics with Diffusion/Adsorption Mechanisms to enhance Bakken CO2-EOR Modeling***" published in the 53rd US Rock Mechanics/Geomechanics Symposium held in New York, NY, USA, 23–26 June 2019.

Abdulaziz Ellafi was responsible to prepare the methodology, analyze the data, validation and writing the paper. Hadi Jabbari is the PhD advisor and was the director of the project.

Abstract

Unconventional liquid-rich tight reservoirs, such as the Bakken Formation have an enormous amount of oil-in-place that any effort to improve the recovery factor through an EOR process is worthwhile. Due to the ultra-low pore structure of the Bakken Fm, the pore connectivity and pore networks are different from those in conventional reservoirs and thus the fluids transport in EOR processes behave differently. In a CO2-EOR process, the adsorption and diffusion play major roles from both perspectives of production performance and CO2 storage. In addition, our better understanding of geomechanics and coupling it with transport phenomenon has a significant impact on a successful CO2-EOR application in shale plays. In this study, we investigate the changes in reservoir permeability and porosity under different conditions to better understand the correlations between molecular

diffusion/adsorption and the stress/strain changes in a typical huff-n-puff process in the Mountrail County, Williston Basin, ND. The stress state during injection, soak, and production may lead to changes in petrophysical properties, fluid/rock molecular interactions, and fluid transport, which are investigated by coupling the geomechanics and fluid flow through a two-way method. This integrated workflow can assist us to understand the relation between geomechanics and CO2-EOR mechanisms in unconventional liquid-rich shale reservoirs.

6.1 Introduction

Nowadays, unconventional reservoirs are a turning point in the global oil and gas industry since these resources have massive reserves with large potential in contributing to hydrocarbon production and ability to gas storage capacity. Ultra-low permeability (nano to micropore size) and low matrix porosity are the main reservoir parameters that distinguish unconventional liquid-rich shale (LRS) reservoirs from conventional resources. Therefore, the combination of long laterals horizontal well and multistage hydraulic fracturing stimulation is a necessary technique to access the unlocked formations by providing more surface area for hydrocarbon between wellbore in the horizontal wells and extremely low pore size in the rock matrix. In North America, the Bakken Petroleum System (BPS) is the largest shale play that has taken attention and interest in oil production. The BPS consists of four units, Upper Bakken Member, Middle Bakken Member, Lower Bakken Member, and the Three Forks Formation. However, the Middle Member and Three Forks formation are only the productive plays since are naturally fractured. Both non-shale units are characterized by the reservoir porosity between 4 to 8% and permeability in the range of micro-Darcy (Yu et al., 2014; Jin et al., 2017). Several studies showed that these units contain from medium

to a large amount of hydrocarbon saturation. Recent reports by U.S. Geological Survey and Energy and Environmental Research Center (EERC) evaluated theirs proven recoverable oil by 0.16 billion m3 (7.4 billion barrels) and initial oil in place in range of 25.43 billion m3 (160 billion barrels) to more than 143 billion m3 of oil (900 billion barrels) (Flannery and Krause, 2006; Continental Resources Inc, 2014; Sorensen et al., 2016). The Bakken oil is a light oil that its composition consists mainly 40% of C1-C4. Hence, oil production depends on the gas expansion mechanism as a primary depletion stage. Moreover, the oil recovery is believed to be less than 8% due to sharply decline in oil production rate when the natural fractured depleted, while slow to no recharge from the matrix rock, because of its extremely low mobility (Kurtoglu, 2013; Sheng, 2014; Yu et al. 2014). Thus, around 3.8 billion barrels of oil is isolated and unrecovered without using unconventional applications like enhanced oil recovery (EOR) methods.

The aim of this paper is to build a reservoir simulation model of CO2 huff-n-puff process case study in the Mountrail County, Williston Basin, ND in order to investigate the coupling effects of the geomechanical with the molecular diffusion/adsorption mechanisms in both perspectives of production performance and storage.

6.2 Carbon Dioxide (CO2) Applications in Unconventional Reservoirs

Hawthorne et al., 2013 reported that any effort to improve the recovery factor through an EOR process is worthwhile and could increase the incremental oil by several billion barrels. Subsequently, applying EOR application, such as CO2 injection is mandatory since it leads to increase recoverable oil from its primary depletion value, improve the long-term well productivity, and contribute the cost-effective production less than other techniques (Shoaib and Hoffman, 2009; Kurtoglu, 2013; Alfarge et al., 2017; Lashgari et al., 2018). According

to the literature review, the CO2 huff-n-puff process is considered as the most effective EOR method for tight formations, such as Bakken Fm. This method performs better than other applications due to several reasons: 1) CO2 injection is characterized by favorable injectivity as a result of continuous gas pathways from fracture and penetrating into the rock matrix to swell oil by diffusion mechanism. 2) CO2 is required low minimum miscibility pressure (MMP) compared to nitrogen and natural gases to develop miscible displacement by reduction in oil viscosity. 3) A lower acid number in LRS oils could help to apply CO2- EOR successfully without considering the negative impact of asphaltenes precipitation. 4) CO2 adsorption trapping mechanism is considered as the significant mode of hydrocarbon storage, where this mechanism in CO2 is up to five times higher than CH4 adsorption in the organic shale rocks (Wang et al. 2010; Kumar et al., 2013; Kurtoglu et al., 2014; Sheng, 2014; Alfarge et al., 2017). Recent research including modeling and simulation studies of CO2 EOR reported that the oil incremental recovery in the Bakken Fm is in range of 5 to 20% using huff-n-puff gas EOR (Shoaib and Hoffman, 2009; Hoffman, 2016). Also, experimental studies results showed promising outcomes of using gas injection application. Based on the rock characterization of the core samples and experimental factors, this method can improve the oil recovery from the shale core sample in range of 30 to 60% (Alharthy et al., 2017; Lashgari et al., 2018).

On the other hand, CO2 sequestration is an important application that combining with EOR to be an effective solution for environmental challenges (Lashgari et al., 2018). This method could be promising targets to capture, utilize, and store a significant amount of CO2 in deep LRS plays. Therefore, the large quantity of CO2 emissions to the atmosphere that causes global warming issues might be reduced. The Bakken Fm is a good example that has the ability to serve as CO2 geological storage since CO2 adsorption mechanism is attractive

mechanism to the rich organic shale formations, such as the Upper and Lower Bakken Members due to their content of total organic content (TOC) in range between 12 to 36 wt.%, presence of clay around 54 wt.%, and kerogen type (Kang et al., 2011; Kim et al., 2017; Jin et al., 2017; Aljamaan et al., 2017). Although CO2 adsorbed on the organic rich rock contribute ineffectively way to increase oil recovery in unconventional reservoirs, CO2 adsorption can be potentially an effective mechanism to minimize greenhouse gas emissions by tapping CO2 in deep shale formations. Jin et al., 2017 addressed that the Bakken reservoir characterization coupling with adsorption phenomenon allow the CO2 to be stored for millions of years in the deep formations without any impact on environment and concerns of sealing failure or leakage. In order to fill the gap in the literature on the quantifying of CO2 adsorption in LRS plays, numerical simulation models are utilized to attempt to field-scale contribution of CO2 adsorption as storage mechanisms (Jessen et al., 2008; Lashgari et al., 2018).

6.3 CO2-EOR Mechanisms

6.3.1 Diffusion Mechanism in the Bakken Fm.

The modeling work will not be efficiently predictable to the field test without considering many physical processes, such as diffusion/adsorption mechanisms and geomechanical-coupled with the fluid flow transport that represents LRS plays. These mechanisms are associated and can be impacted by the reservoir characterizations and geomechanical property (Teklu et al., 2018). Moreover, unconventional reservoirs rely on these mechanisms to enhance the flow ability from the matrix to the fracture networks. The fluid flow through the pores media are governed by gravity drainage, physical diffusion, viscous flow, and capillary forces, where the viscous flow dominated in the fracture networks, while diffusion

flow in the tight pore space of the rock matrix (Jin et al., 2017). The general definition of the molecular diffusion phenomenon is the Brownian motion or composition gradient in a fluid mixture as a result of the molecules movement in the presence of coexisting gas, liquid phases, and solid formation (Mohebbinia and Wong, 2017; Lashgari et al., 2018). Diffusion mass transfer is significant drive mechanism that control the fluid transport in unconventional reservoirs (nano-porous medium), while the flow in conventional reservoirs (micro-porous media) is governed by Darcy flux. Previous publications have approved that the diffusion role has the positive effect on the CO2-EOR performance during huff-n-puff process to mobilize more oil in the tight rock. In contrast, the negative impact has been reported on the oil recovery when the continuous injection process is used (Yu et al., 2015; Alfarge et al., 2017). Yu et al., 2014 performed a series of simulation works for CO2 injection in the Bakken Fm to compare between considering and without considering CO2 molecular diffusion in numerical reservoir models. The incremental oil recovery factor results after 10 years showed that disregarding the CO2 diffusion rate results the solvent concentrates only around the fractures, then the oil recovery factor will be impacted negatively due to difficultly to diffuse into the rock matrix. Therefore, the reservoir simulation outcomes lead to poor prediction of the oil production performance and underestimation of capability to store CO2 in the shale formations. The molecular diffusion term can be determined either experimentally in labs or numerically using reservoir simulation models, which depends on temperature, phase density, critical properties of components, and mole fraction (Sigmund et al., 1976). Furthermore, Alharthy et al., 2017 conducted the molecular diffusion of the Bakken Fm using experimental and simulation works. They concluded that the magnitude of the diffusion mass transform is small in round 5×10-5 cm^2 /s, and flux energy is very slow mechanism. Recently, Torres et al., 2018 modeled reservoir simulation study with high

accuracy to improve the predictability of the reservoir potential after performing CO2-EOR. The simulation results after history matching reported that the CO2 molecular diffusion coefficient is 1.67×10-5 cm^2 /s.

6.3.2 Adsorption Mechanism in the Bakken Fm.

Another important mechanism through CO2 huff-n-puff process is CO2 adsorption in confinement nanopores. This mechanism defines as the amount of adsorbate on the adsorbent through isotherms, which is a function of pressure (gas phase) or concentration (liquid phase). The amount of adsorption depends on the surface characteristics and pore structure of adsorbent material. In addition, this phenomenon describes as the interactions between the adsorbate and adsorbent based on dispersion, electrostatic, and chemical bond, as well as thermodynamic and kinetic energy. These factors play the main role to understand the adsorption behavior for an adsorbent material. The adsorption phenomenon is increased as the material surface area is high compared to material volume ratio. Moreover, the adsorption phenomenon depends on several parameters: pressure, temperature, flow rate, and adsorbent concentration. Several distinctive lithofacies describe the Bakken Rock Unit, where this unconventional reservoir owns unique properties that might or might not play a significant role to success mobility and applicability of penetrating the solvent within the formation and increase oil recovery using CO2-EOR, as well as capability to storage CO2 in underground formations. The literature review assisted to clarify this question by understanding the reservoir characterization and mineralogy coupled with adsorption mechanism. Based on previous studies, the shale units (Upper and Lower Members) classified as an organic matter with nonporous structure and high amount of total organic carbon (TOC) that controls the adsorption capacity of the organic rich shales. Heller and Zoback, 2014, conducted

experimental work to investigate the relationship between gas adsorption capacity and TOC and minerals that represents Barnett, Montney, Marcellus, and Eagle Ford formations. The results showed that the high TOC value, the maximum absolute adsorption capacities, where Barnett and Montney have TOC in range of 5.3% and maximum adsorption around 40.8 gmole/g. Also, the rich shale members contain the kerogen that is the primary organic matter component that has micro porosity, spanning micrometer to nanometer in scale. The kerogen influences the adsorption capacity (oil both adsorbs and absorbs onto kerogen) and diffusion of hydrocarbon molecules (Kumar et al., 2013). As a result, adsorption trapping mechanism might play the key role in these organic-rich formations to store CO2 safely and reduce the climate change. Liu et al., 2013 constructed simulation work to assess the applicability to store CO2 in the New Albany Shale, and the results indicated that 90% of the injected CO2 is trapped via adsorption mechanism. Nuttall, 2010, explained that CO2 adsorption trapping is up to five times higher than CH4 adsorption in the organic shale rocks. Although adsorption mechanism has a negative impact on the CO2 huff-n-puff process due to large amount of gas adsorbed in the formation, CO2 adsorption isotherm results in the Bakken shales showed that capability to trap up to 17 gmole/g of CO2 in the organic shale for CO2 sequestration in tight formations (Jin et al., 2017). Pervious publications clarified that the combination of molecular diffusion and adsorption mechanisms can assist to improve the CO2 penetrating and covering performance for more surface area of organic and inorganic pores as a result of improving oil recovery and CO2 storage capacity. Lashgari et al., 2018 demonstrated reservoir simulation model on the Bakken Fm to study the gas adsorption effect on the production and storage performance. They found that the reservoir permeability is the crucial key that impact adsorption phenomena, where large amount around 33 to 45% of gas tapping in the formation when the molecular diffusion mechanisms is considered during CO2

injection. However, molecular diffusion mechanism is insignificant with high reservoir permeability (100 μD). In addition, the considering of molecular diffusion can be increased the adsorption capacity by 4 to 10 times without diffusion consideration. In contrast, in extremely low reservoir permeability, adsorption capacity does not exceed 24% of the gas injection. The low adsorption capacity as a result of dissolving the diffusion flux in oil to contribute more to oil recovery than adsorption capacity.

6.4 Geomechanics Coupling Effects

Geomechanics module has widely used in oil industry applications to investigate and evaluate many phenomena, such as hydraulic fracture stimulation, reservoir compaction and surface subsidence during depletion, wellbore stability, and recently for coupling consideration of transport and deformation stresses in the formation during CO2-injection EOR (Tran et al., 2005). Modeling of geomechanical effects can count the interaction between solid and fluid flow transport and investigate the impact of stress and deformation of reservoir rock. Geomechanical effects can be simulated by stress-dependent correlations with a linear elastic constitutive model by either 3D two way coupling or 3D one way coupling. In addition, several publications were included the pressure dependent permeability correlation in the use of reservoir simulation to account the changes in reservoir petrophysical properties. In this paper, the proposed model was used two linear-elastic constitutive models with 3D two way coupling to mimic the reservoir fluid flow that affected by geomechanics responses. Jabbari et al., 2015 studied the performance of CO2 huff-n-puff EOR by coupling the reservoir fluid flow with geomechanics to understand the stress and deformation of the Middle Bakken reservoir. The geomechanical effects were counted through porosity and permeability relationships with pressure, temperature, and mean total

stress. They concluded that the reduction in fracture spacing due to considering of the geomechanical effects during CO2 injection can increase the incremental oil recovery by 10%.

Furthermore, Alfarge et al., 2018 examined the effect of coupling of geomechanics module and fluid transport using numerical reservoir simulation on the Bakken and Eagle formations in order to mimic the permeability and porosity reduction in the matrix, fractures, and hydraulic fractures. The linear-elastic constitutive model was used with different aspects of geomechanical effects (3D two way coupling and 3D one-way coupling). The results indicated that CO2 injection performance has been clearly affected by geomechanics coupling. In addition, Bakken CO2-EOR Pilot tests were matched perfectly with stress dependent correlation, while Eagle Ford results were matched with linear elastic models. On the other hand, Kim et al., 2017 reported a study to conduct the performance of CO2 storage under geomechanical effects in shale gas reservoirs using stress-dependent correlations coupled with a linear-elastic model. The results were positive and geomechanical effects showed better performance of CO2 flooding than CO2 injection in the Barnett shale formation.

This research study assists to understand relation between geomechanics and CO2-EOR mechanisms in unconventional reservoir as productive and storage formations through 3D two-way coupling of fluid flow and geomechanics. Limited to no previous publications were examined the geomechanical effects on both diffusion and adsorption mechanisms during CO2 huff-n-puff process.

6.5 Reservoir Model Description

Although there are a fewer pilot tests that show real response during applying EOR applications, the reservoir simulation model can provide a realistic effect of CO2 huff-n-puff process in the Bakken Fm by performing several scenarios to investigate the reservoir performance. In this study, the symmetric model, as shown in Figure 6. 1 was built using compositional reservoir simulator (CMG/GEM). This case study is based on information of the horizontal well in the Bakken Fm in the Mountrail County, Williston Basin, ND.

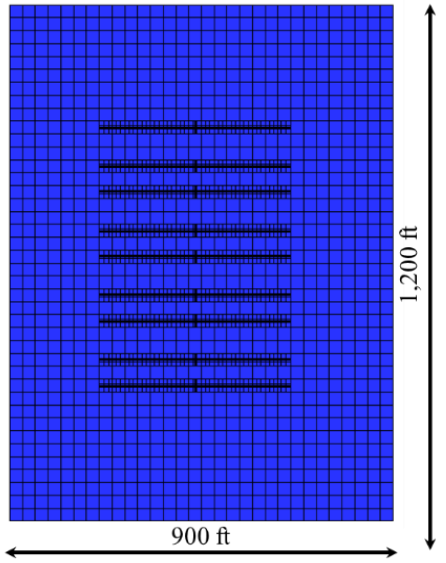

Figure 6. 1. The symmetric model with one stage of hydraulic fracturing.

The field data were gathered from the North Dakota Industrial Commission (NDIC) website, where the well started production through the period from December 2013 to December 2017. After that, the well was shut-in due to a sharp decline in the well productivity as oil depletion in natural and induced fractures. A Cartesian grid system with one stage of hydraulic fracturing was constructed using a local grid refinement (LGR) to mimic the representative chunk of the horizontal well with multi-stage hydraulic fracturing. The grid blocks system in x, y, and y are 30, 40, and 3, respectively and the dimension of the model

is 274×366×43 m (900×1,200×140 ft), as illustrated in Figure 6. 2. Table 6. 1 includes more details about thickness of each layer, the reservoir rock, hydraulic fracturing, and geomechanical properties, where these data were gathered based on the previous Bakken case studied.

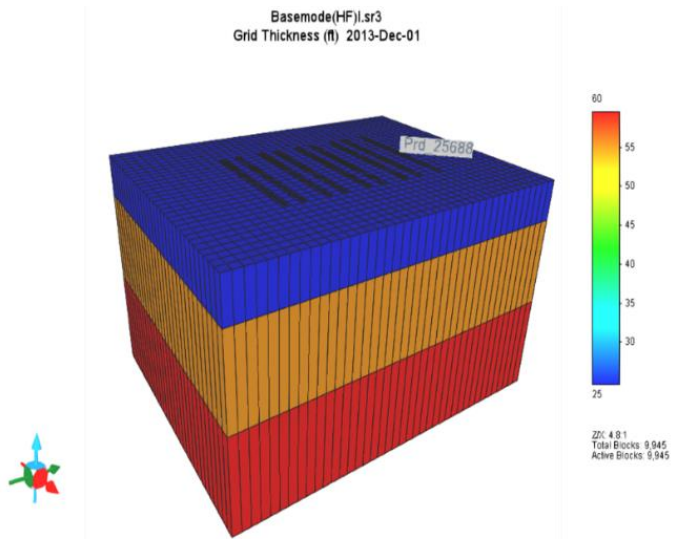

Figure 6. 2. 3D schematic of the reservoir model.

After that, phase behavior model was generated to simulate the Middle Bakken Fm hydrocarbon using the Peng-Robinson equation of state (PR-EOS) in WinProp PVT modeling software.

Table 6. 1 . The Bakken reservoir, hydraulic, and geomechanical properties.

Parameters	Bakken Unit	Value	References
Thickness, ft	Upper Member	25	NDIC, website
	Middle Member	55	
	Lower Member	60	
Matrix Porosity, fraction	Upper Member	0.04	Kumar et al., 2013 & Lashgari et al., 2018
	Middle Member	0.06	
	Lower Member	0.04	
Matrix Permeability, µd	Upper Member	0.010	Yu et al., 2014 & Kumar et al., 2013

	Middle Member	5	
	Lower Member	0.010	
	Upper Member	NA	
Matrix Porosity, fraction	Middle Member	0.0022	Alharthy et al., 2017
	Lower Member	NA	
	Upper Member	NA	
Fractured Permeability, μd	Middle Member	50	Alharthy et al., 2017
	Lower Member	NA	
Initial Water Saturation, fraction	Middle Member	0.40	Jabbari et al., 2015 & Sanaei et al., 2018
Fracture half-length, ft	Middle Member	250	Jabbari and Zeng, 2012 & Sanaei et al., 2018
Fracture spacing, ft	Middle Member	120	Jabbari and Zeng, 2012 & Sanaei et al., 2018
Fracture width, ft	Middle Member	0.01	Jabbari and Zeng, 2012 & Sanaei et al., 2018
Young's modulus, MMpsi	Middle Member	6.5	
Poisson's ratio	Middle Member	0.30	
Compressive strength, psi	Middle Member	16,746	Jabbari et al., 2015
Angle of internal friction, deg	Middle Member	35	
Coefficient of internal, friction	Middle Member	0.85	
Cohesion, psi	Middle Member	3,602	

The typical reservoir fluid composition, as mentioned by Lashgari et al., 2018 was utilized in this step to tune and build compositional model within the Bakken reservoir condition. Furthermore, Table 6. 2 shows several run scenarios that were performed CO2-EOR huff-n-

puff process under condition of 6 months of CO2 injection, 1-month soaking time, and ten years of production. The workflow provides guidance lines to understand the geomechanical effects on the molecular diffusion/adsorption mechanisms.

Table 6. 2 . Summary of simulation case scenarios for CO2 huff-n-puff EOR.

Scenario #	Description
1	Natural depletion before CO_2-EOR process
2	CO_2 injection without considering geomechanical effect
3	CO_2 injection including diffusion mechanisms without considering geomechanical effect
4	CO_2 injection including adsorption mechanisms without considering geomechanical effect
5	CO_2 injection including diffusion and adsorption mechanisms without considering geomechanical effect
6	CO_2 injection with considering geomechanical effect
7	CO_2 injection including diffusion mechanisms with considering geomechanical effect
8	CO_2 injection including adsorption mechanisms with considering geomechanical effect
9	CO_2 injection including diffusion and adsorption mechanisms with considering geomechanical effect

6.6 Results and Observations

As shown in Figure 6. 3 and 6. 4, the history of oil and water data are matched perfectly with simulation results through natural depletion production period. This step is crucial to calibrate, then simulate the production performance for the symmetric model with the field data. Therefore, the optimization processes will be reliable and representative as possible to the field operation.

Table 6. 2 lists several cases that were performed for CO2- EOR huff-n-puff process to investigate the reservoir deformation on the unconventional reservoir mechanisms. Figure 6. 5 illustrates the effect of with and without considering geomechanical effects on the oil recovery factor during natural depletion process.

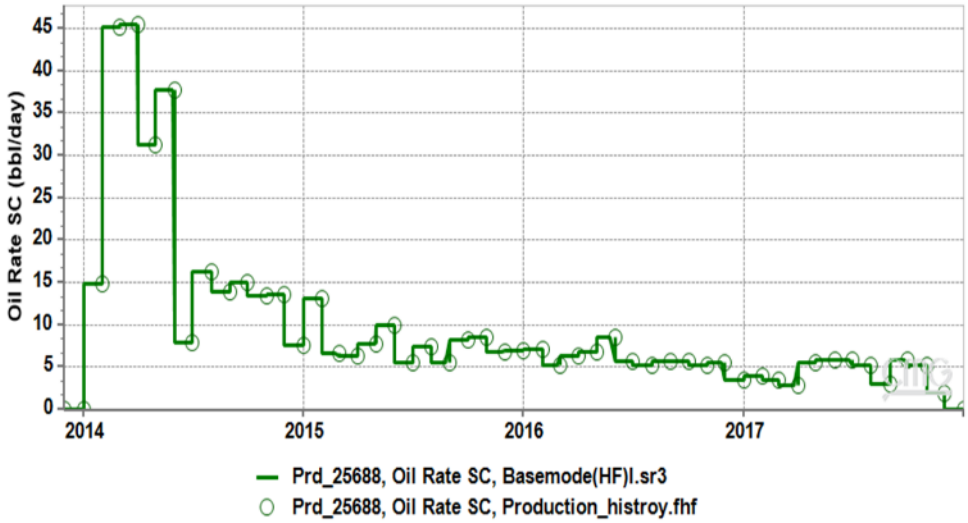

Figure 6. 3. History match of the oil production rate.

As shown in Figure 6. 5, the oil recovery factor results of the model that included the geomechanical property is represented by red line, while green line shows the oil recovery factor of the model without this effect. It is clear that without consideration of porosity/permeability and strain/stress changes results underestimation of the incremental oil recovery by 15.33%. The reasoning for this could be the reservoir elasticity that created more energy to support the reservoir pressure during the natural depletion process. The results are in good agreement with Alfarge et al., 2018 study on the Bakken and Eagle Ford formations.

On the other hand, considering the effect of formation deformation during CO2 injection impacts negatively the oil recovery factor by 5%, as demonstrated in Figure 6. 6. According to Alfarge et al., 2018, the reason behind that is the dilation loading path behavior, as shown in Figure 6. 7. When CO2 injected into the reservoir formation, the reservoir pressure will be increased until the region of the dilation, then the reservoir formation behaves in a plastic manner and could not restore to the original behavior even the injection pressure reaches the equilibrium with average reservoir pressure (Tran et al., 2005; Alfarge et al., 2018).

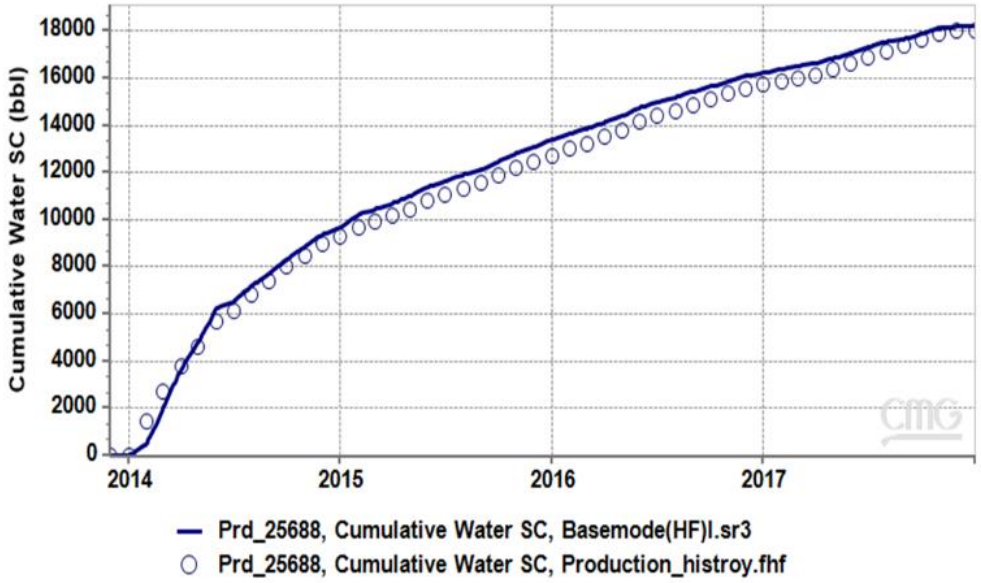

Figure 6. 4. History match of the oil cumulative production.

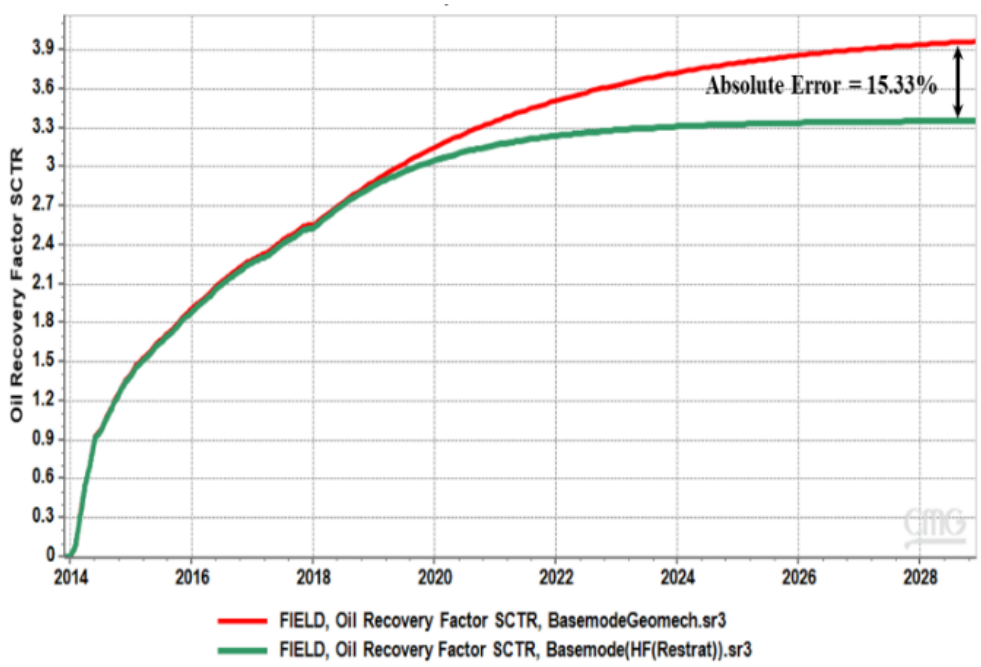

Figure 6. 5. Oil recovery factor through natural depletion process by considering and without geomechanical effects.

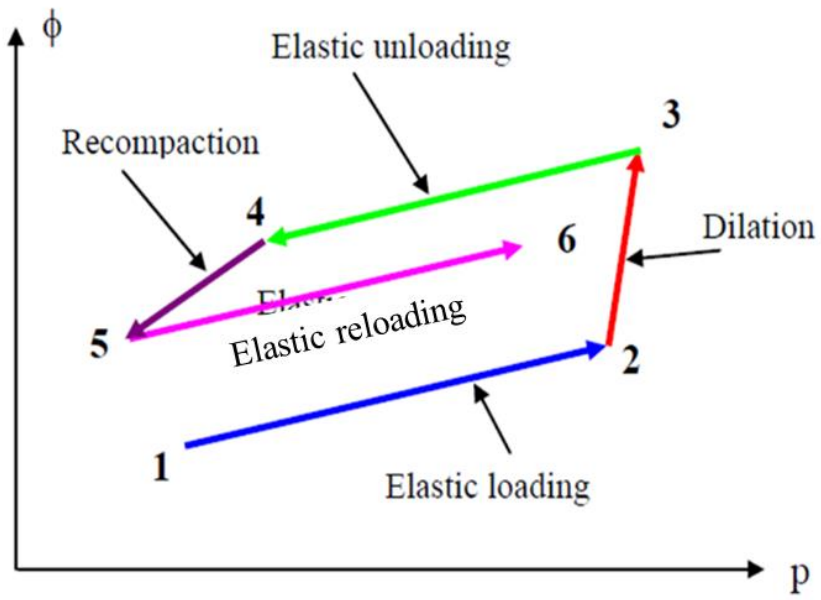

Figure 6. 6. Pseudo dilation behavior (Tran et al., 2005).

Finally, the coupling consideration between the geomechanics and diffusion/adsorption mechanisms shows the Bakken Fm can be able to store CO2 as adsorption phase in the deep underground formation. As shown in Figure 6. 8, when the adsorption mechanism neglected and only diffusion rate is presence, the incremental oil recovery is an overestimated value. The combination between diffusion and geomechanical effects increases the storage capacity in the LRS plays due to energy evolving from molecular diffusion that combined with deformation process and the ability to gas adsorbed into the organic shale. Although the adsorption mechanism has negative results on CO2-EOR huff-n-puff process, adsorption mechanism is beneficial and powerful phenomenon to reduce the global warming issues by capturing, utilize, and storage CO2 safely in the Bakken Fm.

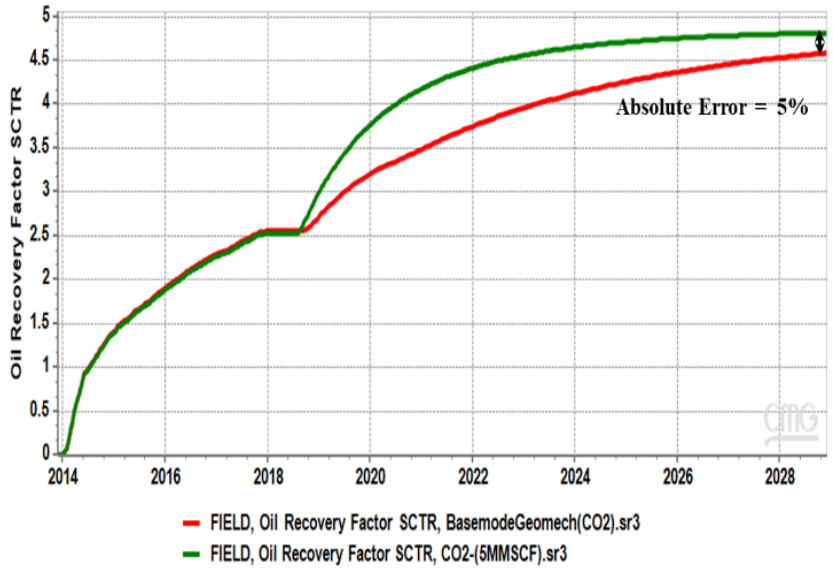

Figure 6. 7. Oil recovery factor through CO2 huff-n-puff process by considering and without geomechanical effects.

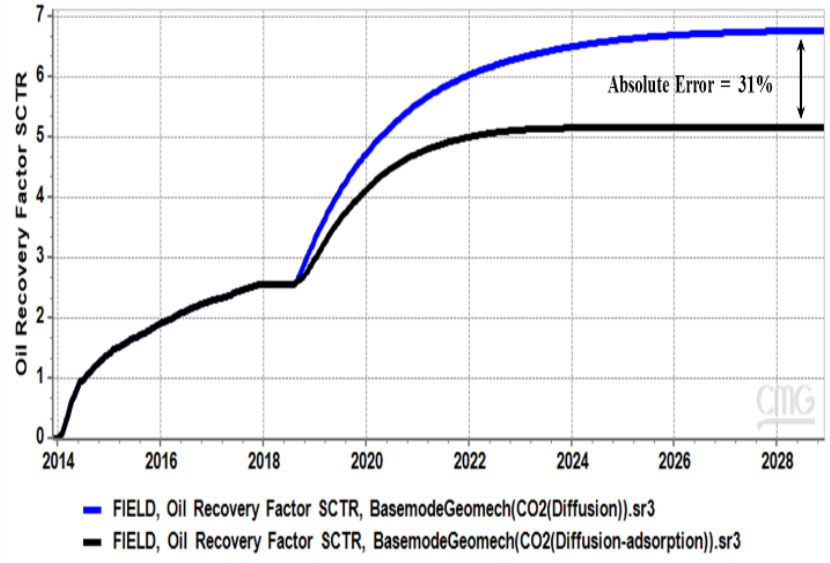

Figure 6. 8. Oil recovery factor through CO2 huff-n-puff process by considering geomechanical effects and diffusion/adsorption mechanisms.

6.7 Conclusions

The objective of this work was to construct a reservoir simulation study with a review of production mechanisms in unconventional reservoirs to better understand the coupling of

geomechanical effects with diffusion/adsorption and their combined effects on the production behavior.

Based on previous works and the results from this study, reservoir simulation models for unconventional plays should include all the factors related to reservoir performance for successful stimulation and EOR design in Liquid-Rich Shale plays (LRS). The molecular diffusion mechanism is the dominated energy in tight pore space to swell more oil from the rock matrix, while adsorption phenomenon controls the storage capacity of the formation surface, especially where it contains high amount of TOC and clay. Using a 3D two-way coupling platform, we investigated the coupling effects of geomechanics and fluid transport during production.

We observed that including the deformation from production in a tight shale play leads to higher recovery factors. In contrast, during CO2 injection, the change in porosity/permeability and strain/stresses yields lower incremental oil recovery factors. The results from this work are in agreement with previous research that the Bakken Fm can be a target for geological storage of waste carbon dioxide.

Finally, CO2-EOR in a tight formation can lead to higher incremental oil recovery (with cost-effective production) and reliable storage of anthropogenic CO2 with minimal environmental footprint.

References

Alfarge, D., M. Alsaba, M. Wei, and B. Bai. 2018. Miscible Gases Based EOR in Unconventional Liquids Rich Reservoirs: What We Can Learn. In Proceedings of the SPE Improved Oil Recovery Conference, Tulsa, Oklahoma, USA, 14-18 April 2018.

Alfarge, D., M. Wei, and B. Bai. 2017. IOR methods in unconventional reservoirs of North America: Comprehensive review. In Proceedings of the SPE Western Regional Meeting, Bakersfield, California, 23-27 April 2017.

Alharthy N, T.W. Teklu, H. Kazemi, R.M. Graves, S.B. Hawthorne, J. Braunberger, and B. Kurtoglu.2017. Enhanced oil recovery in liquid-rich shale reservoirs: laboratory to field. Journal Society of Petroleum Engineers.

Aljamaan H, R. Holmes, V. Vishal, R. Haghpanah, J. Wilcox, and AR. Kovscek. 2017. CO2 storage and flow capacity measurements on idealized shales from dynamic breakthrough experiments. Journal of Energy Fuels 2017;31: 1193–207.

Continental Resources Inc. 2014. Bakken Field Recoverable Reserves, Technical Report.

Flannery, J., and J. Krause. 2006. Integrated Analysis of the Bakken Petroleum System, U.S. Williston Basin. AAPG Annual Convention.

Hawthorne, S. B., C.D Gorecki, J.A. Sorensen, E.N. Steadman, J.A Harju, and S. Melzer. 2013. Hydrocarbon mobilization mechanisms from Upper, Middle, and Lower Bakken reservoir rocks exposed to CO2. In Proceedings of the SPE Unconventional Resources Conference, Calgary, Alberta, Canada, 5–7 November 2013.

Heller, R., M. Zoback. 2014. Adsorption of methane and carbon dioxide on gas shale and pure mineral samples. Journal of Unconventional Oil and Gas Resources.

Hoffman, B.T. An Evaluation of EOR Potential in the Elm Coulee Bakken Formation, Richland County, Montana. In Proceedings of the SPE Rocky Mountain Student Symposium, Butte, MT, 26 Feb 2016.

Jabbari, H., M. Ostadhassan, and M. Rabeie. 2015. Geomechanics Modeling in CO2-EOR: Case Study. In Proceedings of the Unconventional Resources Conference, Calgary, Alberta, Canada, 20-22 October 2015.

Jabbari, H., M. Ostadhassan, and S. Salehi. 2015. Geomecanical Modeling in CO2 Enhanced Oil Recovery. In Proceedings of the 49th US Rock Mechanics / Geomechanics Symposium, San Francisco, CA, 28 June – 1 July 2015.

Jessen, K., G.Q. Tang, and A.R. Kovscek. 2008. Laboratory and simulation investigation of enhanced coalbed methane recovery by gas injection. Journal of Transport in Porous Media.

Jin, Lu., S. Hawthorne, J. Sorensen, L. Pekot, B. Kurza, S. Smith, L. Heebink, V. Herdegen, N. Bosshart, J. Torres, C. Dalkhaa, K. Peterson, C. Gorecki, E, Steadman, and J. Harju. 2017. Advancing CO2 enhanced oil recovery and storage in unconventional oil play—Experimental studies on Bakken shales. Journal of Applied Energy.

Kang, S.M., E. Fathi, R. J. Ambrose, I. Y. Akkutlu, and R. F. Sigal. 2011. Carbon Dioxide Storage Capacity of Organic-Rich Shales. Journal of Society of Petroleum Engineers.

Kim, T.H., J. Cho, and K.S. Lee. 2017. Evaluation of CO2 injection in shale gas reservoirs with multi component transport and geomechanical effects. Journal of Applied Energy.

Kumar, S., B.T. Hoffman, and M. Prasad. 2013. Upper and Lower Bakken Shale Production Contribution to the Middle Bakken Reservoir. In Proceedings of the Unconventional Resources Technology Conference, Denver, CO, 12-14 August 2013.

Kurtoglu, B. 2013. Integrated Reservoir Characterization and Modeling in Support of Enhanced Oil Recovery for Bakken. Ph.D. dissertation, Colorado School of Mines.

Kurtoglu, B., H. Kazemi, R. Rosen, W. Mickelson, and T. Kosanke. 2014. A Rock and Fluid Study of Middle Bakken Formation: Key to Enhanced Oil Recovery. In Proceedings of the SPE/CSUR Unconventional Resources Conference, Calgary, Alberta, Canada, 30 September – 2 October 2014.

Lashgari, H.R., A. Suna, T. Zhanga, G.A. Pope, and L.W. Lake. 2018. Evaluation of carbon dioxide storage and miscible gas EOR in shale oil reservoirs. Journal of Fuel.

Liu, F., K. Ellett, Y. Xiao, and J.A. Rupp. 2013. Assessing the feasibility of CO2 storage in the New Albany Shale (Devonian–Mississippian) with potential enhanced gas recovery using reservoir simulation. International Journal of Greenhouse Gas Control.

Mohebbinia, S and T. Wong. 2017. Molecular Diffusion Calculations in Simulation of Gas floods in Fractured Reservoirs. In Proceedings of the SPE Reservoir Simulation Conference, Montgomery, TX, USA, 20–22 February 2017.

Nuttall, B. 2010. Reassessment of CO2 Sequestration Capacity and Enhanced Gas Recovery Potential of Middle and Upper Devonian Black Shales in the Appalachian Basin. MRCSP Phase II Topical Report, October 2005–October 2010, DOE Cooperative Agreement DE-FC26-05NT42589, OCDO Grant Agreement No. DC-05-13

Oil and Gas Division-North Dakota Industrial Commission (NDIC). 2018. https://www.dmr.nd.gov/oilgas/

Sanaei, A., A. Abouie, M. Tagavifar, and K. Sepehrnoori. 2018. Comprehensive Study of Gas Cycling in the Bakken Shale. In Proceedings of the Unconventional Resources Technology Conference, Houston, Texas, USA, 23-25 July 2018.

Sheng, J. J. 2014. Enhanced oil recovery in shale reservoirs by gas injection. Journal of Natural Gas Science and Engineering, 252-259.

Shoaib, S., and B.T. Hoffman. 2009. CO2 flooding the Elm Coulee Field. In Proceedings of the Rocky Mountain Petroleum Technology Conference, Denver, Colorado, 14-16 April 2009.

Sigmund, P.M. 1976. Prediction of molecular diffusion at reservoir conditions. Part 1. Measurement and prediction of binary dense gas diffusion coefficients. Can. J. Pet. Technol., (April-June): 48-57.

Sorensen, J., B. Kurz, S. Hawthorne, L. Jin, S. Smith, and A. Azenkeng. 2016. Laboratory characterization and modeling to examine CO2 storage and enhanced oil recovery in an unconventional tight oil formation. Elsevier Ltd, 5460-5478.

Teklu, T., X. Li, Z. Zhou, and H. Abass. 2018. Experimental Investigation on Permeability and Porosity Hysteresis of Tight Formations. Journal Society of Petroleum Engineers.

Torres, J.A., L. Jin, N. W. Bosshart, L. J. Pekot, J. A. Sorensen, K. Peterson, P. W. Anderson, and S. B. Hawthorne. 2018. Multiscale Modeling to Evaluate the Mechanisms Controlling CO2-Based Enhanced Oil Recovery and CO2 Storage in the Bakken Formation. In Proceedings of the Unconventional Resources Technology Conference, Houston, Texas, USA, 23-25 July 2018.

Tran, D., L. Nghiem, and L. Buchanan. 2005. An Overview of Iterative Coupling Between Geomechanical Deformation and Reservoir Flow. In Proceedings of the 2005 SPE International Thermal Operations and Heavy Oil Symposium, Calgary, Alberta, Canada, 1-3 November 2005.

Wang, X., P. Luo, V. Er, and S.S. Huang. 2010. Assessment of CO2 Flooding Potential for Bakken Formation, Saskatchewan. In Proceedings of the SPE Unconventional Resources Conference, Calgary, Alberta, Canada, 19–21 October 2010.

Yu W, H.R. Lashgari, K. Wu, S. Kamy. 2015. CO2 injection for enhanced oil recovery in Bakken tight oil reservoirs. Journal of Fuel.

Yu, W., H. Lashgari, and K. Sepehrnoori. 2014. Simulation Study of CO2 Huff-n-Puff Process in Bakken Tight Oil Reservoirs. In Proceedings of the Rocky Mountain Petroleum Technology Conference, Denver, Colorado, 16-18 April 2014.

Yang, S., Wei, Y., Chen, Z., Wu, W., & Xu, J. 2016. Effects of Multicomponent Adsorption on Enhanced Shale Reservoir Recovery by CO2 Injection Coupled with Reservoir Geomechanics. In Proceedings of the SPE Low Perm Symposium, Denver, Colorado, 5-6 May 2016.

CHAPTER 7

Conclusions and Recommendations

7.1 Conclusions

In this dissertation, a comprehensive study was employed to improve oil recovery in unconventional reservoirs. The research findings point out the following:

- We suggest combining static and dynamic diagnostic methods to better estimate fracture geometry through pressure data, diagnostic fracture injection tests (DFIT), micro-seismic fracture mapping, distributed temperature sensing (DTS), production logs, and production data. The full suite of information can provide valuable evidence concerning the details of the treatment and well performance from complicated shale plays.

- Three different cases were observed through diagnostic plots, where mainly the analysis indicates that most of the fracturing fluid was leaked off through the natural fracture surface area and resulted in the estimation of larger values compared to the hydraulic fracture calculated area. These phenomena might represent a secondary fracture set with a high fracture closure stress activated in neighbor stages that was not well-developed in other sections.

- This methodology is a critical factor in the economic development of unconventional reservoirs since the well completion cost is a significant portion of the capital cost

compared to other expenses, and it significantly influences the production rate or ultimate recovery.

- The surfactant as additives modified the rheological properties of HVFRs with produced water by preventing degradation, reducing viscosity, and expanding fluid viscoelasticity, then, the fracturing fluids are able to carry proppant deeper into the secondary and tertiary fractures.

- The surfactant model gives a significant increase by 15% in EUR compared with Linear Gel and HVFRs with produced water (HVFR-PR) due to extended SRV regions.

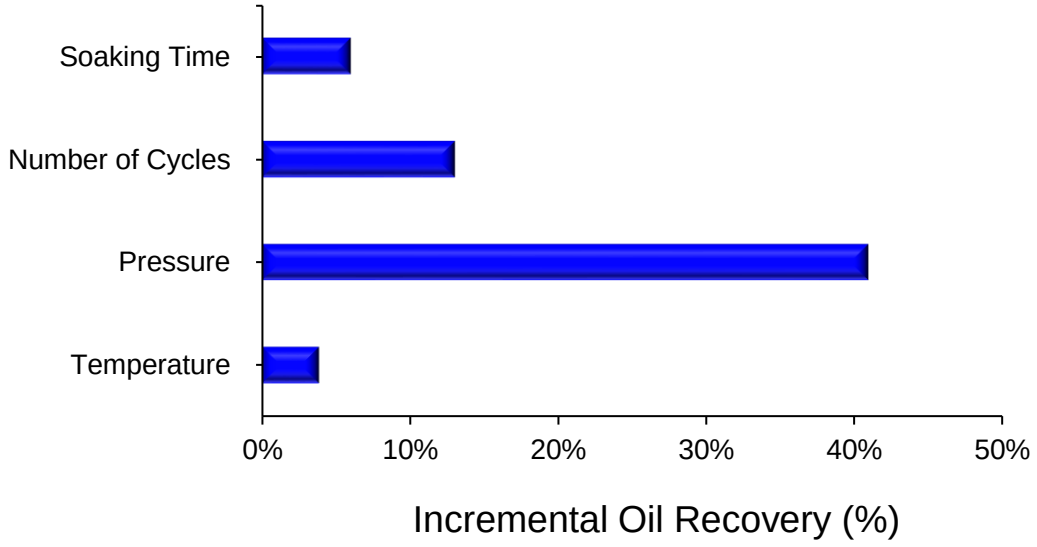

Figure 7. 1. Sensitivity Runs to Reduce Uncertainty in estimation oil recovery.

- The outcomes, as shown in Figure 7. 1 indicated on the effect of the reservoir temperature on the performance of the CO2, where the recoverable oil increases as the temperature increase until reach the optimum depends on the injection pressure phase. On the other hand, high injection pressure yielded higher amount of produced oil.

7.2 Future Work Recommended

The following subjects are suggested for future work in order to conduct a comprehensive study on unconventional reservoirs performance:

- Inclusion of proppant-impact-factors (PIFs) in the calculation of DFIT in order to estimate the effective, and propped contact areas in each stage.
- Combine static and dynamic diagnostic methods to better estimate fracture geometry through pressure data, diagnostic fracture injection tests (DFIT), micro-seismic fracture mapping, distributed temperature sensing (DTS), production logs, and production data. The full suite of information can provide valuable information on the effectiveness of the treatment design and well performance in shale plays.
- Simulation of more case studies are recommended to determine if the adjustment of treatment design from stage to stage can be justified due to the additional cost and treatment job complexities.
- Model the diffusion mechanism in CO2-EOR projects and identify the significant factors that can affect the process on the full-field scale through numerical simulation and sensitivity analysis.
- Conduct comprehensive laboratory experiments on using surfactants as additives to enhance the performance of anionic HVFRs in a High TDS environment, such as in unconventional reservoirs.

References

Ahmadun, F.-R.et al., 2009. Review of technologies for oil and gas produced water treatment. Journal of Hazardous Materials, Volume 139, pp. 530-551.

Ahmed, U., Meehan, D.N., 2016. Unconventional Oil and Gas Resources: Exploitation and Development. CRC Press.

Al Battashi, M., Al Shukaili, S., Al Balushi, S., Al Hatmi, K., & Al Mashrafi, A. (2019, November 11). Treatment of Produced Water with Back Produced ASP. Society of Petroleum Engineers. doi:10.2118/197658-MS

ALL, 2003. Handbook on Coal Bed Methane Produced Water: Management and Beneficial Use Alternatives, ALL Consulting, Ground Water Protection Research Foundation, US Department of Energy, National Petroleum Technology Office, Bureau of Land Management, Tulsa, Oklahoma (July).

Almubarak, T., AlKhaldi, M., Ng, J. H., & Nasr-El-Din, H. A. (2019, August 1). Design and Application of High-Temperature Raw-Seawater-Based Fracturing Fluids. Society of Petroleum Engineers. doi:10.2118/195597-PA

Ba Geri, M., Ellafi, A., Al-Guthmi, S., & Yuanhang, Lu. (2020a). Reducing the Economic Risks of Consuming Freshwater in Hydraulic Fracturing Operation by Using Environmentally Friendly HVFRs. AAPG. ID:59

Ba Geri, M., Ellafi, A., Flori, R., Belhaij, A., & Alkamil, E. H. K. (2019, November 11f). New Opportunities and Challenges to Discover and Develop Unconventional Plays in the Middle East and North Africa: Critical Review. Society of Petroleum Engineers. doi:10.2118/197271-MS

Ba Geri, M., Ellafi, A., Flori, R., Noles, J., & Kim, S. (2019, October 30d). A Comprehensive Review of Formation Damage Caused by High-Viscosity Friction

Reducers: Wolfcamp Case Study. Society of Petroleum Engineers. doi:10.2118/197081-MS

Ba Geri, M., Ellafi, A., Flori, R., Noles, J., & Kim, S. (2019, September 23c). Viscoelastic Characterization Effect of High-Viscosity Friction Reducers and Proppant Transport Performance in High-TDS Environment. Society of Petroleum Engineers. doi:10.2118/196014-MS

Ba Geri, M., Flori, R., Ellafi, A., Noles, J., Essman, J., Kim, S., & Alkamil, E. H. K. (2019, November 11e). Correlated Friction Reduction and Viscoelastic Characterization of Utilizing the Permian Produced Water with HVFRs during Hydraulic Fracturing. Society of Petroleum Engineers. doi:10.2118/197748-MS

Ba Geri, Noles, J., Kim, S., & Ellafi, A. (2020b). New Developed Mathematical Model for Predicting Viscosity Profile and Proppant Transport Utilizing HVFRs Dosage with Produced Water. Society of Petroleum Engineers. doi:10.2118/ 201433-MS

Backstrom, Jesse. 2019 “Strategic Reporting and the Effects of Water Use in Hydraulic Fracturing on Local Groundwater Levels in Texas” The Center for Growth and Opportunity at Utah State University

Bond, C. R. (1985, January 1). North Sea Produced Water Systems. Society of Petroleum Engineers. doi:10.2118/14008-MS

Boschee, P. (2014, February 1). Produced and Flowback Water Recycling and Reuse: Economics, Limitations, and Technology. Society of Petroleum Engineers. doi:10.2118/0214-0016-OGF

Boyer, J., Maley, D., O'Neil, B., Trican Well Service. 2014. "Chemically Enhanced Proppant Transport". 2014. Presented at the SPE Annual Technical Conference and Exhibition, Amsterdam, The Netherlands, 27 – 29 October. SPE-170640-MS

Campin, D. (2019, November 15). The Unknown Risks of Fracking. Unconventional Resources Technology Conference. doi:10.15530/AP-URTEC-2019-198220

Chen, C., Li, X., Wu, B., Zhang, K., & Song, Q. (2019, March 22). Environmental Impact Study and Experience Sharing of Produced Water Reinjection from Unconventional Gas Development. International Petroleum Technology Conference. doi:10.2523/IPTC-19119-MS

Demong, K. L., Sherman, D., & Affleck, B. (2010, January 1). The Tradeoff Between Surfactant Costs and Water Heating to Enhance Friction Reducer Performance. Society of Petroleum Engineers. doi:10.2118/138027-MS

Du, Y., Guan, L., & Liang, H. (2005, January 1). Advances of Produced Water Management. Petroleum Society of Canada. doi:10.2118/2005-060

Ellafi, A. and Jabbari, H (2020b). Understanding the Mechanisms of Huff-n-Puff, CO2-EOR in Liquid-Rich Shale Plays: Bakken Case Study. Society of Petroleum Engineers. doi:10.2118/ 200001-MS

Ellafi, A., Ba Geri, M., Bubach, B., & Jabbari, H. (2019a, August 28). Formation Evaluation and Hydraulic Fracture Modeling of Unconventional Reservoirs: Sab'atayn Basin Case Study. American Rock Mechanics Association.

Ellafi, A., Jabbari, H., Ba Geri, M., & Alkamil, E. (2019b, November 11). Can HVFRs Increase the Oil Recovery in Hydraulic Fractures Applications? Society of Petroleum Engineers. doi:10.2118/197744-MS

Ellafi, A., Jabbari, H., Wan, X., Rasouli, V., Ba Geri, M., & Al-Bazzaz, W. (2020a). How Does HVFRs in High TDS Environment Enhance Reservoir Stimulation Volume? International Petroleum Technology Conference (IPTC) 2020 IPTC-20138

Ellafi, A.; Jabbari, H. Unconventional Well Test Analysis for Assessing Individual Fracture Stages through Post-Treatment Pressure Falloffs: Case Study. Energies 2021, 14, 6747. https://doi.org/10.3390/en14206747

Environment Texas Research and Policy Center, 2013. Keeping water in our rivers strategies for conserving limited water supplies. http://environmenttexas.org/reports/txe/keeping-water-our-rivers (accessed 8.13.15).

Environment Texas Research and Policy Center, 2013. Keeping water in our rivers strategies for conserving limited water supplies.http://environmenttexas.org/reports/txe/keeping-water-our-rivers (accessed 8.13.15).

Esmaeilirad, N., Terry, C., Kennedy, H., Prior, A., & Carlson, K. (2016, August 1). Recycling Fracturing Flowback Water for Use in Hydraulic Fracturing: Influence of Organic Matter on Stability of Carboxyl-Methyl-Cellulose-Based Fracturing Fluids. Society of Petroleum Engineers. doi:10.2118/179723-PA

ExxonMobil, 2017. Hydraulic Fracturing Fluid.

FracFocus, 2012. Chemical Use in Hydraulic Fracturing. http://fracfocus.org/water-protection/drilling-usage.

Freyman, M., 2014. Hydraulic fracturing & water stress: water demand by the numbers. http://www.ceres.org/issues/water/shale-energy/shale-and-water-maps/hydraulicfracturing. water-stress-water-demand-by-the-numbers (accessed 10.20.14).

Gabriel Collins, “New Ways of Thinking About Oilfield Water in the Permian Basin,” Shale Tech 2018, 6 December 2018, Houston, TX

Gabriel Collins, “Trash or Treasure: How is Produced Water's Economic Value Evolving in the Permian Basin?,” Produced Water Society Seminar 2019, 7 February 2019, Sugar Land, TX

Geri, M. B., Ellafi, A., Ofori, B., Flori, R., & Sherif, H. (2019, July 31a). Successful Implementation of High Viscosity Friction Reducers from Laboratory to Field Scale: Middle Bakken Case Study. Unconventional Resources Technology Conference. doi:10.15530/urtec-2019-447

Geri, M. B., Flori, R., & Sherif, H. (2019, July 25b). Comprehensive Study of Elasticity and Shear-Viscosity Effects on Proppant Transport Using HFVRs on High-TDS Produced Water. Unconventional Resources Technology Conference. doi:10.15530/urtec-2019-99

Ghorbani, N., Yan, C., Guraieb, P., Tomson, R. C., Abdallah, D., Aouda, A. B., Al Daghar, T. A. (2016, November 7). An Automated Real-Time Produced Water Composition Measurement Device for Scale Risk Prediction and Prevention. Society of Petroleum Engineers. doi:10.2118/183158-MS

Gu, Y., Yu, S., Mou, J., Wu, D., & Zheng, S. (2020). Research Progress on the Collaborative Drag Reduction Effect of Polymers and Surfactants. Materials Journal

Haghshenas, A., & Nasr-El-Din, H. A. (2014, May 21). Effect of Dissolved Solids on Reuse of Produced Water in Hydraulic Fracturing Jobs. Society of Petroleum Engineers. doi:10.2118/169408-MS

Hu, Y. T., Fisher, D., Kurian, P., & Calaway, R. (2018, January 23). Proppant Transport by a High Viscosity Friction Reducer. Society of Petroleum Engineers. doi:10.2118/189841-MS

Igunnu ET, Chen GZ. Produced water treatment technologies. Int J Low-Carbon Tech 2012.http://dx.doi.org/10.1093/ijlct/cts049.

Jabbari, H., & Benson, S.A (2013, January 1). Hydraulic Fracturing Design Optimization-Bakken Case Study. American Rock Mechanics Association

Jennings, A. R.Jr., Enhanced Well Stimulation Inc.; "Fracturing Fluids – Then and Now". JPT July 1996.

Kakadjian, S., Thompson, J. E., Torres, R., Trabelsi, S., Zamora, F., & Ait Hamlat, Y. (2013, October 8). Stable Fracturing Fluids from Produced Waste Water. Society of Petroleum Engineers. doi:10.2118/167275-MS

Kakadjian, S., Thompson, J., & Torres, R. (2015, March 1). Fracturing Fluids from Produced Water. Society of Petroleum Engineers. doi:10.2118/173602-MS

Khatib, Z., & Verbeek, P. (2003, January 1). Water to Value - Produced Water Management for Sustainable Field Development of Mature and Green Fields. Society of Petroleum Engineers. doi:10.2118/0103-0026-JPT

Kondash, A., Vengosh, A., 2015.Water footprint of hydraulic fracturing. Environ. Sci.Technol. Lett. 2 (10), 276–280.

Kurtoglu, B., H. Kazemi, R. Rosen, W. Mickelson, and T. Kosanke. 2014. A Rock and Fluid Study of Middle Bakken Formation: Key to Enhanced Oil Recovery. In Proceedings of the SPE/CSUR Unconventional Resources Conference, Calgary, Alberta, Canada, 30 September – 2 October 2014

Lebas, R. A., Shahan, T. W., Lord, P., & Luna, D. (2013, February 4). Development and Use of High-TDS Recycled Produced Water for Crosslinked-Gel-Based Hydraulic Fracturing. Society of Petroleum Engineers. doi:10.2118/163824-MS

Li, C., Kong, L., Ostadhassan, M., & Gentzis, T. (2019). Nanoscale Pore Structure Characterization of Tight Oil Formation: A Case Study of the Bakken Formation. Energy & Fuels, 33(7), 6008-6019.

Li, L., Ezeokonkwo, C. I., Lin, L., Eliseeva, K. E., Kallio, W., Boney, C. L., … Samuel, M. M. (2010, January 1). Well Treatment Fluids Prepared with Oilfield Produced Water: Part II. Society of Petroleum Engineers. doi:10.2118/133379-MS

Li, L., Sun, H., Qu, Q., Le, H. V., Ault, M., Zhou, J., … Smith, D. (2014, October 27). High-Temperature Fracturing Fluids Prepared with Extremely High-TDS and Hard Produced Water. Society of Petroleum Engineers. doi:10.2118/170607-MS

Li, S., & Zhang, D. (2019, April 1). How Effective Is Carbon Dioxide as an Alternative Fracturing Fluid? Society of Petroleum Engineers. https://doi:10.2118/194198-PA

Lord, P., Weston, M., Fontenelle, L. K., & Haggstrom, J. (2013, June 26). Recycling Water: Case Studies in Designing Fracturing Fluids Using Flowback, Produced, and Nontraditional Water Sources. Society of Petroleum Engineers. doi:10.2118/165641-MS

Male, F., 2019. Using a Segregated Flow Model to Forecast Production of Oil, Gas, and Water in Shale Oil Plays. Journal of Petroleum Science and Engineering.

Maley, D., Farion, G., Giurea-Bica, G., and O'Neil, B., Trican Well Service LTD. 2013. "NonPolymeric Permanent Clay Stabilizer for Shale Completions". Presented at SPE European Formation Damage Conference and Exhibition, Noordwijk, The Netherlands, 5 – 7 June. SPE-165168.

McMahon, B., MacKay, B., & Mirakyan, A. (2015, April 13). First 100% Reuse of Bakken Produced Water in Hybrid Treatments Using Inexpensive Polysaccharide Gelling Agents. Society of Petroleum Engineers. doi:10.2118/173783-MS

Miller, J.E Review of water resource and desalination Technologies United States of America, 2003.

Mohammad-Pajooh, E., Weichgrebe, D., Cuff, G., Tosarkani, B. M., & Rosenwinkel, K.-H. (2018). On-site treatment of flowback and produced water from shale gas hydraulic fracturing: A review and economic evaluation. Chemosphere, 212, 898–914. https ://doi.org/10.1016/j.chemo sphere.2018.08.145

Montgomery, C. T., and Smith, M. B., NSI Technologies 2010. "Hydraulic Fracturing - History of an Enduring Technology. Journal of Petroleum Technology, volume 62, issue 12, page 26 – 32. SPE-1210-0026-JPT

Motiee, M., Johnson, M., Ward, B., Gradl, C., McKimmy, M., & Meeheib, J. (2016, February 1). High Concentration Polyacrylamide-Based Friction Reducer Used as a Direct Substitute for Guar-Based Borate Crosslinked Fluid in Fracturing Operations. Society of Petroleum Engineers. doi:10.2118/179154-MS

NDSWC, 2019. North Dakota Fracking & Water Use Facts.http://www. http://www.swc.nd.gov/pdfs/fracking_water_use.pdf.

Oil and Gas Division-North Dakota Industrial Commission (NDIC). 2019. https://www.dmr.nd.gov/oilgas/

Oraki Kohshour, I., Leshchyshyn, T., Munro, J., Yorro, M. C., Adejumo, A. T., Ahmed, U., Wedel, D. (2016, August 1). Examination of Water Management Challenges and Solutions in Shale Resource Development - Could Waterless Fracturing Technologies Work? Unconventional Resources Technology Conference. doi:10.15530/URTEC-2016-2461040

Otton, K, and Mercier, T. (2015). Produced Water Brine and Stream Salinity. USGS

Paktinat, J., O' Neil, B. J., Aften, C. W., & Hurd, M. D. (2011, January 1). Critical Evaluation of High Brine Tolerant Additives Used in Shale Slickwater Fracs. Society of Petroleum Engineers. doi:10.2118/141356-MS

Palla, C., Weaver, J. D., Benoit, D., Lu, Z., & Vera, N. (2014, November 10). Impact of Surfactants on Fracture Fluid Recovery. Society of Petroleum Engineers. doi:10.2118/171732-MS

Patel, P. S., Robart, C. J., Ruegamer, M., & Yang, A. (2014, February 4). Analysis of US Hydraulic Fracturing Fluid System and Proppant Trends. Society of Petroleum Engineers. doi:10.2118/168645-MS

Quintero, H., Farion, G., Gardener, D., O'Neil, B., Hawkes, R., Wang, C., … Tsuber, L. (2019, September 23). Successful Application of a Salt Tolerant High Viscous Friction Reducer Technology: Past and Present. Society of Petroleum Engineers. doi:10.2118/196211-MS

Quintero, H., Mattucci, M., Hawkes, R., Zhang, K. and O'Neil, B., Trican Well Service LTD. 2018. "Nano-Particle Surfactant in Hydraulic Fracturing Fluids for Enhanced Post Frac Oil Recovery" Presented at the SPE Canada Unconventional Resources Conference, Clagary, Alberta, Canada, 13 – 14 March. SPE-189780-MS.

Rahm, D. Regulating hydraulic fracturing in shale gas plays: The case of Texas. Energ. Policy 2011, 39 (5), 2974−2981

Ren, K.; Tang, X.; Jin, Y.; Wang, J.; Feng, C.; Höök, M. Bi-objective optimization of water management in shale gas exploration with uncertainty: A case study from Sichuan, China. Resour. Conserv. Recycl. 2019, 143, 226–235.

Rodvelt, G., Yuyi, S., & VanGilder, C. (2015, October 13). Use of a Salt-Tolerant Friction Reducer Improves Production in Utica Completions. Society of Petroleum Engineers. doi:10.2118/177296-MS

Scanlon, B. R.; Reedy, R. C.; Nicot, J.-P. Comparison of Water Use for Hydraulic Fracturing for Shale Oil and Gas versus Conventional Oil. Environ. Sci. Technol. 2014, 48, 12386−12393

Seymour, B., Friesen, D., & Sanders, A. (2018, August 9). Enhancing Friction Reducer Performance in High Salt Conditions. Unconventional Resources Technology Conference. doi:10.15530/URTEC-2018-2902709

Shrestha, N., Chilkoor, G., Wilder, J. et al 2017. Potential water resource impacts of hydraulic fracturing from unconventional oil production in the Bakken shale. Water Research 108: 1–24.

STIM-LAB Proppant Consortium, Report July 2012, Section 3.1 Friction Reducers used in Slickwater Applications.

Sun, H., Stevens, R. F., Cutler, J. L., Wood, B., Wheeler, R. S., & Qu, Q. (2010, January 1). A Novel Nondamaging Friction Reducer: Development and Successful Slickwater Frac Applications. Society of Petroleum Engineers. doi:10.2118/136807-MS

Tang, Clement C., Tiwari, Sanjib, and Cox, Matthew W. "Experimental Characterization of Viscosity and Thermal Conductivity of Aluminum Oxide Nanofluid." Proceedings of the ASME 2013 Heat Transfer Summer Conference.

The Energy Information Administration (EIA). 2019. https://www.eia.gov

Thyne, G., & Brady, P. (2016). Evaluation of formation water chemistry and scale prediction: Bakken Shale. Applied Geochemistry, 75, 107–113. doi: 10.1016/j.apgeochem.2016.10.015

Tomomewo, O. S., Dyrstad-Cincotta N., Mann D., Ellafi, A., Alamooti, M., Srinivasachar, S., Nelson, T. (2020b). Proposed Potential Mitigation of Wastewater Disposal through Treated Produced Water in Bakken Formation. American Rock Mechanics Association, ARMA2020-1254.

Tomomewo, O. S., Mann, D., Ellafi, A., Geri, M. B., Tang, C., Kolawole, O., Ispas, I., Alamooti, M., Onwumelu, C. (2020a). Creating Value for The High-Saline Bakken Produced Water by Optimizing its Viscoelastic Properties and Proppant Carrying Tendency with High-Viscosity Friction Reducers. Society of Petroleum Engineers, SPE-200809-MS.

Torres, L., Yadav, O.P., Khan, E., 2016. A review on risk assessment techniques for hydraulic fracturing water and produced water management implemented in onshore un-conventional oil and gas production. Sci. Total Environ. 539:478–493.

USDOE, 2014. Environmental impacts of unconventional natural gas development andproduction.http://www.netl.doe.gov/research/oil-and-gas/publications(accessed4.24.15).

Van Domelen, M., & Haggstrom, J. (2011, January 1). Methods for Minimizing Fresh Water Requirements in Unconventional Reservoir Fracturing Operations. World Petroleum Congress.

Walters, H. G., Stegent, N. A., & Harris, P. C. (2009, January 1). New Frac Fluid Provides Excellent Proppant Transport and High Conductivity. Society of Petroleum Engineers. https://doi:10.2118/119380-MS

Whitfield, S. (2017, June 1). Permian, Bakken Operators Face Produced Water Challenges. Society of Petroleum Engineers. doi:10.2118/0617-0048-JPT

Xiong, B.; Loss, R. D.; Shields, D.; Pawlik, T.; Hochreiter, R.; Zydney, A. L.; Kumar, M. Polyacrylamide degradation and its implications in environmental systems. Clean Water 2018, 1 (1), 17.

Xu, L., He, K., Ariyaratna, A., & Ogle, J. (2018, February 7). Multifunctional, Salt-Tolerant Friction Reducer Stabilizes Clay Formations and Minimizes the Alteration of Rock Wettability Under Downhole Conditions after Hydraulic Fracturing. Society of Petroleum Engineers. doi:10.2118/189511-MS

Xu, L., Lord, P., He, K., Riley, H., Koons, J., Wauters, T., & Weiman, S. (2017, April 3). Case Study: A Two-Part Salt-Tolerant Friction Reducer System Enables the Reuse of Produced Water in Hydraulic Fracturing. Society of Petroleum Engineers. doi:10.2118/184508-MS

Zhang, N., Schmidt, D., Choi, W., Sundararajan, D., Reisenauer, Z., Freeman, J., … Tomson, M. (2018, June 20). Halite Challenges and Mitigation in the Bakken-Experience of Managing High Saline Produced Water from Hydraulically Fractured Wells. Society of Petroleum Engineers. doi:10.2118/190739-MS